ISSN 0021-9673

VOL. 708 NO. 2 4 AUGUST 1995

THIS ISSUE COMPLETES VOL. 708

JOURNAL OF CHROMATOGRAPHY A

INCLUDING ELECTROPHORESIS AND OTHER SEPARATION METHODS

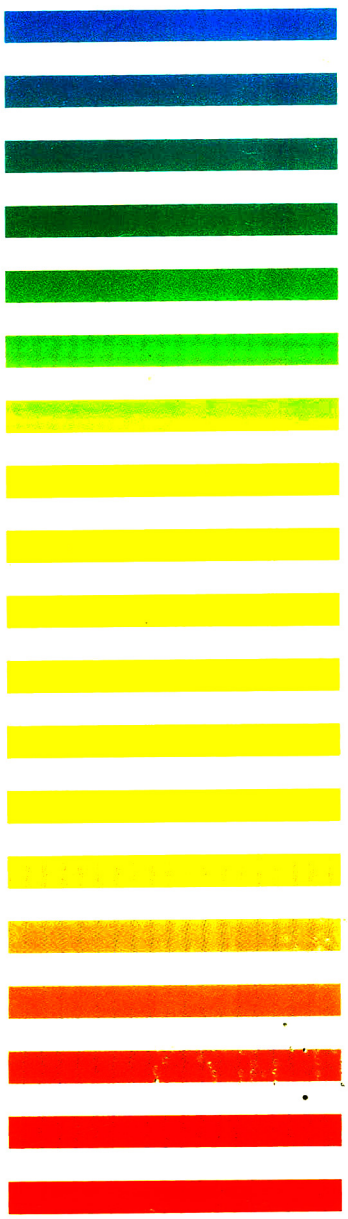

ELSEVIER

JOURNAL OF CHROMATOGRAPHY A

INCLUDING ELECTROPHORESIS AND OTHER SEPARATION METHODS

Scope. The *Journal of Chromatography A* publishes papers on all aspects of **chromatography, electrophoresis** and related methods. Contributions consist mainly of research papers dealing with chromatographic theory, instrumental developments and their applications. In the *Symposium volumes*, which are under separate editorship, proceedings of symposia on chromatography, electrophoresis and related methods are published. *Journal of Chromatography B: Biomedical Applications* —This journal, which is under separate editorship, deals with the following aspects: developments in and applications of chromatographic and electrophoretic techniques related to clinical diagnosis or alterations during medical treatment; screening and profiling of body fluids or tissues related to the analysis of active substances and to metabolic disorders; drug level monitoring and pharmacokinetic studies; clinical toxicology; forensic medicine; veterinary medicine; occupational medicine; results from basic medical research with direct consequences in clinical practice.

Submission of Papers. The preferred medium of submission is on disk with accompanying manuscript (see *Electronic manuscripts* in the Instructions to Authors, which can be obtained from the publisher, Elsevier Science B.V., P.O. Box 330, 1000 AH Amsterdam, Netherlands). Manuscripts (in English; *four* copies are required) should be submitted to: Editorial Office of *Journal of Chromatography A*, P.O. Box 681, 1000 AR Amsterdam, Netherlands, Telefax (+31-20) 485 2304, or to: The Editor of *Journal of Chromatography B: Biomedical Applications*, P.O. Box 681, 1000 AR Amsterdam, Netherlands. Review articles are invited or proposed in writing to the Editors who welcome suggestions for subjects. An outline of the proposed review should first be forwarded to the Editors for preliminary discussion prior to preparation. Submission of an article is understood to imply that the article is original and unpublished and is not being considered for publication elsewhere. For copyright regulations, see below.

Publication information. *Journal of Chromatography A* (ISSN 0021-9673): for 1995 Vols. 683–714 are scheduled for publication. *Journal of Chromatography B: Biomedical Applications* (ISSN 0378-4347): for 1995 Vols. 663–674 are scheduled for publication. Subscription prices for *Journal of Chromatography A*, *Journal of Chromatography B: Biomedical Applications* or a combined subscription are available upon request from the publisher. Subscriptions are accepted on a prepaid basis only and are entered on a calendar year basis. Issues are sent by surface mail except to the following countries where air delivery via SAL is ensured: Argentina, Australia, Brazil, Canada, China, Hong Kong, India, Israel, Japan, Malaysia, Mexico, New Zealand, Pakistan, Singapore, South Africa, South Korea, Taiwan, Thailand, USA. For all other countries airmail rates are available upon request. Claims for missing issues must be made within six months of our publication (mailing) date. Please address all your requests regarding orders and subscription queries to: Elsevier Science B.V., Journal Department, P.O. Box 211, 1000 AE Amsterdam, Netherlands. Tel.: (+31-20) 485 3642; Fax: (+31-20) 485 3598. Customers in the USA and Canada wishing information on this and other Elsevier journals, please contact Journal Information Center, Elsevier Science Inc., 655 Avenue of the Americas, New York, NY 10010, USA, Tel. (+1-212) 633 3750, Telefax (+1-212) 633 3764.

Abstracts/Contents Lists published in Analytical Abstracts, Biochemical Abstracts, Biological Abstracts, Chemical Abstracts, Chemical Titles, Chromatography Abstracts, Current Awareness in Biological Sciences (CABS), Current Contents/Life Sciences, Current Contents/Physical, Chemical & Earth Sciences, Deep-Sea Research/Part B: Oceanographic Literature Review, Excerpta Medica, Index Medicus, Mass Spectrometry Bulletin, PASCAL-CNRS, Referativnyi Zhurnal, Research Alert and Science Citation Index.

US Mailing Notice. *Journal of Chromatography A* (ISSN 0021-9673) is published weekly (total 52 issues) by Elsevier Science B.V., (Sara Burgerhartstraat 25, P.O. Box 211, 1000 AE Amsterdam, Netherlands). Annual subscription price in the USA US$ 5389.00 (US$ price valid in North, Central and South America only) including air speed delivery. Second class postage paid at Jamaica, NY 11431. **USA POSTMASTERS**: Send address changes to *Journal of Chromatography A*, Publications Expediting, Inc., 200 Meacham Avenue, Elmont, NY 11003. Airfreight and mailing in the USA by Publications Expediting.

See inside back cover for Publication Schedule, Information for Authors and information on Advertisements.

0021-9673/95/$09.50

Printed in the Netherlands

VOL. 708, NO. 2 JOURNAL OF CHROMATOGRAPHY A 4 AUGUST 1995

CONTENTS

(Abstracts/Contents Lists published in Analytical Abstracts, Biochemical Abstracts, Biological Abstracts, Chemical Abstracts, Chemical Titles, Chromatography Abstracts, Current Awareness in Biological Sciences (CABS), Current Contents/Life Sciences, Current Contents/Physical, Chemical & Earth Sciences, Deep-Sea Research/Part B: Oceanographic Literature Review, Excerpta Medica, Index Medicus, Mass Spectrometry Bulletin, PASCAL-CNRS, Referativnyi Zhurnal, Research Alert and Science Citation Index)

REGULAR PAPERS

Column Liquid Chromatography

Concentration dependence of the distribution coefficient of maltooligosaccharides on a cation-exchange resin
by S. Adachi (Kyoto, Japan), T. Mizuno (Okayama, Japan) and R. Matsuno (Kyoto, Japan) (Received 28 March 1995) . . . 177

Influence of organic solvent modifier and solvent strength on peak shape of some basic compounds in high-performance liquid chromatography using a reversed-phase column
by D.V. McCalley (Bristol, UK) (Received 28 March 1995) . . . 185

Study on how mobile phase buffer composition effects the retention behavior of the system peak in non-suppressed ion chromatography
by M. Nishimura and M. Hayashi (Kyoto, Japan), A. Yamamoto (Toyama, Japan), T. Horikawa (Nagaoka, Japan) and K. Hayakawa and M. Miyazaki (Kanazawa, Japan) (Received 28 March 1995) . . . 195

Optimization of the determination of amino acids in parenteral solutions by high-performance liquid chromatography with precolumn derivatization using 9-fluorenylmethyl chloroformate
by B. Carratù, C. Boniglia and G. Bellomonte (Rome, Italy) (Received 28 March 1995) . . . 203

Evaluation of solid-phase extraction procedures in peptide analysis
by T. Herraiz and V. Casal (Madrid, Spain) (Received 20 March 1995) . . . 209

Heterogeneity of the bovine κ-casein caseinomacropeptide, resolved by liquid chromatography on-line with electrospray ionization mass spectrometry
by D. Mollé and J. Léonil (Rennes, France) (Received 21 March 1995) . . . 223

Enantiomeric enrichment of partially resolved 4-hydroxy-2-carboxymethylcyclopentanone derivatives by achiral phase chromatography
by E. Loža, D. Loļa, A. Ķemme and J. Freimanis (Rīga, Latvia) (Received 21 March 1995) . . . 231

Enantiomeric separation of a thiazole derivative by high-performance liquid chromatography and micellar electrokinetic chromatography
by R. Furuta and T. Doi (Osaka, Japan) (Received 27 March 1995) . . . 245

Chiral separations of β-blocking drug substances using chiral stationary phases
by J. Ekelund, A. van Arkens, K. Brønnum-Hansen, K. Fich, L. Olsen and P.V. Petersen (Brønshøj, Denmark) (Received 20 March 1995) . . . 253

Characterization of size-permeation limits of cell walls and porous separation materials by high-performance size-exclusion chromatography
by H. Woehlecke and R. Ehwald (Berlin, Germany) (Received 28 March 1995) . . . 263

High-performance size-exclusion chromatographic characterization of water-soluble polymeric substances produced by *Phanerochaete chrysosporium* from free and wheat cell wall bound 3,4-dichloroaniline
by E. Hoque (Oberschleißheim, Germany) (Received 29 March 1995) . . . 273

Gas Chromatography

Gas chromatography of Titan's atmosphere. VI. Analysis of low-molecular-mass hydrocarbons and nitriles with BPX5 capillary columns
by A. Aflalaye, R. Sternberg and F. Raulin (Créteil, France) and C. Vidal-Madjar (Thiais, France) (Received 24 January 1995) . . . 283

Contents (continued)

Retention of halocarbons on a hexafluoropropylene epoxide-modified graphitized carbon black. IV. Propane-based compounds
by T.J. Bruno, K.H. Wertz and M. Caciari (Boulder, CO, USA) (Received 2 January 1995) 293

Determination of N-nitrosodimethylamine in beer by gas chromatography–stable isotope dilution chemical ionization mass spectrometry
by M. Longo, C. Lionetti and A. Cavallaro (Milan, Italy) (Received 3 April 1995) 303

Electrophoresis

Diode laser-induced fluorescence detection in capillary electrophoresis after pre-column derivatization of amino acids and small peptides
by A.J.G. Mank (Amsterdam, Netherlands) and E.S. Yeung (Ames, IA, USA) (Received 1 March 1995) 309

Separation of precolumn-labelled D- and L-amino acids by micellar electrokinetic chromatography with UV and fluorescence detection
by A. Tivesten and S. Folestad (Göteborg, Sweden) (Received 16 March 1995) 323

Capillary zone electrophoretic determination of C_2–C_{18} linear saturated free fatty acids with indirect absorbance detection
by R. Roldan-Assad and P. Gareil (Paris, France) (Received 15 March 1995) 339

SHORT COMMUNICATIONS

Column Liquid Chromatography

Detection of olive oil adulteration by measuring its authenticity factor using reversed-phase high-performance liquid chromatography
by A.H. El-Hamdy and N.K. El-Fizga (Tripoli, Libya) (Received 31 March 1995) 351

Electrophoresis

Performance of a physically adsorbed high-molecular-mass polyethyleneimine layer as coating for the separation of basic proteins and peptides by capillary electrophoresis
by F. Bedia Erim, A. Cifuentes, H. Poppe and J.C. Kraak (Amsterdam, Netherlands) (Received 27 March 1995) . . 356

ERRATA

Erratum to "Determination of phylloquinone in intravenous fat emulsions and soybean oil by high-performance liquid chromatography" [J. Chromatogr. A, 664 (1994) 189]
by F. Moussa (Tours, France) 363

Erratum to "Study of the enantioselective binding between BOF-4272 and serum albumins by means of high-performance frontal analysis" [J. Chromatogr. A, 694 (1995) 81]
by A. Shibukawa, M. Kadohara and J.-y. He (Kyoto, Japan), M. Nishimura and S. Naito (Tokushima, Japan) and T. Nakagawa (Kyoto, Japan) 364

AUTHOR INDEX 365

ELSEVIER

Journal of Chromatography A, 708 (1995) 177–183

JOURNAL OF CHROMATOGRAPHY A

Concentration dependence of the distribution coefficient of maltooligosaccharides on a cation-exchange resin

Shuji Adachi[a,*], Takeshi Mizuno[b], Ryuichi Matsuno[a]

[a]*Department of Food Science and Technology, Faculty of Agriculture, Kyoto University, Sakyo-ku, Kyoto 606-01, Japan*
[b]*Production Station, Hayashibara Co., Ltd., 7-7 Amase-minami, Okayama 700, Japan*

First received 2 February 1995; revised manuscript received 28 March 1995; accepted 28 March 1995

Abstract

The distribution coefficients of glucose, maltose and maltotriose on a cation-exchange resin in the sodium form at 60°C depended on the solute concentration, being larger at higher concentration. The dependence of the coefficient on concentration decreased in the order maltotriose > maltose > glucose. The dependence was explainable by considering the swelling pressure of the resin, which decreased at higher solute concentrations.

1. Introduction

Cation-exchange resins are widely used to separate mono- and oligosaccharides [1–4]. The adsorption of a solute on a resin is characterized by a distribution coefficient, which is defined as the ratio of the solute concentration in the resin phase to that in the external phase. The distribution coefficient is usually obtained at a low solute concentration, and has been considered as an intrinsic value for a combination of the solute and the resin at a constant temperature, and to be independent of the solute concentration. However, dense solutes are often used as samples in practical separation processes on an industrial scale. Ito et al. [5] reported that the distribution coefficient of nistose (fructotriosylglucoside) on a cation-exchange resin in the Na^+ form depended on its concentration, and increased with increase in concentration. However, they did not explain why the coefficient depended on the solute concentration.

In this work, the distribution coefficients of glucose, maltose and maltotriose on a cation-exchange resin in the Na^+ form and containing 4% of divinylbenzene content were obtained at various concentrations. It was found that the swelling pressure of the resin plays an important role in the dependence of the distribution coefficient on the solute concentration.

2. Experimental

2.1. Materials

We used a cation-exchange resin (Dowex) with sulphonate groups and a divinylbenzene content of 4%. The resin was converted into the alkali metal form (Li^+, Na^+ or K^+) or the hydrogen form according to standard procedures [6].

Glucose, maltose, maltotriose and maltotetra-

* Corresponding author.

0021-9673/95/$09.50
SSDI 0021-9673(95)00405-X

ose were products of Hayashibara (Okayama, Japan). The bed voidage of the column packed with the resin was determined using pullulan (Hayashibara) or soluble starch (Nacalai Tesque, Kyoto, Japan). Other chemicals were of analytical-reagent grade.

2.2. Distribution coefficient

The cation-exchange resin was converted into the Na^+ form. The distribution coefficients of glucose, maltose and maltotriose on the resin were determined at 60°C, to prevent microbial growth and owing to the low viscosity at that temperature. Practical separations on an industrial scale have also been carried out at such a temperature. The resin was separated on a sintered-glass filter. The wet resin (about 5.3 g) was placed in a vial, glucose, maltose or maltotriose solutions of a known concentration C_0 were added and kept at 60°C for 30 min, then the external solution was decanted. This was repeated at least three times to attain equilibrium. Finally, the resin was separated on the sintered-glass filter and excess solution on the resin surface was removed with filter-paper. The solute concentration in the filtrate was determined by high-performance liquid chromatography to confirm that the equilibrium concentration was C_0. The wet resin was used to measure the amount adsorbed and to evaluate the apparent density of the resin, ρ_p, by pycnometry.

The filtered resin was weighed (W_R) in an Erlenmeyer flask, then distilled water of volume V_d (usually 50 ml) was added. The flask was gently shaken to desorb the solute for at least 1 h, then the solute concentration in the external solution, C_d, was determined. The distribution coefficient, K, of the solute was evaluated using the following equation:

$$K = \frac{C_d V_d / (W_R / \rho_p)}{C_0} \quad (1)$$

2.3. Determination of the molar volume of a solute

A solute of mass W_S was placed in a volumetric flask of volume V (about 10 ml), which was precisely determined using distilled water. The solute was dissolved in distilled water, which was further added to dilute to the mark at 60°C. The mass of water added, W_w, was precisely measured. The concentrations of the solute, C_S, and water, C_w, were evaluated using the equations

$$C_S = W_S / (M_S V) \quad (2a)$$

$$C_w = W_w / (M_w V) \quad (2b)$$

where M_S and M_w are the molecular masses of the solute and water, respectively.

Under the assumptions that the volumes of a solute and water are independent and that additivity holds, the following equation is obtained:

$$C_w = \frac{1}{v_w} - \frac{v_S}{v_w} \cdot C_S \quad (3)$$

where v_S and v_w are the molar volumes of the solute and water, respectively. Since the v_w value at 60°C can be calculated from the density [7], the v_S value can be calculated if the plot of C_w versus C_S gives a straight line.

2.4. Determination of the equivalent volume of a resin

The equivalent volume, V_e, is defined as the volume of resin per unit equivalent of fixed ions. The V_e values of the resins in the H^+, Li^+, Na^+ and K^+ forms were determined as described [8]. The bed voidage was measured by means of the pulse response, using pullulan as the solute.

2.5. Determination of the swelling pressure of the resin

The resin in the Li^+, Na^+ or K^+ form was packed into a column of 1.52 cm I.D. with a jacket. The bed height was about 44 cm, which was precisely measured in each experiment. Pulse response experiments were performed at 60°C, using 1% (w/v) glucose, maltose and

maltotriose as the samples. Maltotetraose [1% (w/v)] was also used for the resin in the Na^+ form. The eluent was distilled water. The bed voidage was determined from the pulse response curves of pullulan [1% (w/v)]. The pulse response experiments were carried out at three or four different flow-rates for each solute and the elution profiles were monitored using a YRU-883 refractometer (Shimamura Seisakusho, Tokyo, Japan) and recorded on an R-11 strip-chart recorder (Rikadenki, Tokyo, Japan). The elution curves were analysed according to Nakanishi et al. [9] to evaluate the distribution coefficient, K, of each solute. These methods are based on moment analysis of the elution curves.

We have proposed an equation which relates the K value with the swelling pressure of the resin, Π [8]. Assuming that v_S is independent of pressure, the chemical potentials of the solute in the external solution and resin phases, μ_1 and μ_2 are given by the following equations:

$$\mu_1 = \mu(P^0) + RT \ln a_1 + (P_1 - P^0)v_S \quad (4a)$$

$$\mu_2 = \mu(P^0) + RT \ln a_2 + (P_2 - P^0)v_S \quad (4b)$$

where P is the pressure, R is the gas constant, T is the absolute temperature, a is the activity. P^0 is the standard pressure and the subscripts 1 and 2 denote the external solution and resin phases, respectively. Since μ_1 is equal to μ_2 at equilibrium, we can obtain the following equation:

$$\frac{a_2}{a_1} = \exp\left(-\frac{\Pi}{RT} \cdot v_S\right) \quad (5)$$

where $\Pi = P_2 - P_1$ and is the swelling pressure of the resin. The distribution coefficient K is defined as the ratio of the solute concentration in the resin phase to that in the external solution phase. Therefore, the distribution coefficient can be expressed by

$$K = \gamma_0 \exp\left(-\frac{\Pi}{RT} \cdot v_S\right) \quad (6a)$$

where γ_0 is a parameter related to the ratio of the activity coefficient of the solute in the external solution phase to that in the resin phase. Taking the logarithms of both sides of Eq. 6a,

$$\ln K = -\frac{\Pi}{RT} \cdot v_S + \ln \gamma_0 \quad (6b)$$

If Eq. 6b is applicable to the present system, the Π value can be calculated from the slope of the line obtained from the plots of ln K versus v_S.

2.6. Bed shrinkage by dense solute solutions

The resin in the Na^+ form was packed into a column with a water-jacket. The I.D. of the column was 1.52 cm and the bed height was about 44 cm, which was precisely measured in each experiment. The bed was kept at 60°C by circulating thermostated water through the jacket.

A 20% (w/v) solution of glucose, maltose or maltotriose was continuously applied to the bed at a flow-rate of 1.7 ml/min until there was no further bed shrinkage. Usually the volume of the applied solute was about 1.5 times that of the bed. The bed shrinkage was monitored using a video camera. After bed shrinkage had ceased, pulse response studies using soluble starch [1% (w/v)] in the solute solution were performed using the solute as the eluent, to determine the bed voidage when glucose and maltose were used as the solute. The effluent was fractionated using a Type 2112 fractionator (LKB, Bromma, Sweden) and the concentration of soluble starch in each was determined. These experiments were also repeated at solute concentrations of 40 and 60% (w/v).

2.7. Analysis

The concentrations of glucose, maltose and maltotriose were determined using an LC-6A high-performance liquid chromatograph (Shimadzu, Kyoto, Japan) with an St/6DVB-15(N) separation column (Japan Organo, Tokyo, Japan) and a YRU-880 refractometer (Shimamura). Distilled water was used as the eluent. The concentration of soluble starch was measured by the KI–I_2 method [10].

3. Results and discussion

3.1. Distribution coefficients at various solute concentrations

Fig. 1 shows the distribution coefficients at 60°C of glucose, maltose and maltotriose on a resin in the Na^+ form at various equilibrium concentrations. The open symbols represent single-component systems. The closed symbols represent a binary component system which consisted of maltose and maltotriose and where the concentration of maltotriose was fixed at 5.0% (w/v). The distribution coefficients of maltose and maltotriose in the binary system are plotted against their total concentrations. The distribution coefficients of all the solutes depended on their concentrations, and the extent of the dependence was in the order maltotriose > maltose > glucose.

Eq. 6a suggests the reason for this. If the swelling pressure Π is lower at higher solute concentrations, the distribution coefficient might increase. The dependence of the swelling pressure on the solute concentration was studied, and the molar volumes of the solutes were determined as shown below.

3.2. Molar volumes of the solutes

The water concentrations at different solute concentrations were plotted against the solute concentrations and are shown in Fig. 2. The plots gave a straight line for each solute. The molar volume of water at 60°C was 0.0183 l/mol [7]. According to Eq. 3, the molar volumes of glucose, maltose and maltotriose were calculated from the slopes of the respective lines as 0.116, 0.216 and 0.313 l/mol, respectively. The molar volume of maltotetraose, which will be necessary in Fig. 3, was calculated to be 0.416 l/mol by extrapolating the relationship between the molar volume and the molecular mass for the above three solutes.

3.3. Relationship between equivalent volume and swelling pressure

The equivalent volume of the resin was considered as a parameter that related the swelling pressure with the bed shrinkage. The resin in the H^+ form was packed into a column, and the bed voidage of the bed, ε_H, was determined from the pulse response experiments using pullulan as the solute. The equivalent volume of the resin in the H^+ form was calculated to be 0.470 l/equiv.

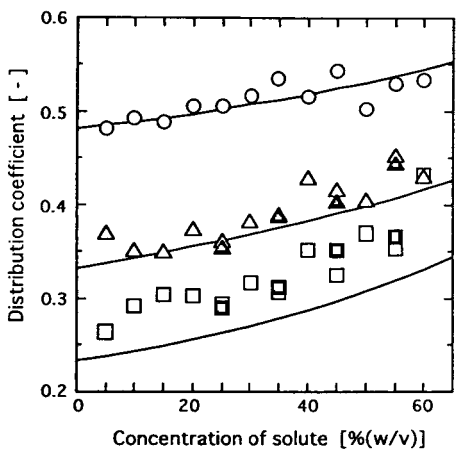

Fig. 1. Distribution coefficients of (○) glucose, (△) maltose and (□) maltotriose at 60°C on a cation-exchange resin in the sodium form. The solid curves are calculated.

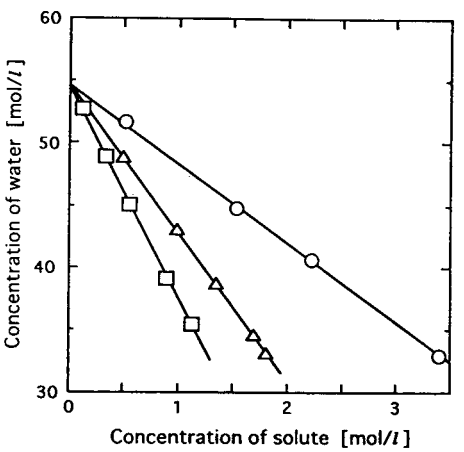

Fig. 2. Concentrations of water in (○) glucose, (△) maltose and (□) maltotriose solutions at 60°C.

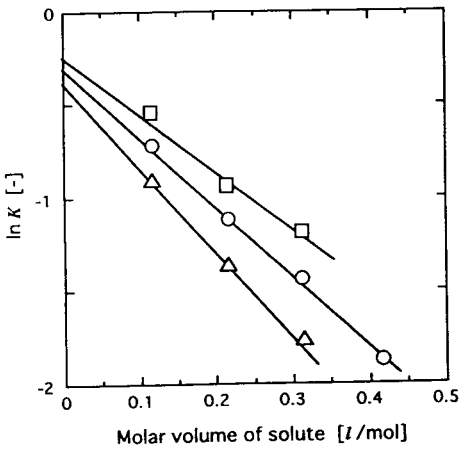

Fig. 3. Estimation of the swelling pressure of a cation-exchange resin in the (△) lithium, (○) sodium and (□) potassium forms. The distribution coefficients were observed at 60°C using distilled water as the eluent. The solutes were glucose, maltose, maltotriose and maltotetraose.

from its exchange capacity and apparent density. The resin was consecutively converted into the Li^+, Na^+ and K^+ forms by supplying LiCl, NaCl and KCl solutions, respectively, and by washing with distilled water. For the resin in each alkali metal form, the distribution coefficients, K, of the maltooligosaccharides and the bed voidage, ε, were measured using distilled water as the eluent. The equivalent volume, V_e, of the resin in each alkali metal form was calculated using the following equation:

$$V_e = \frac{V_{e,H} Z(1-\varepsilon)}{Z_H(1-\varepsilon_H)} \quad (7)$$

where Z and Z_H are the bed heights for the resins in alkali metal and H^+ forms, respectively, and $V_{e,H}$ is the equivalent volume of the resin in the H^+ form.

The swelling pressure of the resin in each alkali metal form was calculated using Eq. 6b. The distribution coefficients of the malto-oligosaccharides were plotted against their molar volumes on a semi-logarithmic scale (Fig. 3). The plots gave a straight line for the resin in each form. The swelling pressure Π and the γ_0 value were evaluated from the slope and the intercept of the line, respectively.

Gregor [11] has proposed a model in which the matrix of an ion-exchange resin is a network of elastic springs, and the equivalent volume of the resin is a linear function of the swelling pressure:

$$V_e = a\Pi + b \quad (8)$$

where the empirical constants, a and b, are characteristic of the resin and independent of the ionic form. Constant b is the equivalent volume of the unstrained resin. It has been reported that this model is applicable for styrene-type [11,12] and dextran gel-type [13] ion exchangers. Since the resin was a styrene type, the model should be applicable. As shown in Fig. 4, the equivalent volume of the resin was linearly related to the swelling pressure, indicating that the model was valid for the resin. The values of constants a and b were calculated to be 1.06×10^{-3} l/equiv. · atm and 0.334 l/equiv., respectively.

The parameter γ_0 was also a linear function of the swelling pressure (atm):

$$\gamma_0 = 1 - 2.60 \times 10^{-3}\Pi \quad (9)$$

This relationship was obtained empirically. Since the activity coefficients in the external solution

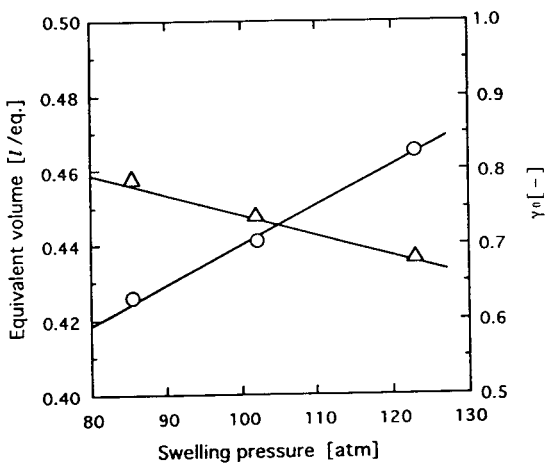

Fig. 4. Experimental relationships (○) between an equivalent volume of resin and the swelling pressure of the resin and (△) between the parameter γ_0 and the pressure.

and resin phases are the same when the swelling pressure is zero, the intercept on the axis should be 1.

3.4. Bed shrinkage by dense solute solutions

The resin in the Na^+ form was packed into a column. Glucose, maltose or maltotriose solutions of 20, 40 and 60% (w/v) were applied consecutively to the bed, and the bed height was read after no further shrinkage occurred. The bed voidage was also measured when glucose and maltose solutions were applied. The bed shrank with increasing solute concentration (Fig. 5). The relationship between the bed shrinkage and the solute concentration, C_S, was empirically expressed by a second-order function for each solute:

$$Z/Z_0 = 1 + cC_S + dC_S^2 \quad (10)$$

where Z and Z_0 are the bed heights at $C_S = C_S$ and $C_S = 0$, respectively, and C_S is in units of % (w/v). The values of the constants c and d were determined to be -4.83×10^{-4} and -6.25×10^{-6}, -6.86×10^{-4} and -5.21×10^{-6}, and -7.00×10^{-4} and -7.50×10^{-6} for glucose, maltose and maltotriose, respectively. The solid curves in Fig. 5 were drawn using these values of c and d.

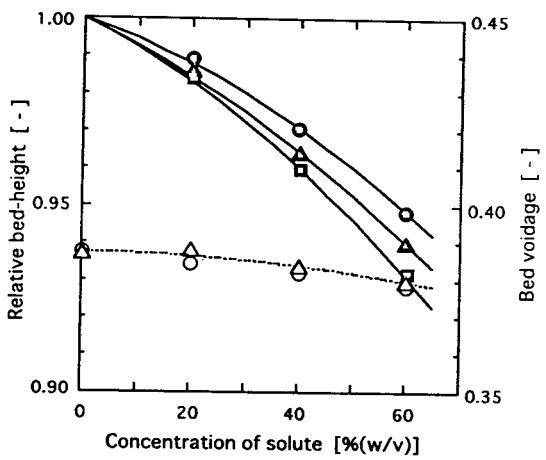

Fig. 5. Effects of the solute concentration on bed shrinkage and bed voidage. The closed and open symbols represent the relative bed height and bed voidage, respectively. ●, ○ = Glucose; ▲, △ = maltose; ■ = maltotriose.

The bed voidage also depended slightly on the solute concentration, as shown in Fig. 5. The bed voidage was not studied when maltotriose was applied, because the relationships between the bed voidage and C_S were similar for both glucose and maltose, and because maltotriose is much more expensive than the other solutes. The bed voidage could be empirically expressed by a second-order function of C_S:

$$\varepsilon = 0.387 - 2.00 \times 10^{-5} C_S - 1.87 \times 10^{-6} C_S^2 \quad (11)$$

where C_S is in units of % (w/v). The relationship of Eq. 11 is shown in Fig. 5 by the dotted curve.

3.5. Calculation of distribution coefficients at various solute concentrations

The bed shrinkage Z/Z_0 and the bed voidage ε at any solute concentration can be evaluated by Eqs. 10 and 11, respectively. The equivalent volume of the resin, V_e, at the concentration is given by

$$V_e = \frac{Z}{Z_0} \cdot \frac{1-\varepsilon}{1-\varepsilon_0} \cdot V_{e,0} \quad (12)$$

where the subscript zero represents the values at $C_S = 0$. The value of $V_{e,0}$ for the resin in the Na^+ form was 0.441 l/equiv. By substituting the V_e value into Eq. 8, the swelling pressure of the resin at the concentration was calculated. The γ_0 value corresponding to the swelling pressure was obtained from Eq. 9. Thus, all the values necessary to calculate the distribution coefficient K at the concentration using Eq. 6a were obtained.

The solid curves in Fig. 1 were drawn according to the procedures described above. The curves for glucose and maltose coincided well with the experimentally observed dependence of the distribution coefficients on solute concentration. For maltotriose, the calculated curve lies slightly below the symbols which represent the experimentally observed distribution coefficients. The reason for the discrepancy is not clear. However, the calculated curve showed a tendency for the distribution coefficient to be larger

at higher concentrations. The distribution coefficient of maltotriose depended most on the concentration among the solutes. This is ascribed to its large molar volume.

References

[1] P. Jandera and J. Churacek, J. Chromatogr., 98 (1974) 55.
[2] R.W. Goulding, J. Chromatogr., 103 (1975) 229.
[3] H.D. Scobell, K.M. Brobst and E.M. Steele, Cereal Chem., 54 (1977) 905.
[4] S. Adachi, T. Watanabe and M. Kohashi, Agric. Biol. Chem., 53 (1989) 3193.
[5] H. Ito, M. Hayashiya, Y. Kajihata and T. Imura, Abstracts of 57th Annual Meeting of the Society of Chemical Engineers, Japan, 1992, p. 152.
[6] K. Kakihana and Y. Mori, Introduction to Ion-Exchange, Hirokawa-shoten, Tokyo, 1969, pp. 43 and 46 (in Japanese).
[7] R.C. Weast (Editor), Handbook of Chemistry and Physics, CRC Press, Boca Raton, FL, 1988, p. F-5.
[8] S. Adachi, T. Watanabe and M. Kohashi, Agric. Biol. Chem., 53 (1989) 3203.
[9] K. Nakanishi, S. Yamamoto, R. Matsuno and T. Kamikubo, Agric. Biol. Chem., 41 (1977) 1465.
[10] H. Fukuba and K. Kainuma, in: M. Nakamura and S. Suzuki (Editors), Handbook of Starch Sciences, Asakura-shoten, Tokyo, 1977, p. 174 (in Japanese).
[11] H.P. Gregor, J. Am. Chem. Soc., 70 (1948) 1293.
[12] G.E. Boyd and B.A. Soldano, Z. Elektrochem., 57 (1953) 162.
[13] S. Yamamoto, K. Nakanishi and R. Matsuno, Ion-Exchange Chromatography of Protein, Marcel Dekker, New York, 1988, p. 137.

ELSEVIER

Journal of Chromatography A, 708 (1995) 185–194

JOURNAL OF CHROMATOGRAPHY A

Influence of organic solvent modifier and solvent strength on peak shape of some basic compounds in high-performance liquid chromatography using a reversed-phase column☆

David Victor McCalley

Department of Chemical and Physical Sciences, University of the West of England, Frenchay, Bristol BS16 1QY, UK

First received 17 January 1995; revised manuscript received 28 March 1995; accepted 28 March 1995

Abstract

Comparative column efficiency and peak asymmetry measurements were made for 16 pyridine derivatives using approximately isoeluotropic mixtures of methanol, acetonitrile and tetrahydrofuran (THF) in combination with phosphate buffer at pH 7.0 on a RP-HPLC column suitable for the analysis of basic compounds. On average, THF and methanol gave significantly better peak shape than acetonitrile, although considerable variations in behaviour for the different derivatives were noted. Methanolic mobile phases yielded straight line plots of $\log k'$ vs. percentage of modifier; nevertheless the increase in k' with decreasing methanol concentration is accompanied by a deterioration in peak shape which varies in extent depending on the nature of the probe compound.

1. Introduction

The difficulty inherent in the analysis of basic compounds by RP-HPLC is still an area of concern. There are important applications, for instance in pharmaceutical analysis, since many drugs contain basic groups. However, the chromatography of basic analytes is also of more general interest since such compounds can highlight the heterogeneity of the RP surface and changes in the surface which can occur with time. Differences can be revealed between apparently similar columns from different manufacturers, and even columns made from different batches of the same manufacturer's product.

Solvents of low viscosity are generally preferred in HPLC due to practical considerations, but also to the improved column efficiencies which may result. The improvement is believed to be due largely to the increased diffusion coefficients of the analytes in the mobile phase in accord with the Wilke–Chang equation [1]. Thus, acetonitrile–water mixtures may be preferred to methanol–water in RP-HPLC. However, few systematic experimental studies have been performed which detail the effect of change of the organic modifier on column efficiency (N) and asymmetry factor (A_s) if the analytes are basic compounds, which are prone to deleterious column interactions, for instance with underivatised column silanol groups. Claessens et al. [2] in a comparative study of eight columns using the probe compounds 2-hexyl- and 2-heptylpyridine, showed that large differences in A_s

☆ Presented in part at *the 19th International Symposium on Column Liquid Chromatography, Innsbruck, 28 May–2 June, 1995.*

0021-9673/95/$09.50
SSDI 0021-9673(95)00404-1

were evident for most columns when simple organic solvent–water mixtures containing either methanol, acetonitrile or THF were used as the modifier, with acetonitrile giving rise to the most asymmetric peaks. In another study, relatively little difference in A_s for pyridine was reported when using acetonitrile–water compared with methanol–water [3] ; pyridine appears to be a more severe probe of column activity under these conditions than 2-substituted derivatives of similar pK_a. In previous work [4], we investigated the performance of a range of different types of RP column using a variety of different probe compounds including pyridine (pK_a 5.2) and the considerably more basic compounds benzylamine (pK_a 9.3), quinine (pK_a 8.5) and nicotine (pK_a 8.0) [5]. It was shown that the performance for pyridine in methanol–water or methanol–phosphate buffer at pH values near the upper limit for silica-based columns, could provide some indication of column performance for the tobacco alkaloids under the same conditions.

In the present study, we have explored further the possible differences in RP column performance with different modifiers, using a set of pyridine derivatives which cover a range of pK_a values and stereochemistry. Our previous results relating compound stereochemistry and pK_a to peak shape using methanol [3] could also be compared for the different modifiers. The analysis of these compounds is of practical significance, since they are environmental pollutants originating from coal tar [6]. The study was performed on Inertsil ODS, a column which was shown to give good results for pyridine derivatives and some more basic compounds containing different structural features, detailed above, at pH 7.0. Analysis of the tobacco alkaloids (pK_a > 8) was demonstrated on the column at this relatively high, and also at low pH [4]. A column giving a reasonable peak shape for pyridine derivatives should give more reproducible data than columns producing very asymmetric peaks [7]. Similarly, we did not want to utilise probe compounds which give severe interaction with the RP surface, since we wished to study a variety of possibly non-optimum mobile phases. We performed the study with mobile phases buffered at pH 7.0. At acidic pH, pyridine derivatives show rather low retention, necessitating low concentrations of organic modifier for analysis. It was felt that differences between the various modifiers might be concealed using largely aqueous mobile phases; however, further studies are necessary to investigate this hypothesis. Furthermore, the collapse of ODS ligands onto the surface of the silica and the change in ionisation state of the surface silanols [4] might produce different results.

Relatively few detailed experimental studies have been performed on the effect of solvent strength (as controlled by the volume fraction of a particular organic modifier) on the retention factor and peak shape of basic analytes. Vervoort et al. [8] showed a correlation between k' and A_s for analysis of a series of basic drugs. Nevertheless, a later report by the same group [7] claimed hardly any correlation between k' and A_s. However, it is difficult to interpret these studies fully due to the lack of experimental detail given. Thus, we also performed some investigation on the effect of change of organic solvent concentration on the peak shape for the same series of basic compounds.

Despite the above justification for the experimental conditions chosen, it should be stated clearly that different combinations of sample type, pH and column can lead to different situations. Column performance as measured by A_s and N measurements may not be consistent for analytes of unrelated structure. Thus, column "A" may perform better for compound "X" while column "B" performs better for compound "Y". Similarly, comparisons of relative column performance may yield different results at different pH. Analysis of compounds with higher pK_a values (e.g. alkyl amines) could also give rise to different results. Nevertheless, the study should give additional information on the selection of optimum mobile phases for the chromatography of basic compounds.

2. Experimental

The HPLC system consisted of an SP 8800 pump, Spectra 100 UV detector with a time

constant of 0.1 s and a 9-μl flow cell (Spectra Physics, San Jose, CA, USA) and valve injector with 5 μl loop (Rheodyne, Cotati, CA, USA). We attempted to keep the dead volume of the system to a minimum, and used a relatively large diameter column in order to limit extra-column effects. N was determined from peak widths at half height ($w_{0.5}$) using the formula $n = 5.54[t_R/w_{0.5}]^2$. A_s was calculated at 10% of the peak height from the ratio of the widths of the rear and front sides of the peak; both measurements were made using a Model 2000 data station (Trivector, Bedford, UK). All results were the mean of at least duplicate injections. The columns used were Inertsil ODS 5 μm, 25 × 0.46 cm I.D. (GL Sciences, Tokyo, Japan) with 14% carbon loading. All analyses were performed at 20°C. Buffers were prepared by dissolving the appropriate quantity of KH_2PO_4 in pure water, and adjusting the pH with KOH solution of the same molar concentration, in order to maintain $[K^+]$ constant. The pH of the buffer was measured before addition of the organic modifier; this avoids difficulties inherent in the measurement of the pH of organic solvent–water mixtures, but does not allow calculation of aqueous–organic pK_a values. Uracil was used as a column void-volume marker for calculation of k'. All pyridine derivatives for HPLC analysis (from Sigma-Aldrich, Poole, UK) were made up at a concentration of 100 mg l^{-1} in the relevant mobile phase. For UV work, approximately 10 mg l^{-1} phosphate solutions of the compounds were utilised, prepared as above.

3. Results and discussion

Previously, we showed that chromatography of pyridine and some alkyl-substituted derivatives can be performed reproducibly on Inertsil ODS using methanol–water (55:45, v/v) without buffers or additives; the compounds are largely unprotonated in this mobile phase [3]. Nevertheless, unbuffered mobile phases can lead to variable ionisation due to concentration effects within the peak, leading to asymmetry [1]; indeed, we found that some derivatives gave very asymmetric peaks in unbuffered acetonitrile–water or THF–water mixtures isoeluotropic with the methanolic mobile phase. Furthermore, unbuffered mobile phases seemed to require long equilibration times and give less reproducible N and A_s values for some analyte/mobile phase combinations. Thus, we performed the study using the three solvents in combination with a pH 7.0 phosphate buffer; in any case buffers are more likely to be used in practice for the analysis of basic compounds. Table 1 shows the effect of varying the nature of the organic modifier in buffered mobile phases, on performance of the same column. Approximately isoeluotropic eluent concentrations were determined empirically; the influence of extra column band broadening should be similar for peaks of similar k'. The overall $[K^+]$ was maintained at 0.0225 M in each experiment in an attempt to maintain competetive ion-exchange interactions of the buffer constant. To ensure that no deterioration of the column took place during the study, the first results obtained were reproduced at the end of the work. Table 1 shows that stereochemical effects noted previously for the derivatives using the methanolic phase are generally reproduced for acetonitrile and THF [3]; peak asymmetry tends to decrease with increasing size and proximity of groups substituted in the region of the basic centre. Differences between column performance for the different solvents appear to be strongly dependent on the nature of the probe compound, even for this related set. Some compounds show little difference (e.g. monosubstituted 2-derivatives) whereas others show major differences (e.g. monosubstituted 4-derivatives). The difference in the results for 2-substituted derivatives from those obtained on most of the columns studied previously [2] may be due to the relative inertness of the column used in the present study. The average A_s for all 16 derivatives using either methanol, acetonitrile or THF was 1.50 (R.S.D. 9.8%), 1.81 (R.S.D. 17.1%) and 1.43 (R.S.D. 8.8%), respectively. Similarly, the average N was 14 300 (R.S.D. 8.6%), 13 900 (R.S.D. 10.2%) and 14 100 (R.S.D. 5.0%). All of the individual compounds studied showed greater A_s in the mobile phase modified with acetonitrile than in those modified with methanol or THF. Acetonitrile also gave a wider range of

Table 1
Effect of organic modifier on column performance data for pyridine and alkyl substituted pyridines

Compound	pK_a (water at 25°C)[a]	k'	N	A_s
Pyridine	5.17	0.59[b]	11 400	1.69
		0.45[c]	11 900	1.78
		0.40[d]	13 200	1.55
2-Methylpyridine	5.96	1.09	14 000	1.45
		0.73	14 000	1.54
		0.74	13 800	1.46
3-Methylpyridine	5.68	1.26	13 100	1.57
		0.96	12 900	1.82
		0.97	13 800	1.61
4-Methylpyridine	6.00	1.23	12 700	1.73
		0.93	11 600	2.12
		0.86	13 400	1.60
2-Ethylpyridine	5.89	2.02	15 300	1.32
		1.69	15 900	1.44
		1.89	15 400	1.32
3-Ethylpyridine	5.80	2.42	14 400	1.53
		1.93	14 100	1.78
		2.30	14 900	1.45
4-Ethylpyridine	5.87	2.53	14 000	1.65
		2.06	12 900	2.31
		2.15	14 500	1.45
2,3-Dimethylpyridine	6.57	2.10	14 700	1.36
		1.35	14 700	1.55
		1.48	14 000	1.46
2,4-Dimethylpyridine	6.74	2.29	14 500	1.46
		1.37	13 900	1.70
		1.53	13 300	1.49
2,6-Dimethylpyridine	6.71	1.98	14 800	1.37
		1.10	14 700	1.55
		1.31	13 600	1.46
3,4-Dimethylpyridine	6.47	2.28	13 300	1.72
		1.60	12 300	2.23
		1.60	13 500	1.51
3,5-Dimethylpyridine	6.09	2.70	14 200	1.55
		1.83	13 900	1.86
		2.21	13 800	1.49
2-Propylpyridine	6.30	3.98	16 200	1.26
		2.87	16 700	1.34
		4.57	15 200	1.25

Table 1. *Continued.*

Compound	pK_a (water at 25°C)[a]	k'	N	A_s
4-Isopropylpyridine	6.02	4.66	14 800	1.50
		3.61	13 400	2.14
		4.59	15 000	1.30
3-Butylpyridine	–[e]	10.75	15 900	1.35
		7.86	15 500	1.60
		13.71	14 200	1.19
4-*tert.*-Butyl pyridine	5.99	7.83	15 300	1.45
		5.80	14 500	2.23
		8.85	14 500	1.27

[a] All pK_a values from Ref. [9] except 2,3-DMP, Ref. [5].
[b] Methanol–phosphate buffer (0.05 *M*) pH 7.0 (55:45, v/v).
[c] Acetonitrile–phosphate buffer (0.0375 *M*) pH 7.0 (40:60, v/v).
[d] THF–phosphate buffer (0.03 *M*) pH 7.0 (25:75, v/v).
[e] Value not available. For comparison purposes, benzene gave $N = 17\,000$ with $A_s = 1.22$ with this column using methanol–water (55:45, v/v).
Flow-rate 1 cm^3 min^{-1}; column Inertsil ODS batch "a"; detector UV at 254 nm. For other conditions, see Experimental.

values for the compounds (shown by the increased R.S.D.). Overall, methanol and THF gave much more similar results.

The differences in column performance for the individual solvents could be due to the different hydrogen bonding abilities of the modifier as noted by Claessens et al. [2]; however, this explanation does not fully account for our results. We believed that different degrees of protonation of the analytes in the different mobile phases could be a contributing factor; protonated analytes can participate in ion-exchange interactions with ionised surface silanols. We monitored the protonation of 2,4-dimethylpyridine (2,4-DMP) and pyridine (highest and lowest pK_a) in acetonitrile–buffer and THF–buffer using a UV method employed previously [3], which is based on the increased absorptivity of the protonated species (see Fig. 1). The approximate pH of the aqueous buffer (measured prior to mixing with organic solvent), which when combined with modifier leads to half protonation of pyridine was 3.2, 3.9 and 4.1 for buffered isoeluotropic methanol, acetonitrile and THF mixtures, respectively; methanol results are calculated from previous data [3]. The corresponding approximate values for 2,4-DMP are 4.6, 5.0 and 5.5, respectively. It should be noted that these are not aqueous–organic pK_a values (see Experimental). The variation in values for the different modifiers may be at least partially due to their appreciably different concentrations in the isoeluotropic mixtures and differing influence on the ionisation of the buffer used. At aqueous pH of 7.0 prior to combination with THF, 2,4-DMP appears to be very slightly protonated, although not measurably protonated in the other two mobile phases. Furthermore, the highest pK_a derivatives 2,4- and 2,6-DMP give slightly increased tailing using THF instead of methanol, in contrast with the average results reported above, although the increases seem hardly significant. We substituted a pH 6.0 buffer for the pH 7.0 buffer in the THF mobile phase. Fig. 1 shows 2,4-DMP to be substantially protonated at this lower pH in combination with THF and the derivative shows greater protonation than in isoeluotropic methanol or acetonitrile mixtures. The k' values for 2,4-and 2,6-DMP fell by ca. 25%, presumably due to decreased interaction with the ODS ligands, whereas low pK_a compounds (e.g. pyridine) showed little change in k'. However, we were unable to detect significant changes in A_s for any of the analytes. A

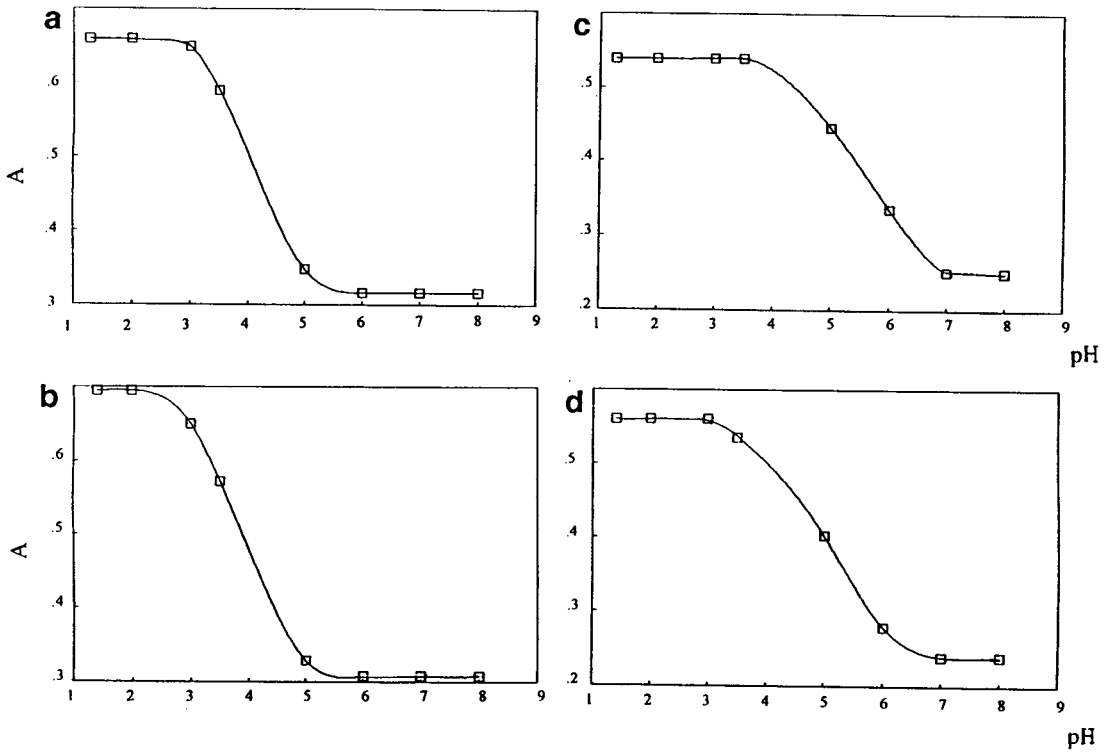

Fig. 1. Plot of UV absorbance at 255 nm (a, b), and 259 nm (c, d) against pH. (a) Pyridine in THF–phosphate buffer (25:75, v/v); (b) pyridine in acetonitrile–phosphate buffer (40:60, v/v); (c) 2,4-dimethylpyridine in THF–phosphate buffer (25:75, v/v); (d) 2,4-dimethylpyridine in acetonitrile–phosphate buffer (40:60, v/v).

difficulty in such investigations is the concurrent change in ionisation of silanols, especially since the pH is in the region of their average pK_a. Furthermore, the competitive effect of buffer K^+ ions may reduce ion-exchange effects. This same factor may also reduce the influence of the relatively small pK_a differences in these analytes on peak tailing, emphasising stereochemical effects. The relative influence of compound stereochemistry and pK_a could vary from column to column, leading to changes in the relative asymmetry of the analytes. Other factors may contribute to the differences in A_s shown for individual compounds with the different modifiers. For instance, spectroscopic studies show distinctly different RP solvation characteristics of methanol–water compared with acetonitrile–water. Increased solvation of the bonded ligands in the latter mobile phase may allow greater penetration of components to the silanols [10].

Finally, we investigated the effect of organic solvent strength on peak shape for these compounds. Methanol was used due to its apparent suitability for chromatography of these compounds and the greater solubility of phosphate buffer in higher concentrations of this solvent. The overall phosphate buffer concentration of the mixture was maintained at 0.0225 *M* throughout the experiments which utilised 25–65% methanol and produced variations in k' of approximately an order of magnitude. For these experiments, we had to replace the column due to some deterioration after prolonged use. The second column, packed with a different batch of the same ODS material, showed improved N and A_s in absolute terms, however, values relative to pyridine are similar to those for the first column, and differences of similar magnitude are also shown in peak shape for the neutral compound benzene. Fig. 2 shows a plot of log k' vs. volume

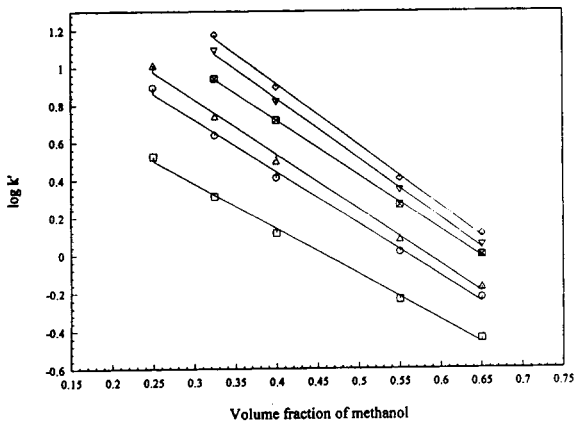

Fig. 2. Plot of log k' against volume fraction of methanol. Column Inertsil ODS batch "b"; detector UV at 254 nm. (□) pyridine, (○) 2-methylpyridine, (△) 3-methylpyridine, (⊠) 2,6-dimethylpyridine, (▽) 3,4-dimethylpyridine, (◇) 3,5-dimethyl pyridine. For composition of mobile phases, see Table 2. For other conditions see Table 1.

fraction of organic solvent in the mobile phase for some of the compounds. The plots are generally linear over the range 25–65% methanol which is fairly typical for RP systems, although not usual for basic compounds, whose plots often give severe curvature [11]. Presumably, the column used was sufficiently inert towards these compounds to give this behaviour without the use of amine additives such as triethylamine. Measurements of k' and corresponding N and A_s are shown in Table 2. Some compounds (e.g. 4-methylpyridine) gave considerable tailing at high k' values. This lends weight to our decision not to use probe compounds giving greater detrimental interaction, which could have prevented observation of any trends by giving extreme tailing under these non-optimum conditions. For all compounds, A_s increases as k' increases. However, A_s of some compounds hardly varies with k' over the ranges studied (e.g. 2-propylpyridine); others show considerable variation (e.g. 4-methylpyridine). These results may merely be a reflection of the relative degree of detrimental interaction of the compound with the column, as influenced by stereochemical and pK_a effects. Fig. 3 shows selected plots of A_s vs. k'; they are approximately linear but have very different slope. N values reflect the trends in A_s values, although some peaks are not sufficiently asymmetric to affect N calculated using the half-height method. The effects of instrumental dead volume are noticeable in reduced N for some peaks with low k'. The variation of A_s with k' can be attributed to overloading of the silanols by the retained basic solutes as discussed by Snyder and co-workers [1,12]. At very low sample concentrations, these sites may preferentially interact with sample molecules but are not overloaded, whereas for more practical sample concentrations, they become saturated. At high k', a greater fraction of the sample band is present in the stationary phase to overload these sites. Our previous monitoring of A_s using injection of 0.05–3.5 μg pyridine with the same column with methanol–phosphate buffer pH 7.0 (55:45, v/v) gives direct evidence of such overloading effects [3]. Nevertheless, the increase in asymmetry with sample amount was somewhat less than that with increase in k' shown in Table 2. It is possible that other factors contribute, such as the decreased ionisation of both sample molecules and silanol groups in mobile phases containing high concentrations of modifier.

Our previous comparisons of A_s for pyridine derivatives were largely between compounds of very similar k' [3]. 4-Substitution with alkyl groups of increasing chain length gives substantial increase in k', and thus should give increased tailing, although the reverse is found for THF and methanolic mobile phases. It is possible that whole molecule stereochemical effects can explain the data [3]; these may be partially obscured by differences in k', since the factors have opposing influence. Use of Table 2 to compare A_s of compounds giving similar k' in different solvents poses conceptual difficulties, because changes in solvent composition lead to other changes (e.g. ligand solvation effects and ionisation effects) noted above.

4. Conclusions

Significant differences in peak shape were obtained for pyridine and alkyl-substituted de-

Table 2
Effect of solvent strength on column performance data for pyridine derivatives

Compound	Mobile phase composition														
	65:35			55:45			40:60			32.5:67.5			25:75		
	k'	N	A_s	k'	N	A_s	k'	N	A_s	k'	N	A_s	k'	N	A_s
Pyridine	0.36	12 600	1.37	0.58	12 500	1.47	1.30	11 700	1.62	2.05	10 900	1.90	3.35	10 800	2.11
2-Methylpyridine	0.59	13 900	1.24	1.03	14 500	1.24	2.57	14 600	1.28	4.33	14 600	1.47	7.79	14 800	1.77
3-Methylpyridine	0.67	13 400	1.35	1.21	13 400	1.42	3.16	12 900	1.53	5.48	12 400	1.87	10.3	12 200	2.34
4-Methylpyridine	0.66	12 600	1.40	1.19	12 700	1.60	3.07	11 900	1.90	5.30	11 200	2.42	9.95	10 900	3.26
2-Ethylpyridine	0.97	14 500	1.15	1.80	15 200	1.14	5.29	15 800	1.16	–[a]	–[a]				
3-Ethylpyridine	1.15	14 300	1.26	2.20	14 000	1.37	6.99	14 200	1.49	–[a]	–[a]				
4-Ethylpyridine	1.18	13 800	1.31	2.27	13 900	1.49	7.16	13 600	1.73	–[a]	–[a]				
2,3-Dimethylpyr.	1.05	16 400	1.19	1.93	14 100	1.19	5.72	13 700	1.31	–[a]	–[a]				
2,4-Dimethylpyr.	1.13	14 100	1.20	2.17	14 400	1.31	6.25	14 500	1.47	11.4	14 200	1.84	–[a]		
2,6-Dimethylpyr.	0.99	14 600	1.15	1.83	14 800	1.19	5.19	15 400	1.23	8.70	15 500	1.42	–[a]		
3,4-Dimethylpyr.	1.11	13 200	1.41	2.20	13 700	1.67	6.51	12 700	2.07	12.3	11 900	2.77	–[a]		
3,5-Dimethylpyr.	1.28	14 100	1.32	2.54	14 000	1.49	7.82	14 400	1.75	15.0	14 000	2.19	–[a]		
2-Propylpyr.	1.67	14 900	1.09	3.47	15 300	1.11	12.1	15 800	1.14	–[a]	–[a]				
4-Isopropylpyr.	1.92	14 000	1.25	4.10	14 400	1.37	15.3	14 600	1.59	–[a]	–[a]				
3-Butylpyr.	3.76	15 000	1.12	9.26	15 900	1.23	–[a]	–[a]	–[a]						
4-*tert.*-Butylpyr.	2.91	13 700	1.20	6.81	14 500	1.34	–[a]	–[a]	–[a]						

Variation of k', N and A_s with solvent strength using Inertsil ODS column. 65:35 = methanol–0.064 *M* phosphate buffer pH 7.0 (65:35, v/v); 55:45 = methanol–0.05 *M* phosphate buffer pH 7.0 (55:45, v/v); 40:60 = methanol–0.0375 *M* phosphate buffer pH 7.0 (40:60, v/v); 32.5:67.5 = methanol–0.033 *M* phosphate buffer pH 7.0 (32.5:67.5, v/v); 25:75 = methanol–0.030 *M* phosphate buffer pH 7.0 (25:75, v/v). For comparison purposes, benzene gave $N = 19\,200$ with $A_s = 1.03$ using methanol–water (55:45, v/v). Column Inertsil ODS batch "b". Other conditions as in Table 1.

[a] Data not obtained due to long retention time.

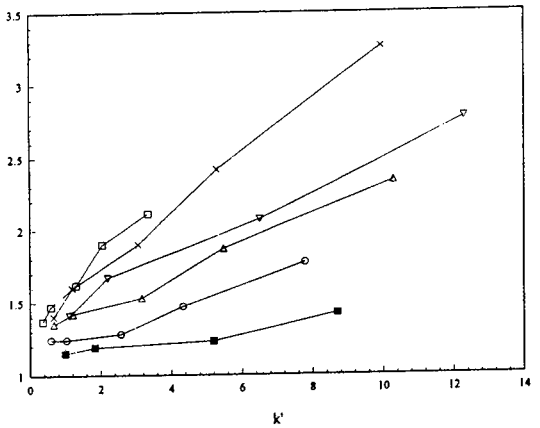

Fig. 3. Plot of A_s against k'. (×) 4-Methyl pyridine; for other symbols see Fig 2. Column Inertsil ODS batch "b". For other conditions see Table 1.

rivatives when using a silica-based RP column, depending on the choice of organic modifier in mobile phases buffered at a pH near the upper limit of such columns. However, the magnitude of these differences varies considerably with the analyte, even within the related set of compounds studied. Differences in protonation of the individual compounds in the different mobile phases were studied as a possible influential factor in explaining the differences in peak shape. However, it appears that the situation is complex, with several possible contributing effects. For the Inertsil ODS column used, mobile phases modified with acetonitrile gave significantly worse results than those modified with methanol or THF; this finding was in general agreement to that in a previous study [2]. Nevertheless, our work in progress indicates that the optimum choice of modifier may depend both on the nature of the analyte and the particular ODS phase utilised. All of these results indicate that the modifier is a neglected but important factor in the optimisation of the chromatography of basic compounds.

Steric hindrance around the basic nitrogen atom of the analyte reduces the influence of silanol effects [12]; this effect can explain why 2-substituted pyridines gave less tailing than 3- or 4-substituted derivatives of similar pK_a with each of the modifiers used. Tailing appears to decrease with increasing size and proximity of groups substituted near the basic centre.

Peak tailing increases for a particular analyte as k' increases with decreasing methanol concentration. The magnitude of this increase depends on the analyte. Steric effects may again explain why 2-derivatives, especially when substituted with larger alkyl groups, show little tailing even at high k' on the relatively inert column utilised in this study. Increased tailing of other analytes may be explained partially in terms of the increased overloading of silanol groups as k' increases; however, it is likely that other factors contribute to this effect.

It should be emphasised that these results were obtained using a single column with a rather narrow range of solutes. More work is necessary using different columns and solutes of entirely different structure, at high and low pH before deciding if any more general conclusions can be drawn.

Acknowledgements

The author thanks M. Norman, University of the West of England, for assistance with the preparation of Figures, GL Sciences for the gift of HPLC columns and Glaxo Research and Development (Ware, UK) for donation of the data station.

References

[1] L.R. Snyder and J.J. Kirkland, Introduction to Modern Liquid Chromatography, 2nd ed., Wiley, New York, 1979.
[2] H.A. Claessens, E.A. Vermeer and C.A. Cramers, LC·GC Int., 6 (1993) 692.
[3] D.V. McCalley, J. Chromatogr. A, 664 (1994) 139.
[4] D.V. McCalley, J. Chromatogr., 636 (1993) 213.
[5] R.C. Weast (Editor), CRC handbook of Chemistry and Physics, CRC Press, Boca Raton, FL, 1st student ed., 1988.
[6] A. Labudzinska and K. Gorczynska, Analyst, 119 (1994) 1195.
[7] R.J. Vervoort, M.W. Derksen and F. Maris, J. Chromatogr. A, 678 (1994) 1.

[8] R.J. Vervoort, F.A. Maris and H. Hindriks, J. Chromatogr., 623 (1992) 207.
[9] J.A. Dean (Editor), Lange's Handbook of Chemistry, McGraw Hill, New York, 13th ed., 1985.
[10] D.M. Bliesner and K.B. Sentell, Anal. Chem., 65 (1993) 1819.
[11] K. Valko, L.R. Snyder and J.L. Glajch, J. Chromatogr. A, 656 (1993) 501.
[12] D. Chan Leach, M.A. Stadalius, J.S. Berus and L.R. Snyder, LC·GC Int., 1 (1988) 22.

ELSEVIER

Journal of Chromatography A, 708 (1995) 195–201

JOURNAL OF CHROMATOGRAPHY A

Study on how mobile phase buffer composition effects the retention behavior of the system peak in non-suppressed ion chromatography

Masayuki Nishimura[a,*], Morimasa Hayashi[a], Atsushi Yamamoto[b], Tatsuji Horikawa[c], Kazuichi Hayakawa[d], Motoichi Miyazaki[d]

[a]*Analytical Applications Department, Shimadzu Corporation, 1 Nishinokyo-kuwabara-cho, Nakagyo-ku, Kyoto 604, Japan*
[b]*Toyama Institute of Health, 17-1, Nakataikoyama, Kosugi-machi, Toyama 939-03, Japan*
[c]*Technological University of Nagaoka, 1603-1, Kamitomioka, Nagaoka 940-21, Japan*
[d]*Faculty of Pharmaceutical Sciences, Kanazawa University, 13-1 Takara-machi, Kanazawa 920, Japan*

First received 17 January 1995; revised manuscript received 28 March 1995; accepted 28 March 1995

Abstract

The effect of mobile phase buffering on the retention behaviour of a system peak in non-suppressed ion chromatography was studied. When a weak base whose pK_a was near to the pH of the mobile phase was added to the mobile phase as a counter ion, the retention of the system peak selectivity shortened while the retention times of the analyte anions did not change. The cause of this phenomenon was thought to be an effect of mobile phase buffering induced by a weak base. Quantitative interpretation was successfully carried out to control the retention time of the system peak. The results allow the separation of analyte anions and control of the retention time of the system peak to be done independently. This method makes it possible to increase the variety of mobile phase compositions in the ion chromatography of anions.

1. Introduction

From the beginning of the history of non-suppressed ion chromatographic analysis of anions [1], an obviously retained vacant peak, the so-called "system peak", has often been observed when an organic acid ion is used as the eluting ion. In a practical sense, the appearance of a system peak has both merits and demerits. The greatest merit is making possible the detection of weakly retained species such as fluoride by narrowing the water dip peak. Trace levels of fluoride detected from a flat baseline by the high-volume injection method [2] provide a notable example. However, in general, the appearance of a system peak prolongs the interval possible between injections and is thus the greatest demerit in terms of throughput in routine analyses. Therefore, if it is possible to control the retention of the system peak so as to have it elute within an adequate period, high-performance separations can be consistent with shorter analytical periods.

The retention behaviour of the system peak has been widely studied [3–8] and it has been clarified that the hydrophobicity of the undissociated organic acid affects the retention of the system peak. Recently, we succeeded in predict-

* Corresponding author.

0021-9673/95/$09.50
SSDI 0021-9673(95)00406-8

ing the retention behaviour of a system peak by assuming a bi-Langmuir sorption isotherm model [5]. With this model, the capacity factor of a system peak (k'_e) had become predictable when the counter ions were a proton and/or a strong base ion.

On the other hand, it has been reported that k'_e selectivity decreased with the use of a weak base as a counter ion when the pK_a of the conjugate acid was near the pH of mobile phase [9], a linear relationship between pK_a and k'_e being observed. However, a quantitative interpretation had not yet been achieved. If the mechanism underlying the retention behaviour is understood quantitatively, it should become possible to control the retention time of a system peak with the added benefit of regaining the usefulness of a great variety of mobile phases which hitherto have been disregarded only by reason of the inadequate retention behaviour of the system peak in each instance.

The aim of this work was to clarify the mobile phase buffer effect on k'_e and to develop a theory which allows k'_e to be predicted under any mobile phase conditions. The control of k'_e in a two-base system, using strong and weak bases, is discussed.

2. Theory

When an n-basic organic acid (H_nA) is dissolved in pure water and the pH is adjusted with a monoacidic base (B) to prepare a mobile phase solution, the following simultaneous equations apply:

$$K_{ai} = [H^+]_m[H_{n-1}A^{i-}]_m/[H_{n-i+1}A^{(i-1)-}]_m \quad (i = 1 \text{ to } n)$$

$$K_{aB} = [H^+]_m[B]_m/[HB^+]_m$$

$$[H^+]_m + [HB^+]_m = \sum_{i=0}^{n} i[H_{n-i}A^{i-}]_m + [OH^-]_m$$

$$[t - H_nA]_m = \sum_{i=0}^{n} [H_{n-i}A^{i-}]_m$$

$$[t - B]_m = [B]_m + [HB^+]_m$$

where the subscript m represents the bracketed species in the mobile phase, K_{ai} represents the ith dissociation constant of H_nA, K_{aB} represents the K_a of the conjugate acid of B and $[t - H_nA]_m$ and $[t - B]_m$ represent the total concentrations of H_nA and B in the mobile phase, respectively. From the above equations, the concentration of an undissociated organic acid in the mobile phase ($[H_nA]_m$) can be represented by $[H^+]_m$, the K_a values and $[t - H_nA]_m$ as follows:

$$[H_nA]_m = \frac{[H^+]_m^n}{[H^+]_m^n + \sum_{i=1}^{n} [H^+]_m^{n-i} \prod_{j=1}^{i} K_{aj}} \cdot [t - H_nA]_m \quad (1)$$

In a system peak zone, $[t - H_nA]_m$ is different from that in the baseline zone. A decrease in $[t - H_nA]_m$ is generally the cause of a decrease in $[H^+]_m$ and $[H_nA]_m$. However, changes in $[H^+]_m$ are suppressed when the solution is strongly buffered, and so the change in $[H_nA]_m$ ($d[H_nA]_m$) becomes small for a given change in $[t - H_nA]_m$ ($d[t - H_nA]_m$).

According to a previous paper [5], the capacity factor of a system peak (k'_e) can be represented as follows:

$$k'_e = \frac{d[H_nA]_m K_d \phi}{\sum_{i=0}^{n} d[H_{n-i}A^{i-}]_m} = \frac{d[H_nA] K_d \phi}{d[t - H_nA]_m} \quad (2)$$

where K_d is the distribution coefficient of the undissociated acid and ϕ represents the phase ratio of the column.

Since K_d is constant while neither the pH of mobile phase nor $[t - H_nA]_m$ changes, k'_e is dependent only on $d[H_nA]_m/d[t - H_nA]_m$. As mentioned above, $d[H_nA]_m/d[t - H_nA]_m$ becomes small when the buffering action in the mobile phase is strong; hence it is obvious that k'_e also becomes small under such conditions. The buffering effect can be changed by selecting a base with a pK_{aB} near to the pH of the mobile phase. Using Eq. 2, it is possible to calculate k'_e if $K_d\phi$ is known. We selected phthalic and salicylic acids as organic acids in the mobile

phase to test the theory in actual analytical systems.

3. Experimental

3.1. Instrumentation and reagents

The ion chromatograph used was an LC-10A (Shimadzu, Kyoto, Japan), which consisted of an LC-10AD pump, a CTO-10A column oven, a CDD-6A electrical conductivity detector, a Rheodyne Model 7125 manual injector and a C-R7A data processor. Shim-pack IC-A1 (d_p = 10 μm, 100 mm × 4.6 mm I.D.) and Shim-pack IC-A3 (d_p = 5 μm, 150 mm × 4.6 mm I.D.) anion-exchange columns designed for ion chromatography (Shimadzu, Kyoto, Japan) were used as analytical columns. The base material of both columns was polymethacrylate resin; the surface of the IC-A3 column is more hydrophobic than that of the IC-A1 column. All reagents were of the highest available purity. Phthalic acid, salicyclic acid, tris(hydroxymethyl)aminomethane (Tris), γ-aminobutyric acid (GABA) and other weak bases containing zwitterions (Wako, Osaka, Japan) listed in Table 1 were used as received. Mobile phases were prepared by dissolving the appropriate reagents in purified water from a Toraypure water-purification system (Toray Industries, Tokyo, Japan).

3.2. Calculation of isotherm

The isotherm for phthalic acid on a Shim-pack IC-A1 column was determined using k'_e values measured for several mobile phase conditions which included proton and/or a strong base as counter ions. The experimental results were fitted to the function $[H_2A]_m$ according to the method established in Ref. [5].

3.3. Analytical conditions

Phthalic acid systems

Ten kinds of bases, as listed in Table 1, were each added to separation solutions of 2.5 m*M* phthalic acid to adjust the pH to 4.08 in each case. A Shim-pack IC-A1 column was employed as the analytical column. The flow rate was 1.5 ml/min and all flow lines including the detector cell were maintained at 40°C by the column oven. A 5-μl volume of pure water was injected for each different mobile phase composition and the retention time of the system peak (negative peak) was measured.

Table 1
pK_{aB} of the bases added to the mobile phase in the phthalic acid system

Base	pK_{aB}
Glycine	2.35
β-Alanine	3.60
γ-Aminobutyric acid (GABA)	4.20
ε-Aminocaproic acid	4.37
Aniline	4.60
Pyridine	5.22
p-Aminophenol	5.82
Bis-Tris[a]	6.55
Imidazole	7.20
Tris(hydroxymethyl)aminomethane	8.08

[a] Bis(2-hydroxyethyl)iminotris(hydroxymethyl)methane.

Salicyclic acid systems

A 5 m*M* salicyclic acid solution was prepared and divided into two equal portions. To one portion was added Tris to adjust the solution pH to 4.17 (solution A). The remaining portion was also adjusted to pH 4.17 by addition of GABA to give solution B. Aliquots of solutions A and B were then combined with stirring in the following ratios (v/v): A : B = 100 : 0, 87.5 : 12.5, 75 : 25, 50 : 50 and 0 : 100. Except for the analytical column (Shim-pack IC-A3) and flow-rate (1.2 ml/min), all other conditions were the same as those used for the phthalic acid systems described above.

4. Results and discussion

4.1. Phthalic acid systems

Because the pK_{a_1} and pK_{a_2} values of phthalic acid, H_2A, are known (pK_{a_1} = 2.9, pK_{a_2} = 5.2,

calculated from data given in Ref. [10]), $[H_2A]_m$ can be calculated for any phthalate-buffered mobile phase which includes a weak base B by solving Eq. 2. $K_d\phi$ was calculated using the bi-Langmuir isotherm equation evaluated previously, as follows:

$$\Gamma_{H_2A} = \frac{570[H_2A]_m}{1 + 30700[H_2A]_m} + \frac{14[H_2A]_m}{1 + 680[H_2A]_m} \quad (3)$$

where Γ_{H_2A} represents the total amount of H_2A adsorbed on the column. Fig. 1 represents the relationship between pK_{aB} and log k'_e. The solid line is the calculated interpolation and the closed squares are the experimental results. Good agreement between the calculated and experimental results confirms that k'_e directly reflects the buffering activity of the mobile phase and is predictable. Moreover, the observed phenomenon that the retention time of a system peak showed a minimum value when the mobile phase was buffered to around pH 5.2 [5,6] can be understood with our model, since the mobile phase buffering action became maximum at pH 5.2, i.e., at the pK_{a_2} of phthalic acid.

4.2. Salicylic acid systems

Salicyclic acid also has been widely employed as an organic acid in mobile phases. The high hydrophobicity of salicyclic acid makes it possible to elute analyte ions at low concentrations. This acid also provides good baseline stability with low background conductivity. Moreover, large peak areas can be obtained even under higher pH (>5) conditions because the acid is monobasic. In a salicyclic acid system, however, the retention time of the system peak is usually long so that the injection intervals are also long. Because of this, the use of salicyclic acid systems has been limited. The proposed technique should be effective in practice. In addition, prediction of k'_e will become easier in this system rather than the phthalic acid system since salicyclic acid is a fairly strong monobasic acid.

A two-base system, using strong and weak bases, was employed with regard to practical usage since it is easier to control the mobile phase buffer activity by changing the concentration of a selected weak base than by attempting to give an adequate base every time.

Using salicyclic acid and two bases, a strong

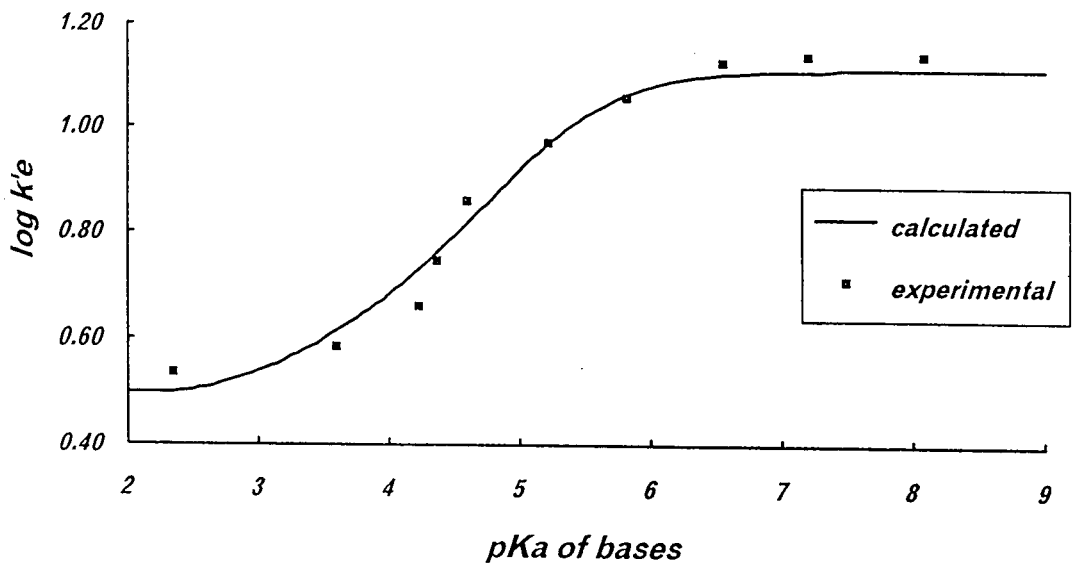

Fig. 1. Relationship between pK_a of a conjugate acid of the added base and the capacity factor of a system peak (k'_e). Solid line, calculated; squares, experimental results.

base, e.g., Tris; B1, and a weak base, e.g., GABA; B2, the equation of charge balance was obtained using known values as follows;

$$[H^+]_m + [t - B1]_m + \frac{[H^+]_m[t - B2]_m}{K_{aB2} + [H^+]_m} = \frac{K_a[t - HA]_m}{K_a + [H^+]_m} + \frac{K_w}{[H^+]_m} \quad (4)$$

where K_w is the ionic product of water, but was neglected because the mobile phase used was acidic. Eq. 4 was rewritten with $[H^+]_m$ as a cubic equation. However, the term in $[H^+]_m^3$ was neglected as the pK_a of salicylic acid (2.98 [11]) is more than ten times larger than $[H^+]_m$. The equation was therefore solved directly using a quadratic equation. In this study, we calculated $K_d\phi$ for conditions at which the concentration of salicyclic acid was known and the pH was adjusted to desired value with only B1. In this case, because [t − B2]m was equal to zero, Eq. 4 was rewritten as a quadratic equation for $[H^+]_m$, and so $[H^+]_m$ was strictly calculated. Moreover, $d[HA]_m/d[t - HA]_m$ could be directly calculated to be 0.830 in this case also. Hence $K_d\phi$ was calculated to be 35.1 with $d[HA]_m/d[t - HA]_m$ and the experimental k'_e (29.2) using Eq. 1.

The k'_e value was then predicted for a two-base system. For this purpose, $d[HA]_m/d[t - HA]_m$ should be solved strictly. First, a new function, $f([H^+]_m)$, is introduced as follows:

$$f([H^+]_m) = \frac{[H^+]_m}{[H^+]_m + K_a}$$

Then $[HA]_m$ is expressed as follows:

$$[HA]_m = f([H^+]_m)[t - HA]_m$$

with this technique, $d[HA]_m/d[t - HA]_m$ can be calculated directly as follows:

$$\frac{d[HA]_m}{d[t - HA]_m} = \frac{df([H^+]_m)}{d[H^+]_m} \cdot \frac{d[H^+]_m}{d[t - HA]_m} \cdot [t - HA]_m + f([H^+]_m) \quad (5)$$

in Eq. 5, $d[H^+]_m/d[t - HA]_m$ is easily calculated because $[H^+]_m$ can be represented as a function of $[t - HA]_m$. With Eq. 5 and the previously obtained $K_d\phi$ value, k'_e for any ratio of B1 and B2 was calculated.

Fig. 2 shows the relationship between the concentration of GABA and k'_e. It is obvious that calculated k'_e (solid line) agreed with the

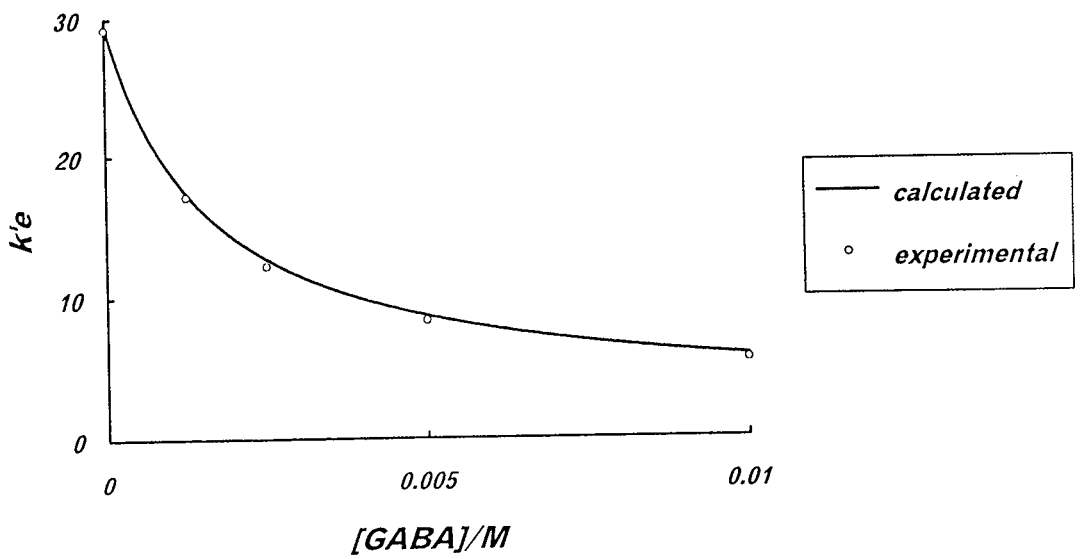

Fig. 2. Relationship between the concentration of GABA and k'_e.

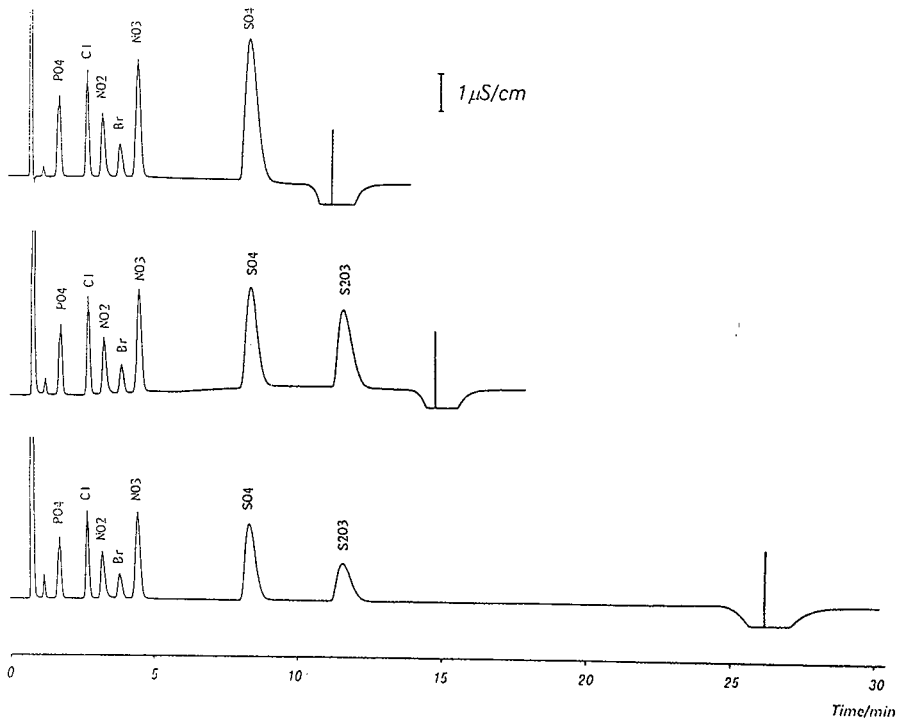

Fig. 3. Comparison of chromatograms obtained under the following conditions: mobile phase, 2 m*M* salicyclic acid (pH 4.0) containing Tris and/or GABA (see text); column, Shim-pack IC-A3; flow-rate, 1.5 ml/min; temperature, 40°C; detection, conductivity; injection volume, 10 μl. The injected samples contained the following anions: PO_4^{3-} 50, Cl^- 10, NO_2^- 12, Br^- 10, NO_3^- 30, SO_4^{2-} 40 and $S_2O_3^{2-}$ 50 mg/l.

experimental k'_e (open circles) very well over the range between 0 and 10 m*M* of GABA added. In this case, it was possible to control k'_e freely from 5 to 30.

Quantitative interpretation of the last aspect of the retention behaviour of a system peak was successfully performed. Especially the use of the salicyclic acid system led to very easy calculations and extended the controllable range of k'_e. Using these results, optimization of the separation of analyte ions and control of k'_e were investigated independently. Fig. 3 presents typical examples of the utility of the present method. The three chromatograms were obtained with mobile phases in which 2 m*M* salicyclic acid was included and the pH values were adjusted to 4.0 with Tris and/or GABA. In the bottom chromatogram, 1.6 m*M* Tris was added to adjust the pH of the mobile phase. Under the conditions applied, k'_e was as large as 28.1. The top chromatogram was obtained with a mobile phase in which 3.0 m*M* GABA was employed as the only base. k'_e was so small that the determination of thiosulfate ($S_2O_3^{2-}$) was impossible owing to interference from the system peak. In the middle chromatogram, 0.8 m*M* Tris and 1.5 m*M* GABA were added to the mobile phase and k'_e was adequate under these conditions. On the chromatograms, the predicted retention times of the system peaks are masked with solid vertical lines. These results indicated that an improvement in ease of use and an extension of the limits of ion chromatography can be realized with the present method.

References

[1] D.T. Gjerde, J.S. Fritz and G. Schmuckler, J. Chromatogr., 186 (1979) 509.

[2] M. Nishimura, M. Hayashi, K. Kayakawa and M. Miyazaki, Anal. Sci., 10 (1994) 321.
[3] A. Yamamoto, A. Matsunaga, M. Ohto, E. Mizukami, K. Hayakawa and M. Miyazaki, J. Chromatogr., 482 (1989) 145.
[4] A. Yamamoto, K. Hayakawa, A. Matsunaga, M. Ohto, E. Mizukami and M. Miyazaki, J. Chromatogr., 627 (1992) 17.
[5] A. Yamamoto, A. Matsunaga, E. Mizukami, K. Hayakawa and M. Miyazaki, J. Chromatogr., 644 (1993) 183.
[6] P.E. Jackson and P.R. Haddad, J. Chromatogr., 346 (1985) 125.
[7] J. Stahlberg and M. Almgrem, Anal. Chem., 61 (1989) 1109.
[8] H. Sato, Anal. Chem., 62 (1990) 1567.
[9] N. Hamada and T. Yagi, Bunseki Kagaku, 39 (1990) 411.
[10] M. Yasuda, K. Yamasaki and H. Ohtaki, Bull. Chem. Soc. Jpn., 33 (1960) 1067.
[11] D.D. Perrin, Nature, 182 (1958) 741.

ELSEVIER

Journal of Chromatography A, 708 (1995) 203–208

JOURNAL OF CHROMATOGRAPHY A

Optimization of the determination of amino acids in parenteral solutions by high-performance liquid chromatography with precolumn derivatization using 9-fluorenylmethyl chloroformate

B. Carratù*, C. Boniglia, G. Bellomonte

Istituto Superiore di Sanità, Laboratorio Alimenti, Viale Regina Elena 299, 00161 Rome, Italy

First received 20 January 1995; revised manuscript received 28 March 1995; accepted 29 March 1995

Abstract

An automatic precolumn derivatization procedure is presented for the determination of amino acids in parenteral solutions by reversed-phase high-performance liquid chromatography. The fluorenylmethyl chloroformate was used as the reagent for derivatization. The optimum conditions for the derivatization reaction, separation and detection were investigated from reproducibility and linearity data. This method has the advantage of automatic precolumn derivatization, a shorter analysis time with optimum separation and high reproducibility of retention times and peak areas for all amino acids with both UV and fluorescence detection.

1. Introduction

Amino acids have traditionally been determined by methods based on ion-exchange chromatography followed by postcolumn derivatization with ninhydrin [1,2]. In recent years, the determination of amino acids using precolumn derivatization and reversed-phase high-performance liquid chromatography (RP-HPLC) separation of the derivatives has become widely accepted and recognized as a powerful method. It requires much shorter analysis time and yields greater sensitivity.

The most common reagents used for amino acid derivatization are *o*-phthalaldehyde (OPA), phenyl isothiocyanate (PITC), 1-dimethylamino-naphthalene-5-sulphonyl (dansyl) chloride and 9-fluorenylmethyl chloroformate (FMOC-Cl) [3–15]. FMOC-Cl has several advantages: it reacts very quickly with both primary and secondary amino acids under alkaline conditions in a buffered aqueous solution, the derivatives are fairly stable and either UV absorbance or fluorescence detection can be applied [16–27].

We report here a procedure for precolumn derivatization with FMOC-Cl and RP-HPLC that we have successfully used for the determination of amino acids in parenteral solutions approved by the Farmacopea Ufficiale Italiana. These aqueous solutions contain 3–19 synthetic L-amino acids (essential and non-essential) with concentrations ranging from 4% to 10%; in order to assess the procedure, we purposely prepared a 6% solution of eighteen L-amino

* Corresponding author.

0021-9673/95/$09.50
SSDI 0021-9673(95)00409-2

acids. The method of Pernigo et al. [28] was adapted and modified to optimize the separation of amino acids. Differences in detection between fluorescence and UV methods, reproducibility and linearity data are presented.

2. Experimental

2.1. Apparatus

The chromatographic system consisted of a Varian Model 9010 HPLC pump, a Perkin-Elmer Model 101 column thermostat (column temperature 32°C), a Varian Aminotag (5 μm) column (150 × 4.6 mm I.D.), a Varian Model 9090 autosampler with a 20-μl loop, a Perkin-Elmer Model LS-1 spectrofluorimeter (excitation at 265 nm, emission at 340 nm) and a Perkin-Elmer Model LC-95 UV detector (265 nm). The data were collected using a Hewlett–Packard Model 3396A integrator.

2.2. Materials

Boric acid, sodium hydroxide, acetonitrile, isopropyl alcohol, methyl alcohol, sodium acetate and glacial acetic acid were purchased from Carlo Erba, 9-fluorenylmethyl chloroformate from Fluka, tetrahydrofuran from BDH and 1-amino-amantadine and amino acids from Sigma.

2.3. Preparation of standard solutions

A 6% amino acid stock standard solution was prepared from each amino acid solution (stored at −30°C) and diluted in 0.5 *M* borate buffer (adjusted to pH 8 with 30% NaOH) to have the following composition (m*M*): isoleucine 3.68, leucine 5.71, lysine 3.28, phenylalanine 1.87, threonine 2.26, tryptophan 0.62, valine 4.30, histidine 2.0, methionine 1.45, arginine 4.43, glycine 3.25, serine 2.45, alanine 3.82, proline 3.86, tyrosine 0.24, taurine 0.16, glutamic acid 2.21 and aspartic acid 1.06.

Norvaline (20 m*M* in borate buffer) was used as an internal standard. All aqueous solutions were prepared with water purified with a Milli-Q water system (Millipore). Solvents were of HPLC grade and chemicals were of the highest purity available.

2.4. Derivatization procedure

A 50-μl volume of test solution and 50 μl of norvaline solution were added to 100 μl of borate buffer in glass sample vials. Subsequent steps followed the autosampler injector programme: 200 μl of FMOC-Cl reagent (30 m*M* in dry acetone) were added, the mixture was quickly shaken and the reaction was allowed to proceed for 10 min at room temperature.

Excess FMOC-Cl was destroyed by addition of 200 μl of 1-amino-amantadine solution (25 m*M* in methyl alcohol) and after 2 min the solution was ready to be injected for HPLC analysis.

2.5. Chromatographic separation

Separation of the FMOC-Cl amino acid derivatives was carried out using a binary gradient. Eluent A was acetonitrile–isopropyl alcohol (90:10) and eluent B was 50 m*M* sodium acetate buffer containing 4% tetrahydrofuran adjusted to pH 4.03 with glacial acetic acid.

The stop time was 75 min after injection; the flow-rate was constant at 1.5 ml/min. The gradient programme used is given in Table 1.

2.6. Quantitative analysis

Amino acid peaks were identified from reference relative retention times of the standard amino acid solution and by adding appropriate amounts of amino acids to the sample. The

Table 1
Eluent gradient programme

Step	Time (min)	A (%)	B (%)
0	15	20	80
1	25	25	75
2	10	30	70
3	10	40	60
4	10	50	50
5	15	80	20
6	5	100	0

external standard method was used for quantification.

The reproducibility of the retention times and peak areas was tested by a series of ten derivatizations of 46.65 m*M* standard solution. The linearity was established by triplicate determinations of five different concentrations of amino acids ranging from 9.36 to 46.65 m*M*.

3. Results and discussion

FMOC-Cl reacts with both primary and secondary amino acids to form highly fluorescent and stable derivatives; the derivatization agent is fluorescent itself and therefore it is essential to remove excess FMOC-Cl with an appropriate reagent. The present procedure uses 1-aminoadamantadine (ADAM) because it is stable and particularly soluble in the borate buffer so that the final volume of the solution is more reproducible [17,21,23]. Most workers have used pentane extraction to remove the excess of the reagent from the derivatized sample; this solvent has the advantage of concentrating the sample, but the transfer of acetone can cause the undesirable extraction of non-polar amino acids [8,17,19].

Further critical aspects of the derivatization procedure are the concentration of the FMOC-Cl solution and the reaction time. To study the effect of these factors on the formation of amino acid derivatives, the reproducibility was determined by a series of ten derivatizations of 46.65 m*M* standard solution with 30 and 15 m*M* FMOC-Cl with reaction times of 3 and 10 min followed by UV and fluorescence detection. The standard solution tested can be considered to be equivalent to a parental solution because of the similar concentration and composition.

Table 2 shows the reproducibility of retention times and normalized peak areas for each amino acid. The results for normalized peak areas show that aspartic acid, glutamic acid and tyrosine

Table 2
Relative standard deviations (%) ($n = 10$) of retention times and peak areas

Amino acid	15 m*M* FMOC-Cl								30 m*M* FMOC-Cl							
	Retention time				Peak area				Retention time				Peak area			
	3 min		10 min		3 min		10 min		3 min		10 min		3 min		10 min	
	UV	FL	UV	FL	UV	FL	UV	FL	UV	FL	UV	FL	UV	FL	UV	FL
Arg	0.29	0.29	0.33	0.29	2.0	2.3	6.3	3.9	0.28	0.27	0.30	0.16	5.7	4.0	1.0	1.5
Tau	0.51	0.32	0.37	0.38	2.0	3.2	4.4	11.4	0.43	0.41	0.21	0.18	7.4	3.5	0.1	3.0
Ser	0.34	0.34	0.39	0.36	1.8	1.8	5.9	3.6	0.37	0.37	0.33	0.32	5.4	4.4	1.1	0.9
Asp	0.38	0.39	0.39	0.40	15.0	13.7	16.4	24.7	0.42	0.42	0.33	0.35	5.0	6.0	1.3	1.4
Glu	0.42	0.45	0.47	0.38	10.0	10.0	14.3	13.8	0.46	0.46	0.35	0.50	5.7	4.7	1.2	2.1
Thr	0.38	0.39	0.43	0.38	3.4	3.5	6.4	4.9	0.42	0.43	0.35	0.33	5.6	4.4	1.1	1.1
Gly	0.43	0.42	0.51	0.39	3.5	2.6	3.9	3.0	0.40	0.40	0.36	0.33	5.7	5.7	0.8	1.4
Pro	0.47	0.51	0.39	0.40	3.2	2.5	6.5	4.8	0.33	0.35	0.26	0.24	5.4	7.9	0.4	1.4
Ala	0.22	0.24	0.35	0.31	2.6	2.2	4.2	2.7	0.30	0.39	0.45	0.45	5.7	6.6	1.0	1.6
Met	0.18	0.18	0.27	0.22	1.8	2.2	4.9	2.6	0.28	0.23	0.22	0.22	5.7	4.1	0.9	1.3
Val	0.15	0.35	0.22	0.18	1.7	1.6	4.3	1.5	0.19	0.20	0.17	0.17	5.6	4.4	0.9	1.7
Phe	0.14	0.13	0.20	0.32	2.3	2.0	3.8	2.5	0.19	0.18	0.11	0.11	6.4	5.4	1.0	1.6
Trp	0.13	–	0.21	–	3.2	–	2.3	–	0.19	–	0.10	–	5.3	–	1.3	–
Ile	0.12	0.12	0.18	0.15	1.7	2.0	4.1	1.4	0.18	0.19	0.11	0.11	5.5	4.2	1.1	1.7
Leu	0.20	0.18	0.18	0.15	1.4	3.0	1.1	1.9	0.18	0.19	0.10	0.10	5.0	3.0	1.0	1.2
His	0.09	0.09	0.11	0.10	9.7	9.3	15.4	16.9	0.19	0.19	0.06	0.06	5.5	13.0	3.1	3.7
Lys	0.09	0.09	0.09	0.10	2.4	3.4	2.1	4.3	0.14	0.15	0.04	0.05	6.8	2.6	0.7	1.6
Tyr	–	–	–	–	–	–	–	–	0.10	0.10	0.02	0.02	9.7	4.7	1.2	2.2
Nor	0.15	0.13	0.21	0.23	1.8	5.2	4.1	1.9	0.19	0.25	0.15	0.21	3.3	1.0	2.0	1.3

Values for derivatization procedure carried out with 15 and 30 m*M* FMOC-Cl with reaction times of 3 and 10 min and with UV and fluorescence (FL) detection.

were the amino acids most sensitive to the reaction conditions. The relative standard deviations (R.S.D.) for aspartic acid and glutamic acid with FMOC-Cl 15 m*M* at reaction times of 3 and 10 min were elevated, whereas tyrosine was not detectable. When the concentration of FMOC-Cl was increased to 30 m*M* with a 3-min reaction time, tyrosine became detectable and the R.S.D. of aspartic acid and glutamic acid decreased to 6.0%, but worsened for the other amino acids.

To avoid carrying out two different analyses for the determination of all amino acids, the reaction time was extended to 10 min and the FMOC-Cl concentration was kept at 30 m*M*. Under these conditions, there was a clear improvement in the R.S.D., which ranged from 0.1 to 3.0% except for histidine (3.7%) because of its low relative fluorescence response [8,29].

The linearity of response was estimated by analysing five different amino acid solutions with total concentrations ranging from 9.36 to 46.65 m*M* obtained by serial dilution. Table 3 shows the correlation coefficients for the analyses carried out with 15 m*M* FMOC-Cl at 3 min and 30 m*M* FMOC-Cl at 10 min with both UV and fluorescence detection; these reaction conditions were selected on the basis of reproducibility data. A regression equation for each amino acid was constructed. Fig. 1 shows the calibration graphs for aspartic acid, glutamic acid and tyrosine under the two different reaction conditions.

In view of the good agreement between the reproducibility and linearity data of the analyses carried out with 30 m*M* FMOC-Cl and a 10-min reaction time, these conditions may be regarded as the most favourable. Fig. 2 shows the amino acid profile for a 46.65 m*M* standard solution.

The results obtained by fluorescence detection were similar to those with UV detection except for tryptophan, which was not detectable by fluorimetry because the fluorescence of the adduct is quenched [30].

Table 3
Correlation coefficients of the linearity test ($n = 3$)

Amino acid	15 m*M* FMOC-Cl, 3 min		30 m*M* FMOC-Cl, 10 min	
	UV	FL	UV	FL
Arg	0.9985	0.9976	0.9991	0.9989
Tau	0.9995	0.9988	0.9999	0.9996
Ser	0.9998	0.9993	0.9994	0.9992
Asp	0.9769	0.9840	0.9995	0.9993
Glu	0.9529	0.9700	0.9993	0.9997
Thr	0.9982	0.9953	0.9996	0.9998
Gly	0.9994	0.9999	0.9991	0.9989
Pro	0.9984	0.9913	0.9993	0.9989
Ala	0.9953	0.9886	0.9992	0.9997
Met	0.9991	0.9987	0.9900	0.9974
Val	0.9994	0.9981	0.9991	0.9990
Phe	0.9993	0.9994	0.9990	0.9983
Trp	0.9986	–	0.9989	–
Ile	0.9996	0.9995	0.9990	0.9990
Leu	0.9990	0.9924	0.9990	0.9990
His	0.9911	0.9860	0.9978	0.9964
Lys	0.9992	0.9983	0.9968	0.9958
Tyr	–	–	0.9999	0.9960

Values were calculated using five data points from amino acid solutions containing 9.36, 18.72, 28.07, 37.50 and 46.65 m*M* of total amino acids.

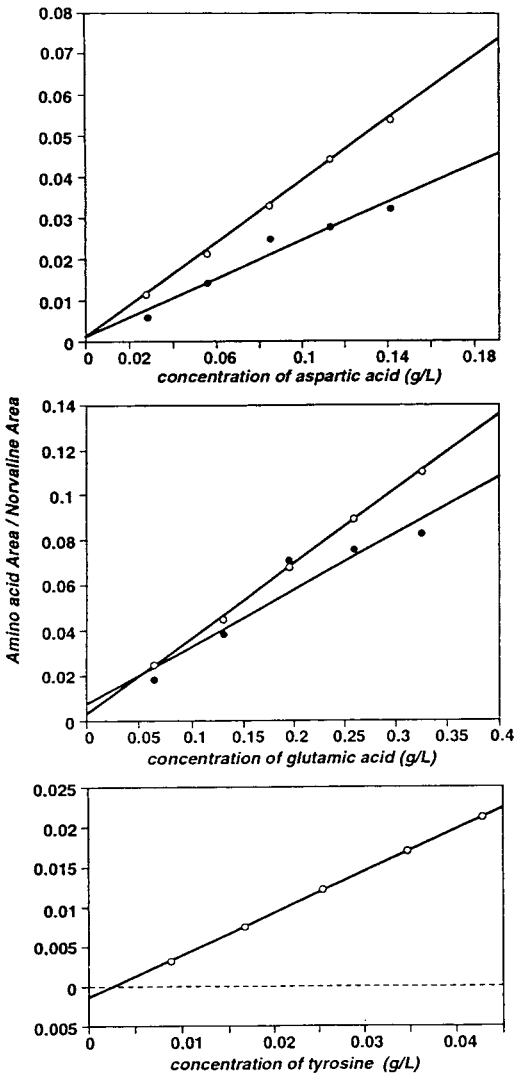

Fig. 1. Linearity for aspartic acid, glutamic acid and tyrosine (UV detection). ● = 15 m*M* FMOC with a 3-min reaction time; ○ = 30 m*M* FMOC with a 10-min reaction time.

The determination of free cystine is not practicable with this method; it is advisable to carry out a second run after oxidation to cysteic acid with performic acid [22,30].

4. Conclusion

The proposed method offers numerous advantages: easy sample preparation, room temperature for the derivatization reaction, high stability of derivatives, simultaneous determination of primary and secondary amino acids, good reproducibility and linearity for solutions over a wide range of concentrations. The analysis requires no specialized equipment other than standard HPLC equipment; to automate the derivatization procedure fully an autosampler is also needed.

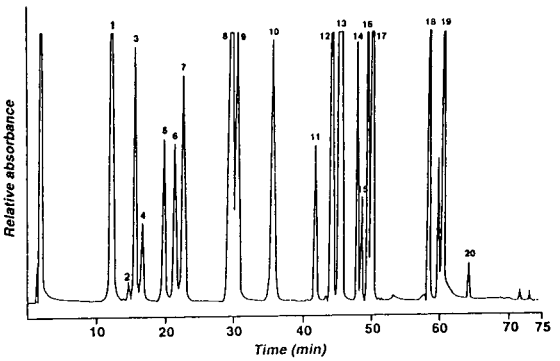

Fig. 2. Chromatogram of 46.65 m*M* amino acid standard solution derivatizated with 30 m*M* FMOC-Cl with a 10-min reaction time and with UV detection (265 nm). The analytical conditions are described in the text. Peaks: 1 = arginine; 2 = taurine; 3 = serine; 4 = aspartic acid; 5 = glutamic acid; 6 = threonine; 7 = glycine; 8 = FMOC-OH; 9 = proline; 10 = alanine; 11 = methionine; 12 = valine; 13 = norvaline; 14 = phenylalanine; 15 = tryptophan; 16 = isoleucine; 17 = leucine; 18 = histidine; 19 = lysine; 20 = tyrosine.

References

[1] D.H. Spackman, W.H. Stein and S. Moore, Anal. Chem., 30 (1958) 1190.
[2] B. Hamilton, Anal. Chem., 35 (1963) 2055.
[3] G.H.T. Wheler and J.T. Russell, J. Liq. Chromatogr., 4 (1981) 1281.
[4] S. Einarsson, S. Folestad, B. Josefsson and S. Lagerkrist, Anal. Chem., 58 (1986) 1638.
[5] S.A. Cohen and D.J. Strydom, Anal. Biochem., 174 (1988) 1.
[6] R. Schuster, J. Chromatogr., 431 (1988) 271.
[7] G. McClung and W.T. Frankenberger, Jr., J. Liq. Chromatogr., 11 (1988) 613.
[8] P. Fürst, L. Pollack, T.A. Graser, H. Godel and P. Stehle, J. Liq. Chromatogr., 12 (1989) 2733.
[9] D.T. Blankenship, M.A. Krivanek, B.L. Ackermann and A.D. Cardin, Anal. Biochem., 178 (1989) 227.

[10] M. Simmaco, D. De Biase, D. Barra and F. Bossa, J. Chromatogr., 504 (1990) 129.
[11] P. Fürst, L. Pollack, T.A. Graser, H. Godel and P. Stehle, J. Chromatogr., 499 (1990) 557.
[12] U. Bütikofer, D. Fuchs, J.O. Bosset and W. Gmür, Chromatographia, 31, No. 9–10 (1991) 44.
[13] P.A. Haynes, D. Sheumack, H. Kibby and J.W. Redmond, J. Chromatogr., 540 (1991) 177.
[14] R. Nathans and D.R. Gere, Anal. Biochem., 202 (1992) 262.
[15] Hua Liu and H.G. Worthen, J. Chromatogr., 579 (1992) 215.
[16] S. Einarsson, B. Josefsson and S. Lagerkrist, J. Chromatogr., 282 (1983) 609.
[17] I. Betnér and P. Földi, Chromatographia, 22, No. 7–12 (1986) 381.
[18] J.S. Niedbalski and D.P. Ringer, Anal. Biochem. 158 (1986) 138.
[19] T. Näsholm, G. Sandberg and A. Ericsson, J. Chromatogr., 396 (1987) 225.
[20] G.E. Kisby, D.N. Roy and P.S. Spencer, J. Neurosci. Methods, 26 (1988) 45.
[21] B. Gustavsson and I. Betnèr, J. Chromatogr., 507 (1990) 67.
[22] E.J. Miller, A.J. Narkates and M.A. Niemann, Anal. Biochem., 190 (1990) 92.
[23] M.F. Malmer and L.A. Schroeder, J. Chromatogr., 514 (1990) 227.
[24] A. Pecavar, A. Golc-Wondra, M. Prosek and E. Skocer, Vestn. Slov. Kem. Drus., 38 (1991) 183.
[25] P.A. Haynes, D. Sheumack, L.G. Greig, J. Kibby and J.W. Redmond, J. Chromatogr., 588 (1991) 107.
[26] H.G. Worthen and H. Liu, J. Liq. Chromatogr., 15 (1992) 3323.
[27] J. Kirschbaum, B. Luckas and W.D. Beinert, J. Chromatogr. A, 661 (1994) 193.
[28] N. Pernigo, D. Faccioli and L. Ravizza, Riv. Tossicol. Sper. Clin., 23 (1993) 1.
[29] G.G. Guilbault, Practical Fluorescence. Theory, Methods and Techniques, Marcel Dekker, New York, 1973, p. 307.
[30] A.F. Fell in J.M. Rattenbury (Editor), Amino Acid Analysis, Ellis Horwood, Chichester, 1981, p. 86.

ELSEVIER

Journal of Chromatography A, 708 (1995) 209–221

JOURNAL OF CHROMATOGRAPHY A

Evaluation of solid-phase extraction procedures in peptide analysis

Tomas Herraiz*, Vicente Casal

Instituto de Fermentaciones Industriales, CSIC, Juan de la Cierva 3, 28006 Madrid, Spain

First received 1 February 1995; revised manuscript received 20 March 1995; accepted 22 March 1995

Abstract

Solid-phase extraction (SPE) procedures for peptide isolation and fractionation, based on non-polar and ionic interactions, were evaluated using small synthetic peptides and casein enzymatic hydrolysates. SPE based on hydrophobic phases is a useful, efficient and rapid procedure for peptide extraction and concentration. It allows a successful peptide fractionation using eluents that contain an increasing content of acetonitrile in the presence of trifluoroacetic acid. Differences regarding selectivity are observed between sorbents. Non-polar interaction with C_{18} sorbents is adequate for the isolation of very polar and hydrophobic peptides. CN sorbents are only adequate for very hydrophobic peptides. PH, CH, C_8 and C_2 sorbents are useful for isolating and fractionating hydrophobic and very non-polar peptides, but generally not for very polar peptides. Ionic solid-phase extraction using Accell Plus cartridges of QMA (quaternary methylammonium) and CM (carboxymethyl) are very useful for the fractionation of peptide mixtures into basic, acidic and neutral pools of peptides. It can be concluded that SPE using these procedures is a useful tool for the isolation and fractionation of peptides from biological and food samples.

1. Introduction

Sample preparation columns based on the principles of solid-phase extraction (SPE) are fast becoming indispensable tools in many areas of research [1]. This technique provides a clean and concentrated extract that simplifies subsequent analysis by removing interfering or cross-reacting components. The use of SPE is growing rapidly because of the current availability of many bonded silica sorbents [2]. These materials make SPE an extremely selective and efficient technique when used before radioimmunoassays, HPLC, GC, MS, TLC or bioassay.

SPE has proved very useful for isolating peptides from biological tissues [3,4]. It appears also to be very promising technique for the extraction and preferential enrichment of peptides with an application to food samples [5–9]. Bennett [10] used octadecylsilica (ODS) cartridges followed by a sequence of a variety of RP-HPLC solvent systems for exploiting the hydrophobic, basic and acidic character of the peptides to be purified. ODS SPE columns have become an important tool in removing salt and polar materials following tissue homogenization, while preferentially enriching the oligopeptide fraction [11]. Higa and Desiderio [12] optimized the recovery of substance P and methionine-enkephalin synthetic peptides from an ODS dispos-

* Corresponding author.

0021-9673/95/$09.50
SSDI 0021-9673(95)00388-6

able cartridge. Optimization of SPE with C_{18} columns has also proved useful for the extraction of peptides from dairy samples [5]. Herraiz et al. [7] recently separated peptides by RP-HPLC following peptide isolation from skim milk using Sep-Pak C_{18} cartridges. Prefractionation of complex mixtures of peptides from cheese using SPE on ODS after gel filtration chromatography has also been reported as a useful technique for the further identification of peptides [8].

In addition to non-polar SPE cartridges, other silica-based ion-exchange Sep-Pak cartridges packed with either a carboxymethyl (CM) cation exchanger or a quaternary methylammonium (QMA) anion exchanger have already been successfully used for the fractionation of pituitary peptides into basic, neutral and acidic pools [13].

An adequate purification of biological samples with a low content of biologically active peptides requires the use of crude fractionation procedures preceding high-resolution RP-HPLC. In addition to the concentration effect obtained with the extraction process, the benefit of the prefractionation of peptides for selective chromatographic resolution has been reported [6]. Many types of bonded materials are currently available that may lead to different selectivities when applied to peptide extraction. Thus, owing to the increasing possibilities of SPE, new research is currently needed to investigate the behaviour of different available SPE sorbents in the isolation and fractionation of peptides. A systematic approach to the fractionation of peptides using SPE would be very useful, because of the heterogeneity of peptides in complex mixtures as biological and food samples. For obtaining a high recovery of a purified peptide, it is necessary to identify the most suitable bonded silica phase and elution conditions. In this regard, the possibility of non-specific irreversible adsorption altering the extraction should be considered [5].

The purpose of this work was to study the isolation and fractionation of synthetic peptides and peptides from casein enzymatic hydrolysates by using SPE with various types of bonded silica phases. This study may contribute to the development of systematic methods for the isolation and prefractionation of peptides in complex mixtures.

2. Experimental

2.1. Synthetic peptides and casein enzymatic hydrolysates

Glutathione, V-G-S-E, G-G-Y-R, K-W-K, P-F-G-K, V-H-L-T-P-V-E-K, (L,D)-L-G-(L,D)-F, W-W, D-R-V-Y-I-H-P-F-H-L-L-V-Y-S, F-L-E-E-V, F-L-E-E-I and F-L-E-E-L were obtained from Sigma (St. Louis MO. USA) and G-G-W-A from Serva (Heidelberg, Germany). Peptides were used without further purification and were selected to cover a range of different size, hydrophobicity (peptides with polar and non-polar amino acids), charge at the pH used (peptide with acidic and basic amino acids) and retention times in a C_{18} RP-HPLC column.

Complex mixtures of peptides were obtained from enzymatic hydrolysates from commercial α- and β-casein as follows: a 1.66 mg/ml concentration in 10 m*M* phosphate buffer (pH 8) of each casein (Sigma), used without further purification, was mixed with 0.5 mg of trypsin from porcine pancreas (Type II crude, Sigma) dissolved in the same buffer (approximate enzyme-to-substrate molar ratio = 1:110). Trypsin was not treated with L-1-tosylamide-2-phenylethyl chloromethyl ketone (TPCK) and has a significant residual activity of chymotrypsin. Proteolysis was carried out at 37°C in a water-bath for 5 h. The enzymatic hydrolysates obtained (30 ml) were acidified to pH 2 with trifluoroacetic acid (TFA) and stored at −20°C until further utilized for SPE. Then, portions (2 ml) were passed through the SPE columns at 1 ml/min. Solutions used as reaction controls were prepared independently with α- and β-casein, but without the addition of trypsin. In the same manner, controls were prepared but lacking the casein.

2.2. SPE disposable cartridges and columns

Disposable SPE columns containing 500 mg of sorbent (40 μm, 60 Å) with a column volume of

2.8 ml were obtained from Varian (Harbor City, CA, USA), containing the following sorbents: C_2(ethyl), C_8(octyl), C_{18}(octadecyl, 18% carbon loading), PH (phenyl), CH (cyclohexyl), CN (cyanopropyl, non-end-capped silica) and CBA (carboxylic acid). Sep-Pak Plus environmental C_{18} cartridges (820 mg of sorbent, 80 μm, 125 Å; 12% carbon loading) and Accell Plus QMA (quaternary methylammonium) and Accell Plus CM (carboxymethyl) ion-exchange Sep-Pak cartridges (360 mg of sorbent, 45 μm, 300 Å) were obtained from Waters (Milford, MA, USA).

CN, C_2, PH, CH, C_8, C_{18}, Sep-Pak Plus C_{18} columns and cartridges were conditioned prior to peptide loading by passing successively 2 ml of methanol (Scharlau, Barcelona, Spain), 2 ml of Milli-Q-purified water and 2 ml of a solution of 0.1% of protein sequencing grade TFA (Sigma) in water. The void volumes were ca. 0.6 ml for Varian SPE columns, 0.8 ml for CM and QMA cartridges and 1.6 ml for Sep-Pak Plus C_{18} cartridges. CBA columns were conditioned with 2 ml of methanol and subsequently with 2 ml of 10 m*M* ammonium acetate buffer (pH 5.5). CM and QMA cartridges were conditioned by passing 2 ml of Milli-Q-purified water and subsequently 2 ml of 10 m*M* ammonium acetate buffer (pH 5.5).

2.3. SPE procedures of synthetic peptides

SPE of synthetic peptides was studied using the following procedures:

(a) A reference sample was obtained by dissolving synthetic peptides in 0.1% of protein sequencing grade TFA (Sigma) in Milli-Q-purified water to provide a peptide concentration of 0.01–0.1 mg/ml. Portions of 2 ml of this solution were loaded and passed slowly (1 ml/min) in duplicate through the following disposable cartridges: C_2, C_8, C_{18}, CN, PH, CH and Sep-Pak environmental C_{18}. The peptide concentration used is adequate for further direct HPLC analysis, allowing an accurate measurement of peptide recovery after SPE. The amount applied did not overload the SPE columns. The unretained fraction was recovered from the outlet of the SPE columns. Then, retained peptides on the sorbent were washed with 2 ml of 0.1% TFA in water. Subsequently, peptides were eluted with fractions containing a stepwise gradient in acetonitrile (ACN) (Scharlau, Barcelona, Spain). Thus, fractions of 2 ml of 0.1% TFA in 20% ACN, 0.1% TFA in 50% ACN, 0.1% TFA in 80% ACN and finally 0.1% TFA in pure ACN were eluted in this order through the columns. Analyses of the recovered peptides present in the unretained, washing and eluting fractions were carried out by injecting 100 μl of every eluting fraction into the RP-HPLC system as indicated below. The recovery of peptides in every collected fraction was calculated by comparison with the peptide peak areas obtained from the sample reference itself that had been chromatographed prior to SPE.

(b) A second sample of synthetic peptides was obtained by dissolving peptides in acetonitrile–10 m*M* ammonium acetate buffer (pH 5.5) (20:80) to provide a peptide concentration of 0.01–0.1 mg/ml. Portions of 2 ml of this solution were eluted slowly (in duplicate) through the Accel QMA and Accell CM Sep-Pak disposable cartridges connected in series, with the CM connected ahead of the QMA cartridges as described previously [13]. The unretained fraction (2 ml) was recovered (first neutral fraction) and subsequently the cartridges were eluted with 2 ml of 10 m*M* ammonium acetate buffer (pH 5.5) containing 20% of acetonitrile (second neutral fraction). The CM and QMA cartridges were disconnected. Subsequently, portions of 4 ml of 10 m*M* ammonium acetate buffer (pH 5.5) containing 20% of acetonitrile plus 1 *M* sodium chloride were passed slowly through the CM cartridge to obtain the basic fraction and through the QMA cartridge to obtain the corresponding acidic fraction.

(c) Another sample of synthetic peptides was dissolved in 10 m*M* ammonium acetate buffer (pH 5.5) to provide a peptide concentration of 0.01–0.1 mg/ml. Portions of 2 ml of the solution of synthetic peptides dissolved in ammonium acetate buffer (pH 5.5) were loaded on to CBA columns (in duplicate). The unretained fraction was recovered (first fraction). Subsequently, the column was washed with 2 ml of ammonium acetate buffer (pH 5.5) (second fraction) and

elution was carried out with two portions of 2 ml of 0.1% TFA in 40% acetonitrile (third and fourth fractions).

RP-HPLC analyses of 100 μl of every collected fraction from the SPE sorbents (CBA, CM, QMA) were carried out to calculate the percentage recovery of each peptide, as indicated above.

2.4. SPE of peptides from enzymatic hydrolysates

Aliquots (2 ml, ca. 150 nmol) of the casein enzymatic hydrolysates were treated as mentioned above for synthetic peptides to achieve the fractionation of casein peptides in non-polar SPE. In ionic SPE, the enzymatic casein hydrolysates were previously lyophilized and dissolved in 2 ml of acetonitrile–10 m*M* ammonium acetate buffer (pH 5.5) (20:80) previously to start the SPE procedure.

2.5. Concentration, enrichment and fractionation of casein peptides by SPE

A narrower fractionation of peptides from casein hydrolysates was carried out following an increase from 10% to 40% of acetonitrile while increasing 5% of acetonitrile in each fraction. On the other hand, enrichment and concentration of peptides were carried out after diluting the enzymatic hydrolysate 50-fold, so that the volumes of 50 ml of that hydrolysate were eluted slowly (1 ml/min) using a peristaltic pump through the SPE column. The rest of the procedure for elution was as mentioned above.

2.6. RP-HPLC separation of peptides

Experimental work was performed in a Waters high-performance liquid chromatograph controlled with a Maxima 820 workstation (Waters, Milford, MA, USA). It was equipped with two M 6000A pumps, an M WISP 710B automatic sample injector and a variable-wavelength absorbance detector (M 481 L spectrophotometer).

Peptide analysis was carried out using a reversed-phase C_{18} Nova-Pak column (150 mm × 3.9 mm I.D.) (Waters). This column provides a good chromatographic separation of peptides [7]. The chromatographic conditions were as follows: eluent A, 0.1% TFA in water and eluent B, 0.1% TFA in acetonitrile; linear gradient from 0% B to 40% B in 70 min, then at 73 min 100% B and at 78 min 100% A (12 min); flow-rate, 1 ml/min; and absorbance detection at 214 nm. Synthetic peptide injections ranged from 2 to 20 nmol and were analysed at least in duplicate. The amount of peptide injected did not overload the HPLC column and the peak areas were measured using a Maxima 820 workstation.

3. Results and discussion

3.1. Isolation and preparative fractionation of peptides using non-polar SPE

The behaviour of preparative non-polar SPE of peptides was first studied with synthetic peptides loaded on to different commercial non-polar bonded silica disposable columns and cartridges. Fig. 1 shows the RP-HPLC of the solution of ten synthetic peptides used as reference for SPE. Peptides were separated with good resolution for an accurate measurement of peak areas. The average residual standard deviation (R.S.D.) for peak areas after five repetitive injections was less than 1.3%). Peptides loaded on to non-polar SPE units were recovered into six different fractions, i.e., the unretained fraction and the fractions corresponding to eluting the column with 0.1% of TFA in Milli-Q-purified water (washing fraction) and 0.1% of TFA in 20, 50, 80 and 100% of acetonitrile. SPE was carried out using TFA that provides an acidic pH and avoids any peptide ionic interaction with negatively charged silanols. TFA increases the peptide hydrophobicity because carboxylic groups are protonated whereas basic residues form ion pairs with TFA [10]. Table 1 shows the peptide recoveries for the different bonded silica columns. The total recovery of a given peptide in the fractions (given as the sum of the percentage

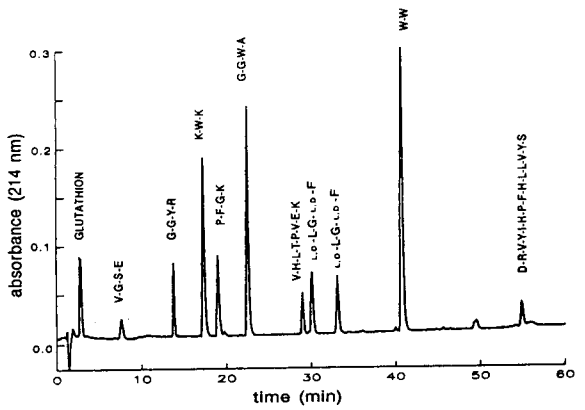

Fig. 1. RP-HPLC of a mixture of synthetic peptides dissolved in 0.1% TFA in water used for studying the selectivity and behaviour of the SPE columns and sorbents. Column, Nova-Pak C_{18} (150 × 3.9 mm I.D.), eluent A, 0.1% (v/v) TFA in water; eluent B, 0.1% (v/v) TFA in acetonitrile; linear gradient from 0 to 40% B in 70 min; flow-rate, 1 ml/min. Duplicate injections of 100 μl were made, using an autosampler. L,D-L-G-L,D-F separates in two diastereoisomeric peaks.

recovery obtained in each fraction) is generally high for most peptides and SPE columns.

Peptides fractionate well in non-polar SPE, depending on their relative polarity or hydrophobicity. Thus, more hydrophobic peptides such as L-G-F, W-W or D-R-V-Y-I-H-P-F-H-L-L-V-Y-S eluted with a higher percentage of acetonitrile, whereas more polar peptides such as glutathione, V-G-S-E or G-G-Y-R could either pass unretained through the SPE sorbent or be eluted in the washing fraction. All peptides elute from the SPE columns with 50% or less of acetonitrile, and no synthetic peptides were recovered with 80% or 100% of acetonitrile. Consequently, the last two fractions are not included in Table 1.

Regarding sorbent selectivity, the comparative study of data of peptide recovery in the eluting fractions exhibits a different retention behaviour between SPE sorbents. Under the experimental conditions employed, a higher hydrophobic interaction between a given peptide and the sorbent is expected to occur when a higher concentration of acetonitrile is needed to elute the peptide from the sorbent. Thus, Table 1 shows that the increasing order of peptide retention because of higher hydrophobic interaction with the sorbent is CN < C_2 < PH < CH < C_8 < C_{18} < Sep-Pak environmental C_{18}. The CN sorbent behaves as a polar sorbent and only allows the retention of more hydrophobic peptides such as W-W and D-R-V-Y-I-H-P-F-H-L-L-V-Y-S. C_2 and PH provide a low retention of the less hydrophobic peptides such as glutathione, V-G-S-E and G-G-Y-R. In contrast, CH, C_8, C_{18} and Sep-Pak C_{18} give a much better preparative isolation and fractionation of peptides. However, C_8 and CH do not retain the very polar peptides sufficiently. In contrast, Sep-Pak C_{18} retains most peptides and is the most suitable when a wide range of peptide polarity and heterogeneity occurs in a sample.

3.2. Isolation and preparative fractionation of casein hydrolysates using non-polar SPE

Further evaluation of peptide SPE was accomplished with a complex mixture of peptides arising from food proteins. Enzymatic hydrolysates of α and β-caseins are used for preparative fractionation and extraction of peptides with non-polar SPE disposable columns. Fig. 2 shows the RP-HPLC of the enzymatic hydrolysate obtained from α-casein. The chromatogram shows a higher number of peptides than those expected from a complete tryptic hydrolysate of α-S1-casein. The reason for this is the existence of an additional activity of chymotrypsin and the fact that bovine α-casein (Sigma) is not a single and pure genetic variant. Nevertheless, the complex mixture of casein peptides obtained is adequate for testing the SPE procedures. Peptides were isolated by SPE and further chromatographed by RP-HPLC, as reported above for synthetic peptides. Table 2 lists the ranges of peptide retention times and peptide recoveries obtained after analysis by RP-HPLC of the peptides isolated from each SPE column and eluting fraction. The peptide recovery in each column and fraction was obtained by comparing the chromatograms of the eluting fractions with the chromatogram of the complete enzymatic hydrolysate before peptide loading into the SPE

Table 1
Fractionation and recovery obtained from a mixture of synthetic peptides in CN, C_2, PH, CH, C_8, C_{18} and Sep-Pak Plus C_{18} column

Peptide	Recovery in the fractions[a] (%)											
	CN column				C_2 column				PH column			
	1	2	3	4	1	2	3	4	1	2	3	4
Glutathione	70	30	0	0	66	39	0	0	53	47	0	0
V-G-S-E	66	26	0	0	56	51	0	0	35	59	0	0
G-G-Y-R	65	32	0	0	18	57	0	0	3	71	22	0
K-W-K	61	32	0	0	16	42	5	0	6	68	18	0
P-F-G-K	66	35	0	0	0	68	22	0	0	0	94	0
G-G-W-A	44	52	0	0	0	12	82	0	0	0	93	0
V-H-L-T-P-V-E-K	55	33	10	0	0	7	72	0	0	0	92	0
L,D-L-G-L,D-F	42	57	2	0	0	0	86	9	0	0	36	71
L,D-L-G-L,D-F	35	58	3	0	0	0	60	13	0	0	20	73
W-W	0	6	86	2	0	0	0	99	0	0	0	100
D-R-V-Y-I-H-P-F-H-L-L-V-Y-S	0	0	58	39	0	0	0	72	0	0	0	108

	CH column				C_8 column				C_{18} column				Sep-Pak Plus C_{18}			
	1	2	3	4	1	2	3	4	1	2	3	4	1	2	3	4
Glutathione	41	58	0	0	33	68	0	0	25	76	0	0	0	7	92	0
V-G-S-E	0	83	0	0	0	33	18	0	0	0	15	0	0	0	85	0
G-G-Y-R	0	5	80	0	0	0	98	0	0	0	101	0	0	0	96	0
K-W-K	0	14	61	0	0	0	95	0	0	0	99	0	0	0	62	19
P-F-G-K	0	0	99	0	0	0	100	0	0	0	101	0	0	0	70	33
G-G-W-A	0	0	91	2	0	0	94	0	0	0	101	0	0	0	2	61
V-H-L-T-P-V-E-K	0	0	86	0	0	0	96	0	0	0	94	0	0	0	27	70
L,D-L-G-L,D-F	0	0	0	96	0	0	10	93	0	0	44	62	0	0	0	99
L,D-L-G-L,D-F	0	0	0	100	0	0	1	99	0	0	14	88	0	0	0	100
W-W	0	0	0	101	0	0	0	103	0	0	0	100	0	0	0	97
D-R-V-Y-I-H-P-F-H-L-L-V-Y-S	0	0	0	96	0	0	0	101	0	0	0	110	0	0	0	103

[a] Fractionation of peptides was carried out as described in the Experimental section. After loading the solution of peptides, four fractions were recovered: (1) unretained fraction; (2) 0.1% TFA in water (washing fraction; (3) 0.1% TFA in 20% acetonitrile; and (4) 0.1% TFA in 50% acetonitrile. Collection fractions of 0.1% TFA in 80% and 100% of acetonitrile did not recover any amount of peptide (result not shown). Data for recovery were obtained in duplicate.

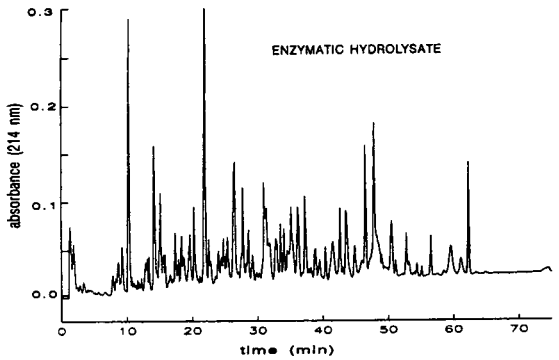

Fig. 2. RP-HPLC of the α-casein enzymatic hydrolysate (Trypsin II, Sigma) used for studying the selectivity and behaviour of the SPE columns and sorbents. Column and conditions as in Fig. 1.

column (Fig. 2). Although Table 2 only shows the results for α-casein, similar relative results were observed for β-casein. As before, peptides from casein distribute into the different SPE fractions, depending on their respective hydrophobicities. In this regard, SPE greatly simplifies peptide samples for further analysis. All peptides elute with 50% or less of acetonitrile, and the total recovery obtained is close to 100% for all columns (the sum of the recovery in each fraction is close to 100% for every column, i.e., the sum of peak areas in all the eluting fractions is equal to the total peak area of the hydrolysate before loading into the SPE column). Therefore, no irreversible adsorption of casein peptides on any of the SPE sorbents seems to occur because all the expected peaks were recovered in the different fractions. Figs. 3 and 4 show the chromatograms of casein peptides isolated using C_2 and C_{18} sorbents. It must be pointed out that no new additional peaks seem to appear in comparison with the chromatogram of the original enzymatic hydrolysate (Fig. 2), which means the absence of artifacts during the SPE procedure.

SPE columns exhibit a similar relative behaviour for the extraction of casein peptides and synthetic peptides. The sorbent's ability to retain peptides by hydrophobic interactions is similar to that observed with synthetic peptides. Thus, Table 2 shows that CN sorbents retain exclusively more hydrophobic peptides (eluting later than 50 min in RP-HPLC and giving a 14% recovery). C_2, PH and CH sorbents behave similarly because they do not retain very polar peptides but provide a good recovery of moderate and very hydrophobic peptides (72, 83 and 83%,

Table 2
Fractionation and recovery of peptides from an enzymatic hydrolysate of α-casein by using different SPE columns

SPE procedure	Fraction in SPE[a]							
	1		2		3		4	
	Δt_r (min)[b]	Recovery (%)[c]	Δt_r(min)	Recovery (%)	Δt_r (min)	Recovery (%)	Δt_r (min)	Recovery (%)
CN	0–46.1	45	0–50.1	45	42.2–59.2	10	52.4–61.9	4
C_2	0–15.1	7	0–24.2	23	19.4–42.2	37	30.6–61.8	35
PH	0–9.8	4	0–15.0	14	14.1–38.4	48	30.8–61.9	35
CH	0–10.1	1	0–14.7	11	12.5–34.7	48	30.6–62.0	35
C_8	–	–	0–10.0	5	9.9–42.1	58	30.8–61.9	36
C_{18}	–	–	0–8.5	2	9.2–38.3	69	30.9–61.8	32
Sep-Pak Plus C_{18}	–	–	–	–	0–27.1	24	10.3–61.8	81

[a] Fractionation of peptides was carried out as described in the Experimental section. The fractions of peptides recovered are as in Table 1.
[b] Range of retention times (min) in which there were found peptides after analysing the collected fractions by RP-HPLC.
[c] Recovery calculated as sum of the total area of the HPLC peaks in the corresponding fraction compared with the total sum of HPLC peaks areas of the complete hydrolysate chromatographed as shown in Fig. 2.

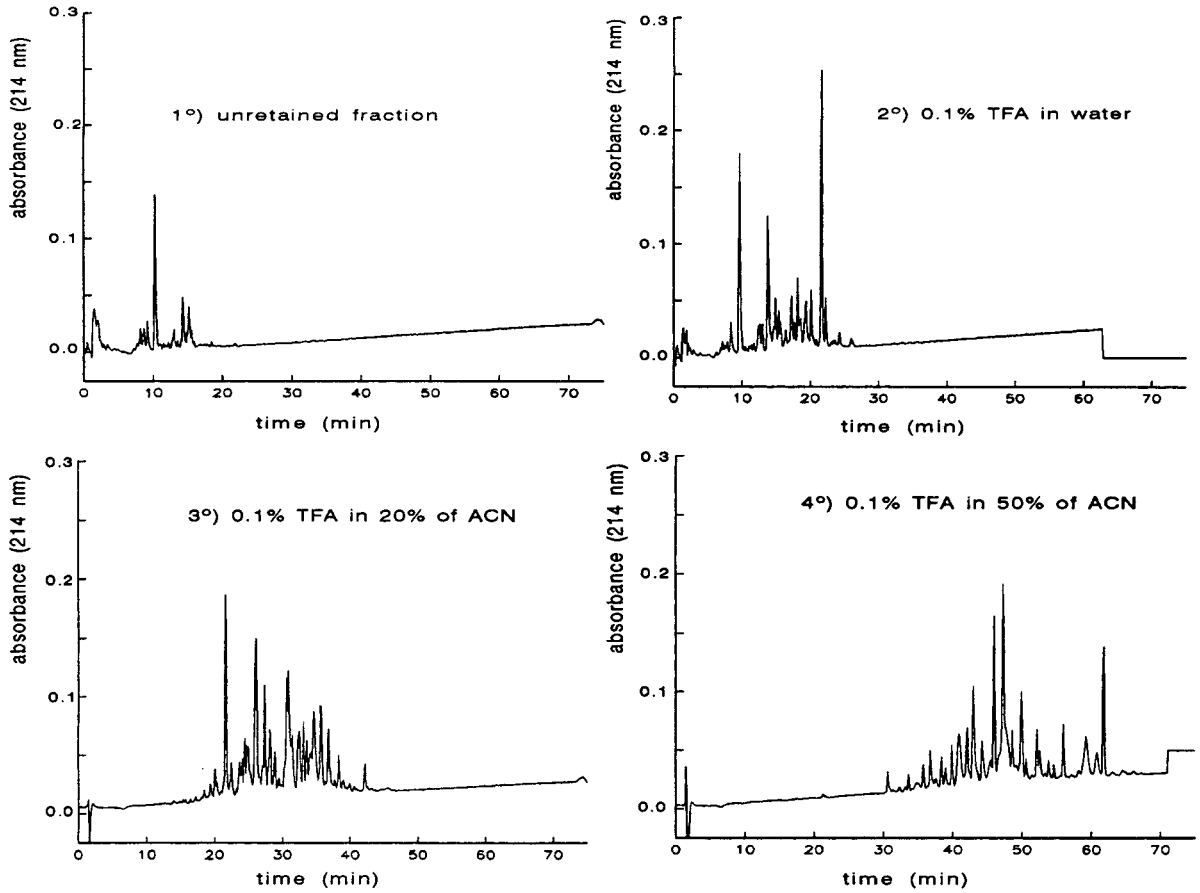

Fig. 3. RP-HPLC of the peptide fractions from an α-casein enzymatic hydrolysate recovered from the C_2 SPE sorbent. (1) Unretained fraction; (2) 0.1% TFA in water; (3) 0.1% TFA in 20% acetonitrile; (4) 0.1% TFA in 50% acetonitrile. Column and conditions as in Fig. 1.

respectively). C_2, PH and CH sorbents also give a good fractionation of the extracted peptides. On the other hand, C_8, C_{18} and Sep-Pak C_{18} retain almost all casein enzymatic peptides with no peptides in the two first fractions (unretained and the washing fractions of 0.1% aqueous TFA).

So far, the results show the suitability of SPE for the preparative extraction and fractionation of peptides. However, a higher preparative purification of peptides may be obtained by small incremental increases in the organic modifier contained in the eluting fractions. Peptides of the casein hydrolysate can be successfully separated into seven fractions from 10% to 40% of acetonitrile. They are collected and subsequently chromatographed by RP-HPLC (Fig. 5). Casein peptides are fractioned as a function of their hydrophobicity, while eluting with an increasing concentration of acetonitrile. In non-polar SPE, peptides adsorb on the sorbent, depending on their hydrophobicity. Thus, more hydrophobic peptides exhibit a higher non-polar interaction with the sorbent and are therefore eluted with a

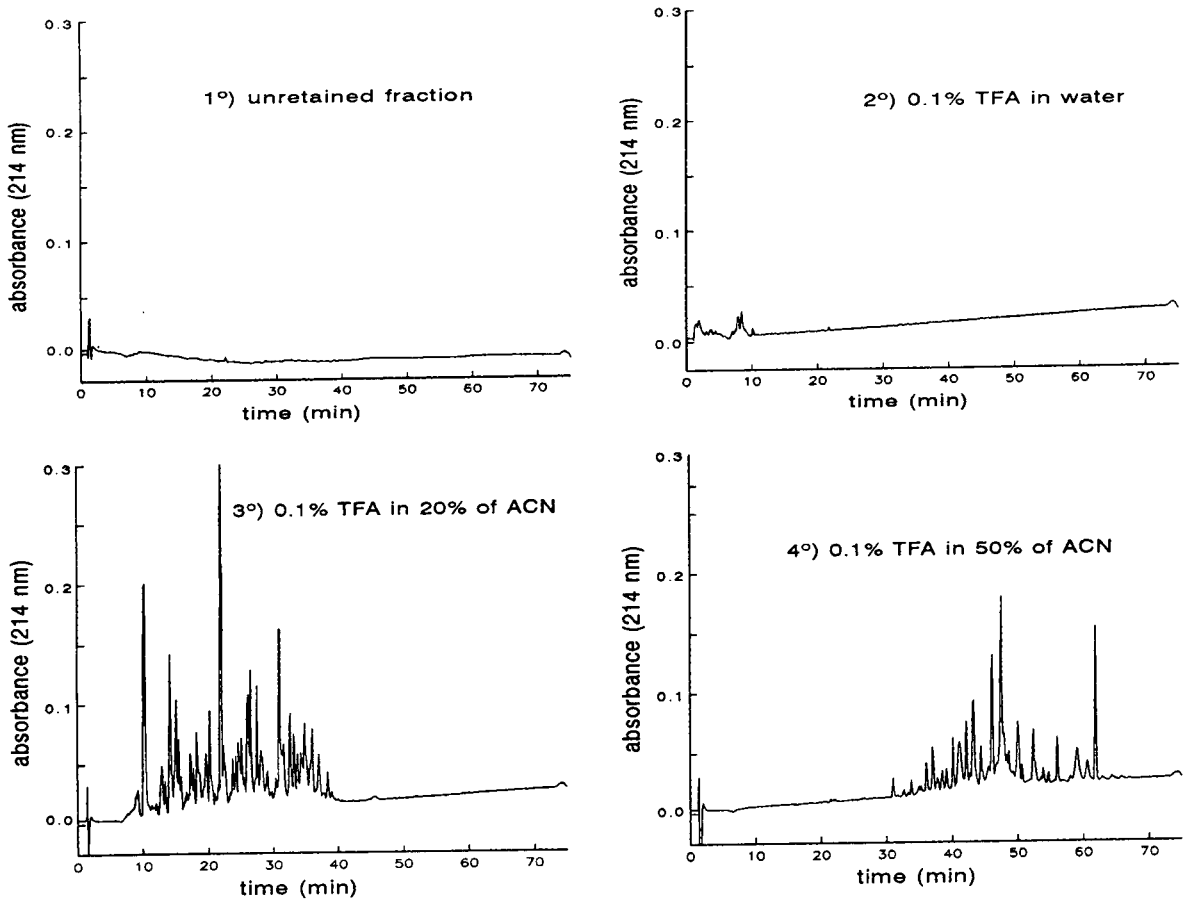

Fig. 4. RP-HPLC of peptide fractions from an α-casein enzymatic hydrolysate recovered from the C_{18} SPE sorbent. (1) Unretained fraction; (2) 0.1% TFA in water; (3) 0.1% TFA in 20% acetonitrile; (4) 0.1% TFA in 50% acetonitrile. Columns and conditions as in Fig. 1.

higher concentration of acetonitrile. In the same manner, those peptides are retained longer in RP-HPLC as expected (Fig. 5).

Selective enrichment and concentration of peptides from diluted casein hydrolysates (1:50) were carried out. After loading 50 ml of a diluted sample of casein peptides, the recovery in the eluting fractions of acetonitrile showed that, except for the CN sorbents, which only adsorb very hydrophobic peptides, giving a recovery of 6%, the rest of the sorbents give a high recovery: C_2 62%, PH 86%, CH 82%, C_8 92%, C_{18} 91% and Sep-Pak Plus C_{18} 99%. These results show that preparative SPE is suitable for the concentration and selective enrichment of trace peptides.

3.3. *Isolation and preparative fractionation of synthetic peptides and protein hydrolysates using ionic SPE*

Peptide isolation and fractionation were also carried out by ion extraction (Table 3). Peptides can be successfully fractionated into basic, neutral and acidic pools using ion-extraction cartridges such as Accell Plus QMA and CM. Table

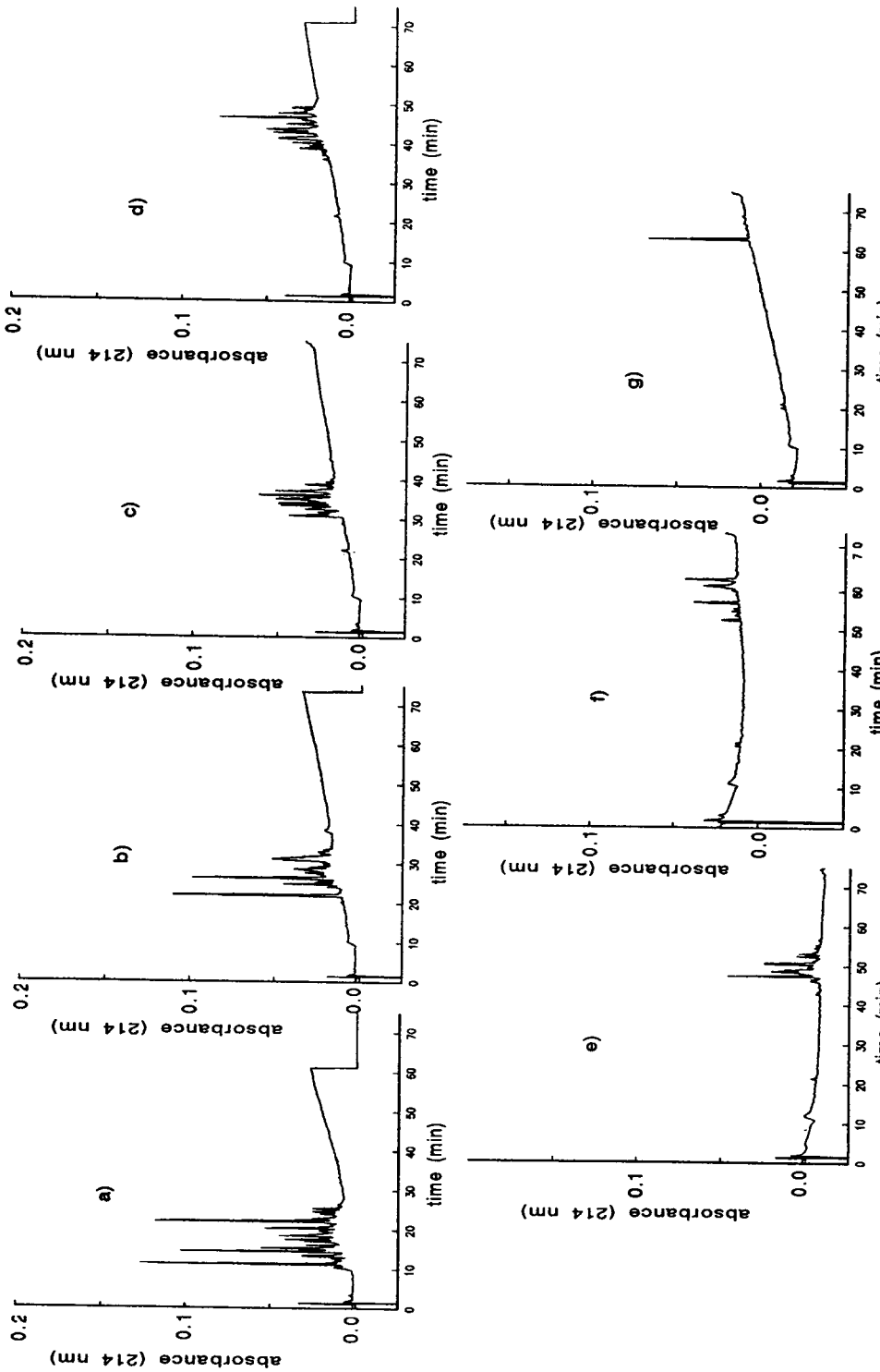

Fig. 5. RP-HPLC of peptide fractions obtained from an α-casein enzymatic hydrolysate after its fractionation in a C_{18} SPE column, using small incremental increases of acetonitrile from 10% to 40%. Fractionation is discussed in the Experimental section. The fractions are (a) 0.1% TFA in 10%, (b) 15%, (c) 20%, (d) 25%, (e) 30%, (f) 35% and (g) 40% of acetonitrile. Column and conditions as in Fig. 1.

Table 3
Fractionation and recovery of peptides from solutions of synthetic peptides in CBA columns and CM and QMA cartridges

Peptide	Recovery in the fractions (%)[a]							
	CBA column				Accell QMA and CM cartridges			
	1	2	3	4	Neutral 1	Neutral 2	Acidic	Basic
Glutathione	46	10	0	0	33	40	25	0
V-G-S-E	87	19	0	0	0	0	80	0
G-G-Y-R	4	33	66	0	0	19	0	65
K-W-K	0	0	85	6	0	0	0	67
P-F-G-K	0	0	100	0	0	29	0	66
G-G-W-A	20	73	1	0	16	83	0	0
V-H-L-T-P-V-E-K	0	0	92	7	4	25	30	37
L,D-L-G-L,D-F	10	82	7	0	21	83	0	0
L,D-L-G-L,D-F	3	75	20	0	19	81	0	0
F-L-E-E-V	39	55	0	0	0	0	98	0
F-L-E-E-I	11	59	30	0	0	0	96	0
F-L-E-E-L	0	50	25	0	0	0	99	0
W-W	0	0	99	1	0	10	88	0
D-R-V-Y-I-H-P-F-H-L-L-V--Y-S	0	0	102	0	0	0	0	96

[a] Fractions are as mentioned in Experimental section. Fractions in CBA are as follows: (1) unretained fraction; (2) 10 m*M* NH_4OAc (pH 5.5); (3) 0.1% TFA in 40% acetonitrile; (4) 0.1% TFA in 40% acetonitrile. Fractions in CM and QMA: neutral 1, unretained fraction; neutral 2, 10 m*M* NH_4OAc (pH 5.5) in 20% acetonitrile; acidic fraction from QMA cartridge, 10 m*M* NH_4OAc (pH 5.5) in 20% acetonitrile + 1 *M* NaCl; basic fraction from CM cartridge, 10 m*M* NH_4OAc (pH 5.5) in 20% acetonitrile + 1 *M* NaCl. Data for recovery were obtained in duplicate.

3 shows that acidic peptides such as F-L-E-E-V, F-L-E-E-I and F-L-E-E-L or V-G-S-E elute in the acidic fraction, whereas G-G-Y-R, P-F-G-K, K-W-K and D-R-V-Y-I-H-P-F-H-L-L-V-Y-S elute in the basic pool. Other peptides appear in the neutral pool. This behaviour agrees with the results reported previously using these cartridges [13].

The basic peptides are efficiently retained in CBA sorbents. At the pH used (5.5), the carboxylic chain of the sorbent is mainly negatively charged whereas peptides with more basic residues (R,K,H) are positively charged and retained on the sorbent. Other sorbents such as SCX (benzenesulphonate), SAX (trimethylaminopropyl) and NH_2 (aminopropyl) were also tested, but the results were poor compared with QMA, CM and CBA and are not included here.

Finally, the enzymatic hydrolysate was also fractioned in the Accell cartridges as shown in Fig. 6. Thus, peptides are extracted into three different pools. From this result, peptides from the α-casein enzymatic hydrolysate seem to appear mainly in the neutral and acidic pools whereas almost no peaks appear in the basic fraction in Fig. 6.

The presence of chromatographic interferences that may co-elute with peptides, possible peptide overlapping, and their presence in very low concentrations are common problems in the HPLC analysis of peptides in food samples and biological fluids. In this regard, SPE should become a necessary preliminary purification step. Peptides can be successfully isolated and further fractioned using appropriate SPE columns and sorbents. The results show the suitability of the SPE procedures based on hydrophobic interaction for preparative extraction, fractionation and enrichment of peptides. However, the correct SPE disposable column must be chosen, depending on the characteristics of the peptides involved. Thus, CN and C_2 sorbents

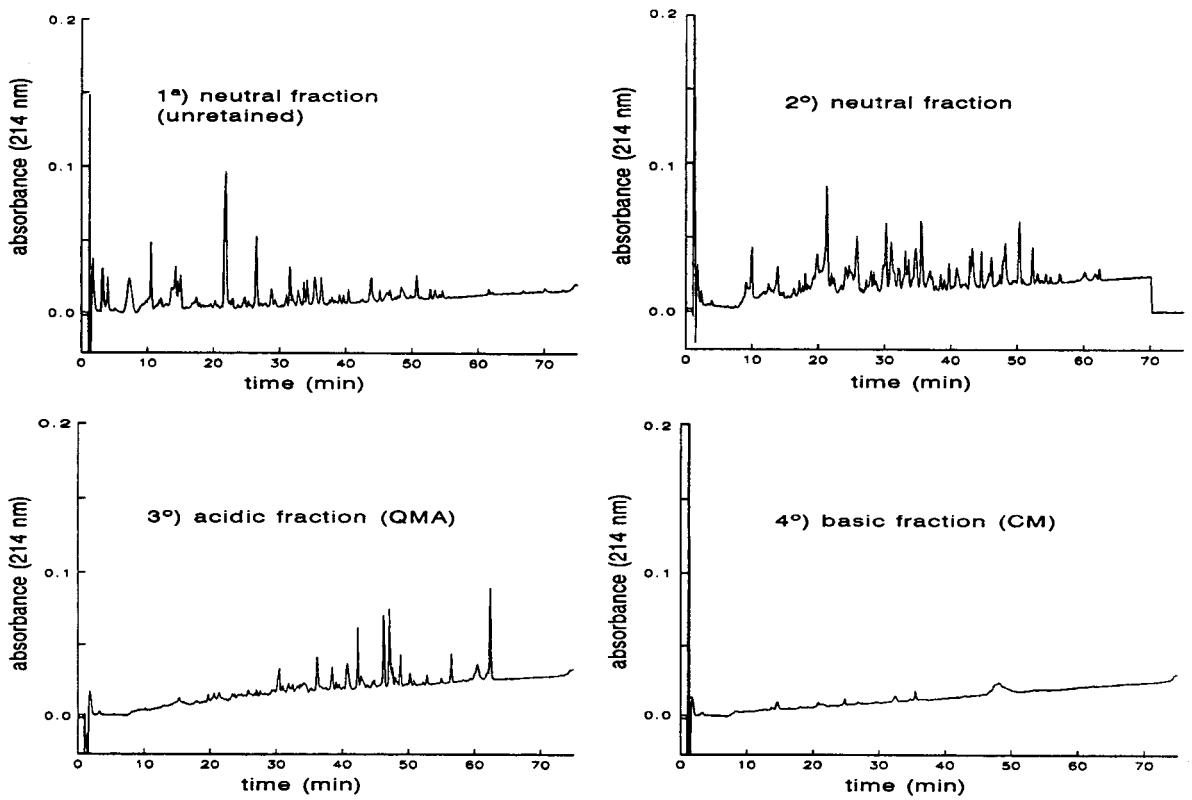

Fig. 6. RP-HPLC of peptide fractions from an α-casein enzymatic hydrolysate recovered from the Accell CM and QMA cartridges. (1) Neutral fraction (unretained); (2) neutral fraction; (3) acidic fraction eluted from QMA cartridge; (4) basic function eluted from CM cartridge. Column and conditions as in Fig. 1.

would be useful for hydrophobic peptides, CH, PH, C_8 for medium and high hydrophobic peptides and C_{18} and Sep-Pak environmental C_{18} for very polar and also hydrophobic peptides. In the non-polar interaction of peptides, as the carbon loading of the SPE column increases and the polarity of the bonded phase decreases, the k' value of peptides increases (i.e., the retention increases). For unknown peptides, it is possible to test several SPE procedures in order to select the most appropriate one or to use non-polar SPE with the highest peptide retention such as a C_{18} packing. Using several SPE procedures could also provide some information on the characteristics of unknown peptides. SPE provides a good recovery and reproducibility in the extraction of peptides, whereas irreversible adsorption is very low and there is an absence of artifacts. This was proved by comparing the HPLC traces from the SPE eluting fractions with those of the initial samples before loading peptides into the SPE column. Using SPE, RP-HPLC mapping of peptides can be simplified and impurities or interferences removed prior to chromatographic analysis. However, it must be pointed out that very large peptides or proteins could be unretained in SPE if they do not pass through the pores of the sorbent. On the other hand, SPE based on ionic interaction could efficiently fractionate peptide mixtures into neutral, acidic and basic pools as shown previously [13]. Ionic SPE would avoid peptide overlapping and improve the resolution while removing peptide interferences present in the sample.

4. Conclusion

SPE is a very useful technique for the preparative isolation, fractionation and purification of peptides from complex mixtures. It provides a rapid and effective way to clean up and concentrate peptides for subsequently RP-HPLC analysis.

Preparative fractionation of peptides requires a correct selection of SPE sorbent, depending on peptide polarity and charge. SPE based on hydrophobic phases is a useful, efficient and rapid procedure for the extraction of peptides after elution with eluents containing an increasing content of acetonitrile in the presence of 0.1% TFA. The increasing order of peptide retention due to the highest hydrophobic interaction between peptides and the sorbent is CN < C_2 < PH < CH < C_8 < C_{18} < Sep-Pak Plus C_{18}. The overall recovery of peptides is high, as proved for synthetic peptides and enzymatic hydrolysates. Concerning sorbent selectivity, it must be pointed out that very polar peptides should be isolated using sorbents with a high retention ability such as C_8, C_{18} or Sep-Pak Plus C_{18}. Very hydrophobic peptides could be isolated with less hydrophobic sorbent such as CN or C_2. Medium and high hydrophobic peptides could be efficiently isolated and fractioned with PH and CH sorbents. SPE with a C_{18} sorbent could be employed for unknown peptides or peptides with a wide range of polarity to provide complete adsorption of most peptides (polar and non-polar). Using several SPE procedures might be useful to provide information on peptide polarity and charge when dealing with unknown peptides. On the other hand, ionic SPE using QMA and CM cartridges simultaneously provides an efficient fractionation and isolation of peptides by charge into neutral, acidic and basic pools as proved for synthetic peptides and casein hydrolysates.

Acknowledgement

The authors thank the CICYT (Spanish government) for its financial assistance from the projects ALI94-0773 and ALI94-0217-C02-02.

References

[1] B. Tippins, Nature, 334 (1988) 273.
[2] F.J. Al-Shammary, J. High Resolut. Chromatogr., 13 (1990) 309.
[3] H.P.J. Bennett, A.M. Hudson, C. McMartin and G.E Purdon, Biochem J., 168 (1977) 9.
[4] H.P.J. Bennett, A.M. Hudson, L. Kelly, C. McMartin and G.E. Purdon, Biochem. J., 175 (1978) 1139.
[5] A. Voirin, J-F. Letavernier and B. Sebille, J. Chromatogr., 553 (1991) 155.
[6] P. Bican and A. Spahni, Int. Dairy, J., 3 (1993) 73.
[7] T. Herraiz, V. Casal and M.C. Polo, Z. Lebesm.-Unters.-Forsch., 199 (1994) 265.
[8] T.K. Singh, P.F. Fox, P. Hojrup and A. Healy, Int. Dairy J., 4 (1994) 111.
[9] D. Gonzalez de Llano, T. Herraiz and M.C. Polo, in L.M. Nollet (Editor) Handbook of Food Analysis, Marcel Dekker, New York, in press.
[10] H.P.J. Bennett, J. Chromatogr., 266 (1983) 501.
[11] P. Angwin and J.D. Barchas, J. Chromatogr., 231 (1982) 173.
[12] T. Higa and D.M. Desiderio, Int. J. Pept. Protein Res., 33 (1989) 250.
[13] H.P.J. Bennett, J. Chromatogr., 359 (1986) 383.

ELSEVIER

Journal of Chromatography A, 708 (1995) 223–230

JOURNAL OF CHROMATOGRAPHY A

Heterogeneity of the bovine κ-casein caseinomacropeptide, resolved by liquid chromatography on-line with electrospray ionization mass spectrometry

Daniel Mollé, Joëlle Léonil*

Institut National de la Recherche Agronomique, Laboratoire de Recherches de Technologie Laitière, 65 rue de St-Brieuc, 35042 Rennes Cedex, France

First received 12 January 1995; revised manuscript received 21 March 1995; accepted 21 March 1995

Abstract

Microheterogeneity occurs in the population of caseinomacropeptides (residues 106–169 of κ-casein) due to variation in the extent and type of oligosaccharide linked to this phosphoglycopeptide. Although caseinomacropeptide A variant (CMP_A) was poorly resolved using reversed-phase high-performance liquid chromatography (RP-HPLC) with spectrophotometric detection, it could be analysed with on-line electrospray-ionization mass spectrometry (ESI-MS). From the already established O-linked glycan chains at least fourteen glycosylated forms of CMP_A were identified, besides the non-glycosylated and multiphosphorylated (1, 2 or 3 phosphate groups) peptides, giving a maximum number of eighteen known forms. Major subcomponents in CMP_A are disialylated species. A maximum of three out of the five potential glycosylation sites were found to be substituted with carbohydrate chains in the most highly glycosylated forms, which may contain up to six N-acetylneuraminic acid residues per molecule. A minor form, diphosphorylated with one disialylated chain, was also detected. From these results, it was shown that the on-line coupling of HPLC with ESI-MS offers a very promising alternative for the analysis of complex mixtures.

1. Introduction

Caseinomacropeptide (CMP) is a polypeptide of 64 amino acid residues (106–169) derived from the C-terminal part of bovine κ-casein. It is released by chymosin (EC 3.4.23.4) action during the primary phase of milk clotting. Some biological functions of CMP have been reported including a growth promoting effect on bifidobacteria [1], suppression of gastric secretion [2,3], depression of platelet aggregation [4], inhibition of oral actinomyces adhesion to cell membranes [5] and inhibition of cholera toxin binding to its receptor [6]. CMP exists as an heterogeneous mixture since it carries both genetic variations (four genetic variants, A, B, C and E are known [7]) as well as carbohydrate and phosphorylation sites responsible for the polymorphism of its precursor. κ-Casein displays mucin-type carbohydrate chains comprising N-acetylneuraminyl (NeuAc), galactosyl (Gal) and N-acetylgalactosamine (GalNAc) residues [8]. A monosaccharide alditol, $GalNAc_{OH}$, and four

* Corresponding author.

0021-9673/95/$09.50
SSDI 0021-9673(95)00386-X

oligosaccharide alditols Galβ(1-3)GalNAc$_{OH}$, NeuAcα(2-3)Galβ(1-3)GalNAc$_{OH}$, Galβ(1-3)-[NeuAcα(2-6)]GalNAc$_{OH}$ and NeuAcα(2-3)Gal-β(1-3)[NeuAcα(2-6)]GalNAc$_{OH}$ have been identified in mature bovine κ-casein [9]. Another source of heterogeneity is the variable level of phosphorylation, ranging from 1 to 3 phosphate groups [10–12]. Thus, from 7 to 10 subcomponents have been reported for the bovine κ-casein [10,11]. However, the distribution of carbohydrate units on the κ-casein molecule still remains unclear.

The complete structural analysis of κ-casein requires isolation of the individual constituents. The majority of the studies reported so far have been accomplished using two chromatographic methods, anion exchange and high-performance size exclusion [11,13], in order to separate the subcomponents of κ-casein. These subcomponents are then enzymatically or chemically cleaved for further analysis of their carbohydrate and phosphorus content. However, these methods are time-consuming and limited by the poor chromatographic resolution obtained. Therefore the number of subcomponents, as well as their precise structure are, as yet, not definitively established neither for κ-casein nor, consequently, for CMP. On account of the potential applications of CMP in pharmacology a better knowledge of this peptide is required. Thus a method for identifying the different molecular forms of CMP would be valuable. It has become increasingly clear that the carbohydrate chains play a critical role in the functional properties of these glycoproteins [14]. In a previous publication, we have reported a procedure for isolating CMP from whey, using cation-exchange chromatography and its subsequent analysis by RP-HPLC [15]. Since the separation of glycoproteins is still a challenging task, because of the occurrence of glycoforms with little difference in size or charge, the emergence of a soft ionization technique such as the electrospray method (ESI) has expanded the capability of liquid chromatography–mass spectrometry (LC–ESI-MS). The present work describes the first use of two combined methods, RP-HPLC and ESI-MS, for the analysis and characterization of the CMP$_A$ subcomponents.

2. Experimental

2.1. Purification of caseinomacropeptide A

CMP$_A$ was isolated from the milk of an individual homozygous cow A/A at the locus κ-casein A variant, according to the method previously described [15] based on the hydrolysis of κ-casein by chymosin, followed by chromatography on a S-Sepharose Fast Flow column (Pharmacia Biotech, Saint-Quentin, Yvelines, France). CMP was found to be 97% homogeneous, based on amino acid composition [15].

2.2. RP-HPLC–ESI-MS analyses of caseinomacropeptide A

The three RP-HPLC columns that were used in order to optimize the separation of the different subcomponents of the CMP$_A$ were: Superspher 100 RP-18 (150 × 2.1 mm I.D., 5 μm particle size) (Merk, Darmstadt, Germany); Nucleosil C_{18}-AB (125 × 2.1 mm I.D., 5 μm particle size) (Macherey-Nagel, Strasbourg, France); Delta-Pack C_{18} (300 Å, 150 × 2 mm I.D., 5 μm particle size) (Waters, Milford, MA, USA). The mobile phase was delivered by a Waters 625 LC pump. The gradient elution was performed with acetonitrile as the organic modifier, at 40°C and at a flow-rate of 0.2 ml/min. Solution A was 0.1% TFA dissolved in double-distilled water (v/v) and solution B was 0.1% TFA dissolved in acetonitrile–double distilled water (80:20, v/v). After equilibration of the column with 27% of solution B, samples were applied to the column and eluted by increasing the concentration of solution B as follows: 0–40 min, 27–47%; 40–42 min, 47–80%. Eluted peaks were detected by absorbance at 214 nm using a Waters 990 Series photodiode array detector.

The mass spectrometer API I Sciex (Thornhill, Ont., Canada) was a single-quadrupole mass spectrometer equipped with an atmospheric-pressure ionization ion source. API I Sciex was operated in the positive mode. Multiply-charged protein ions were generated by spraying the sample solution through a fused-silica capillary of 75 μm I.D., introduced into a stainless steel capillary held at high potential. The voltage on the sprayer was usually set between 5 and 5.5 kV. A coaxial air-flow along the sprayer was provided to assist the liquid nebulization; the nebulizer pressure was usually adjusted within the range of 0.3–0.4 MPa. For the infusion experiment, the sample was delivered to the sprayer by a syringe infusion pump (Model 22, Harvard Apparatus, South Natick, MA, USA). The liquid flow-rate was usually set at 5–10 μl/min for sample introduction. For analysis by RP-HPLC coupled with ESI-MS, splitting of the liquid flow was achieved by a low-dead volume connection and the column effluent was diverted partly to the mass spectrometer (15% of the effluent) and partly to the UV detector (85% of the effluent). This arrangement permitted a straightforward correlation of the total-ion current (TIC) trace with the UV trace. The interface between the sprayer and the mass analyser consisted of a small conical orifice of 100 μm diameter. The potential on the orifice was 80 V. A gas curtain, formed by a continuous flow (0.8–1.2 l/min) of nitrogen in the interface region, served to break up any clusters. The instrument m/z scale was calibrated with ammonium adduct ions of poly-(propylene glycol)s. All protein mass spectra were obtained from the signal averaging of multiple scans. HPLC–ESI-MS experiments were performed while scanning the m/z range 800–2400 at a step-size of 0.33 amu and a dwell time of 0.5 ms. UV absorbance was detected simultaneously with the MS signal and registered with Tune 2.0 software Sciex. Molecular masses were determined from the measured m/z values for the protonated molecules. Data were collected on an Apple Macintosh Quadra 900 computer and were processed using the software package Mac Spec 3.2 Sciex. The reconstructed molecular mass profile was obtained by using a deconvolution algorithm (Mac Spec 3.2 Sciex).

3. Results

3.1. Optimization of the separation of caseinomacropeptide by RP-HPLC

Fig. 1 shows the RP-HPLC–UV traces of CMP_A using three different C_{18} columns (Superspher, Nucleosil, Delta-Pack) eluted with the same mobile phase composition, i.e. water–acetonitrile containing TFA. The injected amount (50 μg) and conditions of elution gradient were identical for all three columns. The UV profile provides a series of closely related peaks reflecting the heterogeneity of CMP_A. In order to improve the separation conditions, the gradient slope, the temperature (37, 45, 55°C), the mobile phase system (acetonitrile, acetonitrile–2 propanol, ammonium acetate buffer pH 6.5) as well as ion-pairing (TFA, acetic acid), were all modified. However, despite all efforts it was not possible to separate the different constituents of CMP_A (data not shown). The Delta-Pack column was found to give the best

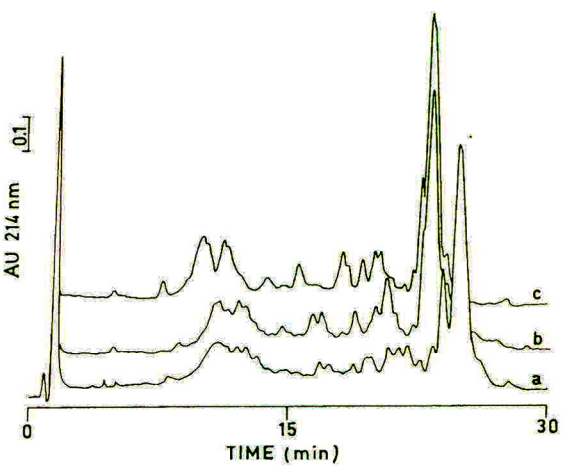

Fig. 1. RP-HPLC elution profile of caseinomacropeptide A variant on (a) Superspher (b) Nucleosil (c) Delta-Pack columns C_{18}. Linear gradient from 21–37% acetonitrile containing 0.1% TFA.

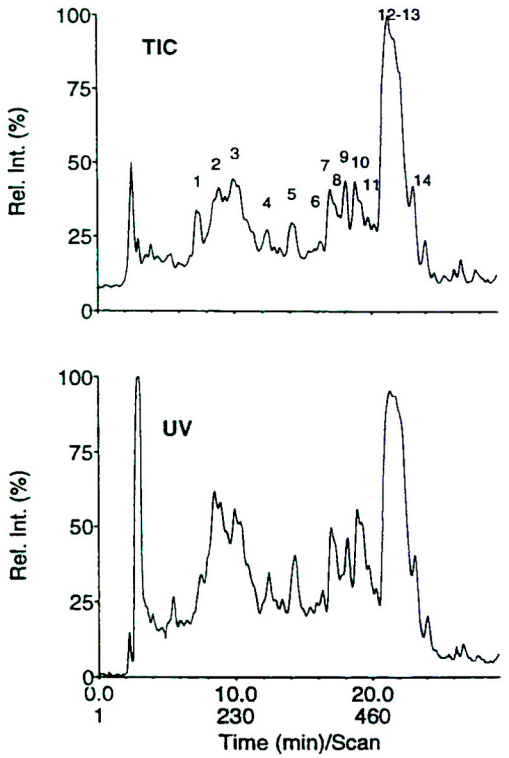

Fig. 2. RP-HPLC spectra of caseinomacropeptide A variant with total ion current (top), as measured by ESI-MS and UV monitoring at 214 nm (bottom).

separation for this complex mixture with an elution acetonitrile gradient containing 0.1% TFA and hence this was used for the coupling with ESI-MS. The major peak, which appeared at a retention time (t_R) of 22 min in Fig. 1c, has been identified as a carbohydrate-free CMP_A [15]. Earlier eluted peaks (t_R 8–20 min) were assigned to glycosylated forms but nothing was known about their carbohydrate content.

3.2. Analysis of caseinomacropeptide A by on-line RP-HPLC–ESI-MS

The reconstructed total ion current (TIC) chromatogram of CMP_A is shown in Fig. 2 (top), for CMP_A injected on the Delta-Pack column. Aliquots of 150 μg were loaded onto the column at a flow-rate of 0.2 ml/min with a split of about 1:7 into the ES source. This chromatogram correlates well with the UV-absorbance profile (Fig. 2, bottom). Peak intensities in TIC and UV absorbance are different because they are based on different physical measurements [16]. The analysis of glycophosphopeptides, and in particular the determination of M_r, was aided by using the two dimensional display or contour plot, in which the individual ions for each scan are plotted as their m/z vs. run time or scan number. Closely related glycoforms are identified by the appearance of a typical diagonal pattern of lines with their respective intensities [17]. This is illustrated in Fig. 3 for the more heavily glycosylated forms observed in the early region of the plot. The M_r of each form can thus be calculated from the contour plot, using the m/z values of any given ion series falling on the same vertical line. These values are presented in

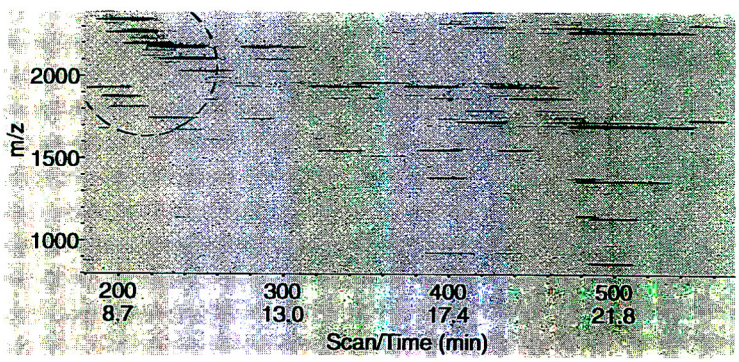

Fig. 3. Two-dimensional display of the ions (contour plot) observed in the HPLC–ESI-MS of caseinomacropeptide A variant. The multiply charged ions of glycoforms are highlighted.

Table 1 (2nd column). As anticipated from our earlier studies, some peaks are not homogeneous and therefore give several masses. As examples, representative spectra of the peaks 2 and 12–13 are shown in Fig. 4A,B respectively. The mass spectrum extracted from each chromatographic peak is characterized by a series of ions having m/z values corresponding to multiple protonated forms of the molecule. Ions from peak 2 were observed at m/z 2336.2, 2262.9, 2191.6, 1927.3, 1868.9, and 1810.8, indicating the coelution of several components. Two series of ions were found, one at m/z 2336.2 and 1868.9 and the other at m/z 2262.9 and 1810.8, which can be related to the $[M+4H]^{4+}$ and $[M+5H]^{5+}$ charged ions. From the measured m/z values for the multiply charged ions and their charge states, the molecular masses were 9339.28 and 9048.88, respectively, for these two components. The low level of the remaining ions in the spectrum

Table 1
Observed molecular masses of the peaks in the UV trace and TIC (Fig. 2) and assignments of different subcomponents of caseinomacropeptide with their calculated molecular masses

Peak No.	Observed M_r	Subcomponent structure of CMP	Calculated M_r
1	3478.40 ± 0.03	–	–
2	9632.82 ± 0.81[a]	CMP_A-3E	9630.92
	9339.28 ± 0.04	CMP_A-2E 1C/D[b]	9339.66
	9048.88 ± 0.04	CMP_A-1E 2C/D[b] or 2E 1B	9048.42
	8759.56 ± 0.70[a]	CMP_A-3C/D[b] or 1E 1C/D 1B	8757.17
3	8684.66 ± 0.74	CMP_A-2E	8683.10
	8392.51 ± 0.42	CMP_A-1E 1C/D[b]	8391.85
	8102.11 ± 0.42	CMP_A-2C/D[b] or 1E 1B	8100.60
4	8683.73 ± 0.74	CMP_A-2E	8683.10
5	7735.48 ± 0.04	CMP_A-1E	7735.27
6	7814.96 ± 1.42[a]	CMP_A (2*P*)-1E	7815.16
7	7736.38 ± 0.69	CMP_A-1E	7735.27
8	2764.56 ± 0.05	–	–
9	6867.88 ± 0.30	CMP_A (2*P*)	6867.33
	7152.97 ± 1.36	CMP_A-1B	7152.85
10	7735.91 ± 0.51	CMP_A-1E	7735.27
	7444.86 ± 0.68[a]	CMP_A-1C/D[b]	7444.10
11	6947.96 ± 0.57[a]	CMP_A (3*P*)	6947.23
12	6868.24 ± 1.08	CMP_A (2*P*)	6867.33
13	6788.04 ± 0.74	CMP_A (1*P*)	6787.42
14	6935.09 ± 1.00[a]	κ-CN (105–169)	6934.60

CMP_A (1*P*) (residue 106–169 of κ-casein) indicates the monophosphorylated carbohydrate-free form in this table. Symbols A, B, C, D, E, are described in Fig. 5.
[a] Determined by infusion.
[b] C and D (C/D), having the same mass, cannot be discriminated by MS analysis.
nd Not determined.

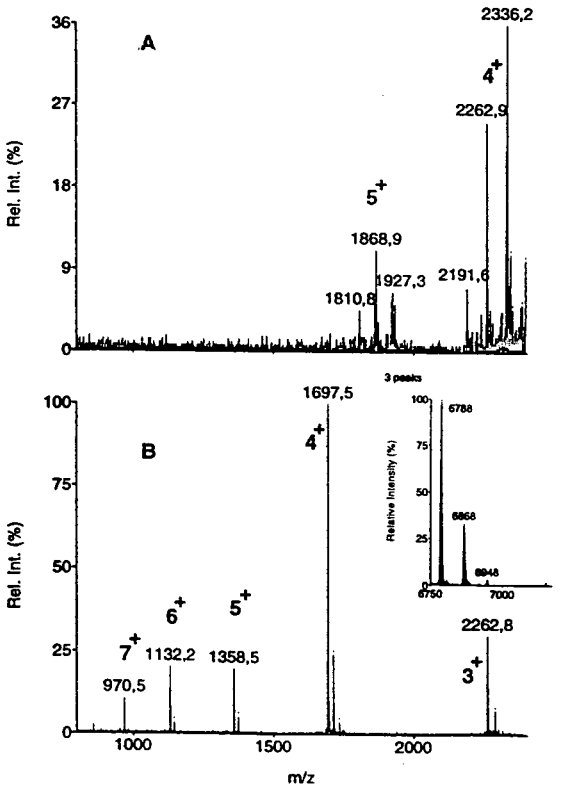

Fig. 4. Mass spectra of peak 2 (A) and peak 12–13 (B) from Fig. 2. Insert in graph B shows the reconstructed molecular spectra. The number of positive charges is indicated at the top of each peak.

precluded their mass determination by Sciex algorithm. However, in the case where only one charge state is observed the m/z difference between related ion signals, as described above for glycoforms, may be used to determine its charge state. For example, only a single charge state is observed for the species detected at m/z 1927.3. The m/z difference of 58.4 between m/z 1927.3 and 1868.9 can be assigned to the mass difference of a NeuAc moiety (M_r NeuAc/5 = 291.6/5) if the charge state is 5. The M_r was determined as 9631.5 ($1927.3 \times 5 - 5$). In order to confirm the M_r of the minor components, higher concentrations of these components were required. Hence each minor peak in RP-HPLC was collected, lyophilized and directly analysed in a carrier solvent by ESI-MS, at a flow-rate of 5 μl/min. The masses of these components are indicated by an asterisk in Table 1. In the spectrum shown in Fig. 4B for peak 13, the predominant M_r measured was 6788.04 ± 0.74, which is in good agreement with the calculated value (6787.42) from the known sequence for the non-glycosylated CMP_A variant [18]. Interestingly, this spectrum reveals the presence of a second distribution pattern of ion peaks (m/z 1145.8, 1374.5, 1717.5, 2290.5) that gives a calculated M_r value of 6867, differing from the non-glycosylated form by 80 amu. These data are consistent with the presence of mono- and di-phosphorylated carbohydrate-free CMPs [11]. In addition, a very minor form with three phosphate groups was also observed in the deconvoluted mass spectrum shown in the Fig. 4B insert. As a linear dependence of the ESI signal upon concentration was observed [19], mono-, di- and triphosphorylated forms occur in the ratios 78%, 20% and 2%, respectively. This implies, of course, that uniform ESI mass spectrometry response of the closely related species was assumed.

Overall, there are fifteen different masses obtained from the CMP analysis by HPLC–ESI-MS within the mass range 6936–9633. Peaks 1 (M_r 3478) and 8 (M_r 2764) were impurities and were not investigated further. The structures of five carbohydrate units reported to be linked to CMP [9] are described in Fig. 5. From these data and mass increments, in excess of the known non-glycosylated peptide mass, the glycan structures shown in Table 1 were assigned to the different peaks separated by HPLC. All masses reported are within 0.02% of those expected for the proposed structures. The same masses recovered along the chromatogram with varying t_R were considered as being different molecular species. Their occurrence is easily attributable to the fact that the same carbohydrate units are linked to different positions in the peptide chain, leading to different t_R values. Peak 18 is a minor component which may correspond to the sequence 105–169 of non-glycosylated κ-casein, κ-CN(105–169), subsequent to the cleavage of the bond Ser104–Phe105. Such a specificity of chymosin has not been reported. However, this kind of cleavage is known for other aspartic

A GalNAc

B Galβ(1-3)GalNAc

C NeuAcα(2-3)Galβ(1-3)GalNAc

D
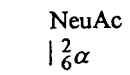

Galβ(1-3)GalNAc

E
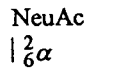

NeuAcα(2-3)Galβ(1-3)GalNAc

Fig. 5. Structure of the five carbohydrate chains of mature bovine κ-casein [9]. M_r (average): A = 221.2, B = 383.3, C = 674.6, D = 674.6, E = 965.8.

proteinases [20]. At least eighteen different molecular species were identified in CMP_A and consequently in κ-casein A, including non-glycosylated and multiphosphorylated forms.

4. Discussion

We describe here the characterization of a complex mixture of glycophosphopeptides, arising from residues 106–169 of κ-casein, by use of the combination of RP-HPLC and ESI-MS. No single method has been reported to be adequate for the analysis of CMP, but ESI-MS has proved to be a powerful method for the characterization of such mixtures, especially when there is some difficulty in separation by HPLC as seen in Fig. 1. Using this means, the maximum number of subcomponents of CMP_A found in this study was twice as high as that previously reported [11]. The sialylated species were detected as the major subcomponents in CMP_A (Table 1) and the NeuAcα(2–3)Galβ(1–3)[NeuAcα(2–6)]Gal-NAc_{OH} tetrasaccharide containing two NeuAc was shown to be the most dominant sugar chain. This confirms the hypothesis that the ratio of disialylsaccharide chains may be high in CMP subcomponents with a high content of carbohydrate chains [21]. As expected from the reverse-d-phase separation (Fig. 1), these forms are eluted earlier. The average distribution of the different sugar chains A, B, C, D and E was estimated to be 0.8, 6.3, 18.4, 18.5 and 56% respectively, following alkaline borohydride treatment and analysis of the carbohydrates linked on the κ-casein molecule [9]. These data are consistent with our results except for the existence of species containing GalNAc (A), which are not detected under our ESI-MS analysis conditions. This suggests that either these species are present in very small quantities, and consequently at levels that are below the detection limit of the experimental set-up used, or that they do not exist. It cannot be precluded that the monosaccharide A is an artefactual component formed by alkaline β-elimination during the isolation of carbohydrate chains from κ-casein [9]. The points of attachment for carbohydrates are four Thr residues (131, 133, 135 or 136, and 142) and one Ser141 of the peptide chain [11,12]. The maximum number of glycosylation sites deduced from our results was three out of five potential sites. Consequently a maximum of six NeuAc groups can be linked per peptide chain, which is not in agreement with the value of ten obtained for the κ-casein B variant by Vreeman et al. [11]. The latter result was based on the determination of NeuAc from chromatographic fractions. No evidence of such masses was found in MS analysis. This discrepancy may be explained by genetic factors since variant B is known to be more efficiently glycosylated than variant A [22]. From our data, one can conclude that only a part of the potential glycosylation sites are substituted for the variant A κ-casein. There is an ambiguity about the structural assignment of three masses, i.e. those with M_r 9048, 8759 and 8102. For each, two possible distributions of carbohydrate chains can be considered. We cannot discriminate between these two structures with this approach. One potential alternative is to use ESI-MS–MS analysis to this end, as well as to locate the three Thr/Ser residues which are glycosylated. Efficient strategies are based on enzymatic digestion

of the glycoprotein into smaller fragments followed by a selective detection of O-linked glycopeptides by comparison of mass spectral data obtained before and after deglycosylation. Glycopeptides are then chosen for MS–MS analysis in order to locate the attachment sites. The same procedure involving degradation of the large molecule to smaller fragments is, of course, valid for the location of the phosphorylation sites. In this work, we have demonstrated the occurrence of triphosphorylated forms consistent with the literature [11]. However, of the three phosphorylation sites in κ-casein only two of are known. Ser127 and Ser149 are partly and completely phosphorylated, respectively [23]. Therefore, the third phosphate group might occur on either potential acceptor, Thr135 or Thr145, located in a tripeptide recognition site [23]. Another interesting result is the finding of a diphosphorylated form of CMP_A with only one E chain. Such a structure has not been reported previously. The low abundance of di- and triphosphorylated carbohydrate chains indicates that multiphosphorylation drastically inhibits the ability of the κ-casein molecule to be glycosylated. It is noteworthy that all glycosylation and phosphorylation sites are positioned on a short segment of the polypeptide chain involving only 20 amino acid residues.

To conclude, the results presented here demonstrate that the combination of RP-HPLC online with ESI-MS is a powerful method for the precise determination of the masses of a large number of glyco- and phosphopeptides within a heterogeneous mixture. As shown from the example of CMP_A, structural details of different molecular forms can be easily obtained when both the peptide and oligosaccharide chains are known. This procedure is rapid and a great amount of information can be obtained from one chromatographic run. The approach described here should be suitable for solving a wide variety of protein and peptide analytical problems.

Acknowledgement

The authors wish to thank Drs J.C. Mercier and P. Martin for helpful discussions.

References

[1] N. Azuma, K. Yamauchi and T. Mitsuoka, Agric. Biol. Chem., 48 (1984) 2159.
[2] L.S. Vasilevskaya, Fiziol. Zhur. SSSR imemi I.M. Sechenova, 64 (1978) 871.
[3] M.P. Chernokov and E.Y. Stan and L.S. Vasilevskaya, Vopr. Pitaniya, 5 (1979) 22.
[4] P. Jollès, S. Lévy-Toledano, A.M. Fiat, C. Soria, D. Gillessen, A. Thomaidis, A. Dunn and F.W. Caen, Eur. J. Biochem., 158 (1986) 379.
[5] J.R. Neeser, A. Chambaz, S.D. Vedovo, M.J. Prigent and B. Guggenheim, Infect. Immun., 56 (1988) 3201.
[6] Y. Kawasaki, H. Isoda, M. Tanimoto, S. Dosako, T. Idota and K. Ahiko, Biosci. Biotechnol. Biochem., 56 (1992) 195.
[7] L. Ferretti, P. Leone and V. Sgaramella, Nucleic Acids Res., 18 (1990) 6829.
[8] H. Van Halbeek, L. Dorland, J.F.G. Vliegenthart, A.M. Fiat and P. Jollès, Biochem. Biophys. Acta, 623 (1980) 195.
[9] T. Saito and T. Itoh, J. Dairy Sci., 75 (1992) 1768.
[10] M. Takeuchi, E. Tsuda, M. Yoshikawa, R. Sasaki and H. Chiba, Agric. Biol. Chem., 49 (1985) 2269.
[11] H.J. Vreeman, S. Visser, C.J. Slangen and J.A.M. Van Riel, Biochem. J., 240 (1986) 87.
[12] C. Zevaco and B. Ribadeau-Dumas, Milchwissenschaft, 39 (1989) 206.
[13] H. Kawakami, Y. Kawasaki, S. Dosako, M. Tanimoto and I. Nakajima, Milchwissenschaft, 47 (1992) 688.
[14] T.W. Rademacher, R.B. Parekh and R.A. Divek, Annu. Rev. Biochem., 57 (1988) 785.
[15] J. Léonil and D. Mollé, J. Dairy Res., 58 (1991) 321.
[16] M.E. Hemling, G.D. Roberts, W. Johnson, S.A. Carr and S.A. Covey, Biomed. Environ. Mass Spectrom., 19 (1990) 677.
[17] V. Ling, A.W. Guzzetta, E. Canova-Davis, J.T. Stults, W.S. Hancock, T.R. Covey and B.I. Shushan, Anal. Chem., 63 (1991) 2909.
[18] J.C. Mercier, G. Brignon and B. Ribadeau-Dumas, Eur. J. Biochem., 35 (1973) 222.
[19] J.W. Metzger, C. Kempter, K.H. Wiesmüller and G. Jung, Anal. Biochem., 219 (1994) 261.
[20] H.B. Drohse, B. Foltmann, Biochem. Biophys. Acta, 995 (1989) 221.
[21] M. Takeuchi, E. Tsuda, M. Yoshikawa, R. Sasaki and H. Chiba, Agric. Biol. Chem., 48 (1989) 2789.
[22] G. Robitaille, K.F.N.G. Kwai-Hang and H.G. Monardes, J. Dairy Res., 58 (1991) 107.
[23] J.C. Mercier, Biochimie, 63 (1981) 1.

ELSEVIER

Journal of Chromatography A, 708 (1995) 231–243

JOURNAL OF CHROMATOGRAPHY A

Enantiomeric enrichment of partially resolved 4-hydroxy-2-carboxymethylcyclopentanone derivatives by achiral phase chromatography

Einārs Loža*, Daina Loļa, Andrejs Ķemme, Jānis Freimanis

Latvian Institute of Organic Synthesis, Aizkraukles str. 21, Rīga, LV-1006, Latvia

First received 3 February 1995; revised manuscript received 21 March 1995

Abstract

Enantiomeric purity of the chromatographic peaks of partially resolved (*R*)-4-hydroxy-2-carboxymethyl-2-cyclopentenone (**4**), (*R*)-4-hydroxy-2-methoxycarbonylmethyl-2-cyclopentenone (**2**), (*S*)-4-benzoyloxy-2-carboxymethyl-2-cyclopentenone (**5**), (*R*)-4-methoxy-2-carboxymethyl-2-cyclopentenone (**6**), (*R*)-4-methoxy-2-methoxycarbonylmethyl-2-cyclopentenone (**7**) and (−)-5-oxa-6-oxoprostaglandin E_1 C(15) epimers (**1A**) and (**1B**) in achiral normal-phase chromatography on silica gel is dependent on the fraction which is being examined. The mentioned substances exhibit an enantiomer enrichment at the beginning of the chromatographic peak and a gradual depletion in the following parts. The observed enantiomer enrichment effect can be explained by a mechanistic concept which assumes a preferred association between the antipodes of the solute.

1. Introduction

In spite of being contradictory to the generally accepted concept that for chromatographic methods to produce differences in retention times of enantiomers either the stationary phase or the mobile phase must be optically active, in the last decade experimental data suggesting that this assumption is not generally valid have been obtained [1–9]. This problem has been reviewed recently along with its possible explanations [10].

The most confusing examples concern the resolution of racemates by means of chromatographic methods in a totally achiral system [1,8]. Szczepaniak and Ciszewska [1] explained their results for the resolution of D,L-amino acids by achiral ion-exchange chromatography as a consequence of different free energies of formation of the particular enantiomer complexes and hence the differences in the distribution coefficients. Similarly, complex formation has been held responsible for the resolution of ^{14}C-labelled lactic acid enantiomers by Cecchi and Malaspina [8], who used precoated TLC plates with copper(II) acetate. On the other hand, the above results are contradictory in terms of the common opinion that chiral recognition can be effected only by another chiral molecule, and that with optically inactive reagents all enantiomers will have the same reaction rate and equilibrium constants.

The second group of optical resolution of enantiomers by achiral chromatography pertains to the resolution of enantiomers from mixtures

* Corresponding author.

0021-9673/95/$09.50
SSDI 0021-9673(95)00385-1

in which one of them is already in excess. Actually such a chromatographic system cannot be considered as totally achiral because of the presence of a chiral component, an enantiomerically enriched substrate. Consequently, in this case changes in enantiomeric composition (or enantiomeric enrichment) can be interpreted by an enantiomeric differentiation induced solely by an already existing enantiomeric excess during chromatography [2–7,9]. Enantiomeric enrichment of partially resolved substances by achiral phase chromatography has been observed in the cases of nicotine [2], mono- and dipeptide derivatives [3,5,6], 9-methyl-$\Delta^{5(10)}$-octalin-1,6-dione [4], 1,1′-bi-2-naphthol, 1-anthryl-2,2,2-trifluoroethanol, chloromezanone, benzodiazepine camazepam [6], hydroxycineole [7] and sulfoxides [9]. This effect seems not to be limited by any particular chromatographic method or sorbent; these examples cover traditional column chromatography [3,4], flash chromatography [9] and preparative HPLC [2,5–7] using columns packed with normal- and reversed-phase silica gel [3–5,7,9], a cation exchanger [2], aminopropylsilica gel [6] or alumina [9]. However, in some cases the choice of the sorbent was crucial, e.g., the enantiomeric differentiation during chromatography failed on changing aminopropylsilica gel to an unmodified sorbent [6].

2. Experimental

2.1. General

Optical rotation measurements were conducted on a Perkin-Elmer (Überlingen, Germany) Model 141 polarimeter at 20°C. ^{1}H NMR spectra were recorded at room temperature with WH-90/DS and WM-360 spectrometers (Gilberstreifen, Germany) in deuterochloroform using tetramethylsilane (TMS) as internal standard. Mass spectra were recorded on a MS-50 mass spectrometer (AEI, Manchester, UK) operating at an ionizing potential of 70 eV. IR spectra were recorded with a Perkin-Elmer (V. Frölunda, Sweden) Model 580 B spectrophotometer.

2.2. Materials

All the solvents were purified before use by routine techniques. Optically enriched (*R*)-4-hydroxy-2-methoxycarbonylmethyl-2-cyclopentenone (**2**), (*R*)-4-hydroxy-2-carboxymethyl-2-cyclopentenone (**4**), (*S*)-4-benzoyloxy-2-carboxymethyl-2-cyclopentenone (**5**), (*R*)-4-methoxy-2-carboxymethyl-2-cyclopentenone (**6**) and (*R*)-4-methoxy-2-methoxycarbonylmethyl-2-cyclopentenone (**7**) were synthesized in our laboratory by published procedures [11,12].

2.3. Chromatography

Analytical and preparative normal-phase HPLC were conducted on a Laboratórni Přístroje (Prague, Czechoslovakia) chromatograph using a 150 × 3 mm I.D. column packed with Separon SGX (5 μm) (Tessek, Prague, Czechoslovakia) and a 250 × 10 mm I.D. column packed by Elsiko (Moscow, Russian Federation) with Silasorb SPH 600 (9 μm) (Lachema, Brno, Czechoslovakia), respectively. A differential refractometer in series with a spectrophotometer were used as detectors. The same mobile phases were used for preparative and analytical HPLC runs (see Tables 2–4). In the optical enrichment experiments by preparative HPLC, 0.3 ml of solution containing 30–50 mg of substrate was introduced into the injector loop and chromatographed at a flow-rate 5 ml/min. A 600 × 25 mm I.D. column (LKB, Bromma, Sweden) packed with Silasorb 600 silica gel (30 μm) was employed for column chromatography. TLC analyses were performed on DC-Alufolien Kieselgel 60 F_{254} plates (Merck, Darmstadt, Germany).

2.4. Syntheses

(R)-4-Hydroxy-2-carboxymethyl-2-cyclopentenone (**4**)

4-Hydroxy-2-methoxycarbonylmethyl-2-cyclopentenone (**2**) (3.5076 g, 20.6 mmol, $[\alpha]_{365}^{20} = -589.8$ ($c = 1.057$, CH_3OH)) and 0.1 *M* HCl (40 ml) were stirred under reflux for 3 h. To the reaction mixture was added pyridine (0.28 ml, 3.5 mmol) and the solvent was evaporated. The

residue was chromatographed on silica gel (120 g) with $CHCl_3$–dioxane–AcOH (65:35:1.5, v/v/v) as eluent to give 2.9623 g (92%) of pure **4**. R_F [$CHCl_3$–dioxane–AcOH (65:35:1, v/v/v)] 0.28. $[\alpha]_{365}^{20} = -488$ ($c = 1.00$, CH_3OH). ^1H NMR (360 MHz), δ: 7.49 (d, $J = 2.6$, 1H), 5.05 (ddd, $J =$ 2.6, 2.2 and 6.0, 1H), 3.34 (s, 2H), 2.88 (dd, $J = 6.0$, 18.8, 1H), 2.39 (dd, $J = 2.2$, 18.8, 1H). MS, m/z (%): 156 (1) $[M]^{+\cdot}$, 138 (60) $[M - H_2O]^{+\cdot}$, 110 (44) $[M - HCOOH]^{+\cdot}$, 96 (100) $[M - CH_3COOH]^{+\cdot}$.

Tetrahydropyranyl 4-iodobutyrate

To a saturated solution of *p*-toluenesulfonic acid in CH_2Cl_2 (50 ml) under an argon atmosphere was added 4-iodobutyric acid (4.87 g, 22.8 mmol) and freshly distilled dihydropyran (12.45 ml, 136.5 mmol) and the resulting solution was stirred at room temperature until the initial compound had disappeared (1.5 h). To the reaction mixture was added triethylamine (0.5 ml, 3.6 mmol), the solvent was evaporated and the residue was dried under vacuum to give 7.5 g of crude product. For a further synthesis, tetrahydropyranyl 4-iodobutyrate was used without an additional purification. R_F [benzene–EtOAc (14:1, v/v)] 0.32. ^1H NMR (90 MHz), δ: 5.96 (m, 1H), 3.72 (m, 2H), 3.24 (t, 2H), 2.48 (t, 2H), 2.13 (m, 2H), 1.70 (m, 6H). IR (film, cm^{-1}): 1742. MS, m/z (%): 197 (36) $[M - C_5H_9O_2]^+$, 171 (2) $[M - I]^+$, 169 (14) $[M - COOC_5H_9O]^+$, 85 (100) $[C_5H_9O]^+$.

(R)-4-Hydroxy-2-(3'-tetrahydropyranyloxycarbonylpropyl)oxycarbonylmethyl-2-cyclopentenone

To a solution of (*R*)-**4** (2.9623 g, 19.0 mmol) with $[\alpha]_{365}^{20} = -488$ ($c = 1.00$, CH_3OH) in dry dimethylformamide (30 ml) under an argon atmosphere was added Cs_2CO_3 (3.25 g, 10.0 mmol) and the reaction mixture was stirred at 50°C for 1 h. To the reaction medium was added a solution of crude tetrahydropyranyl 4-iodobutyrate [prepared from 4.87 g (22.8 mmol) of 4-iodobutyric acid as described above] in dimethylformamide (25 ml) and the resulting mixture was stirred at 50°C for 6.5 h. The dark mixture was diluted with EtOAc (500 ml), washed with 1% $NaHCO_3$ (3 × 150 ml) and saturated NaCl (100 ml) and dried (Na_2SO_4). Before drying, to the EtOAc extract was added triethylamine (TEA) (0.5 ml, 3.6 mmol). The solvent was removed and the residue (12.4 g) was chromatographed on silica gel (150 g) with hexane–EtOAc–*iso*–PrOH–TEA (50:50:1:0.1, v/v) (900 ml) and (20:80:1:0.1, v/v) (800 ml) as eluents to give 4.55 g (73.5%) of pure product. $[\alpha]_{365}^{20} = -203$ ($c = 1.06$, CH_3OH), -210 ($c =$ 1.03, $CHCl_3$). R_F [hexane–EtOAc–dioxane (7:5:3, v/v/v)] 0.20. ^1H NMR (90 MHz), δ: 7.43 (m, 1H), 5.98 (m, 1H), 4.98 (m, 1H), 4.18 (t, 2H), 3.78 (m, 2H), 3.27 (m, 2H), 3.09 (s, 1H), 2.84 (dd, 1H), 2.47 (t, 2H), 2.41 (dd, 1H), 2.01 (m, 2H), 1.73 (m, 6H). MS, m/z (%): 139 (51) $[M - O(CH_2)_3COOC_5H_9O)]^+$, 138 (51) $[M - CH_2 = CHCH_2COOC_5H_9O - H_2O]^{+\cdot}$, 110 (100) $[M - HCOO(CH_2)_3COOC_5H_9O]^{+\cdot}$, 84 (9) $[C_5H_8O]^{+\cdot}$. IR (CH_2Cl_2, cm^{-1}): 3605, 3458, 1740, 1719, 1646.

(R)-4-Trimethylsilyloxy-2-(3'-tetrahydropyranyloxycarbonylpropyl)-oxycarbonylmethyl-2-cyclopentenone (**3**)

To a solution of the above-prepared (*R*)-4-hydroxy-2-(3'-tetrahydropyranyloxycarbonylpropyl)oxycarbonylmethyl-2-cyclopentenone (4.55 g, 13.9 mmol) with $[\alpha]_{365}^{20} = -210$ ($c = 1.03$, $CHCl_3$) in dry benzene (17 ml) under an argon atmosphere were successively added hexamethyldisilazane (3.00 ml, 14.2 mmol) and chlorotrimethylsilane (0.92 ml, 7.2 mmol), and the reaction mixture was stirred at room temperature for 3 h. The solvent and volatiles were evaporated and the residue was dissolved in Et_2O–hexane (1:1, v/v) (200 ml) and stored at −18°C overnight. The solution was filtered, washed with Et_2O–hexane (1:1, v/v) (30 ml) and evaporated to give 5.00 g (90.0%) of pure **3**. $[\alpha]_{365}^{20} = -258$ ($c = 0.96$, $CHCl_3$). R_F [hexane–EtOAc–dioxane (7:5:3, v/v/v) 0.65. ^1H NMR (90 MHz), δ: 7.31 (m, 1H), 5.96 (m, 1H), 4.92 (m, 1H), 4.15 (t, 2H), 3.73 (m, 2H), 3.23 (m, 2H), 2.76 (dd, 1H), 2.44 (t, 2H), 2.33 (dd, 1H), 1.99 (m, 2H), 1.69 (m, 6H), 0.18 (s, 9H). MS,

m/z (%): 314 (3) $[M-C_5H_8O]^{+\cdot}$, 211 (35) $[M-O(CH_2)_3COOC_5H_9O]^+$, 182 (39) $[M-HCOO(CH_2)_3COOC_5H_9O]^{+\cdot}$, 85 (87) $[C_5H_9O]^+$, 75 (100) $[(CH_3)_2SiOH]^+$. IR (CH_2Cl_2, cm^{-1}): 1739, 1717, 1646.

(−)-5-Oxa-6-oxoprostaglandin E_1 (**1A**) *and (−)-5-oxa-6-oxo-15-epi-prostaglandin E_1* (**1B**)

The (*RR* + *SS*)-diastereomer of 1-iodo-3-terahydrofuranyloxy-1-octene [13] (4.27 g, 13.2 mmol) under an argon atmosphere was dissolved in dry Et_2O (70 ml) and to this solution at −30°C was slowly (ca. 5 min) added 3.31 *M* *n*-BuLi hexane solution (4.18 ml, 13.8 mmol). The reaction mixture was stirred at −30 to −25°C for 15 min, then powdered pentynylcopper (1.46 g, 11.2 mmol) was added in one portion. The yellow suspension was stirred at −25 to −20°C for 15 min, cooled to −70°C and (*R*)-**3** (5.00 g, 12.5 mmol, $[\alpha]_{365}^{20} = -258$ (c = 0.96, $CHCl_3$)) solution in Et_2O (35 ml) was slowly (ca. 20 min) added at −70 to −65°C. Stirring was continued at −70°C for 10 min, then the mixture was allowed gradually to warm to −40°C during 30 min. To the yellowish brown suspension was added glacial AcOH (1.5 ml, 26.2 mmol), the cooling bath was removed and the mixture was stirred for 15 min. The reaction mixture was diluted with EtOAc (100 ml), filtered and the precipitate was washed with EtOAc (2 × 50 ml). The green filtrate was evaporated, the residue was dissolved in dioxane (100 ml), and to the solution was added 0.1 *M* HCl (100 ml). The reaction mixture was stirred at room temperature for 3 h, saturated with crystalline NaCl, extracted with EtOAc (3 × 150 ml), washed with saturated NaCl (50 ml) and dried (Na_2SO_4). Before drying, to the extract was added triethylamine (0.2 ml, 1.4 mmol). The solvent was evaporated and the residue (9.49 g) was chromatographed on silica gel (100 g) with hexane–dioxane–AcOH (58:42:1, v/v/v) (1000 ml) and (20:80:1, v/v/v) (300 ml) as eluents to give 3.948 g of product containing mainly the isomers **1A** and **1B**. Spatial orientation of the C(15) OH group was ascribed on the basis of the observations that usually the 15α-isomer of prostaglandins and their derivatives in normal-phase chromatography is more polar than the corresponding 15β-isomer [14]. A 0.9333-g amount of the isomer mixture **1A** + **1B** was chromatographed on silica gel (110 g) with $CHCl_3$–acetone–AcOH (40:60:1, v/v/v) (1000 ml) as eluent. Each of the less polar isomer **1B** and more polar **1A** were divided into five consecutive fractions, which after evaporation and exhaustive drying afforded 0.3351 g (0.03276, 0.10181, 0.08790, 0.07577 and 0.03685 g) of **1B** (30.5%) and 0.3298 g (0.03946, 0.04593, 0.06661, 0.09981 and 0.07797 g) of **1A** (30.0%). **1A:** $[\alpha]_D^{20}$, see Table 3, entry 6. R_F [$CHCl_3$–acetone–AcOH (50:50:1, v/v/v)] 0.18. ^1H NMR (360 MHz), δ: 5.78 (dd, 1H), 5.57 (dd, 1H), 4.18 (dt, 1H), 4.13 (q, 1H), 4.10 (q, 1H), 4.09 (dt, 1H), 2.79 (dd, 1H), 2.60 (dd, 1H), 2.55 (dd, 1H), 2.50 (m, 1H), 2.43 (t, 2H), 2.39 (m, 1H), 2.36 (dd, 1H), 1.98 (q, 2H), 1.53 (m, 2H), 1.30 (m, 6H), 0.89 (t, 3H), O*H* and COO*H* are not indicated. IR (THF, cm^{-1}): 3439, 3058, 1748, 1740. MS was recorded for methyl ester of **1A:** R_F [$CHCl_3$–acetone–AcOH (50:50:1, v/v/v)] 0.31. MS, *m/z* (%): 348 (0.2) $[M-2H_2O]^{+\cdot}$, 295 (0.6) $[M-H_2O-C_5H_{11}]^+$, 202 (7) $[M-2H_2O-HCOO(CH_2)_3COOCH_3]^{+\cdot}$, 177 (17) $[M-H_2O-C_5H_{11}-HO(CH_2)_3COOCH_3]^+$, 149 (48) $[M-H_2O-C_5H_{11}-HCOO(CH_2)_3\ COOCH_3]^+$, 101 (100) $[(CH_2)_3COOCH_3]^+$. Isomer **1B:** $[\alpha]_D^{20}$, see Table 3, entry 6. R_F [$CHCl_3$–acetone–AcOH (50:50:1, v/v/v)] 0.27. ^1H NMR (360 MHz), δ: 5.73 (dd, 1H), 5.60 (dd, 1H), 4.17 (dt, 1H), 4.15 (q, 1H), 4.13 (q, 1H); 4.12 (dt, 1H), 2.79 (dd, 1H), 2.61 (dd, 1H), 2.55 (dd, 1H), 2.50 (m, 1H), 2.43 (t, 2H), 2.40 (m, 1H), 2.35 (dd, 1H), 1.98 (q, 2H), 1.53 (m, 2H), 1.30 (m, 6H), 0.89 (t, 3H), O*H* and COO*H* are not indicated. IR (CH_2Cl_2, cm^{-1}): 3600, 1748, 1736, 1718. MS was recorded for methyl ester of **1B:** R_F [$CHCl_3$–acetone–AcOH (50:50:1, v/v/v) 0.36. MS, *m/z* (%): 348 (0.5) $[M-2H_2O]^{+\cdot}$, 295 (2) $[M-H_2O-C_5H_{11}]^+$, 202 (5) $[M-2H_2O-HCOO(CH_2)_3COOCH_3]^{+\cdot}$, 177 (16) $[M-H_2O-C_5H_{11}-HO(CH_2)_3COOCH_3]^+$, 149 (24) $[M-H_2O-C_5H_{11}-HCOO(CH_2)_3COOCH_3]^+$, 101 (100) $[(CH_2)_3COOCH_3]^+$.

Table 1
Crystal data and experimental conditions for X-ray analysis of **4**

Formula	$C_7H_8O_4$
Molecular mass	156.65
Crystal dimensions (mm)	0.10 × 0.35 × 0.45
Crystal system	Triclinic
Space group	$P\bar{1}$
a (Å)	4.691 (1)
b (Å)	5.351 (1)
c (Å)	14.345 (2)
α (°)	97.23 (1)
β (°)	95.64 (1)
γ (°)	96.48 (1)
V (Å^3)	354.8 (1)
Z	2
Calc. density (g/cm^3)	1.46
μ (Mo Kα) (cm^{-1})	0.8
Radiation	Mo Kα
λ (Å) (graphite monochromator)	0.7107
Diffractometer	Syntex $P2_1$
Maximum value (sin θ/λ)	0.596
Measured reflections	1424
Unique reflections	1255
Observed reflections	922
R (F)	0.0481
Max. residual electron density (e/Å^3)	0.20

2.5. X-ray diffraction studies

A racemic crystal for X-ray measurements of compound **4** was grown from a mixture of hexane and ethyl acetate. The reflection intensities were collected on a Syntex (Cupertino, CA, USA) $P2_1$ single-crystal diffractometer using graphite-monochromated Mo Kα radiation ($\lambda = 0.71069$ Å). The structure was solved by a direct method using the program SHELXS 86 [15] and refined by SHELXS 76 implemented on an IBM-PC/AT [16]. During refinement, absorption correction (program DIFABS) was applied [17]. Crystallographic data for **4** are listed in Table 1.

Results and discussion

We studied the phenomenon of enantiomeric enrichment of a partially resolved material by achiral-normal phase chromatography on silica gel working with cyclopentanone derivatives.

In connection with our recent efforts to prepare 5-hetero-6-oxoprostaglandins E_1 [18–20] we targeted the synthesis of optically active 5-oxa-6-oxoprostaglandin E_1 (**1A**) (Fig. 1). 4-Hydroxy-2-methoxycarbonylmethyl-2-cyclopentenone (**2**) partially resolved [enantimeric excess (*ee*) ca. 40%] by enzymatic methods [11] served as a starting compound for this synthesis. Cuprate addition of a racemic prostaglandin ω-chain to an appropriately modified synthon **3** followed by a hydrolysis of protective groups afforded the desired prostanoid **1A** as a mixture along with its C(15) epimer **1B**.

It was envisaged that the *ee* of each of the isomers **1A** and **1B** should be the same as for the starting synthon **2** provided that the chiral centre on a C(4) atom [or C(11) atom according to prostaglandin nomenclature] would not suffer racemization under the reaction conditions outlined in Fig. 1.

The epimer mixture **1A** + **1B** was purified from by-products using routine column chromatography on silica gel, but a further isolation of the individual C(15) isomers **1A** and **1B** was performed by preparative HPLC. Each of the baseline-separated chromatographic peaks of 5-oxa-6-oxoprostaglandin E_1 C(15) epimers **1A** and **1B** were divided into two parts in their maxima (Fig. 2).

Optical rotation measurements (at five wavelengths) of the samples obtained revealed apparent enantiomeric enrichment (changes in the optical purity really reflect changes in *ee*, as will be discussed later) of both C(15) epimers in the beginning of the chromatographic peak (*a*, *c*) and depletion in the last part (*b*, *d*) (Fig. 2 and Table 2).

The observed changes in optical purity of eluate were not due to undetected impurities or unexpected racemization during the chromatographic process because of the following considerations. (1) The ratios of optical rotation of the samples $a:b$ or $c:d$ (see Fig. 2 and Table 2) at the five wavelengths were constant, indicating an identical shape of the optical dispersion curve of the material obtained from both parts of the chromatographic peak. (2) Optical rotation values of the isomers **1A** and **1B** obtained by

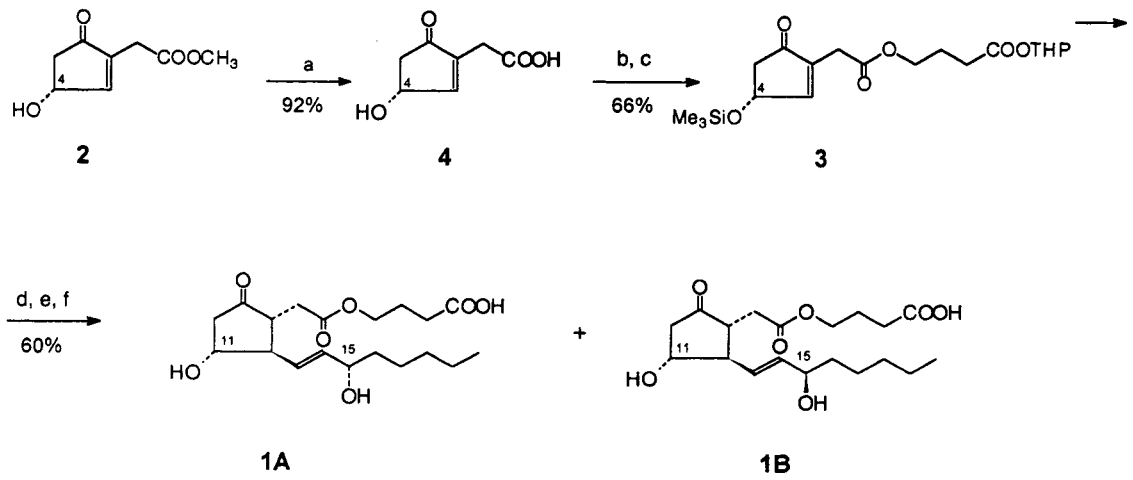

a) 0.1N HCl, reflux. b) Cs_2CO_3 / $I(CH_2)_3COOTHP$ / DMF. c) Me_3SiCl / $(Me_3Si)_2NH$.
d) $LiCu(\text{vinyl-}C_5H_{11})(-C{\equiv}C-C_3H_7)$. e) 0.1N HCl-dioxane, 1:1. f) Chromatography.

Abbreviations: THF - tetrahydrofyranyl, THP - tetrahydropyranyl.

Fig. 1. Synthesis of **1A** and **1B**.

collecting all the corresponding chromatographic peak were nearly the same as calculated from the divided samples (Table 2), i.e., an overall depletion of one antipode in the part of eluate was equivalent to its enrichment in the other as required by the mass balance. (3) HPLC analysis of the samples *a–d* (Fig. 2) did not reveal impurity peaks; further, both *a* and *b* or *c* and *d* were chromatographically (HPLC and TLC) and spectroscopically (NMR) non-distinctive. (4) The observed changes of the optical rotation were not due to racemization because it is impossible to imagine a reasonable process changing simultaneously to the same extent all four different stereogenic centres of a prostanoid molecule, but epimerization of a few of them should be easily detectable by HPLC and NMR.

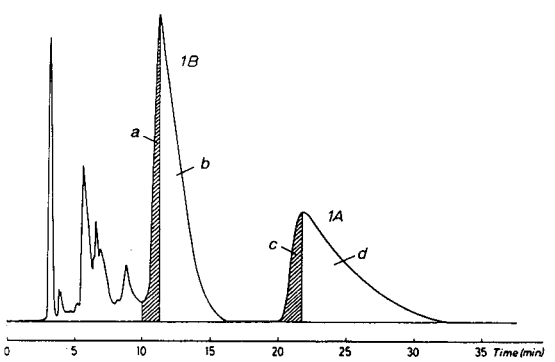

Fig. 2. HPLC separation of (−)-5-oxa-6-oxoprostaglandin E_1 C(15) epimers **1A** and **1B**. Conditions: mobile phase, hexane–ethyl acetate–acetic acid (20:80:1, v/v/v); column, 250 × 10 mm I.D., Silasorb SPH 600 (9 μm); injection volume, 0.3 ml; flow-rate, 5 ml/min; detector, refractometer.

Several experiments were carried out revealing that the optical enrichment of prostanoids **1A** and **1B** during chromatography was not accidental but really was an intrinsic feature persistent to the chromatographic system under consideration.

First, it was established that each of the preliminary separated single isomers **1A** and **1B** on passing through a new preparative HPLC

Table 2
Optical rotation data ($[\alpha]_\lambda^{20}$, in CH_3OH) for samples of prostaglandin E_1 analogues **1A** and **1B** obtained by dividing the corresponding preparative HPLC peaks into two parts in their maxima

λ (nm)	Compound **1B**					Compound **1A**				
	$[\alpha]_\lambda^{20}$ of divided[a] chrom. peak		Ratio of $[\alpha]_\lambda^{20}$ for	$[\alpha]_\lambda^{20}$ calculated[b] for full peak	$[\alpha]_\lambda^{20}$ of full peak	$[\alpha]_\lambda^{20}$ of divided[a] chrom. peak		Ratio of $[\alpha]_\lambda^{20}$ for	$[\alpha]_\lambda^{20}$ calculated[b] for full peak	$[\alpha]_\lambda^{20}$ of full peak
	a	*b*	*a* : *b*			*c*	*d*	*c* : *d*		
589	−30.3	−11.3	2.67	−15.3	−16.5	−24.3	−11.2	2.17	−14.0	−14.3
578	−31.9	−11.9	2.68	−16.2	−17.4	−25.1	−11.7	2.20	−14.7	−15.1
546	−37.7	−14.1	2.67	−19.1	−20.3	−30.4	−13.9	2.19	−17.4	−17.9
436	−82.8	−31.3	2.65	−42.3	−45.1	−68.6	−31.2	2.20	−39.2	−40.6
365	−201.3	−79.9	2.52	−105.8	−112.3	−173.5	−79.2	2.19	−99.4	−103.5
Mass (%)[c]	21.3	78.7			100	21.4	78.6			100
c	1.63	1.62			1.90	1.67	1.65			1.87

Eluent, hexane–ethyl acetate–acetic acid (20:80:1), v/v/v); for other conditions of HPLC separation, see Experimental.

[a] For designations *a*, *b*, *c* and *d*, see Fig. 2.

[b] Optical activity $[\alpha]$ of full chromatographic peak was calculated by the equation $[\alpha] = \Sigma[\alpha]_n m_n$ where $[\alpha]_n$ is the optical activity of part *n* of the peak and m_n is the relative mass of part *n* with respect to the full peak.

[c] With respect to the full peak.

column gave an optically enriched material in the first portion of the chromatographic peak and gradually depleted in the following portions (Table 3; entries 1 and 2).

The same was true using the isomer **1A** of different optical purity obtained in the previous optical enrichment experiments (Table 3; entries 3 and 4). These results indicated that the enrichment was not due to a column contaminated with an unknown chiral compound and further strengthened our confidence that there were no undetected impurities in the sample responsible for the observed effect. Changing the eluent from hexane–ethyl acetate–acetic acid (20:80:1, v/v/v) to chloroform–acetone–acetic acid (60:40:1, v/v/v) diminished the observed effect (Table 3; entry 5). The enantiomer enrichment effect remained after changing the HPLC column to the usual LC column, although the changes in optical purity were not so expressive (Table 3, entry 6).

Being interested in this unexpected phenomenon, we also examined the chromatographic behaviour of 4-hydroxy-2-carboxymethyl-2-cyclopentenone (**4**) and several its derivatives, **2**, **5**, **6** and **7** (see Table 4).

Surprisingly, virtually all of the compounds tested showed a similar effect: an optical enrichment in the first part of the chromatographic peak and gradual depletion in the following parts of the peak (Table 4). On the basis of the optical rotation measurements depicted in Table 4, one can easily confirm that the arguments (1) and (2) proposed to prove the reliability of an enantiomeric enrichment phenomenon for prostanoids **1A** and **1B** still remain valid. The same applies to HPLC, TLC and NMR analysis; samples obtained from divided chromatographic peaks by preparative HPLC of the corresponding cyclopentenone derivatives were non-distinctive. Since the cyclopentenone molecules **2** and **4–7** possess only one stereogenic centre, excluding racemization of the compound during chromatography is more difficult. However, in our case this was not a cause because the values of the total optical activity of fractionated samples were equal to those before chromatography (Table 4). In addition, it has been shown [12,21] that protonation of 4-hydroxy-2-carboxymethyl-2-cyclopentenone (**4**) and its methyl ester **2** in moderately acidic media and chromatographic purification do not affect the stereogenic centre of the molecule.

Unfortunately, we were not able to find an alternative direct method to detect the enantiomeric purity of the samples; the only criterion to judge changes in enantiomeric ratios were the optical rotation measurements. Nevertheless, optical rotation data obtained at five wavelengths combined with chemical purity control (analytical HPLC and TLC) provide a sufficiently reasonable basis to consider that our results really reflect the changes in enantiomeric excess during chromatography of the investigated compounds, although in a relative sense; however, this does not change the point of the matter.

The experimental data obtained fit a mechanistic concept for the explanation of an enantiomeric enrichment effect which is based on thermodynamically non-ideal behaviour of molecules, i.e., on molecular interactions [3,4].

Retention in liquid chromatography is a complex process involving solute interactions in both the mobile and stationary phases that are difficult to describe exactly [22]; nevertheless, a simplified working hypothesis assuming bilayer formation (solvent interaction model) on the surface of adsorbent would be the following.

It is evident that the molecular surrounding of, e.g., the (−)-isomer in the enantiomerically enriched [(−)] > [(+)] mixture (or a solution of their mixture) is different from the molecular surrounding of the corresponding (+)-isomer in the same mixture. Statistically, *homo*-associations (−)···(−) in this case numerically exceed *cross*-associations (−)···(+), which in turn exceed *homo*-associations (+)···(+). The thermodynamics of these interactions may or may not be the same, thus affecting these statistical ratios. On the other hand, interactions of the both (−)- and (+)-antipodes with a sorbent should be identical (provided that distortions induced by thermodynamically non-ideal behaviour of molecules are ignored) forming the first layer of adsorbed molecules which contains both enantiomers in amounts close to their initial

Table 3
Optical purity changes across the chromatographic peaks of prostaglandin E_1 analogues **1A** and **1B** in achiral normal-phase chromatography

Expt. No.	Substrate	Method	Eluent composition (v/v)	$[\alpha]_D^{20}$[a] (mass-% of peak)	$[\alpha]_D^{20}$ calculated[b] for full peak	$[\alpha]_D^{20}$ of full peak
1	**1A**	HPLC	Hexane–EtOAc–AcOH (10:90:1)	−32.8 (25.9); −13.8 (36.6); −9.7 (37.5)	−17.2	−16.2[c]
2	**1B**	HPLC	Hexane–EtOAc–AcOH (25:75:1)	−40.8 (17.8); −22.8 (34.9); −12.0 (47.1)	−20.9	−19.8[c]
3	**1A**	HPLC	Hexane–EtOAc–AcOH (10:90:1)	−26.3 (23.3); −8.8 (76.7)	−12.8	−12.0[c]
4	**1A**	HPLC	Hexane–EtOAc–AcOH (10:90:1)	−33.8 (20.8); −30.4 (42.0); −17.0 (37.2)	−26.1	−27.1[c]
5	**1A** + **1B**	HPLC	$CHCl_3$–acetone–AcOH (60:40:1)	**1B:** −25.0 (21.8); −15.1 (78.2) **1A:** −24.9 (25.2); −15.1 (74.8)	−17.3 −17.6	−16.5[d] −14.3[d]
6	**1A** + **1B**	LC	$CHCl_3$–acetone–AcOH (60:40:1)	**1B:** −16.4 (9.8); −19.0 (30.4); −16.2 (26.2); −15.4 (22.6); −11.5 (11.6) **1A:** −16.9 (12.0); −18.2 (13.9); −16.7 (20.2); −15.1 (30.3); −13.2 (23.6)	−16.4 −15.6	−16.5[d] −14.3[d]

For conditions of HPLC and LC separations, see Experimental.

[a] $[\alpha]_D^{20}$ values of chromatographic fractions (c = 1.00–1.15, CH_3OH) are given in order of their elution from the column; the first fraction in the experiments 1–5 covers the chromatographic peak from the beginning up to its maximum point. Optical rotation was measured at 589 (D line), 578, 546, 436, and 365 nm; analysis of the data obtained allowed the same conclusions to be drawn as from the measurements depicted in Table 2.

[b] Footnote b, Table 2.

[c] Before chromatography.

[d] Purified with hexane–EtOAc–AcOH (20:80:1, v/v/v) as eluent. Value taken from Table 2.

Table 4
Optical purity changes across the chromatographic peaks of cyclopentenones **2** and **4–7** in achiral normal-phase HPLC

Compound and eluent composition (v/v)	$[\alpha]_\lambda^{20}$ (c = 0.58–1.45, CH_3OH)						Ratio of $[\alpha]_\lambda^{20}$ for $a:b:c$
	λ (nm)	Divided peak[a]			Before chrom.	Calculated[b] for full peak	
		a	*b*	*c*			
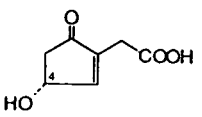 **4**	589	37.9	29.5	21.4	26.9	27.5	1.77 : 1.38 : 1
	578	37.6	29.1	21.2	26.5	27.2	1.77 : 1.37 : 1
	546	36.0	28.0	20.3	25.4	26.1	1.77 : 1.38 : 1
	436	−53.8	−41.0	−31.7	−39.2	−39.2	1.70 : 1.29 : 1
	365	−1215.0	−938.8	−706.5	−874.0	−887.7	1.72 : 1.33 : 1
Hexane–EtOAc–AcOH (20:80:1)	Mass (%)[c]	16.9	41.0	42.1			
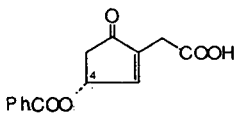 **5**	589	−97.7	−95.1	−65.5	−78.8	−79.1	1.49 : 1.45 : 1
	578	−101.0	−99.1	−73.4	−82.1	−85.1	1.38 : 1.35 : 1
	546	−114.9	−112.0	−77.1	−92.6	−93.1	1.49 : 1.45 : 1
	436	−171.3	−167.5	−115.4	−137.9	−139.1	1.48 : 1.45 : 1
	365	157.5	152.4	86.0	129.9	116.3	1.83 : 1.77 : 1
Hexane–EtOAc (70:30)	Mass (%)[c]	21.0	23.0	56.0			
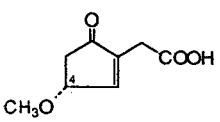 **6**	589	3.8	2.0		2.4	2.4	1.90 : 1
	578	5.5	3.3		3.1	3.8	1.67 : 1
	546	2.8	1.6		1.1	1.9	1.75 : 1
	436	−54.2	−34.9		−37.2	−39.3	1.55 : 1
	365	−651.2	−414.4		−435.3	−468.8	1.57 : 1
Hexane–EtOAc (40:60)	Mass (%)[c]	23.0	77.0				
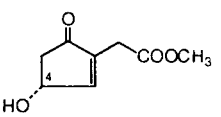 **2**	589	19.4	14.8	12.6	15.4	15.0	1.54 : 1.17 : 1
	578	19.9	15.3	13.1	15.6	15.5	1.52 : 1.17 : 1
	546	19.2	14.6	12.7	15.2	14.9	1.51 : 1.15 : 1
	436	−24.6	−19.5	−16.1	−19.0	−19.4	1.52 : 1.21 : 1
	365	−609.6	−473.8	−396.8	−475.8	−476.6	1.54 : 1.19 : 1
Hexane–EtOAc (30:70)	Mass (%)[c]	22.0	42.8	35.2			
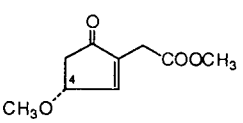 **7**	589	7.6	5.4			5.8	1.41 : 1
	578	9.4	6.7			7.2	1.40 : 1
	546	4.7	3.0			3.3	1.51 : 1
	436	−88.9	−72.7			−75.6	1.22 : 1
	365	−1090.8	−879.7			−917.9	1.24 : 1
Hexane–EtOAc (40:60)	Mass (%)[c]	18.1	81.9				

For conditions of HPLC separations, see Experimental.
[a] Fractions from divided chromatographic peak are given in the order of their elution from the column; fraction *a* covers the chromatographic peak from the beginning up to the maximum point.
[b] Footnote b, Table 2.
[c] With respect to the full peak.

statistical ratio. If the (−)-isomer energetically prefers *cross*-associations (−)···(+) to *homo*-associations (−)···(−) the second layer of more weakly associated molecules should contain both enantiomers in a ratio different from the initial ratio or, in our example, increased in the (+)-isomer compared with the initial ratio. As a result, the partition coefficient of the (+)-isomer between the stationary and the mobile phases will be larger than that of the (−)-isomer {provided that all the time [(−)] > [(+)]} and hence the first fractions of the eluate will be enriched in the (−)-isomer.

If this mechanistic concept is applicable to interpret the enantiomeric enrichment phenomenon, there should be the following consequences: (1) if *cross*-associations of solutes are preferred to *homo*-associations, the first fractions of eluate will be enriched in the enantiomer present in excess; (2) if *homo*-associations of solutes are preferred to *cross*-associations, the outcome will be the opposite, i.e., the last fractions will be enriched in the enantiomer present in excess; (3) apparently, one might under the most favourable circumstances be able to separate not more than the excess enantiomer from the residual racemic mixture by this procedure. It is noteworthy that the character of enantiomeric enrichment (enriched at the beginning of the chromatographic peak or vice versa) should not be susceptible to the retention mechanism (type of adsorbent).

All our optical resolution experiments by achiral normal-phase chromatography gave an eluate enriched in the first fractions with the enantiomer present in excess {an example of a reversed enantiomeric enrichment (i.e., the eluate enriched in the last fractions of the chromatographic peak) can be found in the Ref. [3]}. Consequently, according to the above-discussed mechanistic concept, in our case *cross*-associations of enantiomers should be favoured over *homo*-associations. Trying to find evidence for such a behaviour, we found that crystalline enantiomerically enriched cyclopentanone derivatives **1A**, **4** and **5** all tend to crystallize as racemates. This observation indicates that enantiomeric crystal packing forces of **1A**, **4** and **5** are stronger than homomeric ones. Moreover, in the case of racemic **4**, X-ray structural investigations were performed. A perspective view of the molecular packing of **4** in the unit cell with crystallographic labelling of atoms is shown in Fig. 3.

Two kinds of hydrogen bonds of an intermolecular nature were found in the crystal structure of **4** (Table 5). The shortest of them includes two hydrogen bonds (e.g., O3–H103···O2) which are generated by an inversion centre; they bond enantiomeric molecules (antipodes) in the crystal via carboxyl groups. The second kind of hydrogen bonds is formed by hydroxy and oxo functions of the cyclopentenone **4** molecule, and they are responsible for bonding of infinite chains parallel to shorter diagonals of the *ab* planes of the crystal.

Another explanation of the enantiomeric enrichment phenomenon is based on an assumption

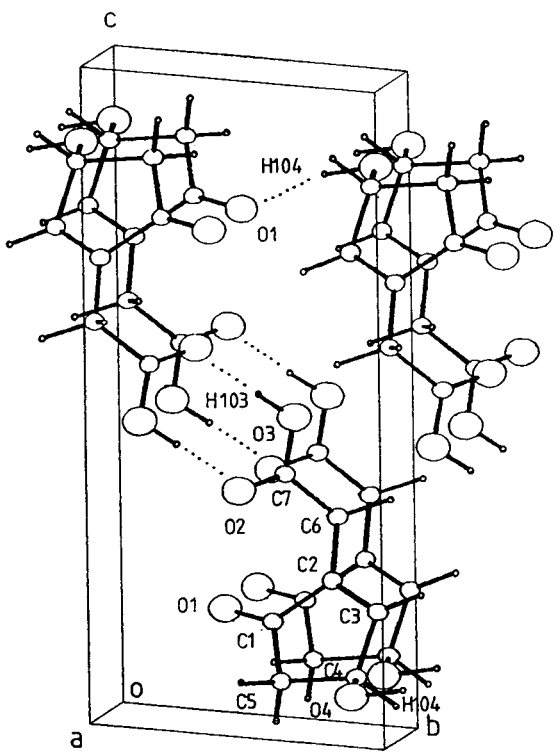

Fig. 3. Perspective view of the molecular packing of (±)-**4** in the unit cell.

Table 5
Intermolecular hydrogen bonds in **4**

D–H···A	D–H (Å)	D···A (Å)	H···A (Å)	Angle at H (°)	Acceptor symmetry
O3–H103···O2	0.93 (4)	2.674 (3)	1.75 (4)	175 (3)	$-x, -y, -z$
O4–H104···O1	1.01 (4)	2.813 (3)	1.83 (4)	164 (4)	$1+x, 1+y, z$

that differences in retention times of the racemate and an individual antipode could be due to different mobilities of more or less stable *homo*- and *hetero*-associates during chromatography [2,5,6]. On the other hand, it is well known [23] that carboxylic acids tend to form dimeric associates via carboxyl groups, especially in an aprotic medium. We tested the analytical HPLC mobilities of compounds **1A** and **4** [the amount of samples chromatographed was 15 μg in 3 μl and the eluent was hexane–EtOAc–AcOH (10:90:1)]. Unfortunately, we were not able to find any statistically credible retention time differences for racemic and optically active forms of these substances. The obtained retention times (retention time values are given in the form $x \pm$ S.D., where x is the mean value and S.D. is the standard deviation) were as follows: (±)-**1A**, 12.74 ± 0.23 (five injections); (−)-**1A** {$[\alpha]_D^{20} = -33.8$ ($c = 1.02$, CH_3OH)}, 12.73 ± 0.30 (five injections); (±)-**4**, 7.69 ± 0.32 (six injections); and (*R*)-**4** {$[\alpha]_D^{20} = +37.9$ ($c = 0.96$, CH_3OH), *ee* ca. 100%}, 7.72 ± 0.33 min (six injections). Moreover, according to the structures of cyclopentenones given in Table 4, carboxylic acids **4**, **5** and **6** should be able to form the strongest H-bonds. H-bonding of the secondary alcohol **2** should be less strong than in the case of the above carboxylic acids but the cyclopentenone **7** is not capable of forming H-bonds at all. Nevertheless, the data given in Table 4 indicate that there are no substantial enantiomer enrichment differences among the compounds of these groups. Apparently, in the case of cyclopentenones **2** and **4–7** the capability to form H-bonds and hence more stable associates does not play a crucial role in ensuring the enantiomeric enrichment during chromatography. It is likely that other kinds of associates, e.g., formed by Van der Waals forces, could also be of great importance.

Summing up the observations made by other investigators [2–7,9] and guided by our experience, it seems reasonable to assume that the enantiomeric differentiation proceeds in a relatively dense medium where the formation of more organized structures than in solution is possible. Such a medium could be, e.g., on the surface of the absorbent [3,4]. Moreover, the observations [5–7] that enantiomer differentiation increases up to a point on increasing the amount of sample loaded and experiments performed by Diter et al. [9] showing that changes in the length of chromatographic column (sixfold!) only slightly affected the enantiomeric enrichment strongly suggest that the main part of the optical resolution proceeds directly after loading the column, maybe even under overloaded conditions [5].

Acknowledgements

This work was supported by grant No. 447 from the Latvian Council of Science, Latvia.

The authors are grateful to Drs. Ivars Turovskis, Solveiga Rozīte and Ivars Dipāns, all at the Latvian Institute of Organic Synthesis, for carrying out ^{1}H NMR, MS and IR spectral measurements.

References

[1] W. Szczepaniak and W. Ciszewska, Chromatographia, 15 (1982) 38.
[2] K.C. Cundy and P.A. Crooks, J. Chromatogr., 281 (1983) 17.

[3] R. Charles and E. Gil-Av, J. Chromatogr., 298 (1984) 516.
[4] W.L. Tsai, K. Hermann, E. Hug, B. Rohde and A.S. Dreiding, Helv. Chim. Acta, 68 (1985) 2238.
[5] A. Dobashi, Y. Motoyama, K. Kinoshita and S. Hara, Anal. Chem., 59 (1987) 2209.
[6] R. Matusch and C. Coors, Angew. Chem., Int. Ed. Engl., 28 (1989) 626.
[7] R.M. Carman and K.D. Klika, Aust. J. Chem., 44 (1991) 895.
[8] L. Cecchi and P. Malaspina, Anal. Biochem., 192 (1991) 219.
[9] P. Diter, S. Taudien, O. Samuel and H.B. Kagan, J. Org. Chem., 59 (1994) 370.
[10] J. Martens and R. Bhushan, J. Liq. Chromatogr., 15 (1992) 1.
[11] I.G. Veinberga, J.F. Freimanis and H.A. Kažoka, Bioorg. Khim., 17 (1991) 760.
[12] D.O. Loļa, J.F. Freimanis, I.V. Vosekalna and A.J. Liepiņa, Zh. Org. Khim., 24 (1988) 1422.
[13] V.R. Korics, G.P. Sokolovs, J.F. Freimanis, O.V. Sahartova, I.A. Mīlmanis, M.B. Fleišers, V.T. Glēzers, A.F. Mišņevs and J.J. Bleidelis, Zh. Org. Khim., 21 (1985) 305.
[14] A.K. Banerjee, B.J. Broughton, T.S. Burton, M.P.L. Caton, A.J. Christmas, E.C.J. Coffee, Crowshaw, C.J. Hardy, M.A. Heazell, M.N. Palfreyman, T. Parker, L.C. Saunders and K.A.J. Stuttle, Prostaglandins, 22 (1981) 167.
[15] G.M. Sheldrick, in G.M. Sheldrick, C. Krüger and R. Goddard (Editors), SHELXS-86. Crystallographic Computing 3, Oxford University Press, Oxford, 1985, pp. 175–189.
[16] G.M. Sheldrick, SHELXS-76. Program for Crystal Structure Determination and Refinement, University of Cambridge, UK, 1976; 400 Atomic Version, Ch. Weizmann Institute of Science, Rehovot, Israel, 1979; Implemented on IBM PC/AT, 1987.
[17] N. Walker and D. Stuart, Acta Crystallogr., Sect. A, 39 (1983) 158.
[18] E.V. Loža, D.O. Loļa, J.F. Freimanis, I.V. Turovskis and S.H. Rozīte, Izv. Akad. Nauk Latv. SSR, Ser. Khim., 2 (1989) 234.
[19] E.V. Loža, D.O. Loļa, J.F. Freimanis, I.V. Turovskis, S.H. Rozīte and I.V. Dipāns, Izv. Akad. Nauk Latv. SSR, Ser. Khim., 4 (1989) 472.
[20] E.V. Loža, D.O. Loļa, J.F. Freimanis, I.V. Turovskis, E.E. Liepiņš, S.H. Rozīte and O.V. Sahartova, Zh. Org. Khim., 26 (1990) 1024.
[21] D.O. Loļa, J.F. Freimanis, I.V. Turovskis and M.P. Gavars, Zh. Org. Khim., 26 (1990) 1919.
[22] C.F. Poole and S.K. Poole, Chromatography Today, Elsevier, Amsterdam, 1991, pp. 375–453.
[23] D. Hadži, in S. Patai (Editor), The Chemistry of Acid Derivatives, Part 1, Wiley, Chichester, 1979, pp. 213–266.

ELSEVIER

Journal of Chromatography A, 708 (1995) 245–251

JOURNAL OF CHROMATOGRAPHY A

Enantiomeric separation of a thiazole derivative by high-performance liquid chromatography and micellar electrokinetic chromatography

Ritsuko Furuta*, Tadashi Doi

Environmental Health Science Laboratory, Sumitomo Chemical Co., Ltd., 3-1-98, Kasugade Naka, Konohana-ku, Osaka 554, Japan

First received 20 December 1994; revised manuscript received 27 March 1995; accepted 27 March 1995

Abstract

Enantiomeric separation of a thiazole derivative, (±)-(*RS*)-4-[1-(2-fluoro-4-biphenylyl)ethyl]-2-methylaminothiazole, can be achieved by HPLC using a β-cyclodextrin (CD)-bonded stationary phase. The effects of the type of CD, organic modifiers in the mobile phase and mobile phase pH on the retention and resolution were studied and optimum conditions were established. The enantiomers of the compound were also separated by micellar electrokinetic chromatography with β- or γ-CDs as chiral additives. The retention behaviour of some structurally related compounds was examined with the two techniques and the results were compared.

1. Introduction

A newly synthesized thiazole derivative, (±)-(*RS*)-4-[1-(2-fluoro-4-biphenylyl)ethyl]-2-methylaminothiazole (SM-8849) (Fig. 1), demonstrating immunomodulating anti-rheumatic activity [1,2], has an asymmetric carbon and has been synthesized as a racemate. Enantioselective analytical methods are essential for studying the activity and kinetics of its individual enantiomers in the pharmacological and toxicological fields.

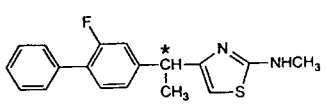

Fig. 1. Structure of SM-8849.

Cyclodextrins (CDs) are torus-shaped cyclic oligosaccharides containing six to twelve D-(+)-glucopyranose units. The interior of the CD cavities is relatively hydrophobic, thus allowing them to form inclusion complexes with a variety of molecules. Based on this ability to form stereospecific inclusion complexes, they have been successfully used for chiral separations in many chromatographic methods. Among the latter, HPLC is the most popular, with two different approaches designed for the application of CDs: (1) the use of chemically bonded CD stationary phases [3–9] and (2) the use of CDs as mobile phase components of reversed-phase (RP) systems [10–14]. Recently, the number of

* Corresponding author.

0021-9673/95/$09.50
SSDI 0021-9673(95)00403-3

papers on chiral separations by CE with CDs has also been increasing. In the CE technique, various modes have been used as in HPLC, that is, capillary zone electrophoresis (CZE) [15–19], capillary gel electrophoresis [20–22] and micellar electrokinetic chromatography (MEKC) [23–25].

We earlier reported chiral separations of agricultural chemicals by HPLC using CD-bonded stationary phases and by CD-modified MEKC (CD-MEKC) and discussed the possible mechanisms of chiral recognition [26–29].

In this investigation, we achieved the chiral separation of SM-8849 by using a β-CD-bonded stationary phase in RP-HPLC and the effects of the structure of the CD, organic modifiers in the mobile phase and mobile phase pH on retention and resolution were assessed. In addition, the enantiomers were also separated by CD-MEKC using β- or γ-CDs. The retention behaviour of SM-8849 analogues with the two methods was compared.

2. Experimental

2.1. Apparatus

HPLC separations were performed using a liquid chromatographic system which consisted of a Model L-6200 pump equipped with a Model L-4000 variable-wavelength spectrophotometric detector (Hitachi, Tokyo, Japan). The column temperature was controlled with a Shodex AO-30C oven (Showa Denko, Tokyo, Japan). Cyclobond I, II and III columns (250 mm × 4.6 mm I.D.) packed with 5-μm spherical silica gel with chemically bonded β-, γ- and α-CDs, respectively, were purchased from Advanced Separation Technologies (Whippany, NJ, USA).

CE experiments were performed with a Beckman (Palo Alto, CA, USA) P/ACE System 2100 capillary electrophoresis system. The capillary cartridge (Beckman) contained a 75-μm I.D. untreated fused-silica capillary that was 57 cm in total length and 50 cm to the detector.

2.2. Chemicals

SM-8849, its enantiomers and structurally related compounds were supplied by the Research Laboratories of Sumitomo Pharmaceuticals (Osaka, Japan), α- and β-CDs were purchased from Kanto Chemical (Tokyo, Japan), γ-CD and HPLC-grade acetonitrile were obtained from Wako (Osaka, Japan) and Sudan IV and other organic solvents and reagents were of analytical-reagent grade from Kanto Chemical or Wako. Water was processed through an RO/NANO Pure II system (Barnstead, Dubuque, IA, USA).

2.3. HPLC separation

Experiments were carried out with Cyclobond I (β-type) unless specified otherwise. The mobile phase for the RP mode was prepared by mixing an organic solvent with 0.1% triethylammonium acetate (TEAA) buffer, filtered through a 0.45-μm membrane filter and degassed before use. That for polar-organic mode was acetonitrile containing 5 or 0% of methanol and very small amounts of glacial acetic acid and triethylamine (≤0.3%). Sample solutions were prepared by dissolving compounds in methanol or acetonitrile to give a concentration of 0.1 mg/ml. In each case, a 5-μl portion of sample solution was injected. The column temperature was kept at 20°C. The flow-rate was 0.5 ml/min for the RP mode and 1.0 ml/min for the polar-organic mode, and the detector was set at 248 nm. The void volume was determined by injecting methanol and the elution order of enantiomers was examined by injecting a sample spiked with one of the enantiomers.

2.4. CE separation

The operating conditions were as follows: applied voltage, 15 kV for MEKC or 10 kV for CZE; temperature, 25°C; detection, UV at 254 nm; and sample introduction, 1-s pressure. The injection end was the anode. The separation solution for MEKC was 100 m*M* sodium dodecyl sulfate (SDS) and 2 *M* urea in 100 m*M* borate–50 m*M* phosphate buffer (pH 9.0) containing 50 m*M* β-CD unless specified otherwise. That for CZE was 5 *M* urea in 25 m*M* phosphate buffer (pH 2.5) containing various concentrations of β-CD. Sample solutions (0.2 mg/ml) were pre-

pared by dissolving each compound in methanol followed by mixing with the separation solution in a ratio of 1:4 (v/v). For MEKC, Sudan IV was added to the separation solution to measure the migration time of the micelle. The elution order of enantiomers was examined in a similar manner to the HPLC separation.

3. Results and discussion

3.1. HPLC separation

Chiral separation of SM-8849 was investigated and achieved first with a CD-bonded phase in the RP mode. The polar-organic mode for CD-bonded phases has recently been reported by Chang et al. [30]; it can resolve enantiomers that cannot be separated in the RP or normal-phase modes. SM-8849 has functional groups which can interact with CDs through hydrogen bonding and the polar-organic mode can be considered applicable. Therefore, this mode with α-, β- and γ-CD-bonded phases was also investigated using acetonitrile containing appropriate amounts of methanol, glacial acetic acid and triethylamine as mobile phases. SM-8849 was not retained on the stationary phases, however, and demonstrated no enantiomeric separation. The following experiments were performed in the RP mode.

Chiral recognition of CDs

The effect of the type of CD on the chiral recognition of SM-8849 was investigated using α-, β- and γ-CD-bonded columns.

Chiral recognition was dependent on the type of CD, that is, the cavity diameter. The enantiomers of SM-8849 were separated only on the β-CD-bonded column (Table 1). This is reasonable because the size of the β-CD cavity is thought to match that of molecules similar to biphenyl or naphthalene [31]. The elution order of the enantiomers was first the (+)-(*S*)- and then the (−)-(R)-isomer. This result indicates that the (−)-(*R*)-enantiomer forms a more stable inclusion complex than the (+)-(*S*)-enantiomer with β-CD.

Table 1
Enantiomeric separation of SM-8849 on cyclodextrin-bonded columns

Column	k_1'[a]	α[b]	Mobile phase[c]
Cyclobond I (β-)	4.94	1.09	25:75
Cyclobond II (γ-)	4.49	1.00	22:78
Cyclobond III (α-)	5.65	1.00	22:78

[a] k_1' = Capacity factor of the first-eluted enantiomer.
[b] α = Separation factor.
[c] Acetonitrile–0.1% TEAA buffer (pH 6.0) (v/v).

Effect of organic modifier

Because CDs form inclusion complexes with various hydrophobic compounds, organic solvent molecules in the mobile phase compete with the solute for occupation of the CD cavity. The effect of the hydrophobicity or the bulkiness of the organic modifier in the mobile phase on the separation of SM-8849 was investigated using primary and secondary alcohols and acetonitrile. Each organic solvent concentration was adjusted so that the capacity factor of the first-eluted enantiomer was about 5. 2-Propanol, 1-butanol and 2-methyl-1-propanol could not be used owing to the high column pressure or low miscibility for adjusting the capacity factor.

As shown in Table 2, smaller alcohols tend to give better separation factors and resolutions. This can be explained as follows: an increase in the bulkiness and hydrophobicity of the alcohol would increase its interaction with the CD cavi-

Table 2
Effects of organic modifiers on the separation factor, α, and the resolution, R_s

Organic modifier[a]	α	R_s	log K_a[b]
Acetonitrile (25:75)	1.09	0.94	–
Methanol (55:45)	1.06	0.45	−0.49
Ethanol (37:63)	1.07	0.47	−0.03
1-Propanol (20:80)	1.05	0.32	0.57
2-Butanol (15:85)	1.00	0.00	1.19
2-Methyl-2-propanol (20:80)	1.00	0.00	1.68

Column, Cyclobond I.
[a] Mobile phase, organic modifier–0.1% TEAA buffer (pH 6.0) (v/v).
[b] Logarithm of the association constant for the β-CD–alcohol complex [32].

ty, reflected in the association constant, log K_a [32], in Table 2, and thus its ability to compete with the solute. Acetonitrile was found to provide much better resolution than alcohol systems, and was therefore chosen as the mobile phase in subsequent experiments.

The (+)-(*S*)-enantiomer always eluted first with any of the organic solvents used.

Effect of pH

Because SM-8849 is a secondary amine, an influence of pH on its retention behaviour was predicted. Therefore, the effects of changing the pH of the mobile phase were investigated.

The capacity factor and the resolution significantly increased with increase in pH up to 5.0 and the best resolution was obtained at pH 6.0, as shown in Table 3. At pH 7.0, the peak broadened and the resolution decreased, although the reason was not clear.

The dissociation constant of SM-8849 was established to be between 4 and 6 in 50% methanol solution in a preliminary experiment. In general, the binding strength of the charged species to the CD cavity is smaller than that of the corresponding neutral species, presumably owing to diminished hydrophobic interactions between the charged guest molecule and the non-polar cyclodextrin cavity. This is in line with the change in retention behaviour mentioned above.

In spite of the fact that the acetonitrile content in the mobile phase and the column used were the same as those used in the previous section, the retention time at pH 6.0 obtained in this experiment was almost doubled (see Tables 1 and 3). The acetonitrile content was therefore adjusted so that the retention time of the first-eluted peak was about 40 min in the subsequent experiments.

Although better resolution is generally expected at lower temperature, as confirmed in a previous experiment [26], temperature effects were not investigated in this work. Fig. 2 shows the chiral separation of SM-8849 under the optimum conditions. The elution order of the enantiomers did not change throughout the investigation.

Table 3
Effects of pH on the capacity factor, k'_1, the separation factor, α, and the resolution, R_s

pH	k'_1[a]	α	R_s
3.5	2.06	1.06	0.26
4.0	4.04	1.07	0.64
5.0	9.99	1.08	1.02
6.0	9.93	1.08	1.05
7.0	9.74	1.08	0.91

Column, Cyclobond I; mobile phase, acetonitrile–0.1% TEAA buffer (25:75, v/v).
[a] k'_1 = Capacity factor of the first-eluted enantiomer.

3.2. CE separation

High-resolution chiral separation of SM-8849 enantiomers was achieved by MEKC. In this case β- and γ-CDs could be successfully used as chiral additives with better resolution obtained with β-CD (Table 4), differing from the HPLC case. When α-CD was used, SM-8849 did not interact because the size of the CD cavity is too small, and therefore it migrated with the micelle. The (−)-(*R*)-enantiomer eluted first when either β- or γ-CD was used. In MEKC, CDs are not solubilized by the micelle and migrate with the same velocity as the electroosmotic flow. Consequently, stable inclusion-complex formation of the solute with CDs provides a faster migration

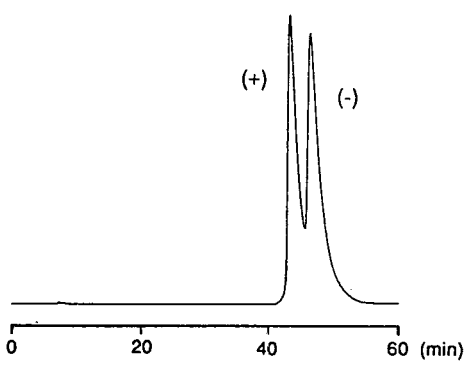

Fig. 2. Enantiomeric separation of SM-8849 by HPLC with Cyclobond I. Mobile phase, acetonitrile–0.1% TEAA buffer (pH 6.0) (25:75, v/v); for other conditions, see text.

Table 4
Enantiomeric separation of SM-8849 by MEKC

CD	$\tilde{k}_1'$[a]	α[b]	R_s[c]
α-	∞	1.00	0.00
β-	15.3	1.25	4.31
γ-	10.2	1.08	1.99

Separation solution, 100 m*M* SDS and 2 *M* urea in 100 m*M* borate–50 m*M* phosphate buffer (pH 9.0) containing 50 m*M* CD.
[a] $\tilde{k}_1'$ = Capacity factor of the first-eluted enantiomer calculated according to the equation derived by Terabe et al. [33].
[b] α = Separation factor.
[c] R_s = Resolution.

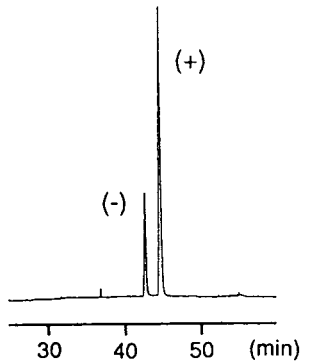

Fig. 3. Enantiomeric separation of SM-8849 spiked with the (+)-(*S*)-enantiomer by MEKC with β-CD. Separation solution, 100 m*M* SDS and 2 *M* urea in 100 m*M* borate–50 m*M* phosphate buffer (pH 9.0) containing 50 m*M* β-CD; for other conditions, see text.

under experimental conditions where the electroosmotic flow is stronger than the electrophoretic mobility of the micelle [24]. Namely, the (−)-(*R*)-enantiomer of SM-8849 forms a more stable inclusion complex with CDs than the (+)-(*S*)-enantiomer as well as on the β-CD-bonded stationary phase.

Because SM-8849 is positively charged at low pH, CZE with a chiral additive can be considered applicable. Consequently, CZE separation with various concentrations of β-CD at low pH was tried. A 5 *M* concentration of urea was added to increase the solubility of the β-CD in this experiment. However, enantiomeric separation could not be achieved, even when 50 m*M* β-CD was added. The lowest concentration of β-CD allowing effective separation of the SM-8849 enantiomers in MEKC was 20 m*M*, although baseline separation was not achieved at this concentration ($R_s = 1.18$).

An electropherogram of SM-8849 spiked with the (+)-(*S*)-enantiomer in MEKC using β-CD as a chiral additive is shown in Fig. 3.

3.3. Retention behaviour of structurally related compounds

The retention behaviour of SM-8849 analogues was investigated using the HPLC and MEKC methods with β-CD established in this study, to obtain comparative information on chiral recognition by CD. Table 5 gives the results obtained for the capacity factors of the first-eluted enantiomers and the separation factors and resolutions of the enantiomers, showing that the enantioselectivity differs between the two methods.

The biphenyl group of SM-8849 is probably included in the CD cavity when an inclusion complex with β-CD is formed [31], although NMR spectroscopic studies are needed to confirm this. The data for compounds **1** (SM-8849) to **3** indicate that the biphenyl group plays an important role in chiral recognition with these methods. From the comparison of compounds **1** and **2**, a biphenyl group without a fluoro substituent is preferable for chiral recognition by β-CD in both methods. Compound **3**, which has a phenyl group that is too small for the β-CD cavity, instead of a biphenyl group, did not show an enantiomeric separation. This illustrates that the relative sizes of the CD cavity and the enantiomer to be complexed are of critical importance for chiral recognition: a tighter fit of molecules is preferable. With the HPLC method, compound **3** was less retained on the stationary phase than compounds **1** and **2**, that is, it demonstrated less interaction with the CD. With the MEKC method, however, the capacity factor of **3** was found to be about the same as that of **2**, although less than that of **1**. In this case, inter-

Table 5
Retention behaviour of structurally related compounds of SM-8849 using HPLC and MEKC methods with β-CD

No.	Compound	HPLC			MEKC		
		k_1'[a]	α[b]	R_s[c]	$\tilde{k}_1'$[d]	α	R_s
1[e]	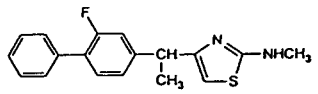	6.25	1.08	0.72	14.48	1.25	4.33
2	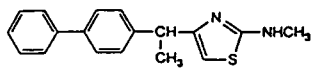	5.75	1.09	0.88	8.95	1.33	7.70
3	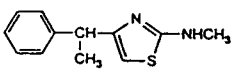	1.63	1.00	0.00	7.95	1.00	0.00
4	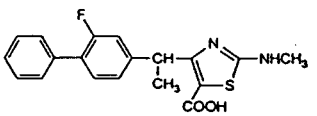	8.97	1.08	1.03	0.37	1.00	0.00
5	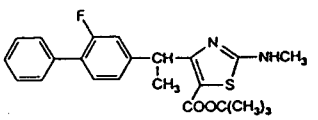	7.08	1.05	0.26	150.60	1.00	0.00
6	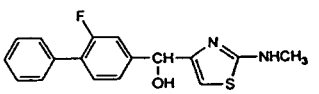	4.27	1.00	0.00	8.07	1.11	3.11
7	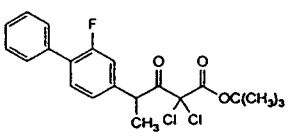	2.78	1.00	0.00	10.29	1.03	0.66
8	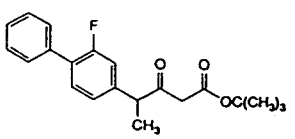	4.24	1.00	0.00	67.67	1.00	0.00

HPLC conditions as in Fig. 2, except the mobile phase was acetonitrile–0.1% TEAA buffer (pH 6.0) (27:73); MEKC conditions as in Fig. 3.

[a] k_1' = Capacity factor of the first-eluted enantiomer.

[b] α = Separation factor.

[c] R_s = Resolution.

[d] $\tilde{k}_1'$ = Capacity factor of the first-eluted enantiomer [33].

[e] SM-8849.

pretation is more complicated because a solute distributes among the micelles, aqueous phase and CDs.

The carbonyl group on the thiazole ring influences the retention and resolution differently with the two methods. Compound **4**, having a 5-carboxy-2-methylaminothiazole ring, showed the best resolution among the HPLC data, while no resolution was apparent with MEKC. The carboxyl group exerts a positive effect, probably by hydrogen bonding with the secondary hydroxyl group of the CD in HPLC, but it has a negative effect in MEKC, because the solute mainly distributes to the aqueous phase and does not interact with the CD. Although compound **5** interacted strongly with the micelle owing to its high hydrophobicity and it showed no resolution in the MEKC case, slight enantiomeric separation was evident with HPLC.

Compound **6**, which has a hydroxyl group attached to the chiral centre, was separated only with the MEKC method. Both methods exhibited low enantioselectivity for compounds **7** and **8**.

4. Conclusions

The enantiomers of SM-8849 can be successfully separated by HPLC and MEKC using CDs. With both methods, chiral recognition is dependent on the type of CD, and inclusion complex formation between the biphenyl group of the solute and the CD cavity is considered to be an important factor in the chiral recognition. These HPLC and MEKC methods can also be applied to structurally related compounds, and will be used complementarily for studies of biological action and activity, dynamics and kinetics, in addition to quality control.

References

[1] C. Abe, F. Nishikaku and Y. Koga, Int. J. Immunother., 7 (1991) 1.
[2] F. Nishikaku and Y. Koga, Immunopharmacology, 25 (1993) 65.
[3] D.W. Armstrong and W. DeMond, J. Chromatogr. Sci., 22 (1984) 411.
[4] D.W. Armstrong, T.J. Ward, R.D. Armstrong and T.E. Beesley, Science, 232 (1986) 1132.
[5] D.W. Armstrong, S.M. Han and Y.I. Han, Anal. Biochem., 167 (1987) 261.
[6] D.W. Armstrong, Y.I. Han and S.M. Han, Anal. Chim. Acta, 208 (1988) 275.
[7] C. Bertucci, E. Domenici, G. Uccello-Barretta and P. Salvadori, J. Chromatogr., 506 (1990) 617.
[8] S. Li and W.C. Purdy, J. Chromatogr., 543 (1991) 105.
[9] J. Florance and Z. Konteatis, J. Chromatogr., 543 (1991) 299.
[10] D. Sybilska, J. Żukowski and J. Bojarski, J. Liq. Chromatogr., 9 (1986) 591.
[11] M. Gazdag, G. Szepesi and L. Huszár, J. Chromatogr., 351 (1986) 128.
[12] J. Żukowski, D. Sybilska, J. Bojarski and J. Szejtli, J. Chromatogr., 436 (1988) 381.
[13] A. Walhagen and L.-E. Edholm, Chromatographia, 32 (1991) 215.
[14] D. Sybilska, A. Bielejewska, R. Nowakowski, K. Duszczyk and J. Jurczak, J. Chromatogr., 625 (1992) 349.
[15] S. Fanali, J. Chromatogr., 474 (1989) 441.
[16] S. Fanali, J. Chromatogr., 545 (1991) 437.
[17] M.W.F. Nielen, Anal. Chem., 65 (1993) 885.
[18] T.E. Peterson, J. Chromatogr., 630 (1993) 353.
[19] H. Nishi, Y. Kokusenya, T. Miyamoto and T. Sato, J. Chromatogr. A, 659 (1994) 449.
[20] A.S. Cohen, A. Paulus and B.L. Karger, Chromatographia, 24 (1987) 15.
[21] A. Guttman, A. Paulus, A.S. Cohen, N. Grinberg and B.L. Karger, J. Chromatogr., 448 (1988) 41.
[22] I.D. Cruzado and G. Vigh, J. Chromatogr., 608 (1992) 421.
[23] T. Ueda, F. Kitamura, R. Mitchell, T. Metcalf, T. Kuwana and A. Nakamoto, Anal. Chem., 63 (1991) 2979.
[24] H. Nishi, T. Fukuyama and S. Terabe, J. Chromatogr., 553 (1991) 503.
[25] K. Otsuka and S. Terabe, Trends Anal. Chem., 12 (1993) 125.
[26] R. Furuta and H. Nakazawa, J. Chromatogr., 625 (1992) 231.
[27] R. Furuta and H. Nakazawa, Chromatographia, 35 (1993) 555.
[28] R. Furuta and T. Doi, J. Chromatogr. A, 676 (1994) 431.
[29] R. Furuta and T. Doi, Electrophoresis, 15 (1994) 1322.
[30] S.C. Chang, G.L. Reid, III, S. Chen, C.D. Chang and D.W. Armstrong, Trends Anal. Chem., 12 (1993) 144.
[31] A.M. Krstulović (Editor), Chiral Separations by HPLC, Ellis Horwood, Chichester, 1989, Ch. 10, p. 209.
[32] Y. Matsui and K. Mochida, Bull. Chem. Soc. Jpn., 52 (1979) 2808.
[33] S. Terabe, K. Otsuka, K. Ichikawa, A. Tsuchiya and T. Ando, Anal. Chem., 56 (1984) 111.

ELSEVIER

Journal of Chromatography A, 708 (1995) 253–261

JOURNAL OF CHROMATOGRAPHY A

Chiral separations of β-blocking drug substances using chiral stationary phases

Jens Ekelund*, Anja van Arkens, Kirsten Brønnum-Hansen, Karen Fich, Lars Olsen, Poul Vibholm Petersen

Chemical Laboratory, National Board of Health, Medicines Division, Frederikssundsvej 378, DK-2700 Brønshøj, Denmark

First received 10 February 1995; revised manuscript received 20 March 1995; accepted 20 March 1995

Abstract

Three chiral stationary phases were evaluated for their usefulness in determinations of optical purity and separations of β-blocking drug substances. The phases were a modified cellulose phase (Chiralcel OD), an immobilized protein (AGP) and a β-cyclodextrin phase (Cyclobond I). These phases were evaluated concerning their practical analytical use for the determination of the enantiomeric purity of non-racemic β-blocking substances. The best phase proved to be Chiralcel OD, which provided excellent separations of almost all β-blocking substances tested and rugged determinations performed with satisfactorily low detection limits. Similar results could be obtained with AGP, but this did not seem to be sufficiently rugged for routine analysis. The β-cyclodextrin phase resulted in poor chiral separations of most β-blocking substances and the usefulness of this phase for analytical purposes seems limited.

1. Introduction

It is well known that the different enantiomers of most optically active drug substances can possess different biological activities. This is also a concern of the regulatory authorities if an optically active compound is to be registered as a drug substance [1,2]. If a compound that is intended to be marketed as a drug is one enantiomer, the regulatory authorities will regard the presence of the other enantiomer, in the raw material or in the finished product, following the same principles as for any other chemical impurity. Hence the need for methods for the determination of one enantiomer in the other has increased. The classical method for the determination of optical purity, also in pharmacopoeial monographs of drug substances, is optical rotation. However, this method is neither very accurate nor precise, and it will be difficult to control the content of enantiomeric impurity at low levels. In recent years, HPLC techniques that are capable of separating and determining enantiomers have been greatly improved. These techniques offer direct and specific determinations of enantiomeric purity. The particular interest in our laboratory has been to develop rugged and precise methods for use for standardization purposes, e.g., as part of testing procedures of drug substances as described in pharmacopoeial monographs. This investigation forms part of a series in which various ap-

* Corresponding author.

0021-9673/95/$09.50
SSDI 0021-9673(95)00384-3

proaches concerning the possibilities of standardized HPLC methods for testing the optical purity of β-blocking drug substances are being evaluated [3].

β-Blocking drug substances most often exhibit a chiral structure and are mostly used as racemic mixtures with the *S*-form being responsible for the desired biological effect. An exception is sotalol, but this is not due to an opposite steric configuration at the chiral centre, but is caused by the ligand nomenclature rules. However, some β-blocking substances are marketed as single enantiomers. In Denmark, eighteen β-blocking drug substances are on the market, three of which are marketed as the pure *S*-form, timolol, bunolol and penbutolol. The remaining fifteen are marketed as the racemic mixture.

Three possible approaches to the separation of chiral substances by HPLC exist: (1) derivatisation of the analyte with a chiral reagent and formation of a diastereomer that can be separated by conventional achiral chromatography; (2) addition of chiral additives to the mobile phase and the use of an achiral stationary phase; and (3) the use of chiral stationary phases.

In our laboratory, the usefulness of determining optical purity by normal-phase HPLC following derivatization with (−)-camphanic acid chloride, (*S*)-(−)-1-phenylethyl isocyanate or 2,3,4,6-tetra-O-acetyl-β-D-glucopyranosyl isothiocyanate has been investigated previously [3]. This reference gives a thorough review and discussion of the literature on chiral separations of β-blockers with the use of derivatization.

Chiral separations performed by the addition of agents to the eluent have been studied with (+)-10-camphorsulphonate [4] and N-benzoxycarbonylglycyl-L-proline [5,6].

The simplest way to separate enantiomers is by direct injection of a sample on to a chiral stationary phase. Several chiral stationary phases have been used for the separation of enantiomers of β-blocking drug substances. Chiral phases consisting of immobilized proteins such as bovine serum albumin (BSA) [7], α-acid glycoprotein (AGP) [8–13], cellubiohydrolase [13–18], ovomucoid [13,19–21] and various modifications of the ovomucoid protein [22,23] have been used to separate enantiomers of β-blockers. The use of non-protein-based phases has also been reported: β-cyclodextrin in both the normal- and reversed-phase modes [13,24,25], Pirkle-type columns [26–29] and cellulose tris(3,5-dimethylphenylcarbamate) [13,30–46].

However, most work seems to have been done only to investigate the separating power and the separation mechanisms of the chiral stationary phases. So far, no work has been done to investigate the suitability of the column materials to determine enantiomeric purity in β-blocking substances at the level where other chemical impurities can be determined by the use of non-chiral analytical HPLC. The aim of this work was to evaluate a number of selected columns for this purpose. All β-blocking drug substances currently on sale in Denmark were included in the investigations in order to evaluate the stationary phases in the best possible way.

From the literature, the most suitable column seemed to be cellulose tris(3,5-dimethylphenylcarbamate) (Chiralcel OD), so such a column was chosen for further investigations. The use of protein-based columns for the separation of enantiomers of β-blocking substances is widespread. Of these protein based phases, α-acid glycoprotein (AGP) is one of the best known and seemed to be the best column to achieve our goal. Most of the Pirkle-type phases seemed less suitable, not because of all low separation power, but because derivatization of the substances is required prior to injection of the sample, thus diminishing the advantage of using a chiral stationary phase compared with a chiral derivatization procedure. One commercially available Pirkle-type phase has been specially designed for the separation of β-blockers without derivatization. However, preliminary work with this phase in our laboratory revealed some unwanted peak-splitting problems due to the temperature dependence of the separations. Further, this phase has been poorly investigated and only for a few substances [29]. Further work to investigate these problems is in progress. Cyclodextrins as stationary phase for the separation of β-blockers are not very useful when operated in the reversed-phase mode. However,

some work has been done with this phase using polar organic solvents as mobile phase, and this approach seems to provide a higher separation power towards β-blockers [25]. Therefore, a cyclodextrin stationary phase was also included in our investigations.

2. Experimental

2.1. Chemicals

Table 1 lists the compounds investigated and the companies from which they were obtained. The pure enantiomeric forms of timolol were supplied by Merck, Sharp & Dohme (Rahway, NJ, USA) and the pure forms of bunolol by Allergan (Irvine, CA, USA). Molecular structures are shown in Fig. 1. All other drug substances were of pharmacopoeial grade. Diethylamine was of analytical-reagent grade from Fluka (Buchs, Switzerland), water was purified by ion exchange prior to use and all other solvents were of analytical-reagent grade from Merck (Darmstadt, Germany).

Table 1
β-Blocking drug substances investigated and their sources

Compound	Company
Acebutolol	Rhône-Poulenc (Essex, UK)
Alprenolol	Hässle (Mölndal, Sweden)
Atenolol	ICI (Cheshire, UK)
Atenolol	Benzon Pharma (Hvidovre, Denmark)
Betaxolol	MEDA (Herlev, Denmark)
Betaxolol	Searle (Mölndal, Sweden)
Bevantolol	Parke-Davis (Ann Arbor, MI, USA)
Bevantolol	Benzon Pharma
Bisoprolol	Merck (Darmstadt, Germany)
Bunolol	Allergan (Irvine, CA, USA)
Carazolol	Upjohn (West Sussex, UK)
Carteolol	Ercopharm (Vedbaek, Denmark)
Metipranolol	Ciba-Geigy (Basle, Switzerland)
Metoprolol	Hässle
Oxprenolol	Ciba-Geigy
Penbutolol	Hoechst (Frankfurt, Germany)
Pindolol	Durascan (Odense, Denmark)
Pindolol	Benzon Pharma
Pindolol	NM Pharma (Sundbyberg, Sweden)
Pindolol	Dumex (Copenhagen, Denmark)
Propranolol	Sigma (St. Louis, MO, USA)
Sotalol	Bristol-Myers (Evansville, IN, USA)
Tertatolol	Servier (Orleans, France)
Timolol	Merck, Sharp & Dohme (Rahway, NJ, USA)

2.2. Apparatus

The chromatographic systems consisted of a Kontron T 414 pump, an LDC SpectroMonitor variable-wavelength detector and a Rheodyne Model 7120 injection valve, an L 6200 pump, an L 4250 UV–Vis detector, an L 5025 column thermostat and an AS 2000A autosampler, all from Merck–Hitachi and a Kontron LC 410 pump with a Kontron Uvikon 735 LC detector. All chromatograms were recorded on a Kipp & Zonen BD-8 recorder. Data were collected on a Hewlett-Packard Model 3359A laboratory data system.

2.3. Columns

The cellulose tris(3,5-dimethylphenylcarbamate) phase was Chiralcel OD (25 cm × 4.6 mm I.D., 10 μm) from Daicel Chemical Industries (Tokyo, Japan). The α-acid glycoprotein phase was a Chiral-AGP column (100 × 4 mm I.D., 5 μm), used in connection with a guard column (10 × 3 mm I.D.) packed with a similar phase, from ChromTech (Norsborg, Sweden). The β-cyclodextrin column was Cyclobond I (25 cm × 4.6 mm I.D.) from ASTEC (Whippany, NJ, USA).
The chromatographic procedures used are given in the discussion section for the various stationary phases.

3. Results and discussion

3.1. Cellulose tris(3,5-dimethylphenylcarbamate) (Chiralcel OD)

Table 2 gives the chromatographic results obtained using the cellulose tris(3,5-dimethyl-

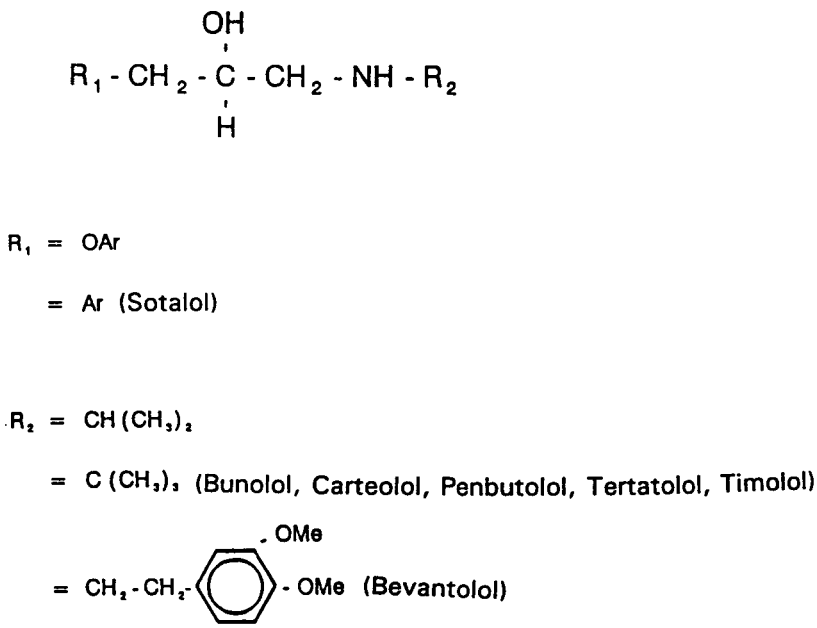

Fig. 1. Structures of the β-blockers investigated.

Table 2
Chromatographic results from the separation of 18 β-blocking substances on the Chiralcel OD stationary phase

Compound	λ (nm)	Eluent[a]	$k'(1)$	$k'(2)$	α	R_s
Acebutolol	320	G	2.77	3.19	1.15	1.6
Alprenolol	275	A	0.35	1.24	3.54	10.9
Atenolol	275	C	0.94	1.75	1.86	4.4
Betaxolol	275	A	0.52	1.57	3.02	10.8
Bevantolol	275	E	0.97	4.10	4.23	9.8
Bisoprolol	275	A	0.69	1.38	2.00	6.9
Bunolol	267	A	0.71	1.42	2.00	6.6
Carazolol	253	C	1.87	2.32	1.24	1.7
Carteolol	275	C	0.48	0.95	1.98	4.1
Metipranolol	275	B	1.08	1.31	1.21	2.2
Metoprolol	275	A	0.69	2.02	2.93	11.8
Oxprenolol	275	D	0.32	1.62	5.06	12.9
Penbutolol	270	A		0.60		
Pindolol	265	F	0.25	1.66	6.64	7.6
Propranolol	290	C	0.90	1.52	1.69	4.6
Sotalol	254	Eluted as a single peak with all mobile phases tested				
Tertatolol	290	D	0.32	1.69	5.28	10.5
Timolol	300	B	0.85	1.07	1.26	2.5

[a] Eluents: A = hexane–2-propanol–DEA (80:20:0.1); B = hexane–2-propanol–DEA (90:10:0.1); C = hexane–2-propanol–DEA (60:40:0.1); D = hexane–2-propanol–DEA (40:60:0.1); E = hexane–2-propanol–DEA (10:90:0.1); F = hexane–2-propanol–DEA (20:80:0.1); G = hexane–ethanol–DEA (90:10:0.1). DEA = diethylamine.

phenylcarbamate) column and the mobile phases listed. The mobile phases chosen for the Chiralcel OD stationary phase were various mixtures of hexane and 2-propanol with the addition of 0.1% diethylamine (see Table 2). These mobile phases were as suggested by the manufacturer of the column. Samples, as salts or free bases, were dissolved in the mobile phase. For the separation studies the sample concentration was 1 mg/ml, 20 μl were injected and the flow-rate was 0.5 ml/min. For information on detection wavelengths, see Table 2. It appears from the results that this column is capable of separating fifteen of the eighteen substances under these conditions. Racemic acebutolol was not separated satisfactorily, racemic sotalol eluted as a single peak and penbutolol was only available in the *S*-form. A chromatogram of racemic timolol is shown in Fig. 2.

Some workers have investigated chiral recognition mechanisms with this stationary phase. In some cases altered capacity factors and reversed retention orders were achieved by the addition of organic alcohols other than 2-propanol to the mobile phase, in this way optimizing the separations [41,43]. Such an approach was attempted with the two compounds that were not separated satisfactorily, acebutolol and sotalol. The alcohols used as alternative modifiers were *tert*-butanol, *n*-butanol, *n*-propanol, ethanol and methanol. For racemic acebutolol an improved separation could be obtained when using hexane–ethanol–diethylamine (90:10:0.1), resulting in $R = 1.6$ (see Table 2). For sotalol, the use of these modifiers in the mobile phase did not offer any improvements. The poor separation of sotalol using the Chiralcel OD column may be due to the lack of an oxygen atom in connection with the aromatic group close to the chiral centre, as compared with the other β-blocking substances.

The possible use of Chiralcel OD as a stationary phase for the determination of optical purity in the two β-blocking drug substances marketed as the pure enantiomeric forms, (*S*)-timolol and (*S*)-bunolol, was validated with respect to specificity, reproducibility, accuracy, linearity, limit of detection and ruggedness, in accordance with the current EEC guideline [47]. For both timolol and bunolol the *R*-form eluted before the *S*-form. For both compounds the chromatographic systems given in Table 2 were used.

Fig. 3 shows a chromatogram of (*S*)-timolol with the addition of 1% of (*R*)-timolol. Linearity of the detector response of (*R*)-timolol added to

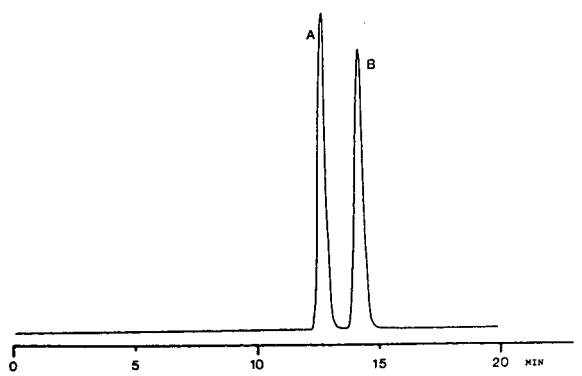

Fig. 2. Chromatogram of racemic timolol. Column, Chiralcel OD; injection volume, 20 μl; sample concentration, 1 mg/ml, detection wavelength, 300 nm. Peaks: A = (*R*)-timolol; B = (*S*)-timolol.

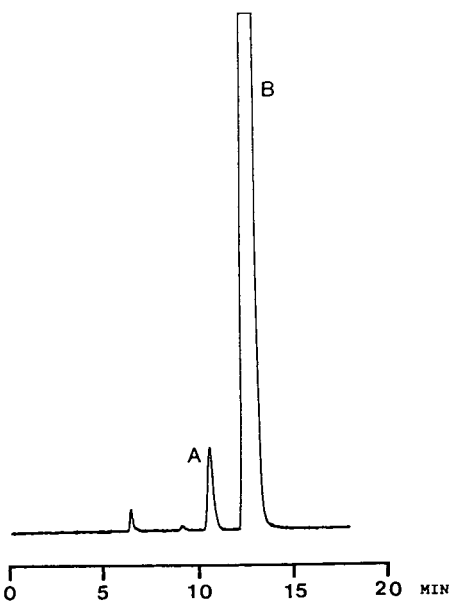

Fig. 3. Chromatogram of (*S*)-timolol spiked with 1% (*R*)-timolol. Column, Chiralcel OD; injection volume, 20 μl; sample concentration, 1 mg/ml; detection wavelength, 300 nm. Peaks: A = (*R*)-timolol; B = (*S*)-timolol.

the (*S*)-form was observed up to a content of 8%. The regression equation (area counts versus percentage added) was $y = 1\,189\,450x + 8274$ ($r = 1.0000$). The corresponding result for (*S*)-bunolol was $y = 21\,254x + 2546$ ($r = 1.0000$). The reproducibility was investigated at a level of 1% of the *S*-form added to the *R*-form; calculations from six determinations resulted in relative standard deviations (R.S.D.s) of 0.84% for (*R*)-timolol and 1.9% for (*R*)-bunolol. The limits of detection were estimated to be ca. 0.1% and 0.05% for (*S*)-timolol and (*S*)-bunolol, respectively.

It was found that the sample solutions were stable for at least 1 week, i.e., no extra peaks appeared in the chromatograms and no detectable racemization occurred in solutions stored at room temperature. The performance of the column was unaltered after several hundred injections and exposure to various mobile phases as described above.

3.2. AGP α-glycoprotein

A thorough evaluation of the ability of this stationary phase to separate β-blocking substances has been reported [13]. It was stated that this column is able to separate a wide range of β-blocking substances. In the present investigation, a procedure suggested by the manufacturer of the column was followed, using mixtures of 2-propanol and 10 m*M* aqueous phosphate buffers as the mobile phase for the separation of β-blockers. A volume of 20 μl of a sample concentration of ca. 0.02 mg/ml was injected, corresponding to an injected amount of 1–2 nmol of substance. The ability of the α-glycoprotein stationary phase to determine the *R*-form as an impurity in the *S*-form was evaluated for both timolol and bunolol. The separation of enantiomeric forms of timolol and bunolol was investigated and the use of a mixture of 1.5% 2-propanol in 20 m*M* phosphate buffer (pH 6.5), delivered at a flow-rate of 0.9 ml/min. These conditions were found to be the optimum when considering both the separation and a reasonable retention time. Detection wavelengths of 220 nm for bunolol and 300 nm for timolol were found to provide the best results. The resolutions for the enantiomers of bunolol and timolol were 1.8 and 2.0, respectively, under these conditions.

Fig. 4 shows a chromatogram of timolol. For both timolol and bunolol the *R*-form eluted before the *S*-form. As described above for the Chiralcel OD column, validation studies were performed according to the EEC guideline [47]. Linearity of the detector response of (*R*)-timolol added to the *S*-form was observed up to a content of 10%. The regression equation (area counts versus percentage added) was $y = 8643x + 1283$ ($r = 0.9997$); the large intercept on the abscissa indicated a small content of the *R*-enantiomer in the (*S*)-timolol raw material. The corresponding results for (*S*)-bunolol were $y = 8296x + 38$ ($r = 0.9998$). The reproducibility was investigated at a level of 1% of the *S*-form added to the *R*-form; calculations from six determinations resulted in R.S.D.s of 4.9% for (*R*)-timolol and 7.6% for (*R*)-bunolol. The limits of detection were estimated to be ca. 0.25% for both (*S*)-timolol and (*S*)-bunolol.

A serious drawback to the use of the AGP stationary phase was discovered during longer series (ca. 6–10 h) of analysis, with the separation power gradually deteriorating, i.e., severe

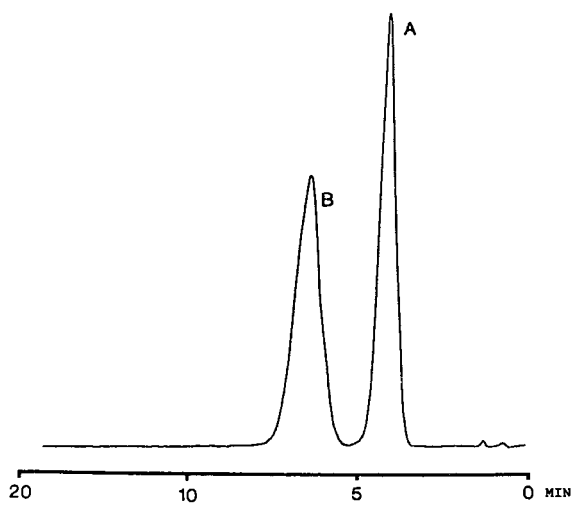

Fig. 4. Chromatogram of racemic timolol. Column, AGP; injection volume, 10 μl, sample concentration, 20 m*M*; detection wavelength, 300 nm. Peaks: A = (*R*)-timolol; B = (*S*)-timolol.

peak broadening and peak splitting were observed. The column could be regenerated by flushing with a 25% solution of 2-propanol for 2 h followed by flushing with water for 1 h. Accordingly, overnight utilization of the column employing automatic injection devices was of limited use.

3.3. β-Cyclodextrin

This column has been used with medium-polarity mobile phases, consisting of mixtures of acetonitrile, methanol, acetic acid and triethylamine, the separation of some β-blocking substances being achieved [25]. Apart from that, no work has been published which indicated that this stationary phase could provide the separation of β-blockers for analytical purposes. Therefore, the separation of the investigated β-blockers was attempted using various compositions of the above-mentioned mobile phase. The sample concentration was 1 mg/ml, the volume injected was 20 μl and flow-rate was 1 ml/min. It should be noted that the order of retention is reversed compared with the Chiralcel OD and the AGP stationary phases, i.e., with the β-cyclodextrin column the *S*-form elutes prior to the *R*-form. The detection wavelengths and the results obtained are given in Table 3. Fig. 5 shows a chromatogram for the separation of a 1:1 mixture of bunolol.

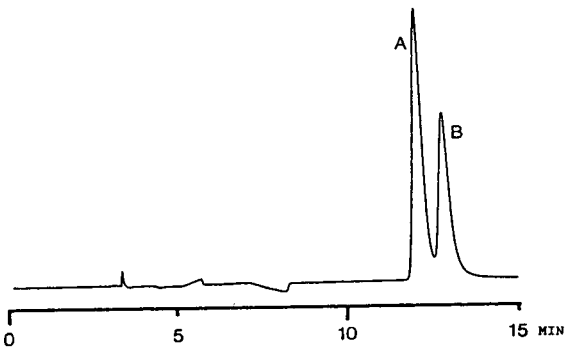

Fig. 5. Chromatogram of 1:1 mixture of (*R*)- and (*S*)-bunolol. Column, Cyclobond I; injection volume, 20 μl; sample concentration, 0.5 mg/ml each; detection wavelength, 300 nm. Peaks: A = (*S*)-timolol; B = (*R*)-timolol.

An attempt was made to separate all eighteen β-blockers, but for the eight substances not listed in Table 3 only very poor or no separations were obtained. The results in Table 3 show the chromatographic parameters for the ten β-blockers able to be separated with the β-cyclodextrin stationary phase. It is clear that the separation power is low with this phase, with α-values in the range 1.04–1.10. In order to evaluate the usefulness of this stationary phase in determining the *R*-form as an impurity in the *S*-form, the reproducibility for (*R*)-timolol added to the *S*-form at

Table 3
Chromatographic results for the compounds that could be successfully separated on the β-cyclodextrin (Cyclobond I) stationary phase

Compound	λ (nm)	Eluent[a]	$k'(1)$	$k'(2)$	α	R_s
Alprenolol	275	A	3.6	3.75	1.04	0.87
Betaxolol	275	B	3.9	4.2	1.07	1.14
Bisoprolol	275	A	5	5.23	1.05	0.70
Bunolol	267	B	2.93	3.19	1.09	1.52
Carazolol	253	B	5.13	5.47	1.07	1.16
Carteolol	275	A	7.27	7.67	1.05	0.96
Metoprolol	275	B	4.2	4.66	1.1	1.9
Propranolol	290	B	3.7	4.0	1.06	1.25
Tertatolol	290	B	3.1	3.3	1.06	1.14
Timolol	300	B	2.9	3.3	1.1	1.96

[a] Eluents: A = acetonitrile–methanol–acetic acid–triethylamine (99:1:0.24:0.36); B = acetonitrile–methanol–acetic acid–triethylamine (97:3:0.24:0.36).

a level of 1% was determined; the R.S.D. from six determinations was 12.5%. For bunolol, the limit of detection of the *R*-form in the *S*-form was ca. 2.5%, an unacceptably high limit of detection which to some extent is due to the fact that the impurity peak, i.e., the *R*-form, elutes after the principal peak, without being sufficiently separated. The high values for the reproducibility and the detection limit show that the β-cyclodextrin phase is not very useful compared with the two other phases tested.

4. Conclusions

Analysis of commercial samples of (*S*)-bunolol and (*S*)-timolol has shown that these contain 0.2–0.8% of the *R*-isomer. Thus, for a useful method for the determination of one enantiomer as an impurity in the other, the detection limit should be not more than 0.1% of the *R*-isomer, in order to provide adequate routine analyses of β-blocker raw materials. These investigations have shown that Chiralcel OD is the best suited for the determination of the enantiomeric purity of β-blockers. Sotalol was the only β-blocker that this column was unable to separate. Otherwise, the column provided separations with sufficiently good peak shapes and with reasonable times of analysis for practical analytical purposes. The column was found to be very stable when used for extended periods of analysis. Further, this stationary phase has been successfully applied to the determination of enantiomeric purity in a finished dosage form [48].

The AGP column also provides acceptable separations of β-blocking substances and with acceptably low detection limits for the determination of enantiomeric purity, even though the amount of substance injected is very small. The AGP column, however, seems to be less rugged in normal laboratory use, with peak broadening occurring after only 6–10 h of use, this being a serious drawback for routine analytical purposes. The β-cyclodextrin column does not provide sufficiently good separations to be used for the determination of the optical purity of β-blockers. Another disadvantage of the β-cyclodextrin phase, when used to separate timolol and bunolol, is that the *S*-form elutes before the *R*-form, the impurity peak eluting on the tail of the main peak, causing an unacceptably high limit of detection.

Acknowledgements

We thank the companies listed in Table 1, who donated the investigated β-blockers and their enantiomers.

References

[1] W.H. De Camp, Chirality, 1 (1989) 2.
[2] Investigation of Chiral Active Substances, Note for Guidance, Commission of The European Communities, Brussels, 1992.
[3] L. Olsen, K. Brønnum-Hansen, P. Helboe, G. Herlev Jørgensen and S. Kryger, J. Chromatogr., 636 (1993) 231.
[4] C. Petterson and G. Schill, J. Chromatogr., 204 (1981) 179.
[5] C. Petterson and M. Josefsson, Chromatographia, 21 (1986) 321.
[6] A. Karlsson, C. Pettersson and B. Björkman, J. Chromatogr., 494 (1989) 157.
[7] E. Kusters and D. Giron, J. High Resolut. Chromatogr. Chromatogr. Commun., 9 (1986) 531.
[8] E. Delee, L. LeGarrec, I. Jullien, S. Beranger, J.C. Pascal and H. Pinhas, Chromatographia, 24 (1987) 357.
[9] J. Hermansson, J. Chromatogr., 325 (1985) 379.
[10] K. Balmer, B. Persson and G. Schill, J. Chromatogr., 477 (1989) 107.
[11] M. Enquist and J. Hermansson, J. Chromatogr., 519 (1990) 285.
[12] C. Vandenbosch, T. Hamoir, D.L. Massart and W. Lindner, Chromatographia, 33 (1992) 454.
[13] C. Vandenbosch, D.L. Massart and W. Lindner, J. Pharm. Biomed. Anal., 10 (1992) 895.
[14] I. Marle, S. Jönson, R. Isaksson, C. Petterson and G. Petterson, J. Chromatogr., 648 (1993) 333.
[15] I. Marle, P. Erlandsson, L. Hansson, R. Isaksson, C. Petterson and G. Petterson, J. Chromatogr., 586 (1991) 233.
[16] Y. Blom and E. Heldin, J. Chromatogr. A, 653 (1993) 138.
[17] C. Vandenbosch, D.L. Massart and W. Lindner, Anal. Chim. Acta, 270 (1992) 1.
[18] J. Hermanson and A. Grahn, J. Chromatogr. A, 687 (1994) 45.

[19] T. Miwa, T. Miyakawa, M. Kayano and Y. Miyake, J. Chromatogr., 408 (1987) 316.
[20] J. Haginaka, C. Seyama, H. Yasuda and K. Takahashi, J. Chromatogr., 598 (1992) 67.
[21] N. Mano, Y. Oda, N. Asakawa, Y. Yoshida, T. Sato and T. Miwa, J. Chromatogr. A, 687 (1994) 223.
[22] J. Haginaka, C. Seyama, H. Yasuda, H. Fujima and H. Wada, J. Chromatogr., 592 (1992) 301.
[23] J. Haginaka, T. Murashima, C. Seyama, H. Fujima and H. Wada, J. Chromatogr., 631 (1993) 183.
[24] D.W. Armstrong, T.J. Ward, R.D. Armstrong and T.E. Beesley, Science, 232 (1986) 1132.
[25] D.W. Armstrong, S. Chen, C. Chang and S. Chang, J. Liq. Chromatogr., 15 (1992) 545.
[26] I.W. Wainer, T.D. Doyle, K.H. Donn and J.R. Powell, J. Chromatogr., 306 (1984) 405.
[27] A.M. Dyas, M.L. Robinson and A.F. Fell, Chromatographia, 30 (1990) 73.
[28] M. Ohwa, M. Akiyoshi and S. Mitamura, J. Chromatogr., 521 (1990) 122.
[29] W.H. Pirkle and J.A. Burke, III, J. Chromatogr., 557 (1991) 173.
[30] Y. Okamoto, M. Kawashima, R. Aburatani, K. Hatada, T. Nishiyama and M. Masuda, Chem. Lett., (1986) 1237.
[31] H. Takahashi, S. Kanno, H. Ogata, K. Kashiwada, M. Ohira and K. Someya, J. Pharm. Sci., 77 (1988) 993.
[32] A.M. Krstulovic, M.H. Fouchet, J.T. Burke, G. Gillet and A. Durand, J. Chromatogr., 452 (1988) 477.
[33] C. Hartmann, D. Krauss, H. Spahn and E. Mutschler, J. Chromatogr., 496 (1989) 387.
[34] D.R. Rutledge and C. Garrik, J. Chromatogr., 497 (1989) 181.
[35] M.S. Ching, M.S. Lennard, A. Gregory and G.T. Tucker, J. Chromatogr., 497 (1989) 313.
[36] H.Y. Aboul-Enein and M.R. Islam, Chirality, 1 (1989) 301.
[37] H.Y. Aboul-Enein and M.R. Islam, J. Chromatogr., 511 (1990) 109.
[38] H.Y. Aboul-Enein and M.R. Islam, Anal. Lett., 23 (1990) 83.
[39] H.Y. Aboul-Enein and M.R. Islam, Anal. Lett., 23 (1990) 973.
[40] C.B. Ching, B.G. Lim, E.J.D. Lee and S.C. Ng, Chirality, 4 (1992) 174.
[41] K. Balmér, P.-O. Lagerström, B.-A. Persson and G. Schill, J. Chromatogr., 592 (1992) 331.
[42] B. Kofahl, D. Henke and E. Mutschler, Chirality, 5 (1993) 479.
[43] H.Y. Aboul-Enein and V. Serignese, J. Liq. Chromatogr., 16 (1993) 197.
[44] V.L. Herring and J.A. Johnson, J. Chromatogr., 612 (1993) 215.
[45] C. Facklam and A. Modler, J. Chromatogr. A, 664 (1994) 203.
[46] P.M. Lacroix, B.A. Dawson, R.W. Sears and D.B. Black, Chirality, 6 (1994) 484.
[47] Analytical Validation. The Rules Governing Medicinal Products in the European Community, Vol. III, Addendum 1, Brussels 1990.
[48] J. Ekelund, I. Litwar and L. Olsen, Poster presented at the 20th International Symposium on Chromatography, Bournemouth, 1994.

ELSEVIER

Journal of Chromatography A, 708 (1995) 263–271

JOURNAL OF CHROMATOGRAPHY A

Characterization of size-permeation limits of cell walls and porous separation materials by high-performance size-exclusion chromatography

Holger Woehlecke, R. Ehwald*

Institute of Biology, Math.-Nat. Faculty I, Humboldt-University, Invalidenstr. 42, D-10115 Berlin, Germany

First received 12 January 1995; revised manuscript received 28 March 1995; accepted 29 March 1995

Abstract

The limiting size of macromolecules for permeation through membranes (cell walls, artificial hydrophilic membranes) as well as size-dependent partitioning within hydrophilic matrices was investigated by HPLC-aided analysis of dextran permeation. The method includes (1) modification of a specially prepared polydisperse dextran probing solution (DPS) by permeation of size fractions through or into the investigated material, (2) fast flow size-exclusion chromatography (SEC) of the modified DPS on a calibrated Superdex-200 HR-column and (3) determination of permeability resp. partition parameters by comparison of the elution profiles of original and modified DPSs. By this method, the mean size limit of permeation through cell walls (cut off), size permeation parameters of hollow fibres, dialysis tubes and ultrafiltration membranes, and the size dependence of partitioning within gel particles can be determined with high accuracy in short time.

1. Introduction

The ultrafiltration properties of microbial and higher plant cell walls are attractive for polymer separation [1–3] and the physiological significance of cell wall permeability is obvious. It refers to retention of soluble polymers in the periplasma, crosslinking of the cell wall matrix, exudation of enzymes and other polymers, protoplast resistance to polymer toxins or lytic enzymes, cell–cell recognition and many other phenomena. The limiting size of polymers for permeation through the cell wall matrix may be altered in the course of extension growth and differentiation or in response to biotic and abiotic stress. Little is known about such changes, as up to now rather laborious methods have been used to measure size limits of cell wall permeation. These methods include observation of the plasmolysis/cytorhysis transition [4], identification of dye-marked polymers in the lumen of plasmolyzed or denatured cells [5,6] and permeation chromatography of polymers on beds of native cells [7], purified cell wall fragments [8] and cell wall microcapsules (CWC) [9–11]. We aimed in a convenient and fast method for estimation of size limits of exclusion resp. membrane permeation of polymers and their size-dependent partitioning, which is generally applicable to different porous and gel-like materials, especially CWC. A straightforward methodical principle was found in the early

* Corresponding author.

0021-9673/95/$09.50
SSDI 0021-9673(95)00407-6

papers of Scherer and collaborators [12,13]. These authors used a method based on GPC fractionation of a polydisperse probing solution of polyethylene glycol (PEG) before and after its equilibration with isolated cell walls or intact cells of bacteria and yeast. The applied GPC fractionation on Biogel was time-consuming and restricted to a small range of PEG molecular size fractions. However, important advantages of Scherer's methodical principle are the possible use of HPLC and its broad applicability to both permeation through membranes and partitioning within matrices. The potency of a method based on a special dextran probing dispersion, a calibrated Superdex 200 column and a HPLC system will be shown in this paper.

2. Experimental

2.1. Materials

Cell wall capsules (CWC) were prepared by denaturation of living plant and yeast cells in ethanol and extraction of ethanol and water-soluble cell contents. Suspension cultured cells of *Chenopodium album* L. earlier used for vesicle chromatography [9], the large sphaeric cells of axenically and autotrophically grown alga *Eremosphaera viridis* De Bary (strain B 228-1 of the collection of the Institute of Plant Physiology, University Göttingen), yeast cells (*Saccharomyces cerevisiae* L., ethanol production strain "Kolin", a kind gift of the Institute of Food Technology, Technical University, Berlin) harvested from an aerobic culture on a glucose/yeast-extract mineral medium in the stationary phase, as well as 1-mm thick slices cut from a 13-mm storage parenchyma cylinder of the potato tuber *Solanum tuberosum* L. (cultivar Quarta) were extracted with 96% ethanol and kept in ethanol at 4°C until analysis. In the case of the large algae and parenchyma cells, plasmoptysis, i.e. bursting of the cell wall by fast penetration of ethanol, was prevented by denaturation of protoplasts in 10% acetic acid before incubation in ethanol. Ethanol-saturated *C. album* cell clusters, *E. viridis* and *S. cerevisiae* cells were dispersed in an excess of a cold (4°C) 1 m*M* $CaCl_2$ solution for one hour. Easily filtrable particles (swollen Sephadex gels, extracted algae cells and cell clusters prepared from the suspension culture) were equilibrated with the buffer used for HPLC by washing the packed material on a sintered glass filter with at least three bed volumes of buffer. Yeast CWCs were equilibrated with the buffer by repeated centrifugation. Vesicular packing material (VP), i.e. enzymatically purified clusters of CWCs, from which the protoplast residue was removed, were obtained from the suspension culture by the procedure earlier described [11]. Alcohol-dried VP was obtained by saturating a fixed bed of the packing material with a mixture of 96% ethanol and *n*-propanol (9:1) and evaporation of the liquid phase in a vacuum rotary apparatus at a water bath temperature of 50°C.

The investigated hollow fibre for blood dialysis consisting of regenerated cellulose [14] was obtained from Kunstseidewerk Pirna (Germany), the dialysis tube Spectra/Por 10 kD from Spectrum (USA), the ultrafilter flat membrane PM-10 from Amicon (USA) and the Sephadex dextran gel beads (G 50 fine and G 75 superfine) from Pharmacia (Sweden).

2.2. Size-exclusion chromatography

SEC was carried out using prepacked Superdex 200 HR 10/30 columns (30 cm × 10 mm I.D., bed consisting of crosslinked agarose with covalently bonded dextran, mean bead diameter 13–15 μm) provided by Pharmacia LKB Biotechnology (Sweden), coupled to a HPLC system (Model 5000 Bio-Rad) and a polarimetric detector (Chiralyser, IBZ Meßtechnik). The sample loop volume of the injector used was 50 μl. An electrolyte solution containing 0.1 or 0.01 *M* phosphate buffer (pH 7), 0.1 *M* NaCl and 0.05% NaN_3 was used as eluent. The constant linear flow-rate was 12.7 mm/min. At this flow-rate, with our system, theoretical plate numbers of 4200 and 1600 were obtained from the peak dispersion of glucose and serum albumin, respectively (the plate count of the column for acetone given by the manufacturer is 10 000).

2.3. Calibration of the molecular size scale

A set of protein standards was used to calibrate the dependence of elution time on molecular size in terms of Stokes' radius. For this purpose, data given by Laurent and Killander [15] were used for the following proteins: γ-globulin (human), alcohol dehydrogenase (yeast), serum albumin (human), peroxidase (horseradish), chymotrypsinogen (porcine), cytochrome C (equine). Providers data (Pharmacia) were available for thyroglobulin (porcine), ferritin (equine), catalase (bovine), aldolase (rabbit) and ovalbumin (hen). The log of the Stokes' radius (r_s) of standard proteins was plotted vs. K_{AV} [16] (Fig. 1). In the course of the experiments we used three Superdex 200 HR 10/30 columns which slightly differed in the elution profile of dextran and the regression parameters between K_{AV} and r_s. Therefore, each column was calibrated separately. With one Superdex column many chromatographic runs (more than 300) could be performed without detectable change in the dextran elution profile.

2.4. Dextran probing solution

From a larger range of commercial preparations, the following dextran preparations were selected as components of the DPS: dextran 162 (No. 59F-0752, Sigma), dextran 60 (control: B7), dextran 15 (control: I) and dextran 4 (control: B) from Serva.

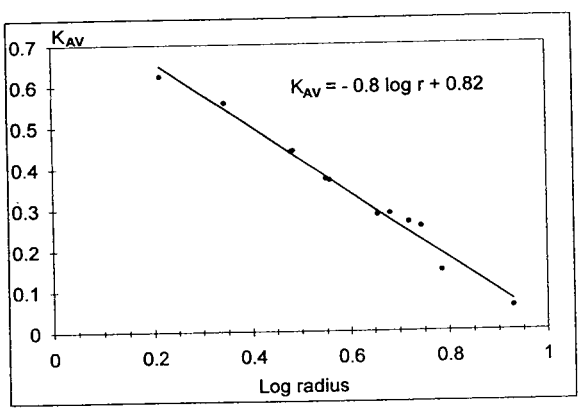

Fig. 1. Calibration curve of the Superdex-200 HR 10/30 column based on proteins with known Stokes' radius.

Computer-aided superposition of elution profiles obtained for these preparations was checked at different mixing ratios to obtain a DPS with nearly equal concentrations of the different size fractions over a wide range of molecular radii (see Results). The DPS has the following composition: 1 g/l dextran 162, 6 g/l dextran 60, 1.5 g/l dextran 15, and 2 g/l dextran 4. The dextrans were dissolved in the elution buffer.

2.5. Permeation procedures

Before dialysis of the DPS against plant CWCs or its partitioning within gel particles, mobile buffer was removed from the wet materials. In the case of the potato slices this was done by blotting on filter paper, with the other materials by suction through a glass filter (larger particles) or a 0.2-μm membrane filter (yeast). Drained materials were mixed with a small volume of DPS (about 1 ml DPS per g wet mass of drained material) and incubated for the given time. By parallel incubations in buffer it was ensured that no optically active material was lost during the incubation. After the incubation time a sample (at least 200 μl) of the external liquid phase (modified DPS) was taken and centrifuged for 10 min at ca. 3000 *g* to ensure absence of particles. In the case of easily filtrable material the modified DPS sample was taken from the outlet of an Econo column (Biorad), whereby particles were kept in suspension in order to avoid compression of soft cells by cohesion forces. In the case of yeast CWCs, the modified DPS was separated from the matrix by centrifugation (3000 *g*, 10 min). For sorption experiments, 0.1 g of alcohol-dried vesicular packing material was allowed to swell in 10 ml of the DPS (final bed volume about 6 ml). Investigation of the hollow fibres and the dialysis tube was carried out by filling their lumen with the DPS and dialysing the sample for different times in a large volume of stirred buffer. The modified DPS was taken as retentate from the lumen. In case of the flat ultrafiltration membranes, both permeate and retentate samples of the DPS were obtained by

the recommended filtration procedure (pressurizing the sample in the Amicon stirred cell 8050).

3. Results

The dextran probing solution (DPS) with a size dispersion fitted to the fractionation range of the Superdex column was obtained by mixing of commercial dextrans as described in the Experimental section. From the symmetric and narrow peaks obtained by rechromatography of the eluted fractions it may be stated, that the elution profile was not influenced by interactions other than size fractionation (Fig. 2).

The principle of the method described in this paper consists in comparison of the original DPS with a modified one, which was obtained by permeation of dextran through hydrophilic membranes or by partitioning within hydrophilic matrices. A computer was used to transform the elution time into Stokes' radius and to give the concentration quotient $Q = C_1/C_2$ of original (C_1) and modified (C_2) DPS to all pairs of pseudomonodisperse dextran fractions with equal Stokes' radius (Fig. 3).

If a volume of the resulting DPS is equilibrated with a similar volume of wet material consisting of cell wall capsules (CWCs) or gel particles, dextran fractions excluded from the cell lumina by the impermeable wall are diluted only by the buffer held in the surface film. Additional dilution by the intracellular liquid space or the intermicellar liquid is expected for permeable dextran fractions. Therefore, Q is not equal for all size fractions, the value being lower for the excluded and higher for the permeable molecules. In case of CWCs with a narrow cut-off and a large volume fraction occupied by free liquid within the cell, a step-like increase of Q at Stokes' radii between the size limits of exclusion and permeation [10] is expected. Figs. 3 and 4 demonstrate that this has indeed been found for CWCs prepared from highly vacuolated plant materials (suspension cells of *C. album*, the unicellular green algae *E. viridis*, and the parenchyma cells of *S. tuberosum*).

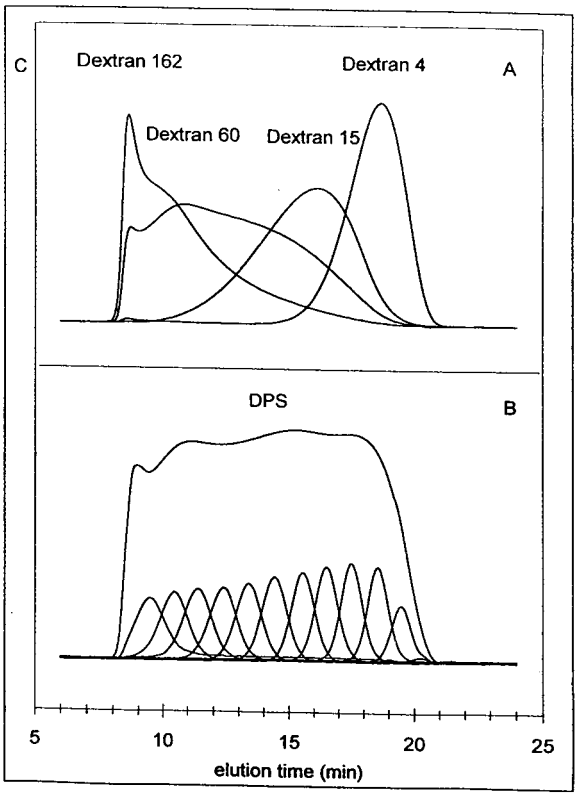

Fig. 2. (A) Elution diagrams of 1% solutions of 4 dextrans used as the components of the dextran probing solution (DPS). (B) Elution diagram of the DPS. Also shown are elution diagrams obtained by rechromatography of pseudomonodisperse fractions of the DPS eluate (0.1 ml) at different elution times (peak elution volume identical with the elution volume at sampling). The peak variance of the pseudomonodisperse fraction at elution time 17.5 min is 0.3 nm in terms of Stokes' radius. The concentration signal C (arbitrary units) is obtained by a polarimetric detector. For details of the chromatographic system see Experimental.

The difference between Q values of excluded and permeable dextran fractions is mainly caused by the large empty intracellular volume of the extracted cells which forms a size-independent dilution space for permeable molecules. The Stokes' radius of a dextran fraction which is diluted by 50% of the internal distribution space (obtained as shown in Fig. 3B) may be defined as mean size limit (MSL) of cell wall permeation. If the matrix volume of the cell wall and cell contents is small in comparison to the intracellular bulk liquid and the permeable compounds

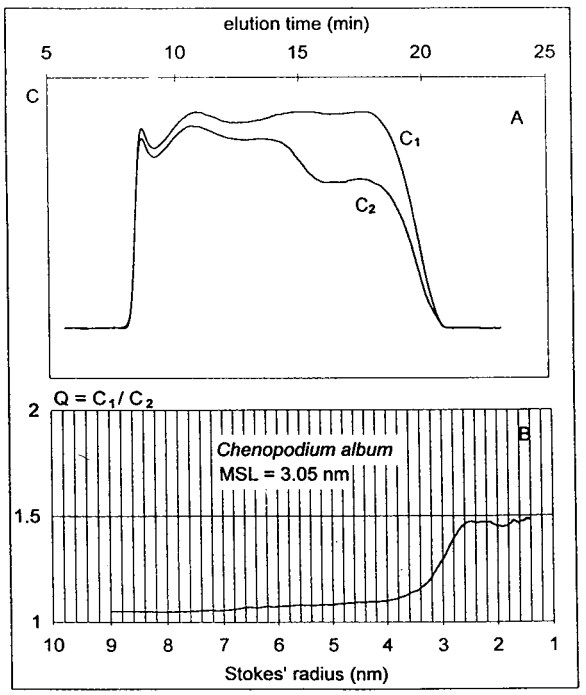

Fig. 3. (A) Diagrams of concentration of original (C_1) and modified (C_2) DPS at different elution time. Equal volumes of a wet (buffer saturated) packed mass of cell capsules prepared from *C. album* were mixed and incubated for 30 min before obtaining the modified DPS by filtration. (B) Diagram of the concentration quotient $Q = C_1/C_2$ at different Stokes' radii obtained by the calibration function shown in Fig. 1. The MSL is the Stokes' radius obtained at the middle of the step in the Q diagram.

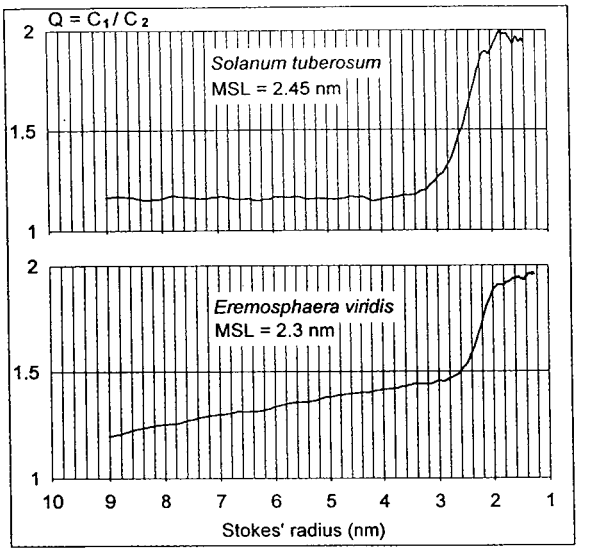

Fig. 4. Q diagrams of cell wall capsules of two different plant materials (obtained as demonstrated in Fig. 3). Incubation period: 30 min in case of *E. viridis*, 6 h in case of potato tissue slices.

have approximately reached an equilibrium partition, the MSL is the Stokes' radius allowing for permeation into half of the cells. The curves obtained with *E. viridis* CWCs did not show a clear size-independence of Q at high molecular size. This peculiarity may have been caused by a rather high content of cell wall ghosts (collapsed cell wall envelops of the mother cells, from which autospores have been released) in the preparation.

If partitioning of dextran fractions with hydrated gel particles is analyzed by our method, the dependence of Q on the Stokes' radius describes the broad size fractionation range which is typical for uniform hydrophilic gels (Fig. 5).

At a molecular size beyond the exclusion limit of the gel, Q is constant ($Q = C$). The difference $Q - C$ found for permeable size fractions is proportional to the partition coefficient of the respective dextran fraction in the matrix (K_{av} value).

$$\Delta Q = Q - C = k \cdot K_{av},$$

where k may be obtained as $(V_g - V_{ex})/(V_d + V_{ex})$, and V_g is the volume of the whole gel sample, V_{ex} the volume of the surface-bound liquid and V_d the volume of the DPS solution. V_{ex} may be derived from dilution of the excluded fractions:

$$V_{ex} = V_d \cdot (C - 1).$$

It is known that size-exclusion characteristics of a concentrated solution of soluble high-molecular-mass dextran (kept in a dialysis tube) is similar to that of a swollen gel of crosslinked dextran at equal dextran concentration [15]. Extracted and rehydrated yeast cells, which are filled with a concentrated dispersion of non-permeable protein [17], show a size fractionation curve which is similar to that of gel materials.

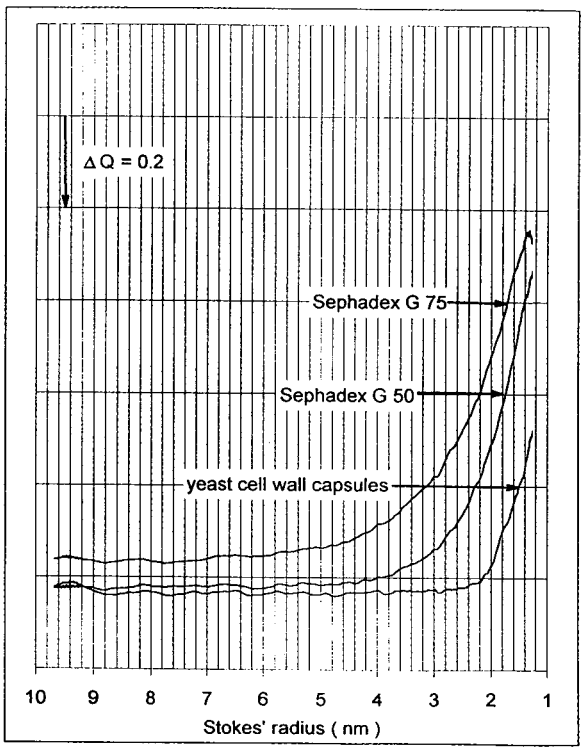

Fig. 5. Q diagrams of gel particles and ethanol-extracted yeast. For clearness, the curves are shifted on the Q scale.

Here, because of the size-exclusion effect of the concentrated polymers, the partition coefficient of permeable dextran molecules is size dependent. The size-exclusion limit obtained from such a system may be interpreted as a cell wall parameter only with caution. It should be checked whether the size-exclusion limit of the included concentrated polymer solution is larger than that of the cell wall.

In the case of yeast cells and small cell clusters of *C. album* it was proved that the values obtained for the size-exclusion limit and the MSL did not increase significantly after an incubation time of 10 or 30 min, respectively (Table 1). However, as the MSL of potato slices increased slightly even after an incubation period of 8 h, especially in case of multilayered tissue slices or cells with thick walls, it seems to be necessary to define the kinetic conditions before a comparative investigation.

In good accordance with the theoretical prediction, the MSL of *C. album* cell walls harvested in the stationary phase (Table 2) gives a value between the size-exclusion limit (ca. 3.4 nm) and the size-permeation limit (ca. 2.8 nm), which were obtained by direct permeation chromatography of polydisperse dextran with CWCs obtained from the same culture [11]. Advantages of the technique described here are the independence of the chromatographic properties of the investigated material, convenience, better reproducibility and higher accuracy. The resolution of the method is sufficient to reproduce small differences in the MSL (0.1 nm) of different batch preparations of CWCs.

In the experiments shown above, the mechanism of separation by the CWC was dialysis (diffusion through a porous membrane). If dried

Table 1
Size-exclusion limit (SEL) of denaturated and ethanol-extracted yeast cells and mean size limit (MSL) of permeation into plant cell wall capsules

Material	Incubation time	SEL, MSL (nm)					
Saccharomyces	5 min			2.2			
cerevisiae	10 min			2.2			
Chenopodium album	30 min		3.5		3.5		
150 μm cell clusters	60 min		3.5		3.4		
	2 h	2.2		2.2		2.2	
Solanum	4 h	2.4		2.4		2.4	
tuberosum	6 h	2.5		2.5		2.4	
1 mm thick slices	8 h	2.6		2.6		2.6	
	25 h	2.8		2.8		2.8	

Table 2
Reproducibility of MSL investigated for batch preparations of deproteinated vesicular packing particles (VP) and cell wall capsules (CWC) obtained from the *C. album* cell culture (incubation time 30 min)

Batch sample	VP (28)					CWC (9.6.)					CWC (16.6)				
	1	2	3	4	5	1	2	3	4	5	1	2	3	4	5
MSL (nm)	3.1	3.2	3.2	3.1	3.2	3.0	2.9	3.0	3.0	3.0	3.2	3.2	3.2	3.2	3.1
Average MSL (nm)	3.16					2.98					3.18				
Standard deviation	0.055					0.045					0.045				

CWCs are allowed to absorb liquid from a polymer solution, the initial mechanism of size separation is ultrafiltration, a mechanism which is important for the dry column technique of vesicle chromatography [3]. Here, Q values of excluded polymers below 1 are obtained. It was questionable whether a higher porosity of the alcohol-dried cell wall might cause entrapping of larger molecules at the beginning of the sorption process (see Ref. [18]), as the size permeation limit of the dehydrated cell wall in pure ethanol or acetone (measured by permeation of polyethylene glycol) is much larger than that of the hydrated wall [19]. However, we did not find a strong difference between the size-exclusion effects of dry and wet CWCs. The MSL of vesicular particles (VP) obtained by the sorption experiments is only slightly larger than that obtained with the same material in a dialysis experiment (Table 3).

The described method can be used to characterize size separation properties for transport through membranes of hollow fibres and dialysis tubes as well as flat ultrafiltration membranes. In our dialysis experiments with hollow fibres and dialysis tubes (Fig. 6), the internal compartment was filled with the DPS.

The volume of this compartment was small in comparison to that of the stirred external compartment. The sample of the retentate (modified

Table 3
Mean size limits (MSL) of vesicular packing particles prepared from *C. album* determined by incubation of ethanol-dried material and moist material of the same batch preparation in the DPS (30 min)

	Dried material (sorption)		Wet material (dialysis)	
MSL (nm)	3.7	3.7	3.5	3.5

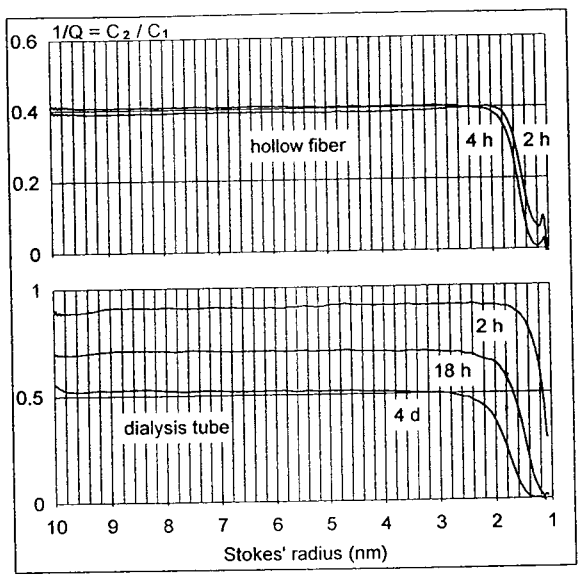

Fig. 6. Diagram of $C_2/C_1 = 1/Q$ of modified DPSs obtained by dialysis of the original DPS from a blood dialysis hollow fibre (regenerated cellulose, length 3 m, internal volume ca. 75 μl, inner diameter 190 μm) and a Spectra-Por CE dialysis tube (cellulose ester, internal volume 2 ml, diameter 7.5 mm, nominal molecular mass cut-off 10 000) into 200 ml of stirred buffer. Samples of the internal modified DPS (retentate) were obtained at the given dialysis times.

DPS) was investigated. If a permeable compound had reached equilibrium partition, its concentration in the modified DPS (C_2) decreased to approximately zero. As expected, the size range of dextran molecules with incomplete retention is clearly dependent on the incubation time. For such experiments, $C_2/C_1 = 1/Q$ is a useful parameter to describe retention. As long as $1/Q$ is constant, impermeability may be assumed (dilution may have been caused only by osmotic water uptake into the lumen). The exclusion limit of the membranes (initially strongly time dependent) may be defined by a threshold of 95% retention, i.e. the critical molecular size for reducing $1/Q$ to 95% of the constant value.

The result of ultrafiltration through a flat membrane is not only dependent on the porosity properties of the membrane but also on flow-rate, concentrations and convective flow along the membrane surface. Separation characteristics of ultrafiltration processes can be conveniently studied by the described chromatographic technique, as demonstrated in Fig. 7.

Volume flow through the membrane produces two modified DPSs: permeate and retentate. Comparison of the modified DPSs with the original one allows for the definition of ultrafiltration parameters, whereby curves of C_1/C_2 may be used in the case of the retentate and of C_2/C_1 in the case of the permeate.

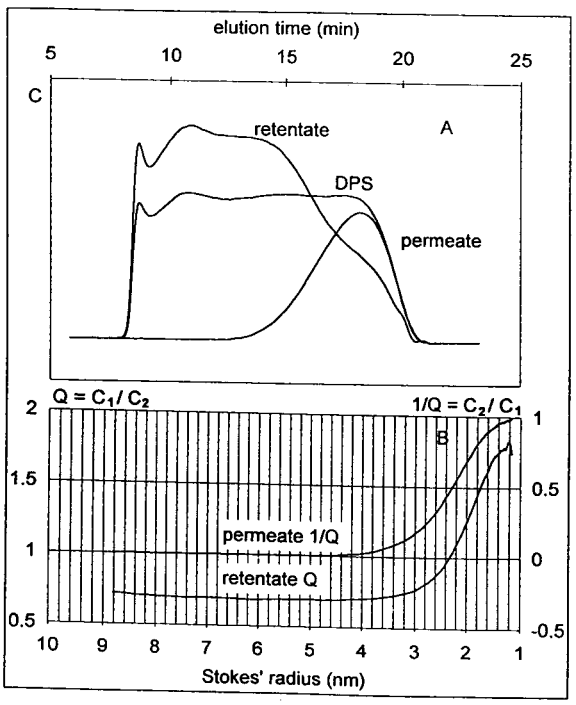

Fig. 7. (A) Diagram of the concentration of eluted dextran from modified DPSs obtained as retentate and permeate in comparison to the original DPS at different elution time. Ultrafiltration membrane: Amicon PM 10. Original volume of DPS: 10 ml, retentate volume: 3 ml. For chromatography, the retentate was diluted with buffer (1/1). (B) Diagrams of concentration quotients suitable for evaluation of the membrane cut off by modified DPDs.

4. Discussion

It should be kept in mind, that values given here as critical molecular size parameters do not refer to the size of the dextran molecules within the investigated matrices, which is difficult to estimate because of the flexibility of the highly hydrated molecules and the influence of the matrix on the large number of their possible conformations [20]. Fortunately, homogeneity of the molecular structure (branching) of the dextran polymers is not essential for our method. It was sufficient to show, that the DPS can be separated into narrow pseudomonodisperse size fractions with defined K_{AV}, as our size estimates are equivalent Stokes' radii, obtained by comparison with the Stokes' radii of the proteins used for GPC calibration. Reference to proteins is an important aspect and seems to be justified because (1) it has been shown that K_{AV} values of proteins and dextrans with equal Stokes' radius (in water) are similar or closely related [15,21,22] and (2) protein permeation into or through porous materials is most significant under both technical and physiological aspects. Cell walls are usually strongly negatively charged matrices. Therefore, the partition parameters and the size permeation limit of ampholytic polyelectrolytes as proteins in the cell wall are not only dependent on their hydrodynamic size but also on electrical field barriers or attraction forces, which are strongly dependent on ion

strength and pH [10,23]. However, as the used DPS and GPC matrix both can be regarded as uncharged, the described method is selective for the steric aspect of cell wall permeability.

In the case of CWSs the step-like change of Q is continuous over a certain range beyond and below the MSL, although for an equilibrium partition with uniform thin-walled capsules a sharp size limit (discontinuous step in Q) may be expected. The width of the experimentally observed step is partly explained by the variability of individual capsules with respect to the size limit of permeation and partly by the chromatographically caused peak variance of monodisperse fractions. Insufficient chromatographic resolution would prevent a discontinuous steep change in Q, even if the separation limit would be a point on the size scale identical for all cells and the permeable fractions were all in equilibrium. In reality, equilibrium can be approximately assumed in case of small thin-walled cells (Table 1). The peak variance of a narrow (pseudomonodisperse) dextran fraction or of a protein (0.3 nm in terms of the Stokes' radius) is similar to the variance of dQ/dr_s near the MSL (Figs. 3 and 4). Obviously, the resolution of the applied GPC system is not sufficient for an optimal description of the small variability of the cells' individual cut-off. Resolution could be improved by the choice of GPC media with a more narrow size fractionation range (and related DPSs) as well as by further improvement of the chromatographic efficiency. However, for many purposes, the variance of the individual cells of a sample with respect to the cell wall cut-off is less interesting than the mean value expressed by the MSL. Good reproducibility and resolution of even small changes in the MSL is possible with the described method (Table 2), and the applied system has a broad measuring range useful for cell wall research (MSL between 2 and 7 nm). For materials with smaller MSL of the cell wall like *Geosiphon* [24] a comparable system involving a Superdex 75 column can be recommended.

Acknowledgements

The authors thank the Deutsche Forschungsgemeinschaft for support and Mrs. Petra Heese and Mrs. Heidemarie Schneider for their excellent technical assistance.

References

[1] M. Sára and U.B. Sleytr, J. Membrane Sci., 33 (1987) 27-49.
[2] R. Kleine, H. Woehlecke and R. Ehwald, Acta Biotechnol., 12 (1992) 243-253.
[3] H. Woehlecke and R. Ehwald, Bio-Forum, 5 (1992) 174-175.
[4] N. Carpita, D. Sabularse, D. Montezinos and D.P. Delmer, Science, 205 (1979) 1144-1147.
[5] O. Baron-Epel, P.K. Gharyal and M. Schindler, Planta, 175 (1988) 389-395.
[6] E. Shedletzky, M. Shmuel, T. Trainin, S. Kalman and D. Delmer, Plant Physiol., 100 (1992) 120-130.
[7] J.P. Gogarten, Planta, 174 (1988) 333-339.
[8] M. Tepfer and I.E.P. Taylor, Science, 213 (1981) 761-763.
[9] R. Ehwald, G. Fuhr, M. Olbrich, H. Göring, R. Knösche and R. Kleine, Chromatographia, 28 (1989) 561-564.
[10] R. Ehwald, P. Heese and U. Klein, J. Chromatogr., 542 (1991) 239-245.
[11] R. Ehwald, H. Woehlecke and C. Titel, Phytochemistry, 31 (1992) 3033-3038.
[12] R. Scherrer and P. Gerhardt, J. Bacteriol., 107 (1971) 718-735.
[13] R. Scherrer, L. Louden and P. Gerhardt, J. Bacteriol., 118 (1974) 534-540.
[14] J. Gensrich and D. Paul, in J.F. Kennedy, G.O. Phillips and P.A. Williams (Editors), Cellulosics: Materials for selective separations and other technologies, Ellis Horwood, London, 1993, Ch. 14, p. 119.
[15] T.C. Laurent and J. Killander, J. Chromatogr., 14 (1964) 317-339.
[16] A.G. Ogston, Trans. Faraday Soc., 54 (1958) 1754.
[17] F.M. Klis, Yeast, 10 (1994) 851-869.
[18] B. Selisko and R. Ehwald, J. Biochem. Biophys. Methods, 27 (1993) 311-325.
[19] R. Ehwald, U. Klein, A. Jäschke, D. Cech and C. Titel, Patent EP 0412507 A1 (1991).
[20] A.M. Basedow and K.H. Ebert, J. Polym. Sci. Polym. Symp., 66 (1979) 101-115.
[21] T.C. Laurent and K.A. Granath, Bioch. Biophys. Acta, 136 (1967) 191-198.
[22] P.L. Dubin and J.M. Principi, Macromolecules, 22 (1989) 10891-10896.
[23] A. Jäschke and D. Cech, J. Chromatogr., 585 (1991) 57-65.
[24] A. Schüßler, E. Schnepf, D. Mollenhauer and M. Kluge, Protoplasma, in press.

ELSEVIER

Journal of Chromatography A, 708 (1995) 273–281

JOURNAL OF CHROMATOGRAPHY A

High-performance size-exclusion chromatographic characterization of water-soluble polymeric substances produced by *Phanerochaete chrysosporium* from free and wheat cell wall bound 3,4-dichloroaniline

Enamul Hoque

GSF-Forschungszentrum für Umwelt und Gesundheit, Institut für Biochemische Pflanzenpathologie, Ingolstädter Landstr. 1, Postfach 1129, D-85758 Oberschleißheim, Germany

First received 14 December 1994; revised manuscript received 29 March 1995; accepted 29 March 1995

Abstract

A high-performance size-exclusion chromatographic (HPSEC) method was developed and optimized for the separation of aq. soluble polymeric xenobiotics. The use of this method for the characterization of aq. soluble polymeric substances produced by *Phanerochaete chrysosporium* cultures from [*ring*-U-^{14}C]-3,4-dichloroaniline ([^{14}C]DCA) and wheat cell wall bound [*ring*-U-^{14}C]-3,4-dichloroaniline was demonstrated by on-line UV detection at 280 nm and radioactivity tracing. The polymeric nature of aq. soluble lignin-like ^{14}C-products was shown by polydispersity and correspondence of the UV signal at 280 nm with the radioactivity trace. The higher polydispersity and molecular mass of lignin-like substances in low-C cultures as compared to those in low-N cultures were found to be associated with lower mineralization rates. Results indicated that the major portion of copolymerized DCA was apparently covalently bound via labile bonds to the α-C atom of the lignin monomer side chains on native wheat cell wall.

1. Introduction

Lignin has been regarded by many scientists as plant's major metabolic sink for the physiological removal of various types of pesticidal xenobiotics from plant intracellular systems via copolymerization. It was reported, for example, that ca. 60–80% of applied 3,4-dichloroaniline could be copolymerized into lignin by wheat plants [1]. As this biopolymer constitutes about 15–25% of the organic substances in some plants [2], it could be considered a major vehicle for the accumulation of diverse types of pesticidal xenobiotics in the natural environment [1]. The biopolymer lignin is formed by cross-polymerization of phenylpropane units via carbon–carbon and ether bonds, and is covalently bound to cell-wall polysaccharides (lignin–carbohydrate complexes, LCC) through hydrogen and ether bonding [3]. The herbicidal xenobiotic 3,4-dichloroaniline (DCA) is shown to be linked to the α-carbon of the phenylpropane side chain of lignin monomers during incorporation into plant lignin [1]. Until now, this group of copolymers has been successfully analysed by ^{1}H NMR spectroscopy, and its molecular mass distribution, e.g. for DCA–lignin, was successfully determined by Sephadex LH-60 chromatography

0021-9673/95/$09.50
SSDI 0021-9673(95)00408-4

[1,4]. In the past, lignin degradation products were analysed by gas chromatography, reversed-phase high-performance liquid chromatography, whereas lignin and lignin–cellulosic substances were characterized by Fourier transform infrared (FTIR) spectrometry, ^{13}C NMR, and pyrolysis gas chromatography–mass spectrometry (Py-GC–MS) [2,3,5]. These methods provide information on the phenolic monomeric constituents of lignin, allowing chemical characterization and significant comparison of treated and untreated materials, but they give no information on the molecular mass distribution of native lignin, oligomers derived from lignin degradation of lignin–carbohydrate complexes [3]. Molecular mass distributions of industrial lignin and lignocellulosics of wheat straw have been investigated by size-exclusion chromatography (SEC) and high-performance size-exclusion chromatography (HPSEC) [3], but HPSEC of lignin–pesticidal complexes for environmental studies, e.g. biodegradation and bioavailability, has not been performed to a great extent. The ubiquitous white rot fungus, *Phanerochaete chrysosporium*, plays an important role in the biodegradation, mineralization and bioavailability of free and lignin-bound pesticides, e.g. chloroanilines, polychlorinated hydrocarbons [6], in agricultural and forest ecosystems. The unique feature of *Phanerochaete chrysosporium* to mineralize a diverse range of xenobiotics, especially in low-N culture media, has been well documented. However, there are controversies about the role of its lignin-peroxidase in mineralization, polymerization or depolymerization of degradation products during bioconversion of free and bound xenobiotics [6].

The intent of the present paper is to describe a newly developed HPSEC method and to demonstrate its applicability to the characterization of aq. soluble polymeric substances produced by the white rot fungus *Phanerochaete chrysosporium* from [*ring*-U-^{14}C]-3,4-dichloroaniline and wheat cell wall [*ring*-U-^{14}C]-3,4-dichloroaniline–lignin metabolite fractions. Such a research is essential not only for the investigation of the ecotoxicological relevance of free and bound pesticidal residues in the environment (mineralization, release, bioavailability), but also for the biological detoxification of contaminated soils or other materials.

2. Experimental

2.1. Chemicals

All chemicals (p.a. grade) and solvents (HPLC grade) used in our studies were obtained either from Riedel-de Haën (Germany) or from Merck (Germany). Water used for the mobile phase of the HPSEC system was four times demineralized using Seralpur pro 90C system (Seral, Ransbach-Baumbach, Germany). The molecular mass calibration standards with peak molecular mass, M_p 1500, 5400, 8000, 19 300, 46 000, 73 500, 95 600, 200 000, 400 000, 780 000 (polystyrolsulphonate Na-salt; Polymer Science Labs., USA) were obtained from Macherey-Nagel (Germany). Blue Dextran (approx. molecular mass $2 \cdot 10^6$) was purchased from Sigma (Germany). Sitka spruce (*Picea sitchensis* L.) milled wood lignin (spruce in situ lignin) standard was prepared according to Lapierre et al. [7].

2.2. HPSEC instrumentation

A Merck-Hitachi HPLC system (L-6200 intelligent pump, Merck, Germany) was equipped with a Rheodyne injector Model 7125, an UV detector (Model 757 absorbance detector, Applied Biosystems, USA), and a HPLC radioactivity monitor (LB 505, Berthold, Germany). It was connected to a HPSEC (size exclusion) column GFC 300-8 with hydrophilic gel surfaces (column dimension, 300 × 7.7 mm I.D.; particle size, 8 μm; pore size, 300 Å; Macherey-Nagel, Germany) with a pre-column GFC 8P (50 × 7.7 mm I.D.) packed with the same gel as used for the main column.

The UV and radioactivity signals were acquired and processed by a PC-based software system Ramona (Raytest, Germany) and a Merck-Hitachi Integrator (D-2500 Chromato-Integrator).

2.3. Chromatographic conditions for HPSEC

During development of the HPSEC system, the effects of Na_2HPO_4 buffer (molarity, pH), $NaNO_3$ (molarity), and the organic additive methanol on the hydrophobic interactions as well as on the separation were studied. The flow-rate of the mobile phase for HPSEC separation was optimized. The optimized system used the following solvent system as mobile phase: 5 m*M* Na_2HPO_4 + 0.1% MeOH (pH 7.0) at a flow-rate of 0.5 ml/min. Samples were dissolved either in 5 m*M* Na_2HPO_4 + 0.1% MeOH, pH 7.0 (soluble products), or in 0.1 *M* Na_2HPO_4, pH 11.18 (polystyrolsulphonate Na-salt standards; Sitka spruce milled wood lignin). The pH of the mobile phase was adjusted using 3 *M* H_3PO_4, and the mobile phase was filtered through 0.2-μm filters (filter type RC 58, Schleicher and Schuell, Germany). Usually 20-μl samples were injected, however, radioactivity traces of the HPSEC analysis of DCA–lignin degradation products were obtained with an injection volume of 100–500 μl. Blue dextran (9.32 μg) and KNO_3 (1% aq. solution) were injected at a volume of 5 μl.

The UV signals were detected at 280 nm at high detector sensitivity (0.01 AUFS) for 20-μl injection volumes and at a low-detector sensitivity (2.0 AUFS) for 100-μl injection volumes. The elution of KNO_3 was monitored at 260 nm, and that of blue dextran at 380 nm.

2.4. Reversed-phase high-performance liquid chromatography

Reversed-phase high-performance liquid chromatography (RP-HPLC) of aq. soluble lignin fractions was performed with a gradient of 89.4% CH_3CN + 0.6% MeOH in H_2O (solvent B) and H_2O (solvent A) on a narrow bore column (250 × 4 mm I.D., 3 μm particle size, stationary phase Spherisorb C_8, flow-rate 0.6 ml/min) as follows: 0 min 30%, 5 min 40%, 10 min 45%, 15 min 50%, 18 min 55%, 20 min 60%, 25 min 75%, 27 min 100%, 29 min 100%, and 30 min 30% B in A. The column was calibrated using the following synthetic, authentic standards: N-(3,4-dichlorophenyl)glucoside (t_R 7.5 min), N-(3,4-dichlorophenyl)succinamide (t_R 15.2 min), N-(3,4-dichlorophenyl)succinimide (t_R 19.0 min), and 3,4-dichloroaniline (t_R 23.7 min) [8].

The detection of UV signals (250 nm, Model 757 absorbance detector, Applied Science, USA) and radioactivity signals (Model Berthold LB 505, Germany) was performed on-line as described for the HPSEC set-up.

2.5. Fermentation conditions

Phanerochaete chrysosporium cultures were maintained in the low-C and low-N media according to Kirk et al. [9] for 21 days, with veratryl alcohol added to the culture media for the stimulation of ligninase production. The concentration of DCA (non-labelled and/or ^{14}C-labelled DCA) was adjusted to 50 μmole/40 ml culture medium, with the radioactivity of [^{14}C]DCA in the treatment group "free DCA + bound [^{14}C]DCA" being half (0.169 μCi) that of the radioactivity applied for the treatment groups "free or bound [^{14}C]DCA" (0.338 μCi). The details of the fermentation conditions will be published elsewhere [10].

2.6. Preparation of wheat cell wall [^{14}C]DCA–lignin metabolite fractions

A wheat cell wall [^{14}C]DCA–lignin metabolite fraction was prepared by pooling the thoroughly extracted insoluble wheat residues from parts of the plant (*Triticum aestivum* var. Goetz) with the highest incorporation of ^{14}C [11]. The final dried wheat cell wall [^{14}C]DCA–lignin metabolite fractions had a consistency of irregular-sized light-brown strips, and showed a specific radioactivity of 5.14 μCi/g.

2.7. Water-soluble wheat cell wall [^{14}C]DCA–lignin degradation products produced by Phanerochaete chrysosporium

The water-soluble wheat cell wall [^{14}C]DCA–lignin degradation products were pooled from low-C and low-N culture filtrates of *Phanero-*

chaete chrysosporium at the end of the fermentation period (21 days) following exhaustive extraction with ethylacetate and *n*-butanol at pH 8.0 and 2.5, and subsequent adjustment of the pH of the unextractable aq. phase to 7.0 [10]. After evaporation in vacuo, the residues from the unextractable aq. phase (pH 7.0) were dissolved in appropriate volumes of 5 m*M* Na_2HPO_4 + 0.1% MeOH (pH 7.0) and analysed as described above.

2.8. Calibration of the HPSEC column by molecular mass (M_p) standards and estimation of molecular mass

The calibration curves of log M_p vs. elution volume, V_e, (see sections 2.1 and 2.3) were generated by Sigma-Plot software (Jandel, USA). The void volume (V_0) was determined by polystyrolsulphonate Na-salt at M_p 780 000 and blue dextran at an M_p of approx. $2 \cdot 10^6$, and the total permeation volume (V_p) was determined by KNO_3 (M_r 102).

The calibration curves of log M_p vs. elution volume (V_e) were used for the estimation of the M_rs of the analytes in our study. However, since we were not able to measure the intrinsic viscosity or radius of gyration by light scattering in our laboratory, all M_rs given for the water-soluble polymeric substances produced by *Phanerochaete chrysosporium* from free and wheat cell wall bound DCA using UV detection (see section 2.3) should be considered as "apparent", i.e. found by "estimation".

2.9. Statistical analysis

The statistical analysis (Student's *t*-test, coefficient of variation, precision, accuracy) of the HPSEC data was carried out using Sigma Plot software according to Hoque [12,13].

3. Results and discussion

3.1. Optimization of HPSEC

Prior to HPSEC optimization, the column system was several times equilibrated with water at a flow-rate of 0.5 ml/min. No separation of polymer standards (M_p 1500–95 600) was achieved on the selected column using 0.1 *M* Na_2HPO_4 (pH 11) as mobile phase. Lowering the pH from 11 to 9 did not result in any major improvement of the separation. However, water (pH 7.0) as a mobile phase showed some improvement of the separation of the polymer standards. Subsequently, the pH of aq. Na_2HPO_4 was adjusted to 7.0, and the effects of solute concentration on the size-exclusion behavior of the polymer standards were studied (Fig. 1). Fig. 1 shows the effects of $NaNO_3$ in the mobile phase [5 m*M* Na_2HPO_4 + 0.1% MeOH (pH 7.0)] on the size-exclusion behavior of the polystyrolsulphonate Na-salt standard with M_p 95 600. The signal intensity of the M_p peak at t_R 14.1 min increased from 21% at 10 m*M* $NaNO_3$ to 100% at 0 m*M* $NaNO_3$. The negative peak in front of the peak at t_R 21.5 min was completely eliminated using the mobile phase without $NaNO_3$ (Fig. 1). Therefore, the addition of $NaNO_3$ in the mobile phase was omitted.

Fig. 2 shows the separation of polystyrolsulphonate Na-salt narrow standards using the

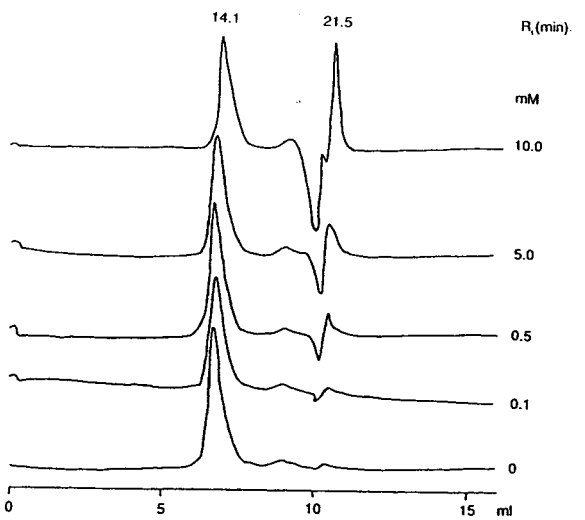

Fig. 1. Effects of $NaNO_3$ in the mobile phase [5 m*M* Na_2HPO_4 + 0.1% MeOH (pH 7.0)] on the size-exclusion behavior of polystyrolsulphonate Na-salt standard M_p = 95 600. Note the increment of the peak at t_R 14.1 min with elimination of the peak at t_R 21.5 min along with the negative peak in front of the peak at t_R 21.5 min.

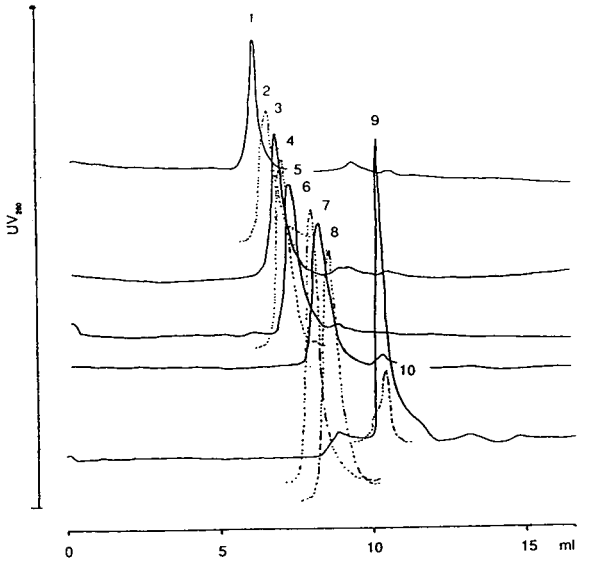

Fig. 2. Separation of polystyrol-sulphonate Na-salt narrow standards using the optimized mobile phase 5 m*M* Na_2HPO_4 + 0.1% MeOH (pH 7.0). The peaks of polystyrol-sulphonate Na-salt standards (indicated by solid and dashed lines) are designated by arabic numbers: 1 = M_p 400 000, 2 = M_p 200 000, 3 = M_p 95 600, 4 = M_p 73 500, 5 = M_p 46 000, 6 = M_p 19 300, 7 = M_p 8000, 8 = M_p 5400, 9 = M_p 1500, and 10 = M_p 102 (KNO_3). A sample equivalent to 50 μg standard was injected each time to obtain the chromatogram.

optimized mobile phase 5 m*M* Na_2HPO_4 + 0.1% MeOH (pH 7.0). The signal-to-noise ratio was improved, the negative peak was eliminated and the difference in the t_Rs of the M_p 1500 and M_p 95 600 peaks was maximized.

The relationship between log M_p and retention volume V_R is shown in Fig. 3. The exclusion limit was found to be M_p 400 000 and the total permeation limit M_p 102.

After optimization of the HPSEC method for polystyrolsulphonate standards, the column was tested for the size-exclusion chromatography of Sitka spruce milled wood lignin, i.e. Spruce in situ lignin [7] (Fig. 4). The Sitka spruce milled wood lignin was shown to be polydisperse with M_p ranging from >102 to >400 000 (Fig. 4).

The standard deviation, precision and accuracy of V_R for polystyrolsulphonate Na-salt standards and Sitka spruce milled wood lignin components were found to be <0.2%, <2.9% and <7.5%, respectively. Thus, within the size-exclu-

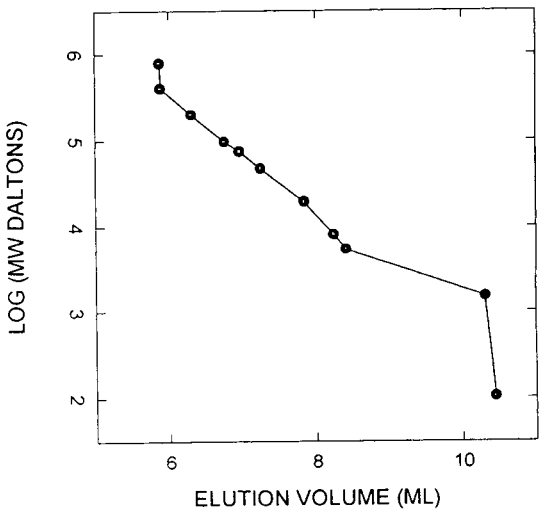

Fig. 3. Relationship between log M_p and elution volume (ml) using the optimized mobile phase 5 m*M* Na_2HPO_4 + 0.1% MeOH (pH 7.0).

sion range between M_p 102 and M_p 400 000, the reproducibility of the size-exclusion chromatographic separation of synthetic (polystyrolsulphonate Na-salt) and natural (Sitka spruce milled wood lignin) polymer standards could be demonstrated.

3.2. Characterization of water-soluble polymeric substances produced by Phanerochaete chrysosporium from free [^{14}C]DCA and wheat cell wall bound [^{14}C]DCA

Fig. 5 shows the UV traces as well as the radioactivity traces of aq. soluble products derived from free [^{14}C]DCA, bound [^{14}C]DCA and free DCA + bound [^{14}C]DCA in the low-N cultures. The correspondence of the UV trace of lignin-like compounds (Fig. 5A) with the radioactivity trace (Fig. 5B) from free [^{14}C]DCA was either due to the polymerization of polar DCA-metabolites or due to the copolymerization of [^{14}C]DCA-degradation products with the ligninase-oxidized veratryl alcohol (veratrylaldehyde). For example, it is reported that ligninase may split the lignin between the C_α and the C_β of the propyl side chain to give benzaldehyde, which could be polymerized like veratrylaldehyde to soluble higher M_r products [14].

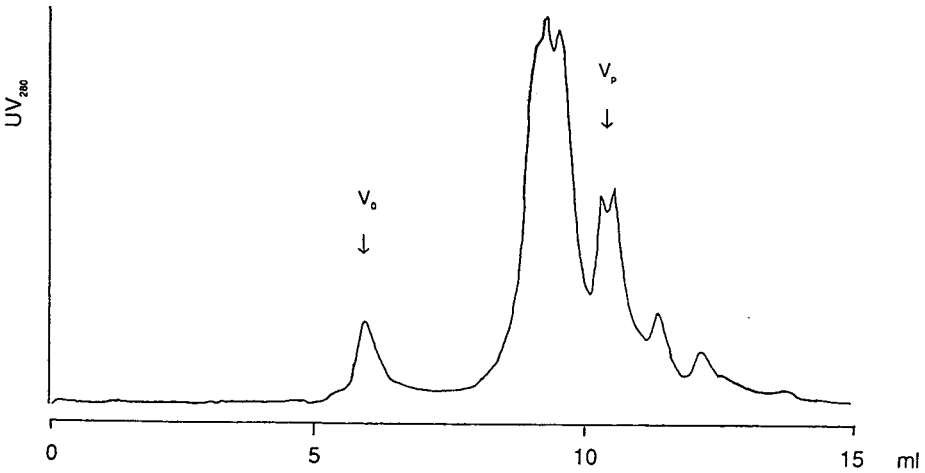

Fig. 4. Separation of sitka spruce milled wood lignin (109 μg in 0.1 *M* Na_2HPO_4, pH 11.18) using the optimized mobile phase 5 m*M* Na_2HPO_4 + 0.1% MeOH (pH 7.0).

The correspondence of the radioactivity trace (Fig. 5D) with the UV trace (Fig. 5C) of aq. soluble ^{14}C-products from bound [^{14}C]DCA showed their polydispersity to be approximately in the same range as that of free [^{14}C]DCA and free + bound [^{14}C]DCA in the low-N cultures of *Phanerochaete chrysosporium*. The low radioactivity trace (Fig. 5F) as compared to the UV trace (Fig. 5E) of the aq. soluble polymer from free DCA + bound [^{14}C]DCA was either due to a low concentration of bound [^{14}C]DCA applied in combination with free, non-labelled DCA (see Experimental) and/or due to increased depolymerization and mineralization of bound [^{14}C]DCA in the presence of free DCA.

In the low-C cultures characterized by lower mineralization rates [10], the radioactivity traces corresponded to the UV traces irrespective of the form (free or bound) and/or combination (free form + bound form) of applied [^{14}C]DCA (Fig. 6). However, similar to the low-N cultures (Fig. 5A,B), the correspondence of the radioactivity trace (Fig. 6B) with the UV trace (Fig. 6A) of the aq. soluble polymer from free [^{14}C]DCA indicated the occurrence of either polyphenolic-type polymerization of [^{14}C]DCA degradation products or copolymerization of [^{14}C]DCA degradation products with ligninase-produced veratrylaldehyde in low-C cultures.

The simultaneous change of the radioactivity trace and the UV trace at 280 nm of the aq. soluble polymer from bound [^{14}C]DCA of low-N and low-C cultures (Figs. 5 and 6) analogous to that from free [^{14}C]DCA suggested a substantial release of bound [^{14}C]DCA from wheat cell wall lignins via cleavage of labile bonds of [^{14}C]DCA to the C_α of lignin monomer side chains [11], and subsequent polyphenolic-type polymerization of [^{14}C]DCA degradation products by *Phanerochaete chrysosporium*.

3.3. Polydispersity of polymeric substances produced by Phanerochaete chrysosporium from [^{14}C]DCA and wheat cell wall [^{14}C]DCA–lignin metabolite fractions

Tennikov et al. [15] have shown that the polydispersity $U_w = (M_z)/(M_w)$ of unknown polymers could be determined by the formula:

$$\text{Polymer polydispersity, } U_w \approx 1 + \frac{\sigma_v}{\Psi(K)V_p} \qquad (1)$$

where σ_v is the width of the chromatogram, V_p is the total permeation volume, $\Psi(K)$ is the slope of the calibration curve, the mass-average molecular mass $M_w = \int_0^\infty f_w(M)\mathrm{d}M$ and $M_z = (M_w)^{-1}\int_0^\infty f_w(M)M^2\mathrm{d}M$ with $f_w(M)$ as the molecular mass distribution (MMD) function. According to Tennikov et al. [15], the slope of the calibration curve $\Psi(K)$ is dependent upon the

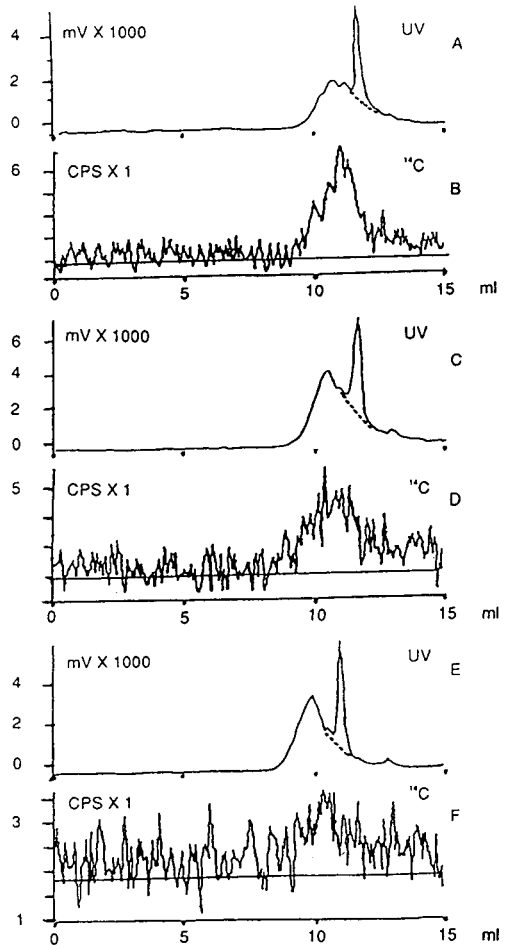

Fig. 5. Dual traces of aq. soluble lignin-like substances (UV at 280 nm) and radioactive substances from low-N cultures following size-exclusion chromatography using the optimized mobile phase 5 m*M* Na_2HPO_4 + 0.1% MeOH (pH 7.0): A = [^{14}C]DCA, UV 280 nm; B = [^{14}C]DCA, radioactivity trace; C = bound [^{14}C]DCA, UV 280 nm; D = bound [^{14}C]DCA, radioactivity trace; E = free DCA + bound [^{14}C]DCA, UV trace; F = free DCA + bound [^{14}C]DCA, radioactivity trace. For E and F, half of the concentrations of bound [^{14}C]DCA (25 μmole) instead of 50 μmole free or bound [^{14}C]DCA for A–D were applied (see Experimental) [10]. Due to the high intensity of the UV signals at 280 nm, the UV traces are given for 100-μl injection volumes for better UV signal resolution, whereas radioactivity traces obtained from 500-μl injection volumes are shown for improved signal-to-noise ratio. Dotted lines indicate the approximate correspondence of UV signal at low-intensity with the radioactivity trace, although at high intensity (500-μl injection volumes) the resolution of the UV signal was lost and corresponded fully to the radioactivity trace.

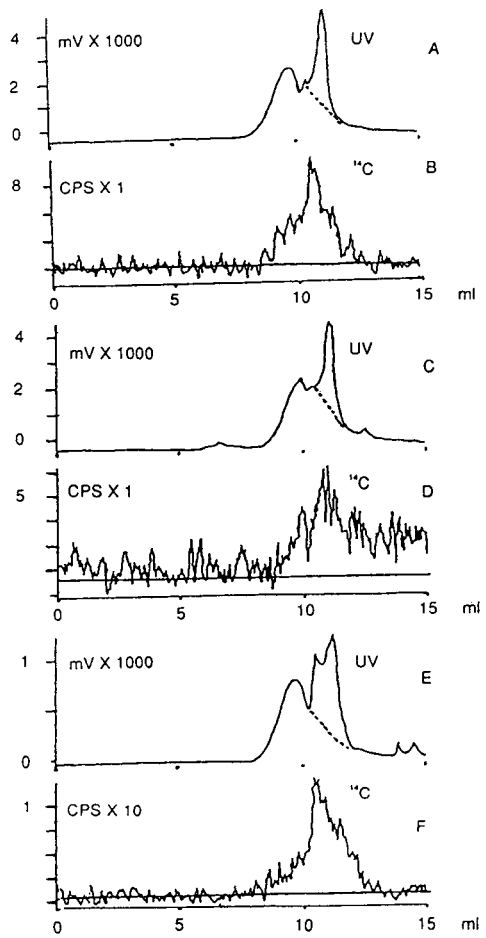

Fig. 6. Dual traces of aq. soluble lignin-like substances (UV at 280 nm) and radioactive substances from low-C cultures following size-exclusion chromatography using the optimized mobile phase 5 m*M* Na_2HPO_4 + 0.1% MeOH (pH 7.0): A = [^{14}C]DCA, UV 280 nm; B = [^{14}C]DCA, radioactivity trace; C = bound [^{14}C]DCA, UV 280 nm; D = bound [^{14}C]DCA, radioactivity trace; E = free DCA + bound [^{14}C]DCA, UV trace; F = free DCA + bound [^{14}C]DCA, radioactivity trace. For E and F, half of the concentrations of bound [^{14}C]DCA (25 μmole) instead of 50 μmole free or bound [^{14}C]DCA for A–D were applied (see Experimental) [10]. Due to the high intensity of the UV signals at 280 nm, the UV traces are given for 100-μl injection volumes for better UV signal resolution, whereas radioactivity traces obtained from 300–500 μl injection volumes are shown for improved signal-to-noise ratio. Dotted lines indicate the approximate correspondence of the UV signal at low-intensity with the radioactivity trace, although at high intensity (300–500 μl injection volumes) the resolution of the UV signal was lost and corresponded fully to the radioactivity trace.

Table 1
Determination of polydispersity (U_w) of polystyrolsulphonate Na-salt standards according to Tennikov et al. [15]

M_p	V_R (ml)	K	$\Psi(K)$	σ_v	U_w
95 000	6.76	0.08	0.19	2.20	2.22
73 500	6.96	0.10	0.21	2.20	1.98
46 000	7.25	0.13	0.24	1.70	1.46
19 300	7.84	0.19	0.27	2.50	1.76
8000	8.24	0.23	0.29	2.10	1.48
5400	8.41	0.24	0.29	2.20	1.52
1500	10.31	0.42	0.27	2.20	1.59

distribution coefficient $K = (V_R - V_0)/(V_p)$ with V_R = retention volume (ml), V_0 = void volume (ml) and V_p = total permeation volume (ml), and could be calculated by the equation:

$$\text{Slope of the calibration graph, } \Psi(K) \approx \begin{cases} \dfrac{1-K}{2}, & \text{if } K > 0.5 \\ K \ln\left(\dfrac{8}{\pi^2 K}\right), & \text{if } K < 0.5 \end{cases} \quad (2)$$

where $\pi \approx 3.1416$.

Using this calculation method, the polydispersity of polystyrolsulphonate Na-salt standards, Sitka spruce milled wood lignin as well as of aq. soluble polymeric substances produced by *Phanerochaete chrysosporium* from [^{14}C]DCA and wheat cell wall [^{14}C]DCA–lignin metabolite fractions was calculated. Table 1 shows that the polydispersity of narrow polystyrolsulphonate Na-salt standards lies within the range 1.48–2.22, which is typical for the narrow GPC standards [$(M_w)/(M_n) = 1.1$–1.2], where M_w is the mass-average molecular mass and M_n is the number-average molecular mass. Thus, the method described by Tennikov et al. [15] for the calculation of polydispersity of unknown polymers was found to be appropriate and justified for the calculation of polydispersity of unknown lignin-like substances in our study.

The polydispersity (U_w) and molecular masses (M_p) of aq. soluble lignin-like substances from the culture filtrates of *Phanerochaete chrysosporium* are summarized in Table 2. In both low-N and low-C cultures, the polydispersity and the molecular mass of aq. soluble lignin-like substances from cell wall bound [^{14}C]DCA were higher than those of free [^{14}C]DCA. The high molecular mass (M_p) of the aq. soluble lignin-like substances of bound [^{14}C]DCA from low-C cultures (Table 2) corresponded to their low mineralization rates [10]. In the low-N cultures, the polydispersity and the molecular mass of lignin-like substances from free DCA + cell wall bound [^{14}C]DCA were higher than those of cell

Table 2
Determination of molecular mass (M_p) and polydispersity (U_w) of lignin-like compunds from culture filtrates of *Phanerochaete chrysosporium* according to Tennikov et al. [15]

Sample	Approx. M_r range ($\times 10^3$)	Mean M_p	V_R^a (ml)	K	$\Psi(K)$	σ_v	U_w
Low-N cultures							
[^{14}C]DCA	0.1–3.7	2814	9.67	0.36	0.29	1.57	1.27
Bound [^{14}C]DCA	0.1–4.4	3081	9.54	0.35	0.29	1.85	1.36
Free DCA + bound [^{14}C]DCA	0.1–5.2	3471	9.35	0.33	0.30	2.22	1.51
Low-C cultures							
[^{14}C]DCA	0.1–15.9	3655	9.26	0.32	0.30	2.59	1.70
Bound [^{14}C]DCA	0.1–385.7	10 543	8.15	0.22	0.29	4.63	3.40
Free DCA + bound [^{14}C]DCA	0.1–15.9	3655	9.26	0.32	0.30	2.59	1.70

[a] Mean V_R of polydisperse signal of lignin-like substances within the size-exclusion limit.

wall bound [^{14}C]DCA, but in the low-C cultures no differences between the two groups could be found. One of the components of the so formed water-soluble polymer from free [^{14}C]DCA, bound [^{14}C]DCA and free DCA + bound [^{14}C]DCA was more polar than DCA–N-glucoside on the reversed-phase C_8 column (see section 2.4; data not shown).

4. Conclusions

The suitability of the described HPSEC method for the separation of lignin-like substances and the aq. soluble xenobiotic polymers is demonstrated. The described method is rapid, reproducible, and allows determination of molecular mass and the polydispersity of unknown water-soluble xenobiotic polymers. The polydispersity (U_w) and the mean molecular mass (M_p) of lignin-like substances were higher in low-C cultures with lower mineralization rates than those in low-N cultures with higher mineralization rates (Table 2) [10,16].

The release of [^{14}C]DCA aglucones from bound forms and the subsequent polymerization of [^{14}C]DCA degradation products (Figs. 5 and 6) did not depend primarily upon the efficiency of mineralization by *Phanerochaete chrysosporium* [10], e.g. in low-N and low-C cultures, but rather on its depolymerization efficiency of crosslinked wheat cell wall lignins, e.g. in low-N cultures as compared to low-C cultures, making labile bonds of [^{14}C]DCA with the C_α of cell wall lignin monomer side chains more accessible to enzymatic and non-enzymatic hydrolytic cleavage (Table 2). Thus, the release of [^{14}C]DCA via cleavage of labile bonds (benzylamine linkage) of DCA to the C_α of lignin monomer side chains [11,17] by *Phanerochaete chrysosporium* could predominately occur. If predominately stable bonds (benzylamine linkage) of DCA to the ring-C of lignin monomers on wheat cell walls [11] should have existed, the release of bound [^{14}C]DCA and the degree of polymerization of [^{14}C]DCA degradation products in low-N and low-C cultures by the white-rot fungus should be expected to be different (Figs. 5 and 6). Indeed, our results were supported by Lange [18] who found that labile bonds of DCA covalently bound to the C_α of the lignin monomer side chains in reference artificial lignin (DEHP)–DCA copolymers account for the entire (ca. 100%) DCA–lignin bonding pattern. Depolymerization of wheat cell wall bound DCA, metabolism and polymerization of released aglucones might be regarded as competitive processes of detoxification and/or mineralization [6].

References

[1] H. Sandermann, Jr., D. Scheel and T. v.d. Trenck, J. Appl. Polym. Sci., 37 (1983) 407–420.
[2] M.E. Himmel, K. Tatsumoto, K. Grohmann, D.K. Johnson and H.L. Chum, J. Chromatogr., 498 (1990) 93–104.
[3] G.C. Galletti and G. Chiavari, J. Chromatogr., 536 (1991) 303–308.
[4] M. Arjmand and H. Sandermann, Jr., Z. Naturforsch., 41c (1985) 206–214.
[5] M.E. Himmel, K.K. Oh, D.R. Quigley and K. Grohmann, J. Chromatogr., 467 (1989) 309–314.
[6] H. Sandermann, D.H. Pieper and R. Winkler, in J.F. Kennedy, G.O. Phillips and P.A. Williams (Editors), Proc. Cellulosics: Pulp, Fibre and Environmental Aspects, Ellis Horwood, London, 1993, pp. 499–503.
[7] C. Lapierre, B. Pollet and B. Monties, in Proc. 6th Int. Symp. on Wood and Pulping Chemistry, Melbourne, Vol. 1, 1991, pp. 543–549.
[8] E. Hoque et al., unpublished results (1994).
[9] T.K. Kirk, E. Schultz, W.J. Connors, L.F. Lorenz and J.G. Zeikus, Arch. Microbiol., 117 (1978) 277–285.
[10] I. Sparrer, Diplom-Thesis, FH Weihenstephan, 1992.
[11] H. Sandermann, Jr., T.J. Musick and P.W. Aschbacher, Agric. Food Chem., 40 (1992) 2001–2007.
[12] E. Hoque, J. Chromatogr., 360 (1986) 452–458.
[13] E. Hoque, J. Chromatogr., 448 (1988) 417–423.
[14] K.E. Hammel, K.A. Jensen, Jr., M.D. Mozuch, L.L. Landucci, M. Tien and E.A. Pease, J. Biol. Chem., 268 (1993) 12274–12281.
[15] M.B. Tennikov, A.A. Gorbunov and A.M. Skvortsov, J. Chromatogr., 509 (1990) 219–226.
[16] E. Hoque et al., unpublished results (1993).
[17] K.T. v.d. Trenck, D. Hunkler and H. Sandermann, Z. Naturforsch., 36c (1981) 714–720.
[18] B.M. Lange, Ph.D. Thesis, Faculty of Biology, Ludwig-Maximilians-University Munich, 1995.

ELSEVIER

Journal of Chromatography A, 708 (1995) 283–291

JOURNAL OF CHROMATOGRAPHY A

Gas chromatography of Titan's atmosphere VI. Analysis of low-molecular-mass hydrocarbons and nitriles with BPX5 capillary columns

A. Aflalaye[a,*], R. Sternberg[a], F. Raulin[a], C. Vidal-Madjar[b]

[a]*LISA, Universités Paris 7 et 12, URA 1404 de CNRS, Centre Multidisciplinaire, Avenue de Général de Gaulle, F-94010 Créteil Cedex, France*

[b]*Laboratoire du Physico-Chimie des Biopolymères, UMR 27 de CNRS, 2 rue Henri Dunant, 94320 Thiais, France*

Received 24 January 1995; accepted 29 March 1995

Abstract

Wall-coated open-tubular capillary columns (0.15 mm I.D., 12 and 25 m long with a 0.25-μm film thickness and 12 m long with a 2-μm film thickness with a chemically bonded stationary phase (5% phenyl–95% dimethylpolysiloxane) were used for the gas chromatographic analysis of various mixtures of low-molecular-mass saturated and unsaturated hydrocarbons and nitriles. Retention indices are given for these solutes at 30°C. Van Deemter curves were also plotted for propionitrile, *n*-hexane and benzene at 30°C for both film thicknesses. Both columns proved efficient and yielded good resolution. The analysis of the experimental band broadening on the basis of Golay's equation indicates the important role of the instrumental contribution to band broadening for columns with thin films of stationary phase.

1. Introduction

As part of the development of a gas chromatographic–mass spectrometric (GC–MS) instrument destined for the Huygens probe of the Cassini mission [1], we are currently studying GC columns which could provide conditions possible for analysing the atmosphere of Titan, the largest satellite of Saturn [1,2].

We have previously studied PLOT [3–5] and WCOT [5,6] capillary columns for the separation of low-molecular-mass hydrocarbons and nitriles, already detected or likely to be present in Titan's atmosphere. In particular, CP-Sil-5 CB WCOT columns of 0.15 mm and 0.10 mm I.D., coated with 100% dimethylpolysiloxane, permit the separation of C_1–C_6 hydrocarbons and C_1–C_4 nitriles with good resolution. The height equivalent to a theoretical plate (HETP) of these columns was as low as about 0.3 mm at low temperature; they also allow a complete separation of the tested mixtures within less than 35 min at 20°C and in less than 15 min with temperature programming. In order to have several possible column options, we extended this study to other types of WCOT capillary columns with a cross-linked bonded stationary phase because of their low bleed. BPX5 capillary columns (SGE Australia), coated with 5% phenyl–95% dimethylpolysiloxane, are slightly

* Corresponding author.

0021-9673/95/$09.50
SSDI 0021-9673(95)00410-6

more polar than the CP-Sil-5 CB. It has already been shown that these BPX5 columns have good separation properties for the simultaneous determination of polar and non-polar high-molecular-mass compounds. However, no data has been available, so far, on their behaviour pertaining to nitriles and on their capacity for analysing mixtures of low-molecular-mass hydrocarbons and nitriles.

We present here a detailed chromatographic study for 0.15 mm I.D. BPX5 columns coated with 0.25-μm (column A) and 2-μm films (column B) at 30°C. We systematically studied the chromatographic behaviour of these solutes on these BPX5 columns of different film thicknesses and lengths. Plate-height studies of test compounds of each chemical family enable the optimum experimental conditions for the separation to be established.

2. Theoretical

The mean plate height, $\bar{H}$, may be written as the sum of various contributions [7,8]:

$$\bar{H} = H_g + H_l + H_c \quad (1)$$

where H_g and H_l represent the gas-phase and liquid-phase contributions to band broadening, respectively, and H_c is the extra-column term due to the instrumental contribution. For an open-tubular column, H_g is related to the outlet carrier gas velocity, u_0, by the Golay equation [9]:

$$H_g = \left[\frac{2D_g}{u_0} + \frac{(1 + 6k' + 11k'^2)}{96(1 + k')^2} \cdot \frac{d_c^2}{D_g} \cdot u_0\right] f = \left(\frac{B'D_g}{u_0} + \frac{C'_{gu_0}}{D_g}\right) f \quad (2)$$

where k' is the retention factor, d_c is the column diameter and f is a pressure corrector factor [7]. This last parameter is close to 1 for low pressure drops and its maximum value is 9/8 at high inlet pressures. D_g is the diffusion coefficient of the solute in the mobile phase at atmospheric pressure. For each solute (Table 1), D_g was calculated according to the Chapman–Enskog equation [10] by using the empirical method for predicting the diffusion coefficients of binary gas-phase systems.

Table 1
Calculated diffusion coefficients at 30°C

Solute	$D_g(H_2)$ (cm^2/s)	$D_g(N_2)$ (cm^2/s)
Methane	0.7115	0.2270
Hexane	0.3275	0.0823
Propionitrile	0.4496	0.1162
Benzene	0.3842	0.0962

The H_l term can be drawn from the following relationship [9]:

$$H_l = \frac{6k'}{(1 + k')^2} \cdot \frac{d_f^2}{D_l} \cdot j u_0 = C_l j u_0 \quad (3)$$

where, d_f is the average thickness of the liquid film, D_l is the diffusion coefficient of the solute in the stationary liquid phase and j is the correction factor for gas compressibility. Assuming that the instrument contribution to the plate height is mainly due to the injection profile, we can have [11]

$$H_c = \frac{\sigma_i^2 u_0^2}{(1 + k')^2 L} = D u_0^2 \quad (4)$$

where σ_i^2 is the variance of the injection profile and L is the column length.

As the correction term f is close to 1, the experimental plate height data can be fitted by the equation

$$H = \frac{B'D_g}{u_0} + C'_g \cdot \frac{u_0}{D_g} + C_l u_0 + D u_0^2 \quad (5)$$

With experiments performed with a single carrier gas, this equation fits the experimental data well. A linear least-squares fit method can be used and good smoothing is generally observed. However, except for B', the relative errors in the determination of the other parameters are as large as 100%. To isolate the C_l term, Giddings and Schettler [7] introduced a method

based on the use of two different carrier gases. The C_1 contribution is obtained from the difference in plate heights observed at a given u_0/D_g value. The instrumental plate height H_c also contributes to this difference in the HETP and must be accounted for, by studying the band broadening of a non-retained compound as a function of mobile phase velocity for two different carrier gases such as hydrogen and nitrogen [8]. At a given u_0/D_g, the difference in plate heights is then due only to the H_c term ($C_1 = 0$). For both carrier gases, H is plotted as a function of u_0/D_g and a linear least-squares fit program is used to determine the coefficients of the plate-height equation.

3. Experimental

3.1. Gas chromatography

Two different WCOT fused-silica capillary columns coated with a film of 5% phenyl–95% dimethylpolysiloxane (BPX5) were studied: a 12-m long column with a film thickness of 0.25 μm (column A) and a 12-m long column with a film thickness of 2 μm (column B). We used a Perkin-Elmer Autosystem gas chromatograph equipped with a flame ionization detector, a thermal conductivity detector and a temperature programmer. It was connected to a PE–Nelson Turbochrom data acquisition system. The detection time constant was set at 50 ms. The injector temperature was 220°C and the detector temperature was 240°C throughout. The split mode was used (with a splitting ratio generally of 60:1) and the sampling techniques were the same as described previously [3]. The solute vapours were injected through the septum with a 1-μl Hamilton gas syringe equipped with a tight stopcock.

The test solutes were propionitrile, hexane and benzene, representing nitrile, alkane and aromatic compounds, respectively.

HETP versus linear velocity of the carrier gas were obtained at 30°C for the selected solutes by injecting a mixture of these solutes with methane, considered as a non-retained compound. Dedicated software (PE–Nelson HETP, developed for this study) was systematically used for determining the HETP from peak broadening.

3.2. Reagents

Allene and cyanogen were obtained from Matheson (East Rutherford, NJ, USA), methylacetylene (propyne) and ethylacetylene (1-butyne) from Baker (Phillipsburg, NJ, USA) and 1,3-butadiene, pentane, hexane and ethylbenzene from Aldrich (Strasbourg, France). All the other C_1–C_4 hydrocarbons tested were obtained from Alphagaz–l'Air Liquide (Bois d'Arcy, France) and were at least 99% pure. 2-Methyl-2-butene, 1-hexene, benzene, cyclohexene, heptane, cycloheptane, 1-octene, octane, acetonitrile, acrylonitrile and propionitrile were obtained from Prolabo (Paris, France), 1-pentene and 3-methylpentane from Fluka (Buchs, Switzerland) and butyronitrile, isobutyronitrile, methacrylonitrile, cyclopropanecarbonitrile, crotononitrile (mixture of *cis* and *trans* isomers) and 3-butenenitrile from Riedel-de Haën (Hannover, Germany). Hydrogen cyanide was prepared by acidification of sodium cyanide with sulphuric acid.

4. Results and discussion

4.1. HETP studies

We systematically applied the theoretical plate-height equation (Eq. 5) to determine the coefficients B', C'_g, C_1 and D. The plate height of test compounds was studied as a function of flow-rate with two different carrier gases. Such an approach enables one to assess the various contributions to solute band broadening and leads to important information. First, for a non-retained compound, it is a convenient way to determine the D term. For retained compounds, it is then possible to approach the C_1 term, once the D term of the retained solute has been calculated.

The D term was determined from a study of

plate height variations with a non-retained compound (methane) using two different carrier gases (hydrogen and nitrogen). The studies were carried out with two different columns with 0.25- and 2-μm stationary phase film thickness.

The variation of H with u_0/D_g, as shown in Fig. 1, indicates higher efficiency when nitrogen is used as the carrier gas. The N_2 curve is systematically lower than the H_2 curve for both columns coated with a thin or thick stationary phase film. The large difference in the efficiencies observed at high u_0/D_g value can be explained ($C_i = 0$) by the instrumental contribution to band broadening, which is very important when H_2 is used as the carrier gas.

The constants B', C'_g and D were determined from the least-squares fit of Eq. 5 to the experimental plate height (Table 2). Table 2 also gives the errors in parameter determination with a 95% confidence interval. In Fig. 1, the corresponding model (solid and dashed lines) fits the experimental data well. For both columns, the B' parameters are close to the theoretical value ($B' = 2$). The use of two different carrier gases led to good precision (about 5%, for a 95% confidence interval) in the determination of the instrumental contribution (D term). Because of the importance of the D term, the errors in C'_g determination are large and the values given in Table 2 are insignificant.

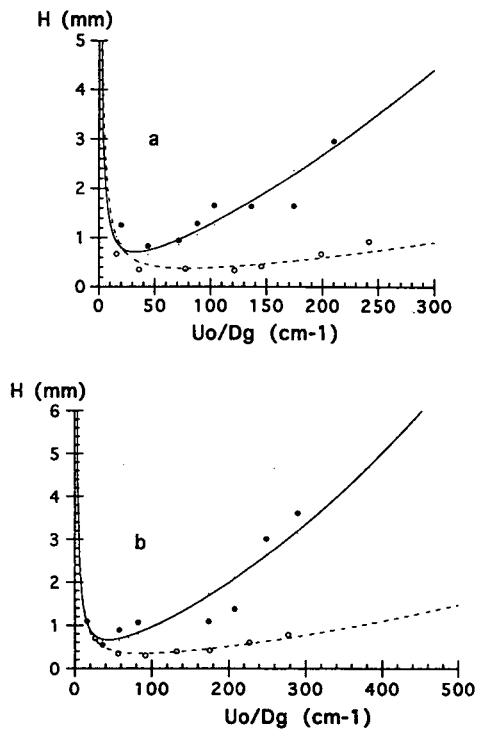

Fig. 1. HETP (H) versus u_0/D_g for methane at 30°C with (●) hydrogen and (○) nitrogen as carrier gases on (a) column A (0.25-μm film thickness) and (b) column B (2-μm film thickness).

Table 2
Coefficients of the plate height equation for a non-retained compound (methane) at 30°C

Column	B' (cm^2/s)	D (s^2/cm)	C'_g (s)
Column A	1.8	$0.10 \cdot 10^{-4}$	$2.0 \cdot 10^{-4}$
(0.25 μm)	0.5	0.03	0.3
Column B	1.9	$0.08 \cdot 10^{-4}$	$1.5 \cdot 10^{-4}$
(2 μm)	0.3	0.04	0.5

Underlineed values correspond to the experimental errors.

The agreement is satisfactory for the D term found with both capillary columns. Considering the time constant of the electrometer (50 ms) as a negligible contribution to the lower efficiencies observed at high flow-rates, the mean variance of the injection profile is $\sigma_i^2 = 0.009$ s^2. In high-speed chromatography using a fluidic injection device [8], the exponential contribution from the current amplifier was the primary source of extra-column band broadening. In the present case it is about 25% of the extra-column contribution and the calculated D coefficient has to be considered as a global term including both electrometer and instrumental contributions. Therefore, the calculated mean variance of the injection profile is overestimated.

Figs. 2 and 3 illustrate the variation of H with u_0/D_g for (A) propionitrile, (B) hexane and (C) benzene on columns with 0.25- and 2-μm film thickness, respectively. The difference in the plate height measured with the two carrier gases (H_2 and N_2), is due to the diffusion of the solute in the stationary phase and to the extra-column contribution. Table 3 lists the coefficients determined by the least-squares fit of Eq. 5 to the experimental data fixing B' at its theoretical

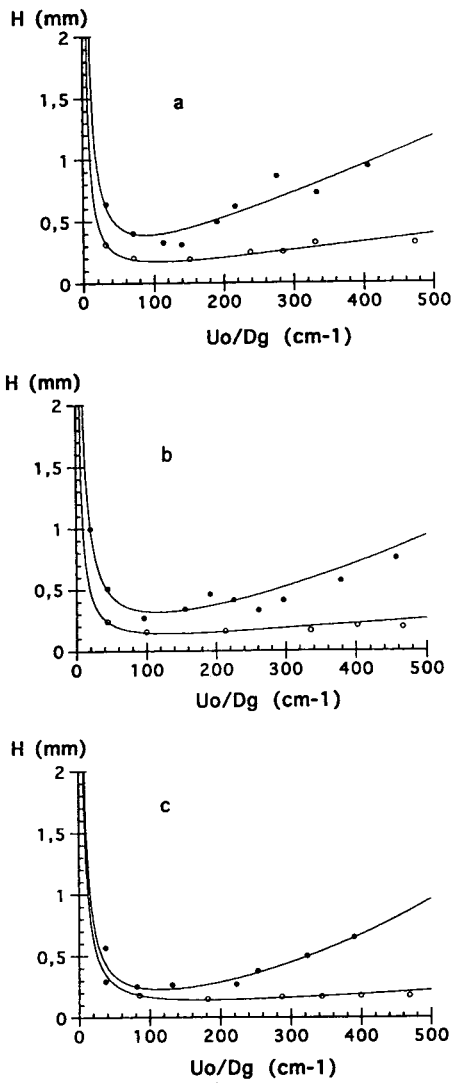

Fig. 2. HETP (H) versus u_0/D_g at 30°C with (●) hydrogen and (○) nitrogen as carrier gases for retained compounds on column A (0.25-μm film thickness). (a) Propionitrile; (b) hexane; (c) benzene.

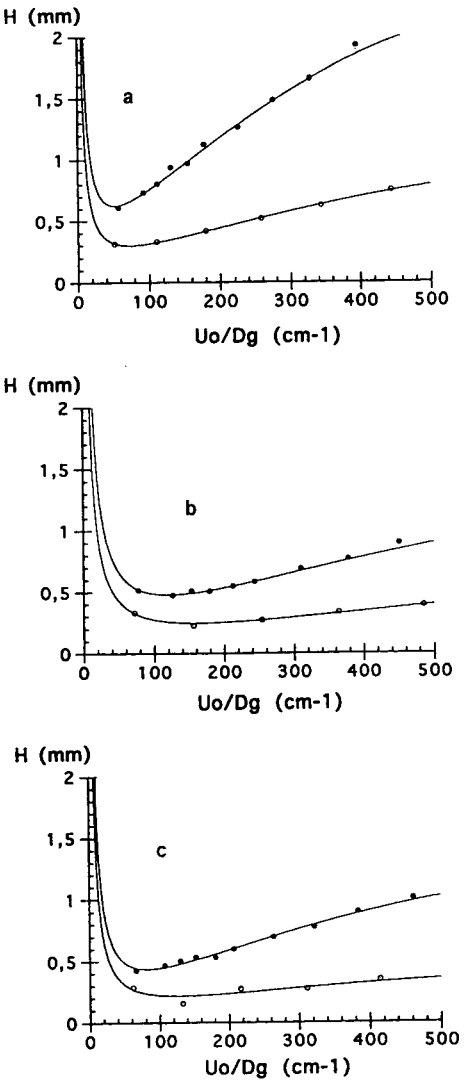

Fig. 3. HETP (H) versus u_0/D_g at 30°C with (●) hydrogen and (○) nitrogen as carrier gases for retained compounds on column B (2-μm film thickness). (a) Propionitrile; (b) hexane; (c) benzene.

value ($B' = 2$) and $D = D_{\text{methane}}/(1 + k')^2$. D was calculated from the D (methane) term previously determined, methane being considered as non-retained solute. For the column of small film thickness (Fig. 2), the extra-column effects are the main contribution to HETP, explaining the lower efficiencies observed when hydrogen is used as the carrier gas.

By plotting $H - H_c$ versus u_0/D_g it is possible to determine the C_1 term. As shown in Fig. 4 for benzene, for instance, when the corrective extra-column term is subtracted, the corrected plate heights almost coincide for both carrier gases with column A of small liquid film thickness. The C_1 term is seven times lower than that observed with the column coated with larger amounts of

Table 3
Coefficients of the plate-height equation for retained solutes at 30°C with $B' = 2$ and D calculated from Eq. 4 with $D_{methane} = 0.09 \cdot 10^{-4}$ s²/cm

Column	Solute	k'	C'_g (s)	C_l (s)	D (s²/cm)	D_l (cm²/s)
Column A (0.25-μm film thickness)	Propionitrile	1.02	$0.01 \cdot 10^{-4}$ 0.2	$5 \cdot 10^{-4}$ 1	$1.8 \cdot 10^{-6}$	
	Hexane	1.04	$0.02 \cdot 10^{-4}$ 0.1	$4 \cdot 10^{-4}$ 1	$1.8 \cdot 10^{-6}$	
	Benzene	2.1	$0.2 \cdot 10^{-4}$ 0.05	$1.5 \cdot 10^{-4}$ 0.4	$0.78 \cdot 10^{-6}$	
Column B (2-μm film thickness)	Propionitrile	7.3	$0.3 \cdot 10^{-4}$ 0.2	$19 \cdot 10^{-4}$ 1	$0.11 \cdot 10^{-6}$	$0.13 \cdot 10^{-4}$
	Hexane	8	$0.2 \cdot 10^{-4}$ 0.04	$8.9 \cdot 10^{-4}$ 0.3	$1.11 \cdot 10^{-6}$	$0.26 \cdot 10^{-4}$
	Benzene	16	$0.05 \cdot 10^{-4}$ 0.1	$10.1 \cdot 10^{-4}$ 0.6	$0.026 \cdot 10^{-6}$	$0.13 \cdot 10^{-4}$

Underlined numbers are the errors on C values.

stationary phase. The same behaviour is observed with the less retained solutes such as propionitrile or hexane.

At 30°C with column B of larger liquid film thickness, the extra-column effects are then considered as less important because the retention of the tested solutes are larger (Fig. 3). The corresponding plate-height curve shows that it is the diffusion in the stationary liquid phase that mainly explains the lower efficiency observed when hydrogen is used as the carrier gas. The C_l term of propionitrile is twice as large as that of hexane, although their k' values are close. A good precision on C_l determination is obtained and the diffusion coefficient of the solutes in the liquid stationary phase D_l were calculated from the C_l term (Eq. 3). That of hexane is twice as small as that found with benzene and propionitrile. The D_l coefficients of propionitrile and benzene are similar, revealing a comparable retention mechanism.

From a practical point of view, the efficiency will be much improved by using a longer column, the instrumental contribution being inversely proportional to the column length. Since the corrected plate height is lower with the column of small film thickness, one will greatly improve the speed and efficiency of analysis by using longer columns of smaller liquid film thickness.

These results explain why in the analytical separations a longer column with a small amount of stationary phase is recommended. The efficiency is improved both by a greater column length and a less important contribution to band broadening, while the analysis speed is increased because of the lower k' values.

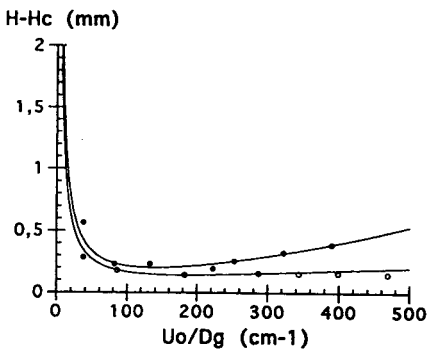

Fig. 4. Correction for extra-column effects. Plot of $H - H_c$ versus u_0/D_g for benzene at 30°C with (●) hydrogen and (○) nitrogen as carrier gases on column A (0.25-μm liquid film thickness).

4.2. Separation of complex mixtures

The theoretical study demonstrates the importance of the instrumental contribution when using H_2 as the carrier gas over the efficiencies observed with column A. In order to lower this

contribution, a longer column was selected (column C) with a total length of 25 m, an I.D. of 0.15 mm and a film thickness of 0.25 μm. Another column having a low instrumental contribution and a length of 12 m (column B) was also used for separating complex mixtures. Analytical separation studies were thus carried out on columns B and C (Fig. 5). Temperature programming was used for both columns in order to shorten the overall analysis time. The low thermal bleeding of the BPX5 columns allows us to use such programming.

The separation of C_1–C_6 hydrocarbons, C_1–C_4 nitriles and some polycyclic aromatic hydrocarbons (PAH) on column C is presented in Fig. 5a. Analytical resolution is achieved for heavy hydrocarbons (above C_4), for all nitriles studied and PAH. The analysis time never exceeds 7 min. However, some co-elutions are observed with light hydrocarbons, particularly C_2.

The separation of C_1–C_6 hydrocarbons, C_1–C_4 nitriles and some PAH on column B is presented in Fig. 5b. The greater film thickness allows a better separation of the light hydrocarbons. The co-elution of methane and C_2 hydrocarbons and the co-elution of ethane and the unsaturated C_2 hydrocarbons have been resolved. However, the co-elution of ethene and ethyne is still observed. Analytical resolution was also achieved for cyanogen, propene and propane, for propyne and allene and for 2-butynitrile, benzene and cyclohexane, with some inversion between the elution times of these compounds. HCN (not injected on column C), is co-eluted with propane and allene. Three new compounds (octane, ethylbenzene and xylene) were also injected as representative of heavy hydrocarbons and PAH, respectively; the analysis time still remains shorter than 10 min.

We also measured the retention indices $I(i)$ (Table 4), of most of the compounds studied in order to ascertain the behavioral pattern of the column in connection with these solutes. The following equation was used:

$$I(i) = 100 \cdot \frac{\log t'_{R(i)} - \log t'_{R(P_z)}}{\log t'_{R(P_{z+1})} - \log t'_{R(P_z)}} + 100Z \qquad (6)$$

where t'_R is the relative retention time, P_z and P_{z+1} correspond to paraffins with z and $z+1$ carbon atoms, respectively, and i corresponds to a solute, the retention time of which is between that of P_z and P_{z+1}.

These retention indices at 30°C (Table 4) vary linearly with the carbon number of the solute for a given chemical family. It should be noted that these experimental data are highly reproducible for all solutes, the relative standard deviation being less than 0.5%.

5. Conclusion

This study has shown that BPX5 columns give a very high resolution for nitriles and confirms the general behaviour of these columns for polar compounds. Consequently, the adsorption of these polar compounds on the stationary phase surface does not change its chromatographic behaviour relative to hydrocarbons. Such columns could be suitable for use in GC–MS studies. Both columns B and C offer a good separation power for saturated and unsaturated hydrocarbons, PAH and nitriles, in a relatively short time, but require temperature programming. Such conditions are not convenient for space GC instrumentation, because they increase markedly the duration of the analytical cycle and the complexity of the instrument and its software. In fact, in the case of the Titan probe, the use of a GC–MS instrument reduces the importance of co-elution problems, especially if the co-eluted compounds have well differentiated chemical properties and consequently different mass fragmentations. This is the case with HCN and propene. Columns B and C are both compatible within the constraints of the Cassini–Huygens mission (temperature between 30 and 100°C, flow-rate about 0.3–0.4 ml min^{-1}, analysis time shorter than 10 min and column head pressure between 0.7 and 0.8 bar). A good separation of heavy hydrocarbons and nitriles is achieved on column C but its length of 25 m is far too great and cumbersome. The length of column B is acceptable and a better analytical resolution is achieved for light hydrocarbons.

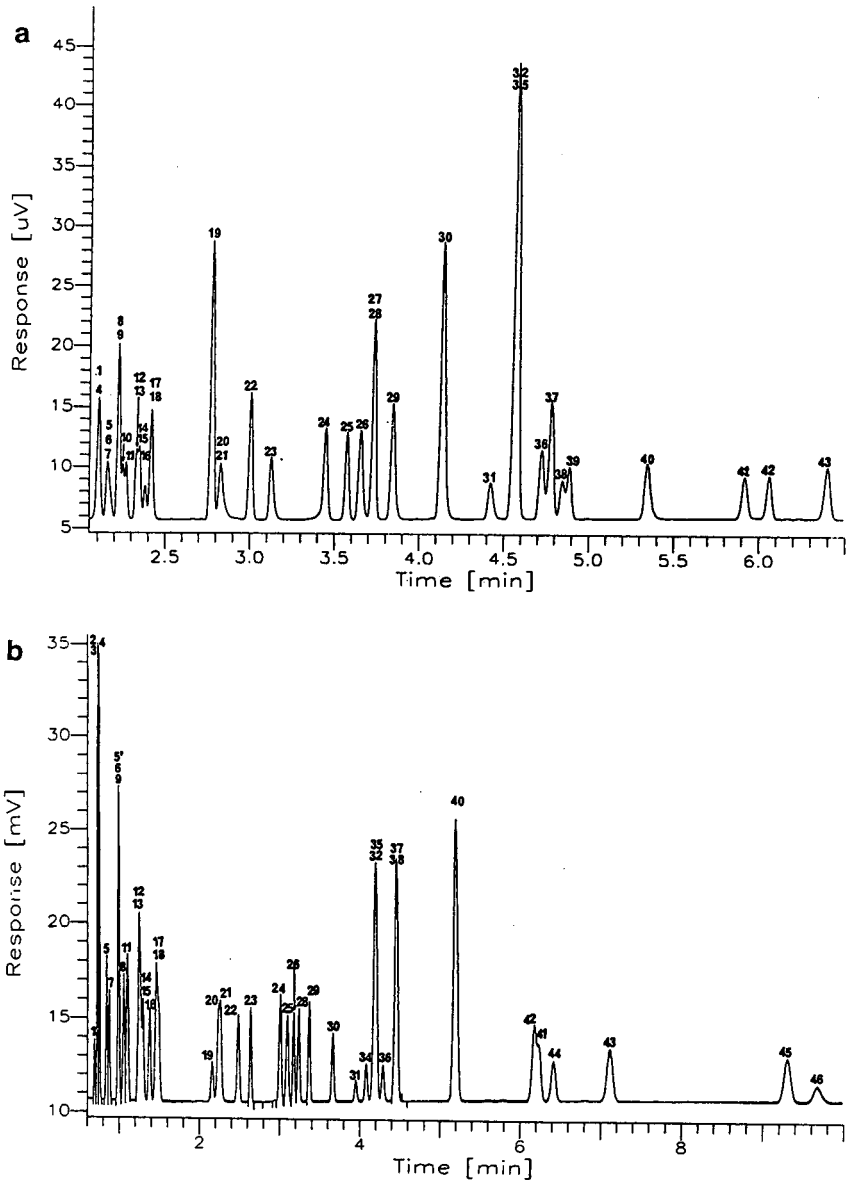

Fig. 5. GC analysis of a gaseous mixture of C_1–C_6 hydrocarbons, PAH and C_1–C_4 nitriles. (a) On a 25 m × 0.15 mm I.D. BPX5 (d_f = 0.25 μm) fused-silica WCOT column. Temperature, isothermal for 1.5 min at 30°C, then increased at 30°C/min to 100°C; carrier gas, H_2; outlet flow-rate, 0.33 ml/min; inlet pressure, 0.8 bar. (b) On a 12 m × 0.15 mm I.D. BPX5 (d_f = 2 μm) fused-silica WCOT column. Temperature, isothermal for 1.6 min at 40°C, then increased at 45°C/min to 100°C; carrier gas, H_2; outlet flow-rate, 0.44 ml/min; inlet pressure, 0.70 bar. Peaks: 1 = methane; 2 = ethene; 3 = ethyne; 4 = ethane; 5 = cyanogen; 5′ = hydrocyanic acid; 6 = propene; 7 = propane; 8 = propyne; 9 = allene; 10 = cyclopropane; 11 = isobutane; 12 = 1-butene; 13 = isobutene; 14 = butadiene; 15 = butane; 16 = *trans*-2-butene; 17 = butyne; 18 = *cis*-2-butene; 19 = 1-pentene; 20 = acetonitrile; 21 = pentane; 22 = 2-methyl-2-butene; 23 = acrylonitrile; 24 = cyclopentane; 25 = 3-methylpentane; 26 = propionitrile; 27 = 1-hexene; 28 = hexane; 29 = methacrylonitrile; 30 = isobutyronitrile; 31 = *cis*- or *trans*-crotononitrile; 32 = 3-butenenitrile; 33 = 2-butynitrile; 34 = benzene; 35 = cyclohexane; 36 = butyronitrile; 37 = cyclohexene; 38 = *cis*- or *trans*-crotononitrile; 39 = *n*-heptane; 40 = cyclopropanecarbonitrile; 41 = toluene; 42 = 1-octene; 43 = cycloheptane; 44 = octane; 45 = ethylbenzene; 46 = xylene.

Table 4
Retention indices of hydrocarbons and nitriles on columns B and C at 30°C

Solute	Retention index	
	Column B	Column C
Propane	300	300
Cyclopropane	356	357
Propyne	339	357
Butane	400	400
1,3-Butadiene	400	400
trans-2-Butene	413	414
cis-2-Butene	426	431
1-Butene	394	394
Isobutene	394	368
1-Pentene	480	510
Acetonitrile	504	500
n-Pentane	500	500
Acrylonitrile	540	544
Cyclopentane	572	573
Propionitrile	595	592
Hexane	600	600
Methacrylonitrile	614	611
Isobutyronitrile	643	638
cis- Or *trans*-crotonitrile	664	661
3-Butenenitrile	680	673
Butyronitrile	694	686
cis- Or *trans*-crotonitrile	699	696
Cyclohexene	689	685
Heptane	700	700

However, ethene and ethyne are still co-eluted. The theoretical study shows the importance of increasing retention times in order to decrease the instrumental contribution to band broadening. Therefore, column B may clearly be selected as one of the chromatographic columns of the GC instrument to be shipped on the Titan probe.

Acknowledgements

The authors warmly thank B. Scotto for his help during this work and J.P. Ballon for linguistic assistance. This work was supported by a grant from the Centre National d'Etudes Spatiales (CNES).

References

[1] F. Raulin, C. Frère, P. Paillous, E. de Vanssay, L. Do and M. Khlifi, J. Br. Interplanet. Soc., 45 (1992) 257.
[2] Proceedings of the Symposium on Titan, ESA Spec. Publ., SP-338, 1992.
[3] L. Do and F. Raulin, J. Chromatogr., 481 (1989) 45.
[4] L. Do and F. Raulin, J. Chromatogr., 514 (1990) 65.
[5] L. Do, Ph.D. Thesis Dissertation, Université Paris 7, Paris, 1993.
[6] L. Do and F. Raulin, J. Chromatogr., 591 (1992) 297.
[7] J.C. Giddings and P.D. Schettler, Anal. Chem., 34 (1964) 1643.
[8] G. Gaspar, R. Annino, C. Vidal-Madjar and G. Guiochon, Anal. Chem., 50 (1978) 1512.
[9] M.J.E. Golay, in V.J. Coates, H.J. Noebels and I.S. Fagerson (Editors), Gas Chromatography 1957, Academic Press, New York, 1958, p. 1.
[10] E.N. Fuller, P.D. Schettler and J.C. Giddings, Ind. Eng. Chem., 58 (1966) 20.
[11] G. Guiochon and C.L. Guillemin, Quantitative Gas Chromatography for Laboratory Analyses and On-line Process Control (Journal of Chromatography Library, Vol. 42), Elsevier, Amsterdam, 1988, p. 93.

ELSEVIER

Journal of Chromatography A, 708 (1995) 293–302

JOURNAL OF CHROMATOGRAPHY A

Retention of halocarbons on a hexafluoropropylene epoxide-modified graphitized carbon black IV. Propane-based compounds

Thomas J. Bruno*, Kelly H. Wertz, Michael Caciari[1]

Thermophysics Division, Chemical Science and Technology Laboratory, National Institute of Standards and Technology, Boulder, CO 80303, USA

Received 2 January 1995; accepted 22 March 1995

Abstract

The retention characteristics of 25 propane-based bromofluorocarbon, chlorocarbon, chlorofluorocarbon, and fluorocarbon fluids have been studied as a function of temperature on a stationary phase consisting of a 5% (m/m) coating of a low-molecular-mass polymer of hexafluoropropylene epoxide on a graphitized carbon black adsorbent. Measurements were performed at 0, 20, 40 and 60°C for R-245ca and R-245cb. Measurements were performed at 20, 40, 60 and 80°C for R-227ca, R-227ea, R-236ea, R-236fa, R-245fa, and R-263fb. Measurements were performed at 40, 60, 80 and 100°C for R-217ba, R-254cb and R-1243b, and at 60, 80, 100 and 120°C for R-280da and R-217caB1. Measurements were performed at 80, 100, 120 and 140°C for R-215aa, R-216ba, R-253fb, R-262da, and R-270aa. Measurements were performed at 100, 120 140 and 160°C for R-215ba, R-225ca, R-225cb, R-243db, R-270da, R-270fa, and R-270fb. Relative retentions as a function of temperature were calculated with respect to the retentions of tetrafluoromethane (R-14) and hexafluoroethane (R-116). Qualitative features of the data are examined, and trends are identified. In addition, the relative retention data were fitted to linear models for the purpose of predicting retention behavior of these compounds to facilitate chromatographic analysis.

1. Introduction

Many laboratories are engaged in a comprehensive research program geared toward the development of new fluids to be used as refrigerants, blowing and foaming agents, and propellants. This research includes the measurements and correlation of thermophysical properties, testing of the compatibility of the materials, measurement of the chemical stability, and studies on their suitability for recycling [1,2]. An important part of these research programs is the chemical analysis of the new developed fluids [3–6]. For several reasons gas chromatography is one of the major quantitative and qualitative analysis methods that is applied to the study of alternative refrigerants, not the least of which are its simplicity and economics of operation [7–9]. Knowledge of the retention characteristics of important fluids on the more useful stationary

* Corresponding author.

[1] Permanent address: Fort Lupton High School, Fort Lupton, CO, USA.

0021-9673/95/$09.50
SSDI 0021-9673(95)00389-4

phases is a valuable tool in the design of effective qualitative and quantitative chromatographic analyses. Determination of the corrected retention parameters, such as the net retention volume, V_N^0 (corrected to a column temperature of 0°C), and relative retentions, $r_{a/b}$, provides the simplest route to achieve these goals.

In previous papers, we presented measurements for 8 methane-based, 18 ethane-based, and 11 ethene-based fluids [10–12]. In this paper, we present measurements on the temperature dependence of the relative retentions, $r_{a/b}$, of 25 propane-based fluids that are commonly encountered in alternative refrigerant research and testing. The studied fluids are listed in the left-hand columns of Tables 1 and 2, along with the accepted code numbers [10,13]. The measurements were made on the packed-column stationary phase that has proven to be very useful for refrigerant analysis: a 5% coating of a low-molecular-mass polymer of hexafluoropropylene epoxide on a graphitized carbon black [10]. The relative retentions were calculated with respect to tetrafluoromethane (R-14) and hexafluoroethane (R-116). In addition to the discussion of qualitative trends in the data, fits to linear models are presented for the logarithms of the relative retentions against thermodynamic temperature, thus providing a predictive capability.

2. Theory

A discussion of the basic definitions, theory and application of corrected retention parameters was presented earlier [10].

3. Experimental

The measurements presented here were performed on a commercial gas chromatograph that had been modified to provide high-precision retention data. All of the experimental details were described earlier [10,11], so only a very general description will be provided here. The chromatograph was modified to maintain a highly stable column temperature, which was measured with a quartz-crystal oscillator thermoprobe (calibrated against a NIST-standard platinum resistance thermometer) that was accurate to within ± 0.01°C. Details of the instrumental modifications were presented earlier [10]. Injection was done via a syringe, and the samples were always introduced at infinite dilution. The carrier gas line to the injection valve was modified to allow the column head pressure to be measured with a calibrated Bourdon-tube gauge. This gauge was calibrated against a dead weight pressure balance traceable to a NIST standard. The column outlet pressure was measured with an electronic barometer that had a resolution of 1.3 Pa (approximately 0.01 Torr). This barometer was also calibrated against a dead weight pressure balance. The column carrier gas flow-rate (corrected for water vapor pressure) was measured with an electronic soap-bubble flow meter. Retention times were measured by a commercial integrator. A Ranque–Hilsch vortex tube was used to provide cooling in the column oven for the subambient temperature measurements [14]. Thermal conductivity detection (TCD) was used with research-grade helium as carrier gas. The TCD was maintained at 125°C for all measurements.

The stationary phase was a commercially prepared packing material consisting of a 5% (m/m) coating of a low molecular mass polymer of hexafluoropropylene epoxide modifier on a 60–80 mesh (177–250 μm) graphitized carbon black [15]. Some representative properties of this modifier and the column preparation procedure were presented earlier [10].

For each retention measurement, five injections were performed at each column temperature. The corrected retention time was simply obtained by subtracting the air retention time as a measure of the void volume (or gas hold up volume). At the start of each series of injections, the requisite temperatures (column, flowmeter, and barometer) and pressures (column head and column exit) were recorded. These replicate measurements furnished the uncertainties used for the error propagation that provided the overall experimental uncertainties that are re-

Table 1
Relative retentions, $r_{a/b}$, and their logarithms, of all of the fluids measured in this study, with respect to tetrafluoromethane, R-14

Name	$r_{a/b}$				$\log(r_{a/b})$			
	0°C (273.15 K)	20°C (293.15 K)	40°C (313.15 K)	60°C (333.15 K)	0°C (273.15 K)	20°C (293.15 K)	40°C (313.15 K)	60°C (333.15 K)
1,1,2,3,3-Pentafluoropropane (R-245ca)	112.0 ± 1.09 0.97%	75.6 ± 0.44 0.58%	54.8 ± 0.18 0.32%	42.7 ± 0.12 0.28%	2.05	1.88	1.74	1.63
1,1,1,2,2-Pentafluoropropane (R-245cb)	63.9 ± 0.36 0.57%	46.4 ± 0.23 0.50%	35.2 ± 0.18 0.51%	28.9 ± 0.06 0.19%	1.81	1.67	1.55	1.46
	20°C (293.15 K)	40°C (313.15 K)	60°C (333.15 K)	80°C (353.15 K)	20°C (293.15 K)	40°C (313.15 K)	60°C (333.15 K)	80°C (353.15 K)
1,1,1,2,2,3,3-Heptafluoropropane (R-227ca)	58.9 ± 0.18 0.31%	43.5 ± 0.32 0.73%	34.4 ± 0.16 0.46%	27.6 ± 0.14 0.50%	1.77	1.64	1.54	1.44
1,1,1,2,3,3,3-Heptafluoropropane (R-227ea)	94.2 ± 0.27 0.29%	65.6 ± 0.76 1.16%	48.6 ± 0.29 0.60%	37.3 ± 0.16 0.44%	1.97	1.82	1.69	1.57
1,1,1,2,3,3-Hexafluoropropane (R-236ea)	100.8 ± .0.85 0.84%	71.8 ± 0.39 0.55%	53.0 ± 0.45 0.85%	41.0 ± 0.23 0.55%	2.00	1.86	1.72	1.61
1,1,1,3,3,3-Hexafluoropropane (R-236fa)	110.6 ± 0.93 0.84%	74.9 ± 0.27 0.36%	55.4 ± 0.24 0.43%	42.7 ± 0.16 0.38%	2.04	1.88	1.74	1.63
1,1,1,3,3-Pentafluoropropane (R-245fa)	110.7 ± .0.97 0.88%	76.1 ± 0.19 0.25%	56.3 ± 0.24 0.51%	43.4 ± 0.23 0.53%	2.04	1.88	1.75	1.64
1,1,1-Trifluoropropane (R-263fb)	60.1 ± 00.34 0.57%	45.4 ± 0.12 0.26%	36.2 ± 0.22 0.62%	29.6 ± 0.35 1.17%	1.78	1.66	1.56	1.47
	40°C (313.15 K)	60°C (333.15 K)	80°C (353.15 K)	100°C (373.15 K)	40°C (313.15 K)	60°C (333.15 K)	80°C (353.15 K)	100°C (373.15 K)
2-Chloroheptafluoropropane (R-217ba)	111.3 ± 0.33 0.30%	83.2 ± 0.25 0.30%	63.5 ± 0.24 0.46%	50.7 ± 0.15 0.30%	2.05	1.92	1.80	1.71
3,3,3-Trifluoropropene (R-1243)	38.1 ± 0.53 1.4%	29.6 ± 0.24 0.8%	24.0 ± 0.36 1.50%	19.8 ± 0.16 0.8%	1.58	1.47	1.38	1.30
	60°C (333.15 K)	80°C (353.15K)	100°C (373.15 K)	120°C (393.15 K)	60°C (333.15 K)	80°C (353.15 K)	100°C (373.15 K)	120°C (393.15 K)
2-Chloropropane (R-280da)	131.5 ± 0.77 0.59%	99.4 ± 0.40 0.40%	76.4 ± 0.31 0.24%	61.1 ± 0.22 0.36%	2.12	2.00	1.88	1.79
n-Heptafluoropropyl bromide (R-217caB1)	217.3 ± 1.30 0.60%	151.4 ± 1.06 0.70	106.9 ± 1.71 1.6%	82.0 ± 0.82 1.0%	2.34	2.18	2.03	1.91
	80°C (353.15 K)	100°C (373.15 K)	120°C (393.15 K)	140°C (413.15 K)	80°C (353.15 K)	100°C (373.15 K)	120°C (393.15 K)	140°C (413.15 K)
1,2,2-Trichloropentafluoropropane (R-215aa)	778.0 ± 5.91 0.76%	506.7 ± 2.22 0.44%	347.7 ± 1.82 0.47%	251.1 ± 2.26 0.90%	2.89	2.71	2.54	2.40
1,2-Dichlorohexafluoropropane (R-216ba)	239.8 ± 2.01 0.84%	169.6 ± 0.51 0.30%	126.0 ± 1.36 1.08%	97.4 ± 0.30 0.31%	2.38	2.23	2.10	1.99
3-Chloro-1,1,1-trifluoropropane (R-253fb)	191.1 ± 0.50 0.26%	135.4 ± 0.79 0.58%	99.9 ± 0.33 0.33%	77.8 ± 0.42 0.54%	2.28	2.13	2.00	1.89
2-Chloro-1,3-difluoropropane (R-262da)	172.7 ± 0.71 0.41%	126.8 ± 1.27 1.00%	95.5 ± 0.33 0.35%	76.2 ± 0.36 0.47%	2.24	2.10	1.98	1.88
2,2-Dichloropropane (R-270aa)	288.9 ± 1.27 0.44%	206.8 ± 0.66 0.32%	155.9 ± 0.41 0.26%	120.5 ± 0.59 0.49%	2.46	2.32	2.19	2.08
1,1,2,2-Tetrafluoropropane, R-254cb	38.0 ± 0.14 0.36%	30.5 ± 0.06 0.21%	25.4 ± 0.10 0.41%	21.8 ± 0.06 0.28%	1.58	1.48	1.41	1.34

continued on p. 296

Table 1. *Continued*

Name	$r_{a/b}$				$\log(r_{a/b})$			
	100°C (373.15 K)	120°C (393.15 K)	140°C (413.15 K)	160°C (433.15 K)	100°C (373.15 K)	120°C (393.15 K)	140°C (413.15 K)	160°C (433.15 K)
1,2,3-Trichloropentafluoropropane (R-215ba)	555.5 ± 6.06 1.09%	382.4 ± 4.47 1.17%	270.6 ± 2.22 0.82%	198.2 ± 0.69 0.35%	2.75	2.58	2.43	2.30
3,3-Dichloro-1,1,1,2,2-pentafluoropropane (R-225ca)	309.6 ± 0.62 0.20%	217.0 ± 1.26 0.60%	160.7 ± 0.41 0.26%	121.9 ± 0.69 0.57%	2.49	2.34	2.21	2.09
1,3-Dichloro-1,1,2,2,3-pentafluoropropane (R-225cb)	305.3 ± 4.30 1.41%	210.3 ± 1.20 0.57%	156.6 ± 1.13 0.72%	118.0 ± 0.55 0.47%	2.49	2.32	2.20	2.07
2,3-Dichloro-1,1,1-trifluoropropane (R-243db)	438.5 ± 1.75 0.40%	302.6 ± 0.91 0.30%	217.4 ± 0.57 0.26%	158.1 ± 0.38 0.24%	2.64	2.48	2.34	2.20
1,2-Dichloropropane (R-270da)	377.6 ± 1.47 0.39%	279.1 ± 1.45 0.52%	197.6 ± 0.83 0.42%	148.6 ± 0.91 0.61%	2.58	2.45	2.30	2.17
1,3-Dichloropropane (R-270fa)	497.8 ± 2.64 0.53%	348.2 ± 3.87 1.11%	253.8 ± 2.33 0.92%	185.5 ± 0.48 0.26%	2.70	2.54	2.40	2.27
1,1-Dichloropropane (R270fb)	377.6 ± 2.76 0.73%	265.9 ± 1.25 0.47%	194.5 ± 0.70 0.36%	147.5 ± 0.74 0.50%	2.58	2.43	2.29	2.17

ported (two standard deviations, 2σ). The column head pressure was maintained uniformly at 137.9 ± 0.3 kPa (approximately 20 p.s.i.g.) for the measurements, although measurements were initially performed at several other pressures to verify consistency in the operation of the chromatograph. The carrier gas flow-rate at the column exit was maintained at 45 ± 0.3 ml/min. Measurements were performed at four temperatures for each fluid. The temperatures were chosen to provide adequate retention to minimize extra-column effects. All samples were obtained from commercial sources in the highest available purity, and were used without further purification.

4. Results and discussion

The relative retentions, $r_{a/b}$, for each fluid with respect to R-14 and R-116 are presented in Tables 1 and 2, respectively. The reported expanded uncertainties (with a coverage factor $k = 2$) are the result of an error propagation performed with the standard deviations obtained from replicate measurements of each experimental parameter. The uncertainties were found to be uncorrelated (as determined by examination of Spearman's ρ and Kendall's τ), and the deviations were found to fit a normal distribution and were therefore treated as being entirely random [16]. In addition to the uncertainty, the coefficient of variation in percent is provided. The precision of the measurements is generally between 0.5 and 1.5%, with the average precision of all the measurements on these compounds being 0.6%. This figure compares very well with the precision of typical retention parameters (generally between 1 and 2%) obtained in other physicochemical gas chromatographic measurements [16]. A plot of $\log(r_{a/b})$ against $1/T$ for each fluid referenced to R-14 is provided in Fig. 1a,b. Similar plots are provided for the fluids referenced to R-116 in Fig. 2a,b.

The expected trend of $r_{a/b}$ with reciprocal temperature is observed for each fluid. There is no evidence of any decomposition at the temperatures at which measurements were performed. It is clear from these plots that good separation is achieved for most of the propane-based compounds on this particular stationary phase. In a few cases, coelution of fluids is observed at the higher temperatures, however.

The temperature-dependent relative retention data were then fitted with the best linear model (simple linear, logarithmic, power, or exponential). The results of these fits are provided in Tables 3 and 4. Included with each fluid are the

Table 2
Relative retentions, $r_{a/b}$, and their logarithms, of all of the fluids measured in this study, with respect to hexafluoroethane, R-116

Name	$r_{a/b}$				$\log(r_{a/b})$			
	0°C (273.15 K)	20°C (293.15 K)	40°C (313.15 K)	60°C (333.15 K)	0°C (273.15 K)	20°C (293.15 K)	40°C (313.15 K)	60°C (333.15 K)
1,1,2,3,3-Pentafluoropropane (R-245ca)	13.9 ± 0.13 0.97%	11.0 ± 0.06 0.58%	9.2 ± 0.03 0.32%	8.1 ± 0.02 0.28%	1.14	1.04	0.96	0.91
1,1,1,2,2-Pentafluoropropane (R-245cb)	7.9 ± 0.05 0.57%	6.7 ± 0.04 0.50%	5.9 ± 0.03 0.51%	5.5 ± 0.01 0.19%	0.90	0.77	0.77	0.74
	20°C (293.15 K)	40°C (313.15 K)	60°C (333.15 K)	80°C (353.15 K)	20°C (293.15 K)	40°C (313.15 K)	60°C (333.15 K)	80°C (353.15 K)
1,1,1,2,2,3,3-Heptafluoropropane (R-227ca)	8.6 ± 0.03 0.31%	7.3 ± 0.05 0.73%	6.5 ± 0.03 0.46%	5.8 ± 0.03 0.50%	0.93	0.86	0.81	0.76
1,1,1,2,3,3,3-Heptafluoropropane (R-227ea)	13.7 ± 0.04 0.29%	10.9 ± 0.13 1.16%	9.2 ± 0.06 0.60%	7.8 ± 0.03 0.44%	1.14	1.04	0.96	0.89
1,1,1,2,3,3-Hexafluoropropane (R-236ea)	14.6 ± 0.17 0.84%	12.0 ± 0.07 0.55%	10.0 ± 0.09 0.85%	8.6 ± 0.05 0.55%	1.17	1.08	1.00	0.94
1,1,1,3,3,3-Hexafluoropropane (R-236fa)	16.1 ± 0.14 0.84%	12.5 ± 0.05 0.36%	10.4 ± 0.04 0.43%	9.0 ± 0.03 0.38%	1.21	1.10	1.02	0.95
1,1,1,3,3-Pentafluoropropane (R-245fa)	16.1 ± 0.14 0.88%	12.7 ± 0.03 0.25%	10.6 ± 0.05 0.51%	9.1 ± 0.05 0.53%	1.21	1.10	1.03	0.96
1,1,1-Trifluoropropane (R-263fb)	8.7 ± 0.05 0.57%	7.6 ± 0.02 0.26%	6.8 ± 0.04 0.62%	6.2 ± 0.04 0.62%	0.94	0.88	0.83	0.70
	40°C (313.15 K)	60°C (333.15 K)	80°C (353.15 K)	100°C (373.15 K)	40°C (313.15 K)	60°C (333.15 K)	80°C (353.15 K)	100°C (373.15 K)
2-Chloroheptafluoro-propane (R-217ba)	18.6 ± 0.06 0.30%	15.7 ± 0.05 0.30%	13.4 ± 0.06 0.46%	11.7 ± 0.04 0.30%	1.27	1.20	1.13	1.07
3,3,3-Trifluoropropene (R-1243)	6.3 ± 0.09 1.40%	5.6 ± 0.04 0.80%	5.1 ± 0.08 0.70%	4.6 ± 0.04 0.80%	0.80	0.75	0.70	0.66
	60°C (333.15 K)	80°C (353.15 K)	100°C (373.15 K)	120°C (393.15 K)	60°C (333.15 K)	80°C (353.15 K)	100°C (373.15 K)	120°C (393.15 K)
2-Chloropropane (R-280da)	24.8 ± 0.15 0.60%	20.9 ± 0.08 0.40%	17.7 ± 0.04 0.24%	15.5 ± 0.06 0.36%	1.40	1.32	1.25	1.19
n-Heptafluoropropyl bromide (R-217caB1)	41.0 ± 0.25 0.60%	31.8 ± 0.22 0.70%	24.9 ± 0.40 1.60%	20.8 ± 0.21 1.000%	1.61	1.50	1.40	1.32
	80°C (353.15 K)	100°C (373.15 K)	120°C (393.15 K)	140°C (413.15 K)	80°C (353.15 K)	100°C (373.15 K)	120°C (393.15 K)	140°C (413.15 K)
1,2,2-Trichloropentafluoropropane (R-215aa)	163.6 ± 1.24 0.76%	117.4 ± 0.52 0.44%	87.9 ± 0.41 0.47%	68.7 ± 0.62 0.90%	2.21	2.07	1.94	1.84
1,2-Dichlorohexafluoropropane (R-216ba)	50.4 ± 0.42 0.84%	39.2 ± 0.12 0.30%	31.9 ± 0.34 1.08%	26.7 ± 0.08 0.31%	1.70	1.59	1.50	1.43
3-Chloro-1,1,1-trifluoropropane (R-253fb)	40.2 ± 0.10 0.26%	31.4 ± 0.18 0.58%	25.3 ± 0.08 0.33%	21.3 ± 0.13 0.59%	1.60	1.50	1.40	1.33
2-Chloro-1,3-difluoropropane (R-262da)	36.3 ± 0.15 0.41%	29.4 ± 0.29 1.00%	24.1 ± 0.08 0.35%	20.9 ± 0.10 0.47%	1.56	1.47	1.38	1.32
2,2-Dichloropropane (R-270aa)	60.8 ± 0.27 0.44%	47.9 ± 0.15 0.32%	39.4 ± 0.10 0.26%	33.0 ± 0.16 0.49%	1.78	1.68	1.60	1.52
1,1,2,2-Tetrafluoropropane, R-254cb	6.5 ± 0.02 0.36%	5.7 ± 0.01 0.21%	5.0 ± 0.02 0.41%	4.5 ± 0.01 0.28%	0.81	0.75	0.70	0.65

continued on p. 298

Table 2. *Continued.*

Name	$r_{a/b}$				$\log(r_{a/b})$			
	100°C (373.15 K)	120°C (393.15 K)	140°C (413.15 K)	160°C (433.15 K)	100°C (373.15 K)	120°C (393.15 K)	140°C (413.15 K)	160°C (433.15 K)
1,2,3-Trichloropentafluoropropane (R-215ba)	128.7 ± 1.40 1.09%	96.7 ± 1.17 1.17%	74.0 ± 0.61 0.82%	58.2 ± 0.20 0.35%	2.11	1.99	1.87	1.77
3,3-Dichloro-1,1,1,2,2-pentafluoropropane (R-225ca)	71.8 ± 0.14 0.20%	54.9 ± 0.33 0.60%	44.0 ± 0.11 0.26%	35.8 ± 0.20 0.57%	1.86	1.74	1.64	1.55
1,3-Dichloro-1,1,2,2,3-pentafluoropropane (R-225cb)	70.7 ± 1.00 1.41%	53.2 ± 0.30 0.57%	42.8 ± 0.31 0.72%	34.7 ± 0.16 0.47%	1.85	1.73	1.63	1.54
2,3-Dichloro-1,1,1-trifluoropropane (R-243db)	101.6 ± 0.41 0.40%	76.5 ± 0.23 0.30%	59.5 ± 0.15 0.26%	46.5 ± 0.11 0.24%	2.01	1.88	1.77	1.67
1,2-Dichloropropane (R-270da)	87.5 ± 0.34 0.39%	70.6 ± 0.37 0.52%	54.1 ± 0.23 0.42%	43.7 ± 0.27 0.61%	1.94	1.85	1.73	1.64
1,3-Dichloropropane (R-270fa)	115.4 ± 0.61 0.53%	88.0 ± 0.97 1.11%	69.4 ± 0.64 0.92%	54.5 ± 0.14 0.26%	2.06	1.95	1.84	1.74
1,1-Dichloropropane (R-270fb)	87.5 ± 0.64 0.73%	67.2 ± 0.32 0.47%	53.2 ± 0.19 0.36%	43.4 ± 0.22 0.50%	1.94	1.83	1.73	1.64

Table 3
Coefficients of the fits of $\log(r_{a/b})$ against $1/T$, with the respective correlation coefficients, with tetrafluoromethane (R-14) as the reference

Name	Model	*m*	*b*	*r*	Temperature range (°C)
1,1,1,2,2,3,3-Heptafluoropropane (R-227ca)	P	1.10	898.82	0.99976	20–80
1,1,1,2,3,3,3-Heptafluoropropane (R-227ea)	P	1.22	2035.09	0.99997	20–80
1,1,1,2,3,3-Hexafluoropropane (R-236ea)	L	676.21	−0.30	0.99996	20–80
1,1,1,3,3,3-Hexafluoropropane (R-236fa)	E	389.63	0.54	0.99999	20–80
1,1,2,3,3-Pentafluoropropane (R-245ca)	E	346.43	0.58	0.99997	0–60
1,1,1,2,2-Pentafluoropropane (R-245cb)	E	322.24	0.55	0.99982	0–60
1,1,1,3,3-Pentafluoropropane (R-245fa)	E	382.37	0.56	0.99996	20–80
1,1,2,2-Tetrafluoropropane, R-254cb	E	325.61	0.56	0.99999	40–100°C
1,1,1-Trifluoropropane (R-263fb)	E	326.24	0.59	0.99997	20–80
2-Chloroheptafluoropropane (R-217ba)	P	1.05	853.99	0.99996	40–100
3,3,3-Trifluoropropene (R-1243)	E	381.19	0.47	0.99992	40–100
n-Heptafluoropropyl bromide (R-217caB1)	E	444.44	0.62	0.99968	60–120
2-Chloropropane (R-280da)	L	727.58	−0.06	0.99987	60–120
1,2,2-Trichloropentafluoropropane (R-215aa)	P	1.19	3059.12	0.99995	80–140
1,2-Dichlorohexafluoropropane (R-216ba)	E	436.34	0.69	0.99994	80–140
3-Chloro-1,1,1-trifluoropropane (R-253fb)	E	457.49	0.63	0.99998	80–140
2-Chloro-1,3-difluoropropane (R-262da)	E	422.27	0.68	0.99996	80–140
2,2-Dichloropropane (R-270aa)	P	1.07	1274.28	0.99980	80–140
1,2,3-Trichloropentafluoropropane (R-215ba)	LG	3.03	20.67	0.99992	100–160
3,3-Dichloro-1,1,1,2,2-pentafluoropropane (R-225ca)	P	1.19	2918.06	0.99999	100–160
1,3-Dichloro-1,1,2,2,3-pentafluoropropane (R-225cb)	P	1.22	3380.21	0.99991	100–160
2,3-Dichloro-1,1,1-trifluoropropane (R-243db)	LG	2.98	20.30	0.99999	100–160
1,2-Dichloropropane (R-270da)	LG	2.76	18.93	0.99899	100–160
1,3-Dichloropropane (R-270fa)	LG	2.88	19.78	0.99999	100–160
1,1-Dichloropropane (R-270fb)	L	1105.50	−0.38	0.99997	100–160

L = linear, P = power, E = exponential, LG = logarithmic.

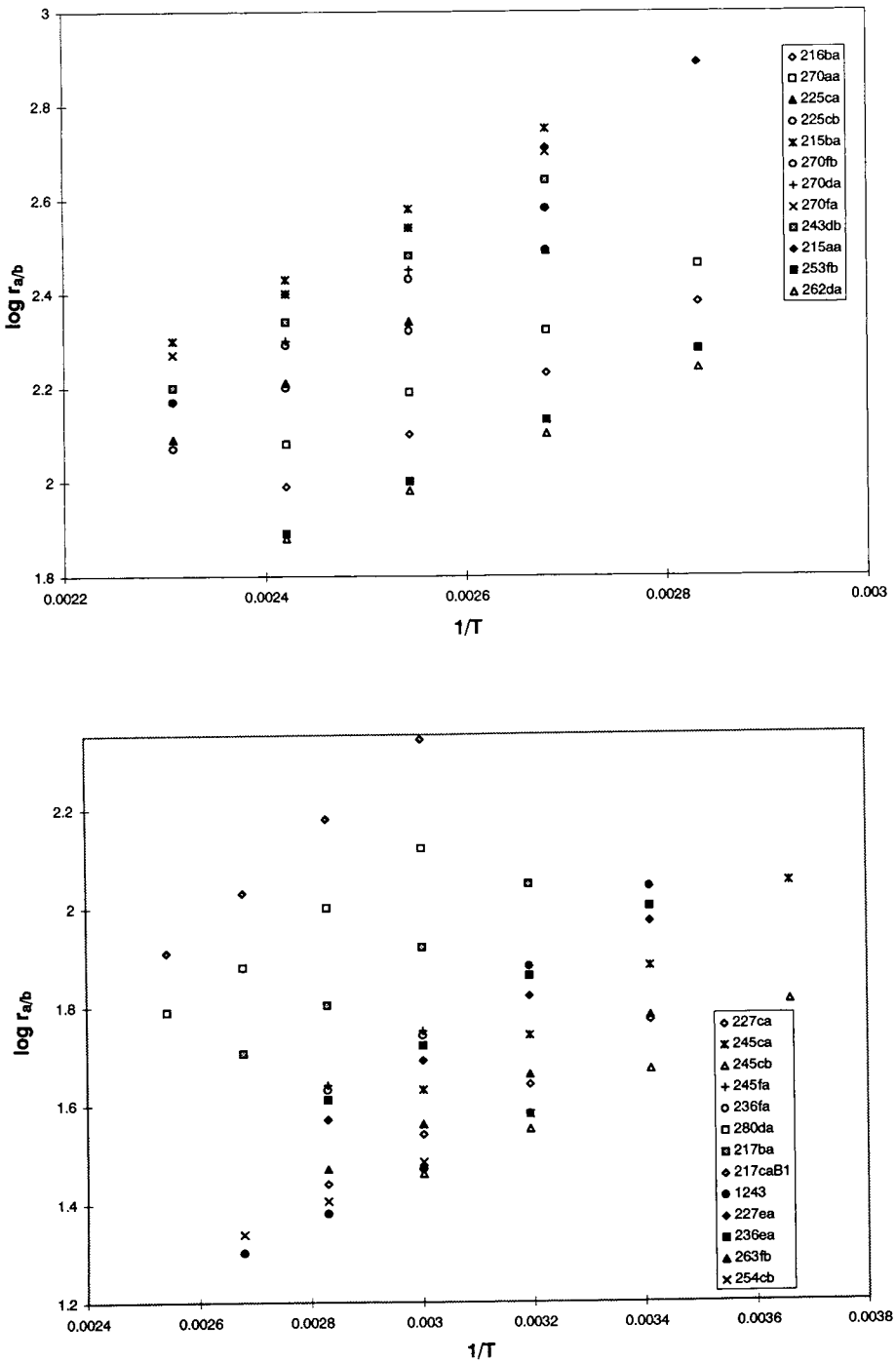

Fig. 1. Plots of the logarithms of the relative retentions (with respect to tetrafluoromethane, R-14) $\log(r_{a/b})$ against $1/T$, for each fluid measured.

coefficients, the Pearson correlation coefficient of the fit, and the temperature range over which the fit was taken.

Many of the measured data obtained for the propane-based fluids are represented very well (within experimental error) with the simple linear model:

$$log\ (r_{a/b}) = m/T + b \quad (1)$$

where m is the slope and b is the intercept. Several were better represented by a logarithmic model:

$$log\ (r_{a/b}) = m\ log\ (1/T) + b \quad (2)$$

an exponential model:

$$log^{\,2}(r_{a/b}) = m/T + b \quad (3)$$

or a power model:

$$log^{\,2}(r_{a/b}) = m\ log\ (1/T) + b \quad (4)$$

The choice of model was based strictly on goodness of fit and statistical significance of the fitted parameters. No physical interpretation is assigned to the coefficients beyond the ability to fit (or account for all of the structure in) the measured data.

5. Conclusions

Measurements of the relative retentions (on a very useful stationary phase) of 25 propane-based halocarbon fluids that are relevant to research on alternative refrigerants have been presented. The logarithms of these data were fitted against the reciprocal thermodynamic tem-

Table 4
Coefficients of the fits of $\log (r_{a/b})$ against $1/T$, with the respective correlation coefficients, with hexafluoroethane (R-116) as the reference

Name	Model	m	b	r	Temperature range (°C)
1,1,1,2,2,3,3-Heptafluoropropane (R-227ca)	E	338.95	0.29	0.99934	20–80
1,1,1,2,3,3,3-Heptafluoropropane (R-227ea)	E	411.97	0.28	0.99990	20–80
1,1,1,2,3,3-Hexafluoropropane (R-236ea)	P	1.18	971.79	0.99994	20–80
1,1,1,3,3,3-Hexafluoropropane (R-236fa)	E	404.73	0.30	0.99968	20–80
1,1,2,3,3-Pentafluoropropane (R-245ca)	P	1.44	3794.79	0.99974	0–60
1,1,1,2,2-Pentafluoropropane (R-245cb)	E	398.31	0.22	0.99998	0–60
1,1,1,3,3-Pentafluoropropane (R-245fa)	E	392.34	0.32	0.99991	20–80
1,1,2,2-Tetrafluoropropane, R-254cb	L	316.43	−0.19	0.99993	40–100°C
1,1,1-Trifluoropropane (R-263fb)	E	289.86	0.35	0.99980	20–80
2-Chloroheptafluoropropane (R-217ba)	L	393.10	0.02	0.99975	40–100
3,3,3-Trifluoropropene (R-1243)	L	276.40	−0.08	0.99976	40–100
n-Heptafluoropropyl bromide (R-217caB1)	E	434.39	0.44	0.99981	60–120
2-Chloropropane (R-280da)	L	451.08	0.04	0.99975	60–120
1,2,2-Trichloropentafluoropropane (R-215aa)	E	454.35	0.61	0.99993	80–140
1,2-Dichlorohexafluoropropane (R-216ba)	E	431.65	0.50	0.99995	80–140
3-Chloro-1,1,1-trifluoropropane (R-253fb)	E	461.44	0.43	0.99998	80–140
2-Chloro-1,3-difluoropropane (R-262da)	E	411.13	0.49	0.99991	80–140
2,2-Dichloropropane (R-270aa)	E	390.81	0.59	0.99974	80–140
1,2,3-Trichloropentafluoropropane (R-215ba)	LG	2.33	15.91	0.99992	100–160
3,3-Dichloro-1,1,1,2,2-pentafluoropropane (R-225ca)	P	1.19	2175.65	0.99998	100–160
1,3-Dichloro-1,1,2,2,3-pentafluoropropane (R-225cb)	P	1.23	2651.06	0.99978	100–160
2,3-Dichloro-1,1,1-trifluoropropane (R-243db)	LG	2.29	15.55	0.99999	100–160
1,2-Dichloropropane (R-270da)	LG	2.07	14.18	0.99814	100–160
1,3-Dichloropropane (R-270fa)	LG	2.18	14.98	0.99994	100–160
1,1-Dichloropropane (R-270fb)	L	826.79	−0.27	0.99996	100–160

L = linear, P = power, E = exponential, LG = logarithmic.

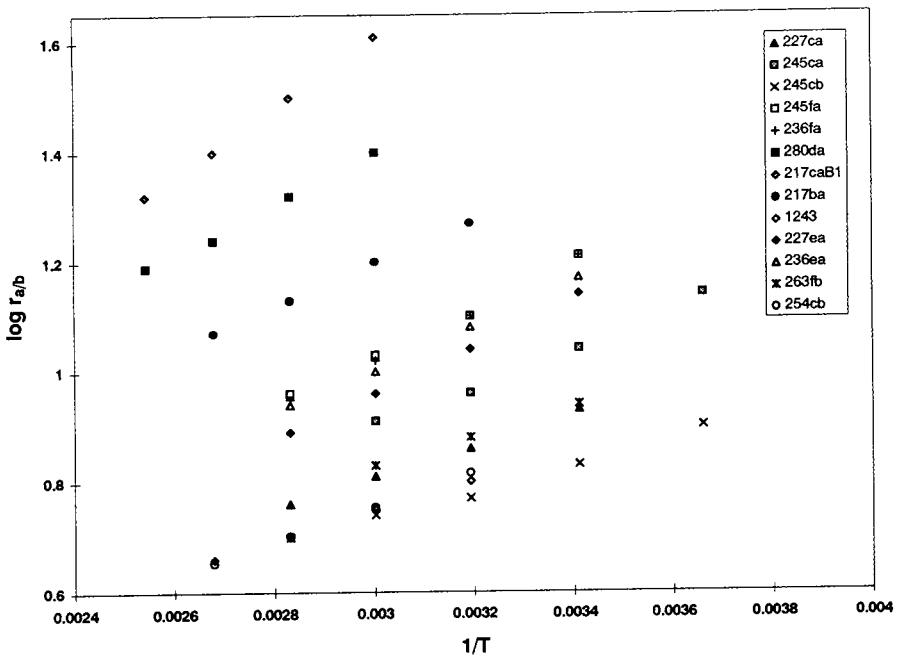

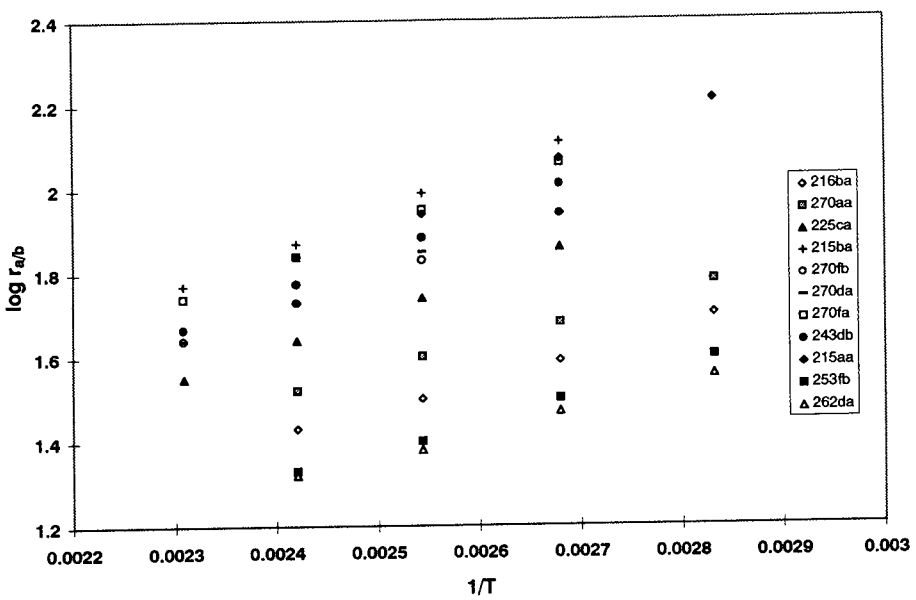

Fig. 2. Plots of the logarithms of the relative retentions (with respect to hexafluoromethane, R-116) $\log(r_{a/b})$ against $1/T$, for each fluid measured.

perature to several linear models. These derived equations can be used for the prediction of the retention behavior of these fluids on this important stationary phase, and therefore can be used for solute identification and also for the design of analytical and preparative-scale separations.

Acknowledgements

The financial support of the Colorado Alliance for Science and the United States Environmental Protection Agency, Stratospheric Ozone Protection Branch (Contract DW13935632-01-0), is gratefully acknowledged.

References

[1] E.J. Lizardos, Maint. Technol., 6 (1993) 17–19.
[2] M.O. McLinden and D.A. Didion, ASHRAE J., 29 (1987) 32–42.
[3] T.J. Bruno, Spectroscopic Library for Alternative Refrigerant Analysis, National Institute of Standards and Technology (U.S.), Special Publication 794, 1990, p. 192.
[4] T.J. Bruno, Strategy of Chemical Analysis of Alternative Refrigerants, National Institute of Standards and Technology (U.S.), Technical Note 1340, 1990, p. 104.
[5] T.J. Bruno, ASHRAE Trans., 98 (1992) 204–208.
[6] T.J. Bruno, ASHRAE Trans., 98 (1992) 210–215.
[7] R.L. Grob (Editor), Modern Practice of Gas Chromatography, John Wiley & Sons, New York, 2nd ed., 1985.
[8] T.J. Bruno, Chromatographic and Electrophoretic Methods, Prentice-Hall, Englewood Cliffs, NJ, 1991.
[9] J.E. Willett, Gas Chromatography, (Analytical Chemistry by Open Learning), John Wiley & Sons, Chichester, 1987.
[10] T.J. Bruno and M. Caciari, J. Chromatogr. A, 672 (1994) 149–158.
[11] T.J. Bruno and M. Caciari, J. Chromatogr. A, 679 (1994) 123–132.
[12] T.J. Bruno and M. Caciari, J. Chromatogr. A, 686 (1995) 245.
[13] T.J. Bruno (Editor), CRC Handbook for the Analysis and Identification of Alternative Refrigerants, CRC Press, Boca Raton, FL, 1994.
[14] T.J. Bruno, Anal. Chem., 58 (1986) 1596.
[15] J.L. Glajch and W.G. Schindel, LC · GC, 4 (1986) 574–580.
[16] J.D. Gibbons and S. Chakraborti (Editors), Nonparametric Statistical Inference, Marcel Dekker, New York, NY, 1992.
[17] T.J. Bruno and D.E. Martire, J. Phys. Chem., 87 (1986) 2430–2436.

ELSEVIER

Journal of Chromatography A, 708 (1995) 303–307

JOURNAL OF CHROMATOGRAPHY A

Determination of N-nitrosodimethylamine in beer by gas chromatography–stable isotope dilution chemical ionization mass spectrometry

Marco Longo*, Claudia Lionetti, Aldo Cavallaro

Presidio Multizonale di Igiene e Prevenzione, Via Juvara 22, 20129 Milan, Italy

First received 16 February 1995; revised manuscript received 3 April 1995; accepted 3 April 1995

Abstract

A sensitive method for the determination of N-nitrosodimethylamine in beer samples is described. The analyte was isolated by distillation and subsequent extraction from the distillate using dichloromethane. Analysis was carried out by gas chromatography combined with positive-ion chemical ionization mass spectrometry. Quantification was performed by stable isotope dilution using [$^2H_6$]-N-nitrosodimethylamine as the internal standard. The measurements exhibited excellent linearity in the range 0.10–4.00 μg kg^{-1} ($r = 0.99999$) and a detection limit of 0.04 μg kg^{-1} was achieved. The between-sample relative standard deviation of the method was 0.73% ($n = 5$) at a concentration level of 0.86 μg kg^{-1}. The recovery of the compound was 78 ± 2.1%. The proposed procedure seems to be a good alternative to the frequently used gas chromatography–thermal energy analysis approach for the determination of N-nitrosodimethylamine.

1. Introduction

The carcinogenic action of N-nitrosodimethylamine (NDMA) has been reported since 1956 [1]. The reaction of nitrogen oxides with alkaloids usually present in germinated malt during the drying process has been established as the primary source of NDMA contamination in beer and other malt beverages [2,3]. Österdahl [4] showed that beer consumption contributes greatly to the average daily intake of NDMA in some countries, even though low levels of contamination (low-ppb scale) are normally detected in beer samples. Therefore, the measurement of small amounts of NDMA in beer is a matter of great concern.

A number of methods for the determination of NDMA and other volatile nitrosamines in foodstuffs and beverages have been developed, based mainly on gas chromatography (GC) coupled with thermal energy analysis (TEA) [5–8]. TEA is a highly sensitive and selective technique for N-nitroso compounds, even though it also responds to some C-nitroso and C-nitro compounds [9]. Unfortunately, owing to its relatively high cost and limited versatility, a TEA detector

* Corresponding author.

0021-9673/95/$09.50
SSDI 0021-9673(95)00417-3

is not an allowable investment for many laboratories. On the other hand, the application of mass spectrometry (MS) as a detection technique for GC has expanded widely in recent years, owing to the increasing importance of GC–MS in analytical chemistry.

GC–MS has been applied extensively in order to confirm the presence of NDMA in samples previously tested by means of other techniques [10–13]. Methods based on GC–MS have sometimes been used for the quantification of NDMA in various matrices [14]. In 1976, Gaffield et al. [15] first reported the higher levels of sensitivity to NDMA achievable by chemical ionization (CI) MS in comparison with electron impact ionization. Actually, most of the ion current in CI is generally carried by the protonated molecular ion $[M+H]^+$ and few fragment ions are observed.

In this paper, a method alternative to TEA detection based on GC–isotope dilution (ID) CI-MS is described. A performance study was carried out in order to assess whether the method was suitable for the determination of NDMA in beer samples in terms of specificity, detection limit, precision and recovery. A careful choice of the GC operating conditions had to be made to avoid interferences from matrix-characteristic compounds giving an ion corresponding to a mass/charge ratio (m/z) of 75. GC optimization trials were performed until a chromatographic resolution sufficient to preclude any potential co-elution was obtained.

2. Experimental

2.1. Chemicals

NMDA and the deuterated analogue $[^2H_6]$NDMA were obtained from Aldrich (Milwaukee, WI, USA) and Cambridge Isotope Laboratories (Woburn, MA, USA), respectively. Methanol and dichloromethane (both of special-reagent grade) and isoamyl alcohol (analytical-reagent grade) were supplied by Carlo Erba (Milan, Italy). All other chemicals were of analytical-reagent grade and were obtained from local sources.

2.2. Sample preparation

Sample preparation was accomplished according to a modified procedure based on the official method II adopted by the Association of Official Analytical Chemists [7,16].

A 200.0-g beer sample was weighed directly into a 500-ml distillation flask containing 40 g of sodium chloride, then 1 ml of 10% sulfamic acid in water was added in order to prevent the artifactual formation of NDMA. The sample was spiked with 50 μl of a standard solution containing 10 μg ml^{-1} $[^2H_6]$NDMA (internal standard) in isoamyl alcohol. The flask was then connected to a distillation apparatus and the distillate (about 75 ml) was collected in a 100-ml flask placed in an ice-bath. The distillate was extracted with three 35-ml aliquots of dichloromethane in a 250-ml separating funnel. The extract was dried by passing it through a glass-wool-plugged chromatographic column containing 30 g of anhydrous sodium sulfate. The dried extract was collected directly in a 250-ml Kuderna–Danish (K–D) evaporator flask (Supelco, Bellefonte, PA, USA) assembled with a K–D concentrator tube (Supelco). After addition of a boiling chip to the K–D flask, a three-ball Snyder column (Supelco) was connected to the K–D evaporator and the extract was evaporated to about 4 ml by heating the tube at 60°C in a water-bath. The final concentration step was carried out by disconnecting the concentrator tube from the flask and attaching the three-ball Snyder column directly to the tube, after addition of another boiling chip. The extract was finally concentrated to 1.0–1.3 ml. The final sample extract volume was accurately measured by means of a precision syringe (Hamilton, Reno, NV, USA). Aliquots of 1 μl beer extract were injected three times successively into the GC–MS system.

2.3. GC–MS analysis

Analyses were performed using an HP5890A gas chromatograph coupled to an HP5989A quadrupole mass spectrometer (Hewlett–Packard, Palo Alto, CA, USA) equipped with a high-energy detector (HED) and operated in the

positive-ion CI mode. Samples were injected via an on-column injector onto a CPWax 52CB (Chrompack, Middleburg, Netherlands) fused-silica capillary column (25 m × 0.25 mm I.D.; 0.2 μm film thickness) connected to a deactivated fused-silica tube (1.5 m × 0.32 mm I.D.) used as a precolumn. Helium was used as the carrier gas at a column head pressure of 50 kPa.

The initial oven temperature was 35°C for 1 min followed by a programme rate of 70°C min^{-1} to 55°C, a 7-min isothermal step, a programme rate of 3°C min^{-1} to 70°C, then a programme rate of 20°C min^{-1} to 180°C. The source temperature was 200°C and the filament emission current and electron energy were 300 μA and 150 eV, respectively. Methane was used as the reagent gas (1.0 Torr source pressure; 1 Torr = 133.322 Pa) for chemical ionization. The spectrometer axis and ion abundance were tuned using perfluorotributylamine as the calibration gas. Quantification was performed by selected-ion monitoring (SIM) of the $[M+H]^+$ ion of NDMA (m/z 75.0) and $[^2H_6]$NDMA (m/z 81.0); the dwell time was 0.100 s per ion.

2.4. Calibration

Standard solutions of NDMA in methanol were prepared at concentrations of 0.2 and 2.0 μg ml^{-1}. Four aliquots of 200.0 g of NDMA-free beer were spiked with 50 μl of internal standard solution (2.5 μg kg^{-1}) and appropriate amounts of the NDMA solutions in order to achieve final concentrations of 0.10, 0.25, 0.50 and 4.00 μg kg^{-1}. A blank beer sample was prepared in a similar way by spiking 200.0 g of NDMA-free beer only with 50 μl of internal standard solution. These calibration samples were prepared and injected into the GC–MS system according to the procedure described above.

3. Results and discussion

3.1. Selectivity

A great lack of specificity in SIM of ions at m/z 75.0 and m/z 81.0 was experienced, as expected. Actually, a number of compounds present in the samples tested gave rise to signals relative to these ions, especially m/z 75.0. Nevertheless, no interfering peaks were observed at the retention time of NDMA in preliminary trials and more than 40 analyses of real samples. Further, the peak shapes of NDMA and its deuterated analogue were compared and checked for symmetry and exact matching (Fig. 1).

3.2. Linearity

A five-level calibration graph was obtained by plotting the peak-area ratios m/z 75.0 and 81.0 versus the known NDMA-to-$[^2H_6]$NDMA amount ratios for the calibration samples and performing least-square regression analysis [17]. The equation obtained showed an excellent linear fit ($r = 0.99999$) and a very low standard error ($s_{y/x} = 5.2642 \cdot 10^{-3}$). The slope ($b$), the intercept ($a$) and the corresponding confidence limits, calculated for three degrees of freedom at the 95% confidence level ($t = 3.18$), were $b = 0.966 \pm 0.0123$ and $a = 0.000362 \pm 0.00909$. It is noteworthy that the confidence interval for the intercept includes the theoretical value of 0.

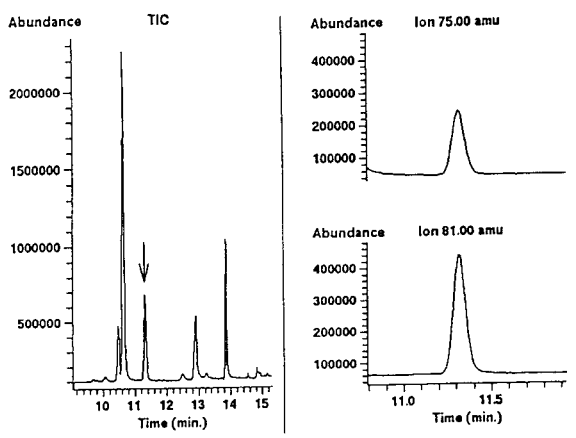

Fig. 1. Total ion chromatogram (TIC) and SIM traces relative to the protonated molecular ion of NDMA (m/z 75.0) and $[^2H_6]$NDMA (m/z 81.0) from a beer sample containing 1.36 μg kg^{-1} NDMA (peak indicated by the arrow in the TIC).

3.3. Limit of detection

The calculated limit of detection [17], defined as the lowest analyte amount yielding a signal equal to the blank signal plus three standard deviations of the blank, was about 0.04 $\mu g\ kg^{-1}$ (8 pg injected). This limit is at least comparable to those usually achievable by means of GC–TEA.

3.4. Precision and analysis of variance

Five 1-μl aliquots of a beer test sample containing 0.86 $\mu g\ kg^{-1}$ of NDMA were analysed on five different days to assess the precision of the method. Each aliquot was injected three times successively into the GC–MS system. The relative standard deviation (R.S.D.) was 0.73%. This value is much lower than that determined for similar concentration levels of NDMA reported previously using methods based on GC–TEA [5,7]. The results obtained were also submitted to a one-way analysis of variance to estimate the contribution of the sample preparation process (random-effect factor; between-sample variation) and the GC–MS measurement (residual value; within-sample variation) to the overall error of the method. The results are summarized in Table 1. A one-tailed F-test was performed to evaluate whether the between-sample mean square was significantly greater than the within-sample mean square. The calculated value of F (2.613) was lower than the critical value of F tabulated at the 95% confidence level ($F_{4,10} = 3.480$), hence there was no evidence of systematic error in the sample preparation step at the concentration level considered.

3.5. Recovery

It is known that precision and accuracy of ID-MS methods are largely insensitive to the recovery rate because all sources of variation are greatly reduced owing to the use of a stable isotopomer as the internal standard. Nevertheless, low recovery rates reduce the sensitivity and could have an indirect adverse effect on the precision of the measurement. Recoveries (R) were calculated by means of the following equation:

$$R\,(\%) = (A/A_{std}) \cdot V \cdot 100$$

Table 1
Results of five replicate analyses of a beer test sample

Aliquot No.	Measurement No. ($\mu g\ kg^{-1}$)			Mean ($\mu g\ kg^{-1}$)	R.S.D. (%) ($n = 3$)
	1	2	3		
1	0.85692	0.86043	0.86008	0.85914	0.23
2	0.85531	0.85804	0.86251	0.85862	0.42
3	0.87123	0.86863	0.85512	0.86499	1.00
4	0.87702	0.86066	0.87823	0.87197	1.13
5	0.84963	0.86088	0.85927	0.85659	0.71
Sample mean:	0.86226				
R.S.D. ($n = 5$)	0.73%				

Determination of the variance components

Source of variation	Degrees of freedom	Sum of squares	Mean square	F-ratio
Between-sample	4	$4.7049 \cdot 10^{-4}$	$1.1762 \cdot 10^{-4}$	2.613
Within-sample	10	$4.5014 \cdot 10^{-4}$	$4.5014 \cdot 10^{-5}$	
Total	14	$9.2063 \cdot 10^{-4}$		

where $A = [^2H_6]$NDMA peak area after a 1-μl injection of test sample solution, $A_{std} = [^2H_6]$NDMA peak area after a 1-μl injection of a standard solution containing 500 ng ml^{-1} of labelled compound in dichloromethane–isoamyl alcohol (95:5) and V = final volume of beer extract collected (ml). The average recovery (mean of five determinations ± confidence limits) was 78 ± 2.1% ($p = 0.05$).

References

[1] P.N. Magee and J.M. Barnes, Br. J. Cancer, 10 (1956) 114.
[2] M.N. Mangino, R.A. Scanlan and J.J. O'Brien, in R.A. Scanlan and S.R. Tannenbaum (Editors), ACS Symposium Series, No. 174, American Chemical Society, Washington, DC, 1981, p. 229.
[3] N.P. Sen, L. Tessier and S.W. Seaman, J. Agric. Food Chem., 31 (1983) 1033.
[4] B.G. Österdahl, Food Addit. Contam., 5 (1988) 587.
[5] S.M. Billedeau, B.J. Miller and H.C. Thompson, Jr., J. Food Sci., 53 (1988) 1696.
[6] A.J. Cutaia, J. Assoc. Off. Anal. Chem., 65 (1982) 584.
[7] N.P. Sen, S. Seaman and M. Bickis, J. Assoc. Off. Anal. Chem., 65 (1982) 720.
[8] S.M. Billedeau and H.C. Thompson, Jr., J. Chromatogr., 393 (1987) 367.
[9] D.H. Fine, D. Lieb and F. Rufeh, J. Chromatogr., 107 (1975) 351.
[10] P.J. Song and J.F. Hu, Food Chem. Toxicol., 26 (1988), 205.
[11] S.R. Dunn, J.W. Pensabene and M.L. Simenhoff, J. Chromatogr., 377 (1986) 35.
[12] B.J. Canas, D.C. Havery, F.L. Joe, Jr., and T. Fazio, J. Assoc. Off. Anal. Chem., 69 (1986) 1020.
[13] C.V. Cooper, Am. Ind. Hyg. Assoc. J., 48 (1987) 265.
[14] R.W. Stephany, J. Freudenthal, E. Egmond, L.G. Gramberg and P.L. Schuller, J. Agric Food Chem., 24 (1976) 536.
[15] W. Gaffield, R.H. Fish, R.L. Holmstead, J. Poppiti and A.L. Yergey, IARC Sci. Publ., 14 (1976) 11.
[16] K. Helrich (Editor), Official Methods of Analysis of the Association of Official Analytical Chemists, A.O.A.C., Arlington, VA, 15th ed., 1990, p. 720.
[17] J.C. Miller and J.N. Miller, Statistics for Analytical Chemistry, Ellis Horwood, Chichester, 3rd ed., 1993, Ch. 5, p. 101.

ELSEVIER

Journal of Chromatography A, 708 (1995) 309–321

JOURNAL OF CHROMATOGRAPHY A

Diode laser-induced fluorescence detection in capillary electrophoresis after pre-column derivatization of amino acids and small peptides

Arjan J.G. Mank[a], Edward S. Yeung[b,*]

[a]*Department of General and Analytical Chemistry, Free University, De Boelelaan 1083 1081 HV Amsterdam, Netherlands*
[b]*Department of Chemistry and Ames Laboratory-USDOE, Iowa State University, Ames, IA 50011, USA*

Received 1 March 1995; accepted 3 April 1995

Abstract

The use of diode laser-induced fluorescence (DIO-LIF) detection in the field of capillary electrophoresis (CE) is examined. A simple but sensitive detection system was constructed. The performance of the system was evaluated with respect to design factors and its sensitivity was compared with the theoretically achievable sensitivity. To enhance the applicability of direct DIO-LIF detection in CE, a derivatization method for amines was developed. A red-absorbing label, consisting of a dicarbocyanine fluorophore with a succinimidyl ester functionality, was synthesized for this purpose. After derivatization of 1×10^{-6} *M* glycine, a detection limit of 0.1 amol was observed for the labeled glycine. Similar detection limits were observed for other amino acids. To show that derivatization preserves the separation efficiency of CE for the analytes examined, 18 amino acids and tyramine were separated with micellar electrokinetic chromatography after labeling. In addition, even labeled peptides, including structurally related enkephalin-type compounds, were separated from each other with zone electrophoresis. To test the applicability of the derivatization method to biological samples, tyramine was determined in urine before and after the consumption of cheese.

1. Introduction

Diode laser-induced fluorescence (DIO-LIF) detection is considered a very promising technique [1]. Diode lasers have several advantageous characteristics: they are small, have a low flicker noise (<0.05%), and the available wavelengths are in the red (>630 nm) to near-infrared region, where the light scattering and fluorescence background are generally low. Diode lasers emitting at 670 nm have been applied in analytical chemistry, especially in combination with liquid chromatography (LC) [2]. Recently, DIO-LIF detection has been combined with capillary electrophoresis (CE) [3].

The low linear velocity (0.01–1 cm s^{-1}) used in CE is favorable for fluorescence detection because it allows multiple excitation of the analytes during the passage through the illuminated volume. In combination with the picoliter-to-nanoliter (pl–nl) volumes of typical CE flow cells, 100 mW of laser light can already result in an irradiance sufficient for excitation saturation

* Corresponding author.

0021-9673/95/$09.50
SSDI 0021-9673(95)00418-1

and/or photodegradation of the analyte, which ultimately determines the detection limit.

The miniaturization of the detection volumes has some disadvantages as well, such as an increased background signal due to scattering and flow-cell fluorescence [4,5]. At longer wavelengths, contributions from these two sources of background are reduced, so that DIO-LIF detection in the red region of the spectrum should be more sensitive than LIF detection at shorter wavelengths. However, because few analytes absorb at wavelengths longer than 630 nm, the direct applicability of DIO-LIF detection is limited. The purpose of this paper is to confirm that DIO-LIF detection is very sensitive and that applicability can be broadened by the introduction of derivatization with a newly developed label for primary and secondary amines.

Higashijima et al. [3] showed the possibility of labeling amino acids with a red-absorbing thiazine-based succinimidyl ester. However, labeling was performed with a very large excess of amino acid compared to the label and only arginine and glycine were present in the reaction mixture. The detection limits for the derivatized compounds were at the 10 pmol level. Fuchigami et al. [6] recently performed labeling with a pyronin succinimidyl ester that is fluorescent in the deep-red region. They reported detection limits for derivatized amino acids of 0.8–4.5 amol using CE with DIO-LIF detection. Separation of the derivatives of arginine, alanine, glycine, glutamic acid and aspartic acid was examined, but broadening and overlap of the peaks interfered with quantitation of the individual compounds.

Therefore, in order for DIO-LIF detection in CE to be useful, the separation power of CE should remain intact and the derivatization reaction should be reasonably efficient even at concentrations lower than those reported before. To achieve this goal we prepared a fluorescence label with a dicarbocyanine fluorophore and a single succinimidyl ester functionality (Fig. 1) [7], which is selective for primary and secondary amino group under slightly alkaline conditions. The absorption and emission maxima of this label lie at 667 ($\epsilon = 187\,000$ l mol^{-1} cm^{-1}) and

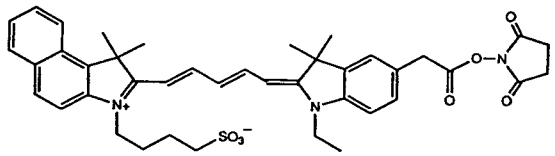

Fig. 1. Chemical structure of the dicarbocyanine label.

689 nm, respectively. The fluorescence quantum yield of the label is 0.23; all values were measured in methanol–water (50:50, v/v). The spectral characteristics of labeled analytes are similar to those of the unreacted label.

The concentration at which the analytes are derivatized here is almost 2 orders of magnitude lower than those reported before. However, due to the limited reactivity of succinimidyl esters, derivatization of the analytes still has to be performed at a much higher concentration than the achievable detection limit for the labeled analytes with CE–DIO-LIF. However, as far as we know, this problem is common to all derivatization-based detection schemes [8].

2. Experimental

2.1. Reagents

Boric acid, sodium hydroxide and methanol were obtained from Fisher Scientific (Pittsburgh, PA, USA). The amino acids and peptides were purchased from Sigma (St. Louis, MO, USA). Sodium dodecylsulfate (SDS) and all other chemicals were obtained from Aldrich (Milwaukee, WI, USA). Solutions were filtered through a 0.2-μm pore size membrane filter before use. The fluorescence label (Fig. 1) was prepared and purified at the Free University (Amsterdam, Netherlands).

2.2. Derivatization

All analytes, except tyramine in urine, were labeled in acetonitrile–borate buffer (pH 9.0, 25 mM). A 75-μl aliquot of the sample solution was mixed with 25 μl borate buffer (pH 9.0, 0.10 M), after which 100 μl of a 5×10^{-4} M solution

of the label in acetonitrile was added. The reaction was performed for 20 min at 65°C. Because succinimidyl esters tend to hydrolyze in aqueous solutions, especially at a higher pH, the concentration of the analyte has to be 2×10^{-7} *M* or higher to ensure quantitative reaction with the label. Below this concentration the reaction yield decreases quickly.

For the determination of tyramine in urine, some pretreatment of the sample was required [9]: 0.5 ml 6 *M* hydrochloric acid was added to 5 ml urine and the mixture was heated at 100°C for 30 min to hydrolyze tyramine–*o*-sulphate [10]. To this solution 5 ml diethyl ether was added and the mixture was mechanically shaken for 10 min and centrifuged at 2000 rpm for 5 min. The organic layer was discarded. The aqueous solution was adjusted to pH 9.6 with borate buffer. Then, 5 ml diethyl ether and 3 g anhydrous sodium sulfate were added in succession. The mixture was shaken and centrifuged as described before. The organic fraction was transferred to a glass centrifuge tube and evaporated to dryness with a stream of nitrogen. The sample was then redissolved in 0.2 ml acetonitrile containing 0.5% triethylamine and 2.5×10^{-4} *M* of the label. The reaction was performed for 45 min at 60°C. Because no water is present in the reaction mixture, tyramine could be derivatized at concentrations as low as 5×10^{-8} *M*.

2.3. Electrophoresis

CE was performed in a 75-cm long fused-silica capillary with an outer diameter of 350 μm and an internal diameter (I.D.) of either 33 or 50 μm (Polymicro Technologies, Phoenix, AZ, USA). The polyimide coating of the capillary was burned off to form a window 45 cm from the injection end (grounded anode end) of the capillary.

Vacuum siphoning was used to inject 2 nl of the sample solution. The injection volume was calculated according to the equation described by Rose and Jorgenson [11]. A run typically consisted of 10-min flush with the running buffer, followed by vacuum injection of the sample and CE at a constant voltage of 30 kV. Both the injection system and the high-voltage power supply were taken from a commercial CE apparatus (ISCO Model 3140, Lincoln, NE, USA).

2.4. DIO-LIF detection

A simple and inexpensive fluorometer designed by us [12] was used as a platform for our DIO-LIF detection system. Because diode lasers are available for less than $100, the laser no longer forms the major part of the costs of the system. To optimize the DIO-LIF detection system, some specific features of diode lasers have to be reckoned with [13]. In contrast to most lasers, diode lasers emit an elliptical beam with a Gaussian intensity profile. For optimum excitation, the major axis of the beam should be oriented along the capillary. This allows the largest amount of light to be coupled into the flow cell. Furthermore, in this geometry the incident laser light is *p*-polarized, which ensures the highest transmission of laser light through the flow cell material.

Diode lasers normally show astigmatism. Because this is in the order of 10–20 μm for index-guided diode lasers, no corrective optics are required for most capillaries. For gain-guided diode lasers this value is 4 times higher and therefore such devices should be avoided. According to Larson et al. [13] the illuminated volume in a 50-μm capillary can be as small as 1.5 pl. In our case, the size of the laser beam was 20×10 μm upon entering the capillary. Although the beam was focused in the center of the capillary, deformation by the capillary wall and astigmatism of the laser beam make an illuminated volume of 10 pl a reasonable estimate [14,15].

To our original design of the fluorometer [12], a number of light shields were added and a *f*/1 biconvex lens, with a 1-cm focal length, is installed to focus the fluorescence collected by the 20 × microscope objective onto the photomultiplier (PMT) (Fig. 2). The diode laser is a 10 mW 670 nm LAS200-670-10 diode laser (Lasermax, Rochester, NY, USA), equipped with a 10 × microscope objective. The excitation filter consists of a combination of a 670 ± 5 nm

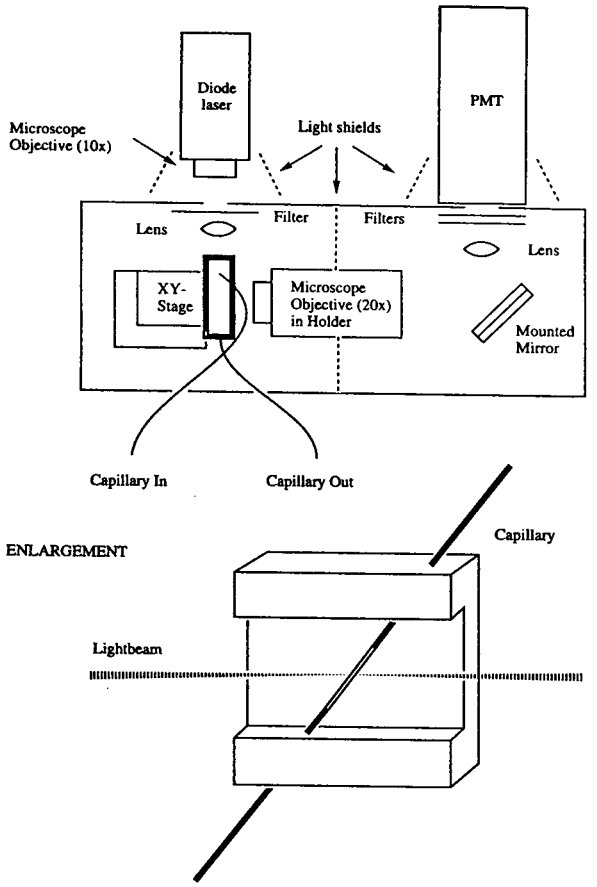

Fig. 2. Schematic diagram of the DIO-LIF detector for CE, including an insert that shows the relative position of the capillary to the excitation beam.

bandpass filter (70% max. transmission) supplied by Omega Optical (Brattleboro, VT, USA) and a standard polarization filter to remove spontaneously emitted light. As a result of the collimating optics and the filters, the excitation power at the capillary is reduced to 3.5 mW.

A 690 ± 5 nm bandpass filter (70% max. transmission, Omega) and a 4-mm RG695 Schott-filter form the emission filter set. A cooled C31034 (RCA, Lancaster, UK) PMT, operated at 1750 V, is used in combination with a SR400 photon counter (Stanford Research Systems, Palo Alto, CA, USA). The data are collected at 5 Hz and stored on the hard disk of a Macintosh Classic computer. Other parts of the DIO-LIF detection represented in Fig. 2 are described in Ref. [12].

3. Results and discussion

3.1. DIO-LIF detection

To determine the sensitivity of the CE–DIO-LIF detection system, 1.0×10^{-6} *M* glycine was labeled and diluted before detection in a 50-μm capillary. The CE conditions were similar to those used in Fig. 3 (see below), but 20 kV were applied across the capillary instead of 30 kV. The labeled glycine and the excess label showed migration times of 20 min and 25 min, respectively. The observed background signal was 1.9×10^5 counts (in 0.2 s), with a (peak-to-peak) noise level of 2.0×10^3 counts. Because the power fluctuations in the output of the diode laser (within 10 min) are less than 0.05%, detection is shot-noise limited.

Fluorescence from the capillary walls is negligible. Raman scattering from the solvent has no recognizable contribution either: its intensity is very low in the red- to near-infrared region of the spectrum and the major peaks of the Raman spectrum of methanol and water lie outside the emission spectral window. Consequently, the background signal can be assumed to consist entirely of elastically scattered light. The addition of another 695-nm bandpass filter reduced both the background signal and the emission collection efficiency by a factor 4. Because detection is shot-noise limited, the observed signal-to-noise ratio was a factor 2 worse. The same negative effect was observed for adding other long-pass filters.

The detection limit for the labeled glycine was 5×10^{-11} *M* or 0.1 amol injected (signal-to-noise ratio = 3, noise = peak-to-peak noise). The signal for labeled glycine was examined for concentrations between 5×10^{-11} *M* and 5×10^{-8} *M*. The slope of the corresponding linear calibration curve was 1.2×10^{14} counts l mol^{-1} with a correlation coefficient of 0.996 (9 data points). This shows that the detector has good linearity

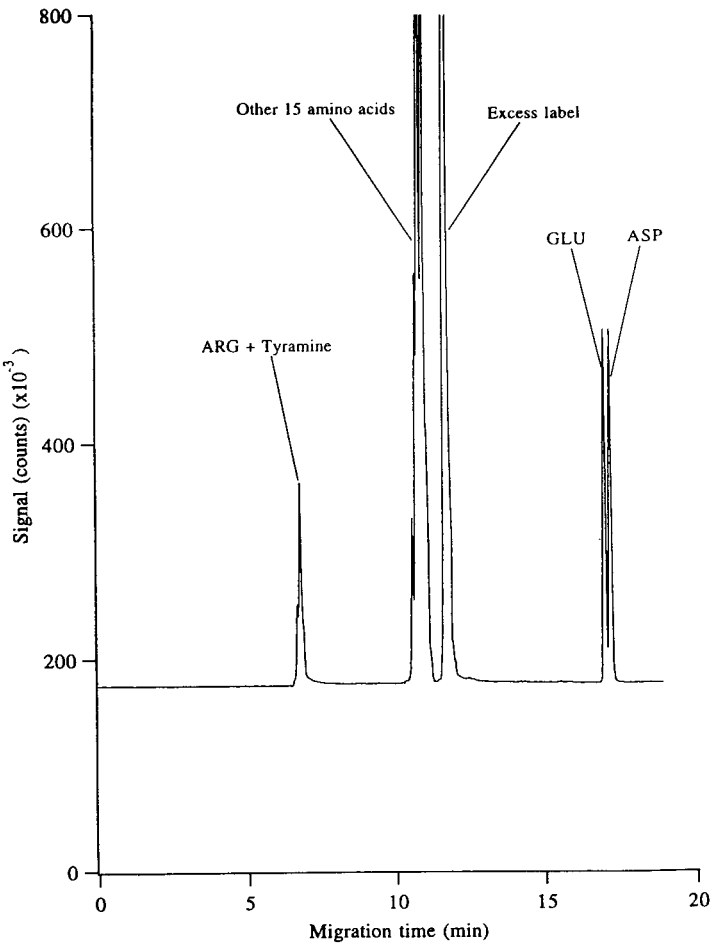

Fig. 3. Electropherogram of a mixture of 18 amino acids plus tyramine, obtained after derivatization. CE conditions: 75 cm capillary (50 μm I.D.); 30 kV; buffer: borate (pH 9.0, 75 m*M*)–methanol (72.5:27.5, v/v).

over a concentration range of at least 3 orders of magnitude. The detection limits observed for the same labeled analyte in 33 μm I.D. capillaries were 1.5-fold worse, due to the difference in pathlength. The observed background signal was similar. Clearly, CE with DIO-LIF detection allows the reliable detection of very low concentrations of red and near-infrared absorbing analytes.

Under the conditions used, dilution on the 50 μm I.D. capillary is negligible and the concentration of the labeled glycine in the migrating sample is the same as the one injected: the migration time of the labeled glycine is 20 min, corresponding to a distance of 45 cm traveled. This indicates a migration velocity of 0.04 cm s^{-1}. At this migration rate, the 3-s observed peak width (at half height) corresponds to 0.12 cm or 2 nl.

To show the different factors that determine the sensitivity of the DIO-LIF detection system, a theoretical estimate can be made of the amount of signal produced per 1-s interval (n_f):

$$n_f = 2.3\epsilon[C_{analyte}]L\Phi_f PC \quad (1)$$

The molar absorptivity (ϵ) of labeled glycine is assumed to be 187 000 l mol^{-1} cm^{-1}, the analyte

concentration ($[C_{analyte}]$) is 5×10^{-11} M at the detection limit, the optical pathlength (L) is 5.0×10^{-3} cm, the fluorescence quantum yield (Φ_f) is 0.23, and the incident radiant power (P) is 1.2×10^{16} photons s^{-1}. C is the collection efficiency of the optical system of the detector, which is limited by three factors: the lens geometric factor (0.042) [16] the filter transmission (0.032), and the PMT quantum efficiency (0.20). Other factors, such as transmission through capillary walls, the lenses and the PMT window, decrease the collection efficiency only 25%. Combining these effects results in a value for C of 2×10^{-4}.

According to Eq. 1, n_f should be equal to 1.2×10^4 counts per 0.2 s (data collection interval) for labeled glycine at the detection limit. This value is only a factor of 2 from the experimental signal of 6×10^3 counts, as derived from the slope of the calibration curve.

Approximating the laser beam cross-section to a 20×10 μm rectangle with a uniform intensity distribution, the formulas described in Ref. [17] can be used to show that every molecule that passes through the detection volume will emit 5.0×10^4 photons. At a concentration of 5×10^{-11} M labeled glycine, only 300 detectable molecules are present in the detection volume. In addition, with a constant migration rate of 0.04 cm s^{-1}, this detection volume is refreshed 4 times per 0.2-s interval. Therefore, a signal of 4 times 300 times 5.0×10^4 photons, or 6.0×10^7 photons, will be produced in the detection volume if the concentration is maintained during the 0.2 s. Correcting for the emission collection efficiency ($C = 2 \times 10^{-4}$) results in an observed signal of 1.2×10^4 counts in 0.2-s, confirming the previously calculated value.

Obviously, the assumptions made concerning the beam shape are not entirely correct, since the actual beam is elliptical and has a Gaussian intensity distribution (see formula 2 in Ref. [13]). In addition, the illuminated volume is somewhat overestimated, because the beam is focused inside the capillary. However, the calculations presented still enable a reasonable estimate of the signal to be expected.

Under the present experimental conditions, photodestruction is not observed. Using flow injection of 5×10^{-10} M labeled glycine and linear velocities between 0.01–0.2 cm s^{-1}, no significant differences in signal height were observed. It should be noted that even if either excitation saturation or photodestruction becomes limiting, a wider excitation beam could be used. With the present 10-μm wide spot on the capillary wall less than one in four of the molecules passing through the capillary actually enters the illuminated volume.

On the detection side, the use of a microscope objective with a larger numerical aperture would obviously improve signal collection. Because detection is shot-noise limited, an equivalent increase in collection efficiency for the background and the signal would still result in a better detection limit. Obviously, sharper bandpass filters may improve the detection limit as a result of the better rejection of scattered light (without a large reduction in the emission collection efficiency). However, such filters are expensive and few analytes have to be detected at a concentration lower than 1×10^{-10} M directly.

3.2. Detection of amino acids

We used the newly developed dicarbocyanine label with a succinimidyl ester functionality to extend the applicability of CE–DIO-LIF detection. Due to the limited reactivity of the functionality, labeling of the amino acids has to be performed at concentrations above 2×10^{-7} M, when aqueous samples are studied. Therefore, derivatization was performed at an analyte concentration of 1×10^{-6} M; detection limits were then determined from serial dilution of the sample after derivatization.

For all amino acids tested, detection limits for the labeled analogs were $(0.5–1.5) \times 10^{-10}$ M. To determine to what extent the separation power of CE was affected by the labeling procedure, a mixture of 18 amino acids (involved in protein synthesis) and tyramine was labeled and subsequently separated by CE. Proline and cysteine were not included: proline did not give an acceptable peak shape and cysteine formed

sulfur–sulfur bonds under the conditions used for labeling.

All electropherograms were recorded by applying 30 kV across the capillary unless mentioned otherwise. By using a 50 μm I.D. capillary and borate (pH 9.0, 75 mM)–methanol (72.5:27.5, v/v) as the buffer, only 5 peaks were observed: labeled arginine and tyramine, 15 labeled monofunctional amino acids, the hydrolyzed label, labeled glutamic acid and labeled aspartic acid (Fig. 3). Arginine and tyramine are not negatively charged at this pH. The 15 labeled amino acids with one carboxylic acid moiety are not well resolved owing to their similar molecular structure. The hydrolyzed label is somewhat smaller than the labeled analytes and has a higher charge-per-size ratio, resulting in a longer migration time. Aspartic acid and glutamic acid contain two carboxylic acid groups that are largely negatively charged. Higher methanol percentages seriously decreased the migration time of the labeled analytes and were avoided for that reason.

For pH values between 8.0–10.0 no change in elution order was observed. Increasing the pH to 11 resulted in a higher effective charge on tyramine and tyrosine due to their phenolic substituent. As a result, separation of the labeled amino acids in the mixture is slightly improved (Fig. 4), although labeled aspartic acid and labeled glutamic acid show the same migration time under these conditions.

Micellar electrokinetic chromatography (MEKC) is often applied to improve the separation of amino acids [18]. However, because the attachment of the label will affect the partition coefficient of the amino acid between the aqueous buffer and the micelle, it is hard to predict the effect of an ionic surfactant on the CE separation of the derivatized amino acids. In practice, the addition of SDS to the borate (pH 9.0, 20 mM)–methanol (72.5:27.5, v/v) buffer

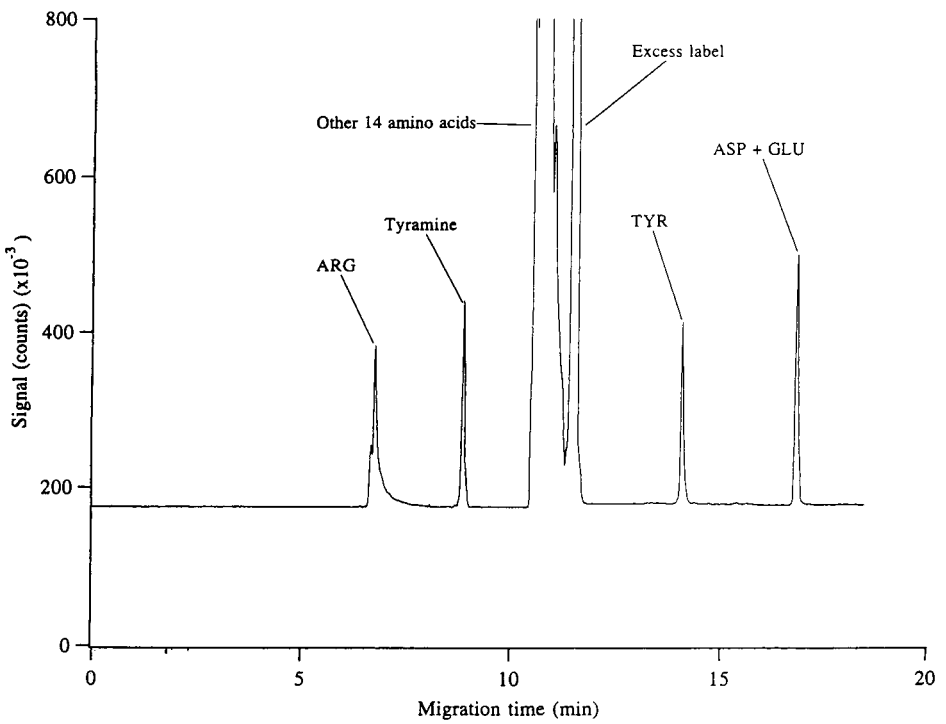

Fig. 4. Electropherogram of a mixture of 18 amino acids plus tyramine, obtained after derivatization. CE conditions: 75 cm capillary (50 μm I.D.); 30 kV; buffer: borate (pH 11.0, 75 mM)–methanol (72.5:27.5, v/v).

had a very large effect. Using 17.5 m*M* SDS the labeled amino acids are well separated on a 33 μm I.D. capillary (Fig. 5), except for labeled tyrosine and labeled glutamine, which have a similar migration time. Changes in pH or SDS concentration allowed separation of the latter two compounds, but resulted in similar migration times for other labeled analytes. Under the conditions used, the excess label is well separated from the analytes. The elution order of the different labeled analytes is almost reversed compared to that observed with conventional CE, because the compounds with a higher charge spent less time in the micelles than the less charged ones. As a result, labeled serine and labeled threonine, which contain hydrophilic residues, migrate faster that labeled glycine, which is obviously smaller. However, the size of the aliphatic part of the amino acid has a small effect as well: labeled valine migrates slower than labeled alanine, which migrates slower than labeled glycine.

It should be noted that only a very small peak is visible for labeled lysine, which contains two primary amine groups. The marked peak represents the lysine that is labeled only once. As was observed for *o*-phthaldehyde (OPA)-labeled analytes previously [19], the multi-labeled lysine is not visible, probably as a result of severe fluorescence quenching. There are two sources of background contamination in the electropherogram. The peaks in the region between 41 and 43 min are associated with the reagent blank. The remaining unmarked peaks are associated with labeled impurities in the amino acids.

The addition of SDS resulted in increased migration times, but all compounds were eluted past the detection window within 45 min. If more methanol is added, the same separation efficiency can only be achieved with an increased

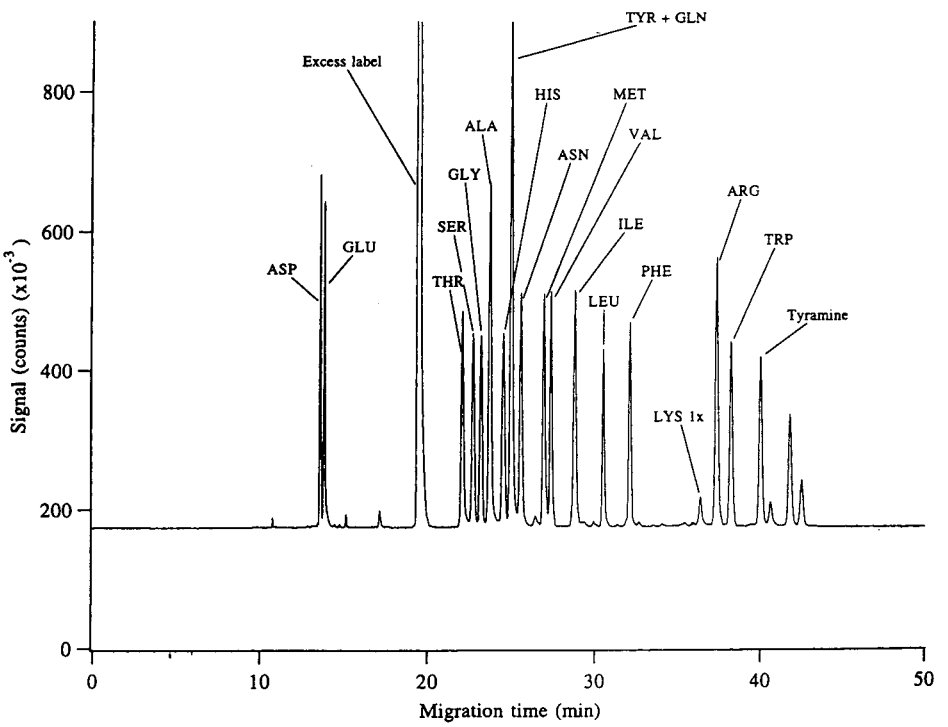

Fig. 5. Electropherogram of a mixture of 18 amino acids plus tyramine, obtained after derivatization. CE conditions: 75 cm capillary (33 μm I.D.); 30 kV; buffer: borate (pH 9.0, 20 m*M*)–methanol (72.5:27.5, v/v) and 17.5 m*M* sodium dodecylsulfate.

SDS concentration. A similar separation in 50 μm I.D. capillaries resulted in somewhat lower resolution. Apparently, the reduced joule heating in the 33 μm I.D. capillary enhanced the separation.

Addition of cyclodextrins to the MEKC buffer has been shown to induce separation of the D- and L-isomers of amino acids [18], even though the size and charge of the isomers are the same. Attempts to separate D- and L-amino acids (DL-alanine, DL-phenylalanine, DL-leucine and DL-methionine were tested) by the addition of α- and β-cyclodextrin in MEKC did not influence the relative migration of the different amino acids or result in any observable enantiomeric separation. Only when γ-cyclodextrin was used, the relative migration of the amino acids was influenced, but still no separation of the D- and L-isomers could be observed. Obviously, the fluorescence label does not allow a selective interaction of the amino acid enantiomers with the cyclodextrins tested [18].

3.3. Detection of peptides

The separation of peptides with CE is largely based on differences in size instead of charge, especially if the same end-groups are present. To examine whether the size of the label hinders the CE separation of small peptides, a mixture of glycine-based peptides was derivatized at 1×10^{-6} *M*. Peptides containing 1–6 glycines were first studied individually to determine their migration times. Baseline separation was achieved in a 33-μm capillary with a buffer consisting of borate (pH 9.0, 75 m*M*)–methanol (65:35, v/v) (Fig. 6). Addition of surfactant did not improve the separation: the smaller peptides are separated more efficiently, but Gly-Gly-Gly-Gly-Gly and Gly-Gly-Gly-Gly-Gly-Gly are still resolved from each other.

Based on this positive result, the separation of two very similar enkephalin-type peptides and related fragments was attempted. These opioid peptides, leucine–enkephaline (Tyr-Gly-Gly-Phe-Leu or T-G-G-P-L) and methionine–enkephaline (Tyr-Gly-Gly-Phe-Met or T-G-G-P-M), represent an important class of neurotransmitters [20]. In the literature, a number of articles related to the analysis of these compounds has appeared using HPLC in combination with precolumn derivatization [21] and CE with UV detection [22]. However, separation of the two related enkephalins was difficult to achieve. Leucine–, methionine–enkephalin and a number of their fragments were derivatized individually at a concentration of 1×10^{-6} *M*. After identification of the peaks, a mixture of these compounds was derivatized.

Because not all fragments of the enkaphalin-type compounds contain a tyrosine unit (with a phenolic substituent), separation was examined at a high pH. With borate (pH 11.3, 75 m*M*)–methanol (65:35, v/v) buffer, most of the labeled fragments are well separated from each other (Fig. 7). Even labeled Leu–and Met–enkephalin can be identified, although baseline separation is not achieved for these two analytes. As can be seen from the electropherogram a significant number of unidentified peaks is present, which originate from impurities and degradation products in the peptide solution.

3.4. Detection of tyramine

Tyramine (4-hydroxyphenethylamine) is an indirectly acting sympathomimetic amine found in cheese, fermented foods and red wine [23]. Previously, tyramine has been determined in urine by HPLC coupled with fluorimetric [10] or electrochemical detection [24]. To show that the combination of derivatization with CE–DIO-LIF detection can also be applied to real samples, it was used to determine the tyramine concentration in the urine of a healthy volunteer before and after eating 100 g of cheddar cheese.

Tyramine is converted to tyramine–*o*-sulphate before it is excreted in urine, which necessitates pretreatment with hydrochloric acid at elevated temperatures. The combination of dilution as a result of this treatment and the fact that many other amines are present in urine make it impossible to perform the labeling prior to the extraction. Pretreatment and derivatization was therefore performed as described in the Experimental section. As can be observed in the

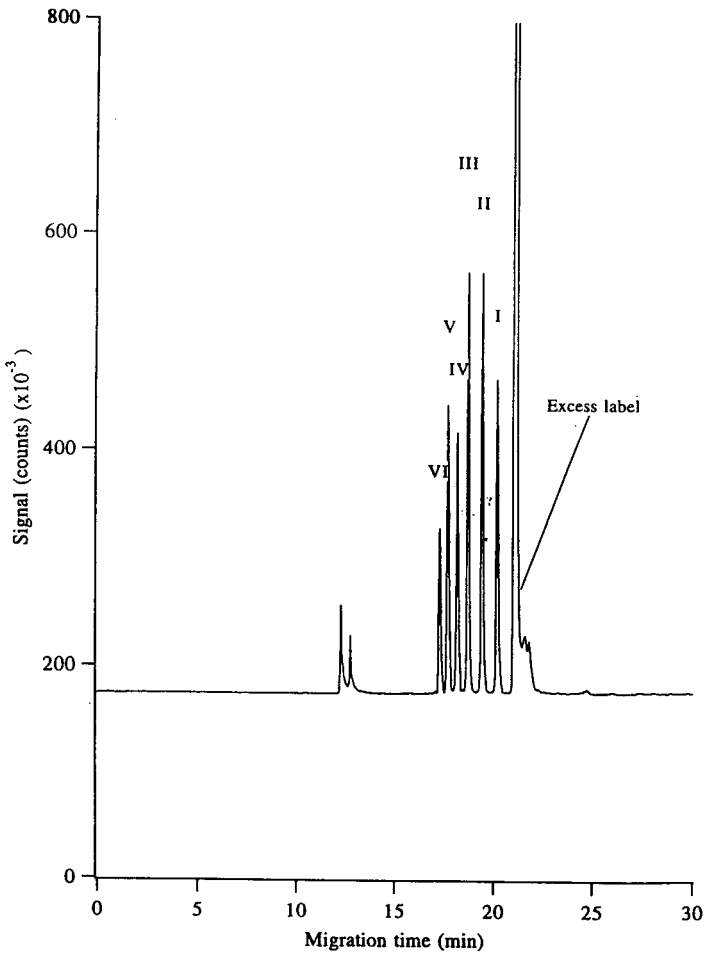

Fig. 6. Electropherogram of a mixture of small peptides [Gly (I), Gly-Gly (II), Gly-Gly-Gly (III), Gly-Gly-Gly-Gly (IV), Gly-Gly-Gly-Gly-Gly (V) and Gly-Gly-Gly-Gly-Gly-Gly (VI)] obtained after derivatization. CE conditions: 75 cm capillary (33 μm I.D.); 30 kV; buffer: borate (pH 9.0, 75 mM)–methanol (65:35, v/v).

corresponding electropherograms, the concentration of tyramine increases almost 2-fold (from 2.5 to 4.7×10^{-6} M) as a result of eating the cheese (Fig. 8). This change is similar to that observed by Koning et al. [10]. Identification was checked by spiking urine with $(1–25) \times 10^{-6}$ M tyramine, followed by the sample preparation procedure described in the Experimental section.

A plot of the peak area versus the concentration showed a linear relation with a correlation coefficient of 0.989 (9 data points). The relative standard deviation of the determination of 5×10^{-6} M tyramine ($n = 5$), 5×10^{-9} M injected, was 4.1%. Clearly, the method described can be applied to the reproducible determination of tyramine in urine. However, it should be noted that the concentrations that are determined here are rather high and further work is necessary to determine the general applicability of derivatization in combination with CE–DIO-LIF detection in other real samples.

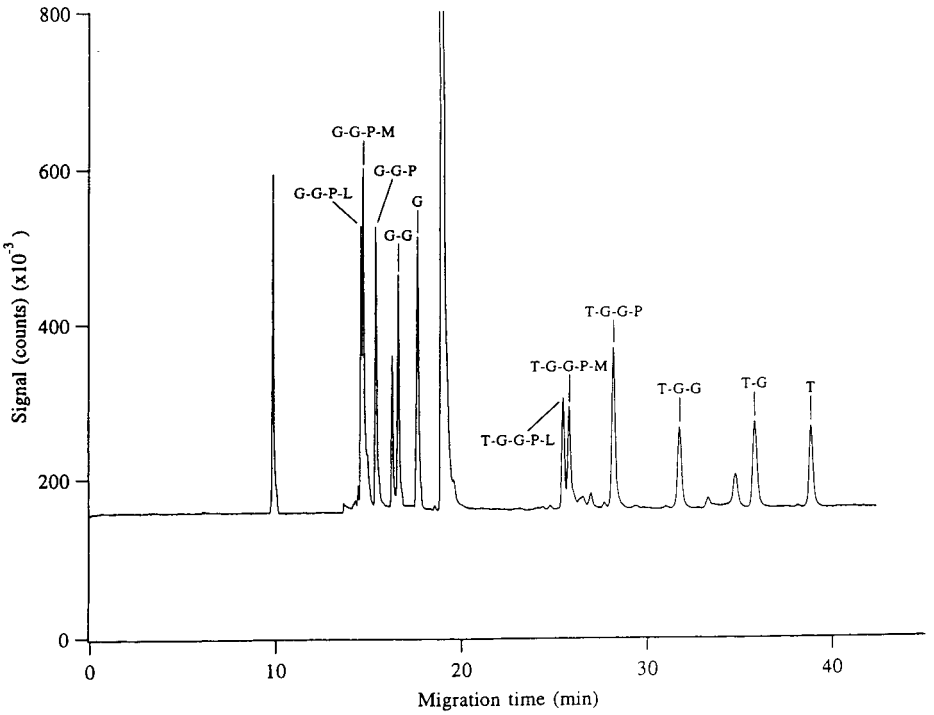

Fig. 7. Electropherogram of a mixture of enkephalines and related fragments, obtained after derivatization. CE conditions: 75 cm capillary (33 μm I.D.); 30 kV; buffer: borate (pH 11.0, 50 mM)–methanol (60:40, v/v).

4. Conclusions

A sensitive DIO-LIF detection system was built for use in CE. The detection limits achieved with this device were compared with theoretical values to identify the factors which influence its performance. To improve the applicability of the system, a derivatization method was developed for primary and secondary amines. A detection limit of 5×10^{-11} M (0.1 amol) was achieved for labeled glycine and similar values were found for other labeled amino acids. It should be noted that due to the limited reactivity of the succinimidyl ester functionality, the analytes were derivatized at a concentration of 1×10^{-6} M in aqueous solutions.

Although the separation power of conventional CE was not sufficient to obtain resolved peaks for all 18 labeled amino acid, micellar electrokinetic chromatography greatly enhanced the separation and nearly all labeled amino acids could be quantified. With conventional (zone) CE a number of labeled peptides with the same end-groups could be separated, despite the large size of the label. Even similar enkephalin-type compounds (and fragments of these compounds) were separable by zone electrophoresis, indicating that labeling does not seriously compromise the high resolving power of CE. Finally, tyramine was determined in urine to show the applicability of the combination of derivatization and CE–DIO-LIF detection to real samples.

It is clear that CE–DIO-LIF detection is a sensitive alternative for the detection of red- to near-infrared absorbing compounds. However, for wide acceptance of the technique its applicability should be broadened. Although the presented results with an amine-selective label

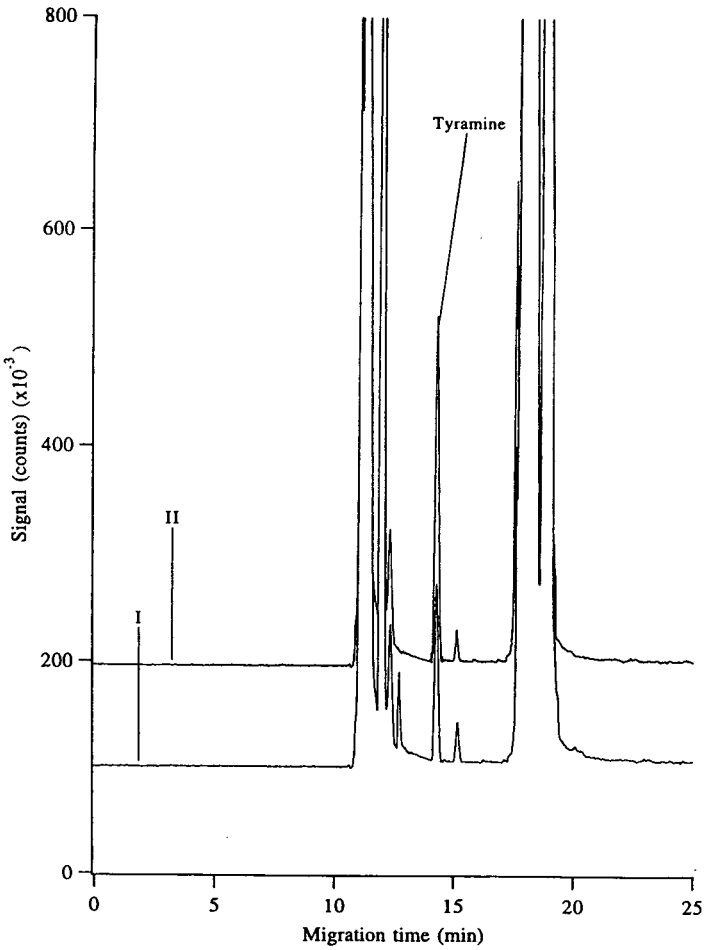

Fig. 8. Electropherograms of urine samples, before (I) and after (II) eating 100 g of cheddar cheese. Both were obtained after extraction and derivatization. CE conditions: 75 cm capillary (50 μm I.D.); 30 kV; buffer: borate (pH 11.0, 50 mM)–methanol (60:40, v/v).

are promising, new labels are required that allow derivatization at much lower concentrations of analyte. The dicarbocyanine fluorophore possesses most of the characteristics required for detection at very low levels, such as a high extinction coefficient at a long wavelength and a high fluorescence quantum yield. However, the succinimidyl ester reactive group is not reactive enough and hydrolyses easily. A more reactive functionality would allow the labeling reaction to be performed with yet lower concentrations of analyte.

At the same time, miniaturization of the derivatization procedure described in this paper would improve the usefulness of the technique as well. Detection of analytes in smaller volumes, such as in single cells, has become possible with the introduction of CE. Cells often contain high concentrations of interesting compounds ($>1 \times 10^{-6}$ M), but they are normally lysed before derivatization is performed. As a result, the concentration in the reaction mixture is much lower. If derivatization could be performed in a very small volume or even inside the cell [25], this problem could be avoided. Investigations involving both the introduction of different re-

active groups on red-absorbing labels and the miniaturization of the derivatization process are being continued.

Acknowledgments

The authors thank ISCO, Inc. for donation of the CE instrument used in this work. The Ames Laboratory is operated for the U.S. Department of Energy by Iowa State University under contract No. W-7405-Eng-82. This work was supported by the Director of Energy Research, Office of Basic Energy Sciences, Division of Chemical Sciences. The Department of General and Analytical Chemistry of the Free University (Amsterdam, Netherlands) and NWO (Den Haag, Netherlands) are gratefully acknowledged for supporting the stay of A.J.G. Mank at Iowa State University.

References

[1] A.J.G. Mank, H. Lingeman and C. Gooijer, Trends Anal. Chem., 11 (1992) 210.
[2] A.J.G. Mank, E.J. Molenaar, H. Lingeman, C. Gooijer, U.A.Th. Brinkman and N.H. Velthorst, Anal. Chem., 65 (1993) 2197–2203.
[3] T. Higashijima, T. Fuchigami, T. Imasaka and N. Ishibashi, Anal. Chem., 64 (1992) 711–714.
[4] S. Wu and N.J. Dovichi, J. Chromatogr., 480 (1989) 141–155.
[5] J.W. Sweedler, J.B. Shear, H.A. Fishman, R.N. Zare and R.H. Scheller, Anal. Chem., 64 (1991) 496.
[6] T. Fuchigami, T. Imasaka and M. Shiga, Anal. Chim. Acta, 282 (1993) 209–213.
[7] A.J.G. Mank, H.T.C. van der Laan, H. Lingeman, C. Gooijer, U.A.Th. Brinkman and N.H. Velthorst, Anal. Chem., submitted.
[8] A.J.G. Mank, H. Lingeman and C. Gooijer, J. High Res. Chromatogr., 11 (1994) 797–798.
[9] D.S. Lho, J.K. Hong, H.K. Paek, J.A. Lee and J. Park, J. Anal. Toxicol., 14 (1990) 77–83.
[10] H. Koning, H. Wolf, K. Venema and J. Korf, J. Chromatogr., 533 (1990) 171–178.
[11] D.J. Rose and J.W. Jorgenson, Anal. Chem., 60 (1988) 642.
[12] E.S. Yeung, P. Wang, W. Li and R. Giese, J. Chromatogr., 608 (1992) 73–77.
[13] A.P. Larson, H. Ahlberg and S. Folestad, Appl. Opt., 32 (1993) 794–805.
[14] T. Tsuda and H. Noda, J. Chromatogr., 471 (1989) 311–319.
[15] F. Maystre and A.E. Bruno, Anal. Chem., 64 (1992) 2885–2887.
[16] Y.F. Cheng and N.J. Dovichi, Science, 242 (1988) 562.
[17] A.J.G. Mank, N.H. Velthorst, U.A.Th. Brinkman and C. Gooijer, J. Chromatogr. A, accepted.
[18] T. Ueda, R. Mitchell, F. Kitamura, T. Metcalf, T. Kuwana and A. Nakamoto, J. Chromatogr., 593 (1992) 265–274.
[19] M.A. Nussbaum, J.E. Przedwiecki, D.U. Staerk, S.M. Lunte and C.M. Riley, Anal. Chem., 64 (1992) 1259–1263.
[20] R.C.A. Frederickson and L.E. Greary, Prog. Neurobiol., 19 (1982) 19.
[21] M. Mifune, D.K. Krehbiel, J.F. Stobaugh and C.M. Riley, J. Chromatogr., 496 (1989) 55–70.
[22] I. Beijersten and D. Westerlund, Anal. Chem., 65 (1993) 3484–3488.
[23] R.C. Causon and M.J. Brown, J. Chromatogr., 310 (1984) 11–17.
[24] P.C. Waldmeier, K.H. Antonin, J.J. Feldtrauer, Ch. Grunenwald, E. Paul, J. Lauber and P. Bieck, Eur. J. Clin. Pharmacol., 25 (1983) 361.
[25] B.L. Hogan and E.S. Yeung, Anal. Chem., 64 (1992) 2841–2845.

ELSEVIER

Journal of Chromatography A, 708 (1995) 323–337

JOURNAL OF CHROMATOGRAPHY A

Separation of precolumn-labelled D- and L-amino acids by micellar electrokinetic chromatography with UV and fluorescence detection

Anna Tivesten, Staffan Folestad*

Department of Analytical and Marine Chemistry, University of Göteborg/Chalmers University of Technology, S-412 96 Göteborg, Sweden

First received 22 December 1994; revised manuscript received 16 March 1995; accepted 27 March 1995

Abstract

Micellar electrokinetic chromatography (MEKC) was examined for the separation of labelled D- and L-amino acids to permit rapid screening of protein amino acid enantiomers in microchemical analytical work. Precolumn chiral derivatization was performed using *o*-phthaldialdehyde/2,3,4,6-tetra-O-acetyl-1-thio-β-D-glucopyranose (OPA/TATG) reagent and the diastereomers formed were detected by UV or fluorescence detection. Optimization of separation buffer pH, ionic strength and surfactant concentration was carried out and was focused on the effective separation window available for the resolution of the amino acid derivatives. The effects of added organic modifiers, methanol, acetonitrile and tetrahydrofuran, on the relative retention of the derivatives were characterized for the purpose of fine tuning the separation selectivity. The resolution of the derivatives of the D- and L-forms of each protein amino acid was very high (mean value of $R_s = 14.3$, range 0.8–28), except for aspartic acid and glutamic acid, whose enantiomers could not be resolved at the alkaline pH studied. A separation of 34 D,L-amino acids in less than 5 min, is demonstrated with only a few peaks co-eluting.

1. Introduction

For the determination of amino acid enantiomers in microchemical analytical work, a microcolumn separation technique such as liquid chromatography (LC) in capillary format or capillary electrophoresis (CE) should be employed. Generally, a higher separation efficiency in a shorter analysis time can be provided by CE than by LC, which is why CE is more attractive to explore for the purpose of obtaining a method for rapid screening of complex samples, e.g., to resolve the D- and L-forms of all protein amino acids in a single run.

In CE, chiral resolution of amino acids can be accomplished basically in two ways, in the direct or the indirect way. The first approach involves the addition of a chiral selector such as cyclodextrins [1–3], crown ethers [4] or copper(II) complexes [5] to the separation buffer or a chiral surfactant such as digitonin [6], N-dodecyl-L-valinate (SDVal) [6–9], glycyrrhizic acid (GRA) [10], β-escin [10] or bile salts [11]. Alternatively, a chiral selector can be incorporated into a

* Corresponding author. Present address: Analytical Chemistry, Pharmaceutical R&D, Astra Hässle, S-43183 Mölndal, Sweden.

0021-9673/95/$09.50
SSDI 0021-9673(95)00391-6

stationary film coated on the inner surface of the separation capillary [12,13]. The use of chiral selectors in CE has recently been thoroughly reviewed by Terabe et al. [14]. Since only a few amino acids exhibit a useful response with UV–Vis absorption or fluorescence detection, most of the studies cited above on chiral selectors involve the separation of amino acids labelled with achiral reagents, e.g., dansyl chloride (DNS) [1,3,5,11], phenyl isothiocyanate (PITC) [6,8–10] or naphthalene-2,3-dicarboxaldehyde (NDA) [2]. The second approach to accomplish chiral resolution, the indirect way, is to utilize chiral labelling, whereby analytes are converted into derivatives with good detection properties and, because the derivatives are diastereomers, an achiral CE separation method can be used. A prerequisite, however, is that the reagent possesses a high optical purity in order to prevent more than one derivative being produced for each chiral analyte. In addition, racemization during derivatization must be avoided. Of several reagents earlier employed for chiral derivatization of amino acids in LC, thoroughly reviewed elsewhere [15], few have so far been examined in CE. Both Marfeys' reagent, as used by Tran et al. [16] and 2,3,4,6-tetra-O-acetyl-β-D-glucopyranosyl isothiocyanate (GITC), as used by Nishi et al. [17], yield derivatives which are amenable to UV detection. Under alkaline conditions more than ten derivatized D,L-amino acids were resolved within 40 min using a sodium dodecyl sulfate (SDS) micellar separation buffer, i.e., separation by micellar electrokinetic chromatography (MEKC). *o*-Phthaldialdehyde (OPA) together with either N-acetylcysteine (NAC) or Boc-cysteine (BocC) was examined by Kang and Buck [18] as a chiral reagent for amino acids in CE. They demonstrated an MEKC separation of six derivatized D,L-amino acids within 30 min with an SDS micellar separation buffer at pH 9.5 containing 5.5% methanol and by using UV absorption detection at 340 nm. In addition, Houben et al. [19] examined OPA–NAC for the determination of the chiral purity of valine by MEKC with UV absorption detection.

In this study, micellar electrokinetic chromatography was examined for the separation of D- and L-amino acids precolumn-labelled with *o*-phthaldialdehyde/2,3,4,6-tetra-O-acetyl-1-thio-β-D-glucopyranose (OPA/TATG). TATG, which is a chiral thiol analogue of GITC, is an inexpensive, commercially readily available chemical which can be obtained in high optical purity. OPA/TATG was selected for this study partly because the derivatives formed with primary amino acids can be detected by UV absorption detection and by conventional and laser-induced fluorescence detection [20] and partly owing to our previous experience with this chiral reagent in LC [21]. In the course of optimizing the overall resolution of the amino acid derivatives in MEKC, separation parameters such as buffer pH, surfactant concentration and concentration of organic modifiers were varied. Our interest here was focused on the derivative retention window, i.e., the effective window available for the separation of labelled amino acids. It was observed that this window was affected in a slightly different way by added organic modifiers than was expected from the results of the MEKC retention window calculated in the traditional way from retention data for Sudan III and acetone. The utility of the MEKC method for the rapid screening of D- and L-amino acids in microchemical analytical work is briefly discussed.

2. Experimental

2.1. Apparatus

MEKC separations were performed using an automated CE instrument, a Model 2050 P/ACE System, from Beckman Instruments (Palo Alto, CA, USA), equipped with a UV absorption detector. Wavelength selection was made with exchangeable filters using a 254-nm filter during the general optimization of the separations and a 340-nm filter for selective detection of the OPA/TATG amino acid derivatives. Occasionally, a laboratory-built CE system was used together with a Shimadzu RF-535 LC fluorescence detector, modified for on-column detection with capillary columns. The excitation and emission wave-

lengths were 350 and 415 nm, respectively. A UG11 bandpass filter was attached to the slit on the excitation side to prevent unwanted stray light from reaching the capillary. Alignment of the capillary in the detector cell housing was made by flowing a 1 m*M* solution of salicylic acid in water–ethanol (95:5, v/v) while adjusting the capillary position to maximize the fluorescence signal.

A high-voltage power supply, Model 2462 (0–30 kV), from Bertan (Hicksville, NY, USA) was used to generate the high voltage over two platinum wire electrodes (Goodfellow Cambridge, Cambridge, UK), each positioned in separation buffer in the glass vials at the injection and detection end of the capillary, respectively. MEKC separations were carried out in both systems using untreated fused-silica capillaries of 50 μm I.D. and 192 μm O.D. from Polymicro Technologies (Phoenix, AZ, USA).

2.2. Chemicals and reagents

Acetonitrile and methanol of HPLC grade were obtained from Rathburn Chemicals (Walkerburn, UK). *o*-Phthaldialdehyde (OPA), 2,3,4,6-tetra-O-acetyl-1-thio-β-D-glucopyranose (TATG), D- and L-amino acids, sodium dodecyl sulfate (SDS), boric acid, anhydrous sodium tetraborate (borax) and sodium hydroxide were all purchased from Sigma (St. Louis, MO, USA). Deionized water was obtained from a Milli-Q system (Millipore, Bedford, MA, USA).

2.3. Procedures

In order to vary the pH of the borate buffers used in the separations, while holding the ionic strength constant, and vice versa, they were prepared according to Bates and Bower [22]. Appropriate volumes of stock solutions of 40 m*M* borax and 0.1 *M* NaOH were mixed and subsequently diluted with deionized water to yield the desired pH and ionic strength. For example, borate buffer of pH ca. 9.5 and ionic strength 40 m*M* was prepared by mixing 37.5 ml of the borate stock solution with 10.6 ml of the sodium hydroxide stock solution and diluting to 100 ml with deionized water. This gave a measured buffer pH value of 9.50–9.55 at ambient temperature, which corresponded to a variation in temperature of ca. ±3°C as calculated from the dependence of pH on temperature for the borax–NaOH buffer system [22]. Measured pH values are quoted for all experiments. The MEKC separation buffers were prepared by dissolving specified amounts of SDS in a small portion of the respective borate buffer. Subsequently, the selected organic modifier, acetonitrile or methanol, and thereafter the rest of the borate buffer were added to the solution to yield the specified concentrations. Finally, the separation buffers were mixed in an ultrasonic bath for 5 min prior to use.

New fused-silica capillaries were pretreated by flushing with 1 *M* NaOH for 10 min followed by rinsing with deionized water and finally with the separation buffer. Between each run in a consecutive series of samples, the capillary was rinsed with 0.1 *M* NaOH, deionized water and separation buffer for 1 min each. Moreover, before each analytical separation, the capillary was equilibrated with the separation buffer by electrokinetic pumping for 2 min.

Acetone and Sudan III were used as markers for the electroosmotic flow and the micellar flow, respectively. A standard solution of these markers (ca. 2% and ca. 18 μM, respectively) was prepared by adding 30 μl of a stock solution of Sudan III (ca. 900 μM) in acetone to 1.5 ml of the separation buffer. Standard solutions of D- and L-amino acids (pH ca. 7) were prepared from 2.5 m*M* stock solutions in 0.1 *M* HCl and neutralized with 0.1 *M* NaOH followed by dilution with deionized water. To make peak identification easier during the MEKC optimization, amino acids were grouped in four standards with 8–10 D- and L-amino acids in each. To control the precision during the measurements, D-methionine was used as a reference compound in each standard. The chiral OPA/TATG reagent solution was prepared by dissolving 8 mg of OPA and 44 mg of TATG in 1 ml of methanol. The borate buffer used for derivatization was prepared from 0.4 *M* boric acid and adjusted to pH 9.5 by adding ca. 1.2 ml of 10 *M* NaOH.

Derivatizations were carried out in a 1-ml glass reaction vial, from which the injection into the CE system was later made. A 75-μl volume of amino acid enantiomer standard solution (100 μM each of the selected D- and L-amino acids) was mixed with 15 μl of borate buffer and then 15 μl of the OPA/TATG reagent were added. The reaction was allowed to proceed for 6 min before the derivatized sample was injected. On the automated CE instrument, injections were made hydrodynamically. Using a separation capillary with a total length of 27 cm (19 cm to the detection window), the injection time on the instrument was set to 2 s (pressure ca. 0.5 p.s.i.). With the laboratory-built instrument, injections were made by gravity. The injection end of the capillary, when placed in the glass vial containing the sample, was elevated 6.5 cm above the level of the detection end of the capillary. An injection time of 30 s was used for a capillary with a total length of 80 cm (44 cm to the window).

3. Results and discussion

Separation of a complex mixture of the derivatives of the protein D- and L-amino acids in a single run where twice as many peaks must be resolved simultaneously, compared with achiral separations of amino acids, is not trivial. Although the exquisite separation power of CE has been elegantly demonstrated, e.g., in separations of biopolymers in gel-filled capillaries where up to 300–400 peaks have been resolved [23–25], there have been few studies on the separation of large sets of small molecules such as amino acids. However, this is not surprising when considering the limits to MEKC resolution, as can be derived from general CE theory. In MEKC the basic equation for resolution between two closely eluting solutes when similar retention factors are assumed, $k'_1 \approx k'_2$, is given by [26,27]

$$R_s = \frac{\sqrt{N}}{4} \cdot \frac{(\alpha - 1)}{\alpha} \cdot \frac{k'_2}{1 + k'_2} \cdot \frac{1 - (t_0/t_{MC})}{1 + (t_0/t_{MC})k'_1} \quad (1)$$

where t_0 is the retention time of the aqueous phase, t_{MC} the retention time of the micellar phase, N the plate number and α the selectivity factor. The retention factor, k', is given by

$$k' = \frac{(t_R - t_0)}{t_0[1 - (t_R/t_{MC})]} \quad (2)$$

where t_R is the retention time of the solute. It should be noted that Eq. 2 is valid only for neutral solutes. However, in most practical cases it can be used to calculate "effective" k' values also for ionized analytes [28], as has been done in this study. Assuming no change in separation efficiency and selectivity, Eq. 1 indicates that the resolution can be optimized by altering the retention factor and the elution range. This MEKC retention window (MRW) over which the analytes are distributed is given by the ratio

$$MRW = t_{MC}/t_0 \quad (3)$$

It should be noted, as pointed out by Rasmussen and McNair [29], that despite the high plate numbers commonly generated in MEKC, for example, 150 000 plates would only give a resolution comparable to conventional HPLC (16 000 plates at $k' = 10$). That comparison was based on the assumption that a similar selectivity is obtained in both systems. The peak capacity, n, i.e., the maximum number of peaks that can theoretically be resolved within the retention window, is given by [28,30]

$$n = 1 + \frac{\sqrt{N}}{4} \cdot \ln\left(\frac{t_{MC}}{t_0}\right) \quad (4)$$

Although the maximum number of peaks that can be resolved in an MEKC system with $N =$ 150 000 is thus well over 100, the peak capacity in practice is much lower, as in conventional HPLC. The best overall resolution that can be attained in MEKC in a separation of a large set of analytes is therefore, as in conventional HPLC, also strongly dependent on the separation selectivity. In addition, in MEKC how well the entire retention window can be utilized for resolving a given set of analytes is of equal importance. CE separations of complex mixtures of amino acid derivatives have recently been compiled by Skocir et al. [31]. Commonly 14–23 amino acid derivatives have been completely or

almost completely resolved within a time frame of 12.5–75 min. This should be compared with a set of the protein D- and L-amino acids, which requires the resolution of more than 30 peaks.

3.1. MEKC separation of OPA/TATG-amino acid enantiomers

The chiral OPA/TATG reagent reacts with amino acids in analogy with other OPA/thiol chiral and achiral reagents that are commonly employed for the precolumn derivatization of primary amines, particularly in LC [15]. The reaction, depicted in Fig. 1, is completed at alkaline pH within a few seconds for most amino acids with the exception of threonine [20]. A feature of the bulky thiol TATG is that the diastereomers formed are relatively stable, no derivative breakdown being observed after 1.5 h. Compared with amino acid derivatives formed with the common achiral reagent OPA/β-mercaptoethanol, the OPA/TATG–amino acid derivatives are more hydrophobic but still highly soluble in aqueous solutions. Further, in comparison with the other two chiral thiols examined so far together with OPA in capillary electrophoresis, NAC and BocC [18,19], TATG gives derivatives which are slightly more hydrophobic (results not shown).

In this study, the aim was to obtain simultaneously a good resolution of both the hydrophilic and hydrophobic OPA/TATG derivatives and to balance this goal with a reasonable total analysis time. The work was carried out mainly in the traditional way through optimization of one experimental parameter at a time. By varying the separation buffer pH, ionic strength, surfactant concentration and concentration of organic solvent, we tried, in each experiment, to spread the analytes evenly over as large a part of the separation window as possible. The degree of utilization of the retention window was judged visually when examining the electropherograms. In addition to the common measure of the MEKC retention window, t_{MC}/t_0 (MRW), in this study we also defined another measure for the purpose of describing the effective window available for separation of the OPA/TATG–amino acid derivatives. This derivative retention window (DRW) is given by by the ratio

$$DRW = t_L/t_F \quad (5)$$

where t_L and t_F denote the retention times for the last- and first-eluting derivatives, respectively. This is a measure which has hardly been discussed in connection with the optimization of the overall resolution in MEKC separations.

During the initial CE experiments, when no micellar system was used, only a few OPA/TATG–amino acid derivatives could be resolved in a single run at alkaline pH. When the anionic surfactant SDS was added to the separation buffer, to provide for hydrophobic interactions, the enlargement of the derivative retention window, DRW, available for separation of the derivatives was a factor of 2–2.5. During optimization, the SDS concentration was varied between 10 and 100 mM in seven steps using 40 mM borate buffer at pH 9.5. Over this concentration range the derivative effective retention factor, k', increased almost linearly. The correlation coefficient (r) for five selected amino aid derivatives, L-serine, D-alanine, L-isoleucine, D-methionine and L-arginine, ranged between 0.999 and 0.992. From the equation for the

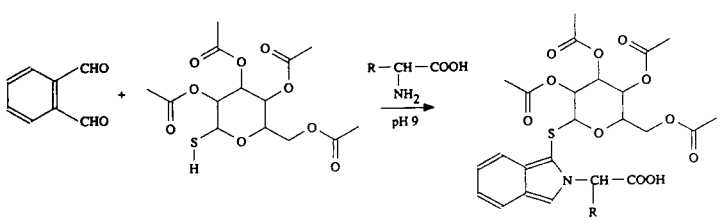

Fig. 1. Reaction of amino acids with the chiral OPA/TATG reagent.

linear dependence of k' on SDS concentration, the critical micelle concentration (*cmc*) can be estimated. In MEKC the retention factor at low micelle concentrations is related to the SDS concentration by [26,32]

$$k' = P_{MW}V([\text{surfactant}] - cmc) \quad (6)$$

where P_{MW} is the partition coefficient of the derivative into the micelles and V is the molar volume of the surfactant. The intercept on plotting k' vs. [SDS] gave a mean value for *cmc* of 2.1. As expected, this value is lower than the *cmc* of 8 m*M* for SDS in pure water (25°C) and agrees well with other *cmc* values reported for SDS in the presence of buffer [32–36]. The best overall resolution of the derivatives was obtained with an SDS concentration between 40 and 50 m*M*; the derivatives were then most evenly distributed over the entire MEKC retention window. At 45 m*M* SDS the values of the *MRW* and *DRW* were 3.66 and 2.97, respectively. The increase in *MRW* with increase in SDS concentration was paralleled by an increase in *DRW*, such that the two showed a constant ratio at all SDS concentrations examined. Although higher SDS concentrations gave some improvement in the resolution between the most hydrophilic derivatives, this could not be balanced by the achievement of a reasonable analysis time because of the drastic increase in retention time for the most hydrophobic derivatives at higher SDS concentrations.

3.2. Dependence of MEKC retention and resolution on pH and ionic strength

The effect of pH on derivative retention and resolution was investigated using a borate buffer with an ionic strength of 40 m*M* and an SDS concentration of 45 m*M*. Between pH 8.5 and 10 no major changes in the elution order of the derivatives were observed. This is what would be expected, considering that the amino acids have their primary amine function(s) derivatized with OPA/TATG, and in the MEKC separation predominantly behave as common weak organic acids, which at this alkaline pH are fully deprotonated. A point here regarding time optimization of the separation is that a higher buffer pH gave a small decrease in retention times without having any large effect on the overall resolution. This was due to a slightly higher electroosmotic flow at high pH, where both t_0 and t_{MC} are similarly affected, with a ca. 3% decrease between pH 9.3 and 10.0. It should be noted that this is mainly a pure pH effect, since the buffers were prepared to have a constant ionic strength while varying the pH. The matter of covariance of ionic strength with change in pH and its effect on the electroosmotic flow has been discussed in detail by Vindevogel and Sandra [36]. In contrast to that study, where the separation buffer concentration was given as its boric acid equivalent, our values of buffer ionic strength also take into account the sodium hydroxide concentration [22]. They observed a slight decrease in electroosmotic flow whereas we observed a slight increase. Moreover, in our study a slight decrease in *MRW* and *DRW* with increase in pH was observed and a pH of 9.5 was chosen as a compromise for further studies. In addition, this separation buffer pH is compatible with the amino acid sample, which after derivatization has a pH just above 9. The choice of pH may also be justified by a higher precision in retention times obtainable at high pH in MEKC, as has been reported by Skocir et al. [31].

The effect of ionic strength on resolution was investigated with a borate buffer of pH 9.5 containing 50 m*M* SDS. As with pH, varying the ionic strength (30–65 m*M* in four steps) did not give any major changes in the elution order of the derivatives. However, both the *MRW* and *DRW* increased with increasing ionic strength to give values of 4.63 and 3.68, respectively, for the 65 m*M* borate buffer. An important aspect in the choice of ionic strength is to have a sufficient buffer capacity in order not to induce excessive peak broadening. During optimization, the variation in plate number for a certain derivative was less than 20% within the respective pH and ionic strength ranges examined. Thus, our changes in buffer pH and ionic strength had only minor effects on separation efficiency. Another aspect of buffer ionic strength is to use as dilute a

separation buffer as possible, since high buffer concentrations gives high currents and accordingly may cause problems with Joule heating. This is particularly important in time optimization, when high voltages are desired to accelerate the separation. In addition, the buffer concentration should match the ionic strength of the injected derivatized sample.

3.3. Dependence of MEKC retention, resolution and selectivity on organic modifier

Addition of organic solvents as modifiers to the separation buffer was examined both for the purpose of widening the retention window and for fine tuning the separation selectivity. The effect of methanol and acetonitrile on the MEKC and derivative retention windows is shown in Fig. 2. An increase in organic solvent concentration from 0 to 12% gave an increase in *MRW* by factors of 2.0 and 2.8 for methanol and acetonitrile, respectively. Despite the difference in effect on *MRW* between the two solvents, it is noteworthy that the increase in size of the effective retention window for derivative separation (*DRW*) was similar, a factor of 1.8 for both methanol and acetonitrile. Hence, although the *MRW* value can be raised from just below 4 to above 10 by the addition of acetonitrile, the *DRW* is less affected (from 2.3 to 4.2). If we look in detail at the effect of organic modifier concentration between 0 and 12%, the decrease in electroosmotic flow is larger with methanol than with acetonitrile, a factor of 1.5 and 1.3, respectively. The electroosmotic flow is therefore slightly higher with acetonitrile than with methanol added to the buffer, a factor of 1.15. This is mainly due to a larger effect on the ζ-potential from methanol compared with acetonitrile [37] and emanates to a large extent from the change in the MEKC separation buffer viscosity and dielectric constant. In addition, the net velocity of the SDS micellar phase was less affected by methanol than by acetonitrile for the same reason. The viscosity increases with increasing concentration (0 to 12%) of organic solvent by factors of 1.35 and 1.12, respectively, for methanol and acetonitrile. It should be noted that the change in retention for the first-eluting derivative was in fact the same as the change in electroosmotic flow, a factor of 1.5 and 1.3 with methanol and acetonitrile, respectively. Thus, the change in retention with addition of organic modifier to the buffer for the most hydrophilic derivatives is due mainly to the change in electroosmotic flow. However, with increasing organic concentration the change in retention of the last-eluting derivatives to the retention of Sudan III is significantly larger with acetonitrile than with methanol, a factor of 1.5 and 1.1, respectively. Hence the most hydrophobic de-

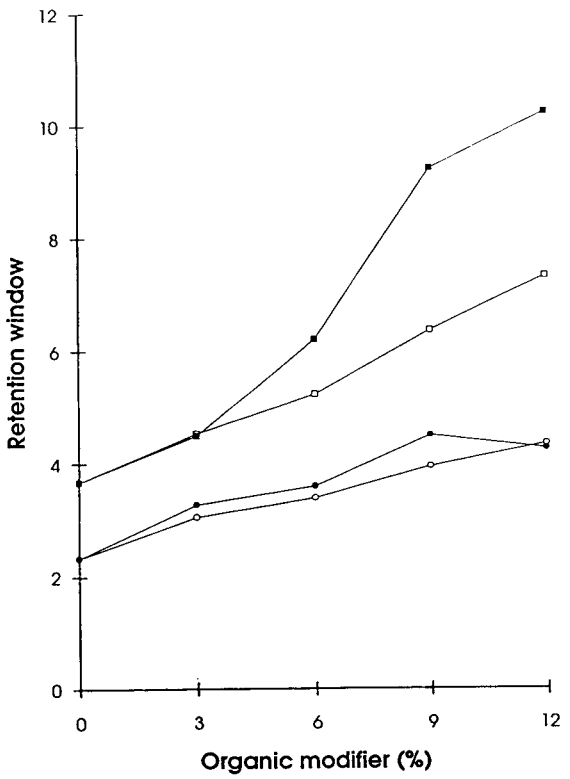

Fig. 2. Retention window dependence on concentration of organic modifier: effect of (□) methanol and (■) acetonitrile on MEKC retention window (t_{MC}/t_0) measured as the ratio of the migration time for Sudan III (t_{MC}) to the migration time for acetone (t_0) and effect of (○) methanol and (●) acetonitrile on OPA/TATG–amino acid derivative retention window (t_L/t_F) measured as the ratio of the migration time for the last-eluting derivative (t_L) to the migration time for the first-eluting derivative (t_F).

rivatives are more strongly retained in the aqueous phase than in the micellar phase with acetonitrile as organic modifier, indicating its higher solvent strength. This resembles the effect of organic modifier on the partitioning of the same OPA/TATG–amino acid derivatives between an aqueous mobile phase and a hydrophobic stationary phase in reversed-phase HPLC [20]. In conclusion, the combination of these two effects (change in electroosmotic flow and solute partitioning between the aqueous buffer–micellar phase) is therefore the likely explanation of why the effective window for derivative retention is actually no larger for acetonitrile than for methanol.

As expected, within the concentration range 0–12%, there was in the main a linear dependence of log k' on organic solvent concentration (negative slope). The correlation coefficient for the four selected amino acid derivatives, D-alanine, D-methionine, L-arginine and L-ornithine, ranged between 0.990 and 0.845 for methanol and between 0.991 and 0.831 for acetonitrile. In addition to the effect of the organic modifier on retention and resolution, there was also a significant increase in plate number with the addition of methanol or acetonitrile to the buffer. This effect was obtained in spite of the fact that the OPA/TATG–amino acid derivatives are highly soluble in aqueous eluents. The increase was most pronounced for late-eluting hydrophobic derivatives, with a ca. 50% higher plate number, but still significant for early-eluting hydrophilic derivatives with a 15–20% increase in N. Initially, tetrahydrofuran was also investigated as an organic modifier in the MEKC separation of the OPA/TATG–amino acid derivatives. In contrast to methanol and acetonitrile, there was no increase in separation efficiency with the use of tetrahydrofuran. Rather, a slightly lower plate number was observed, 80–90% of that obtained with the aqueous SDS buffer solely. This is not surprising considering that tetrahydrofuran has a much lower dielectric constant than acetonitrile and methanol ($\varepsilon = 7.6$, 37.5 and 32.7, respectively), and therefore in general has a lower ability to disperse electrostatic charges via ion–dipole interactions. No further experiments were conducted with tetrahydrofuran.

The effects of methanol and acetonitrile concentration on MEKC separation selectively for OPA/TATG–amino acid derivatives were examined and are shown in Figs. 3 and 4, where the retention is given as the relative retention which was obtained by normalizing the experimentally determined retention time with the retention time for the last-eluting derivative after correction for the time of the non-retained solute. In this way, a graphical overview is obtained of the relative position of the analytes within the effective retention window. Because of the large number of analytes, the data for each solvent are grouped in two separate figures. In general, methanol and acetonitrile gave similar overall elution patterns for the derivatives, although differences were obtained in selectivity on replacing one solvent with the other. In particular, addition of the organic solvents to the separation buffer has a larger effect on the relative retention for the hydrophobic than for the hydrophilic and acidic amino acid derivatives. Moreover, the effect of organic solvent added to the separation buffer on analyte retention is more similar for hydrophobic derivatives than for the hydrophilic derivatives when comparing methanol with acetonitrile. This is further illustrated in Fig. 5a and b by the results for the slope, k, for the OPA/TATG–D- and L-amino acids from a linear regression correlating log k' with organic modifier concentration. In the plots the derivatives have been classified in different groups based on the characteristics of the amino acid side-chain. Apart from the conformational difference between the derivatives of the respective amino acid D- and L-forms, the side-chain constitutes the structural difference between the analytes after derivatization of the primary amine function(s). The side-chain is therefore expected to play a major role in governing derivative retention.

The plots in Fig. 5 shows that with methanol as modifier there is a more coherent pattern than with acetonitrile. It is also shown, as discussed above, that acetonitrile has a larger effect on the distribution of the analytes between the micellar

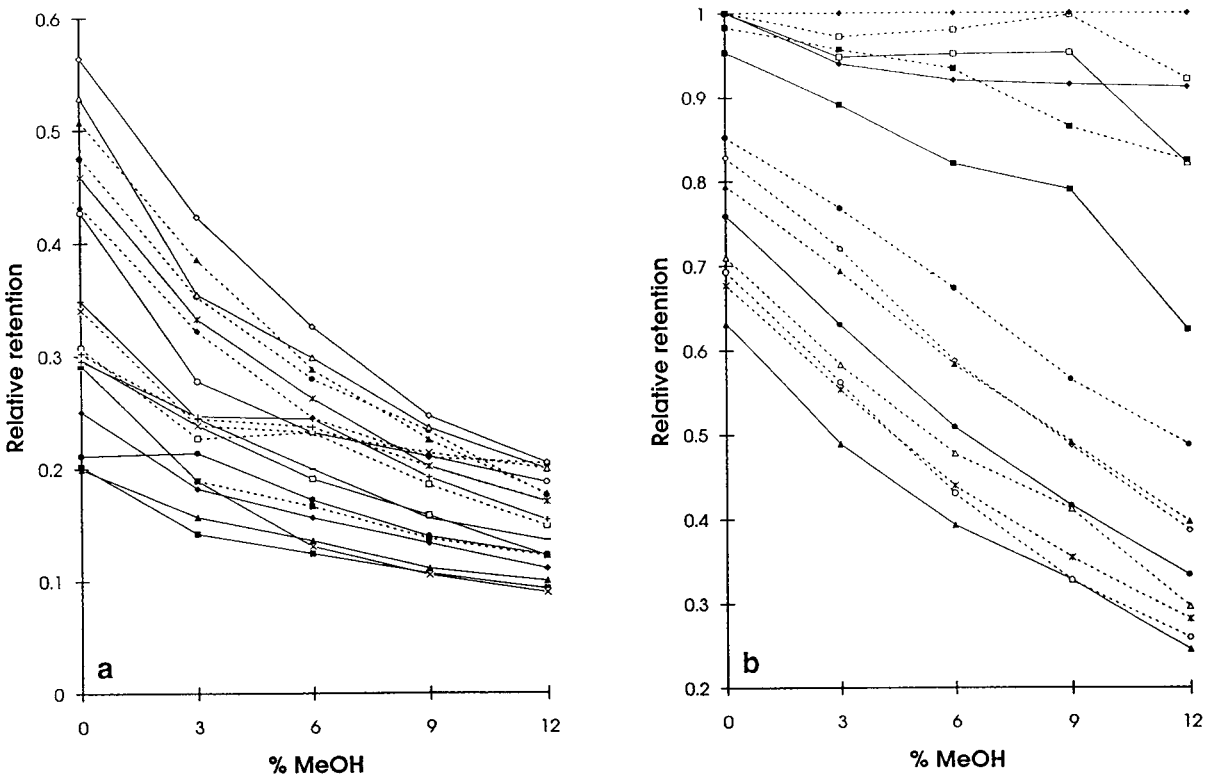

Fig. 3. Effect of methanol concentration on MEKC separation selectivity for OPA/TATG–D- and L-amino acid derivatives. Retention is given as a relative retention by normalizing experimental migration times to the migration time for the last-eluting derivative (t_L) and the electroosmotic flow as $(t_R - t_0)/(t_L - t_0)$. The data are grouped in two separate figures, (a) and (b), for illustration purpose only. The solid and dashed lines denotes the L- and D-form of amino acids, respectively. (a) ■ = Ser; □ = Glu; ◆ = Thr; X = His; ● = Ala; ○ = Trp; △ = Met; ▲ = Tyr; + = Asp; − = Gly; * = Val; ◇ = Phe. (b) ■ = Arg; □ = Orn; ◇ = Phe; ● = Leu; ◆ = Lys; ▲ = Ile; ○ = Trp; △ = Met; * = Val.

and the aqueous phases, particularly for the more hydrophobic derivatives. Considering that the separation buffer pH is well above the ionization constant for the basic amine of histidine (pK = 6.00 [38]), the variation in the slope within the group of basic amino acids is no larger than within the other groups of amino acid derivatives. When using acetonitrile as modifier, compared with methanol, the slightly larger spread in k values within most derivative groups emphasizes the greater effect of acetonitrile on the separation selectivity. In line with this is that more cross-overs in elution order were observed with acetonitrile than with methanol and that these changes were more frequent for the hydrophilic derivatives. This behaviour is in accordance with general observations for solute–micelle interactions in aqueous surfactant systems. Often solubilization of non-polar compounds can be considered as a simple partitioning between the micellar non-polar interior and the aqueous environment in the intermicellar solution, whereas polar compounds can participate in and influence the surfactant aggregation process [35,39]. Therefore, in spite of the fact that all micelles in the separation buffer are altered in the same way by a certain organic modifier, hydrophilic and hydrophobic OPA/TATG–amino acid derivatives may interact to different extents with the different parts of the micelles, thereby experiencing different chemical microenvironments during partitioning.

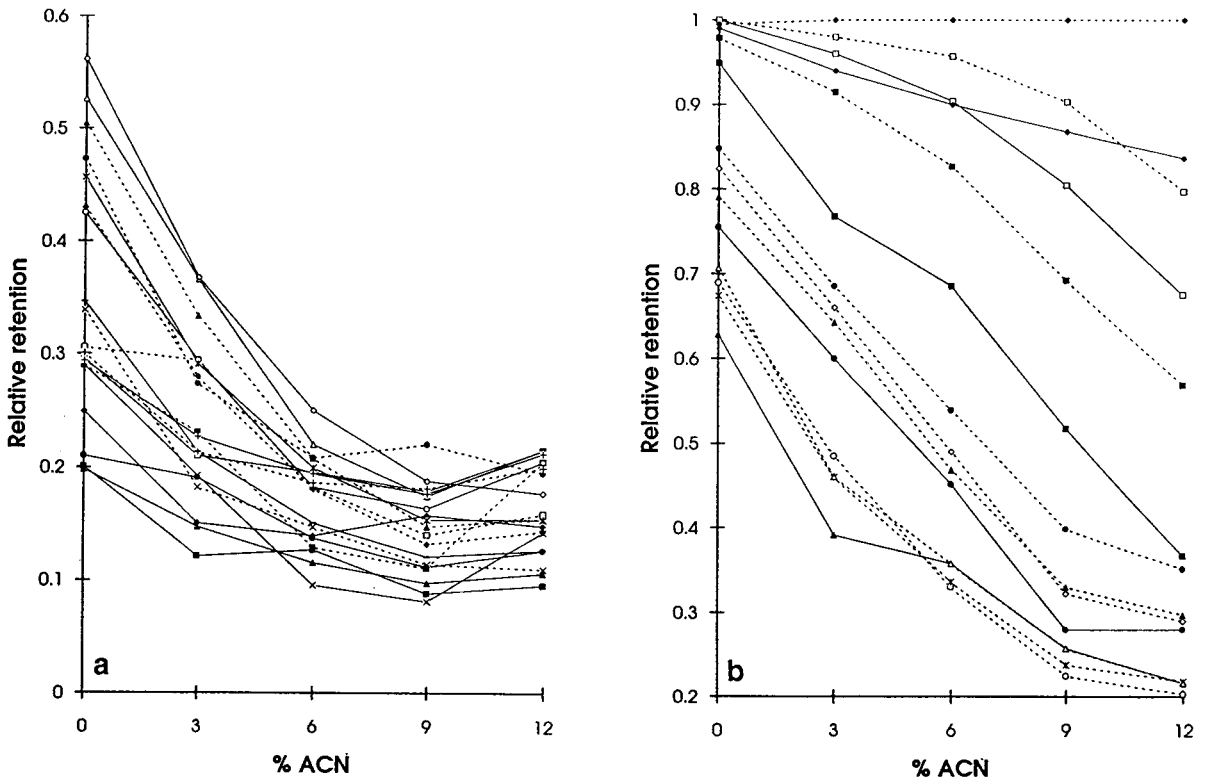

Fig. 4. Effect of acetonitrile concentration on MEKC separation selectivity for OPA/TATG-D- and L-amino acid derivatives. Retention is given as a relative retention by normalizing experimental migration times to the migration time for the last-eluting derivative (t_L) and the electroosmotic flow as $(t_R - t_0)/(t_L - t_0)$. The data are grouped in two separate figures, (a) and (b), for illustration purposes only. Symbols as in Fig. 3.

The changes in relative retention of a certain derivative, relative to the other derivatives, are more parallel for methanol than for acetonitrile. This is probably due to the fact that methanol is incorporated to a greater extent into the micellar structure in a lamellar configuration, in analogy with what has been reported for other alcohols in aqueous surfactant systems [35]. On the other hand, it is likely that acetonitrile to a larger extent modifies the surface of the micelles, in analogy with, e.g., octanenitrile in aqueous surfactant systems [35]. In addition, acetonitrile has a higher dielectric constant than methanol (see above) and therefore a greater ability to disperse the electrostatic charge of the anionic surfactant. Consequently, since polar compounds interact to a greater extent with the surface than with the interior of the micelles, it is likely that acetonitrile may induce more changes than methanol in the MEKC separation selectivity for the hydrophilic derivatives.

When optimizing the overall resolution in the separation of the OPA/TATG–amino acid derivatives, an organic solvent concentration in the range 3–6% was sufficient. The use of higher concentrations unfortunately tended to cluster the peaks at the beginning of the electropherogram, since almost all peaks exhibit a move towards the front in the derivative retention window. At this point it was of interest to examine whether an increase in surfactant concentration could be used as a means to improve the resolution further. However, at an acetonitrile concentration of 4% no significant increase in *DRW* (2.7 compared with 2.8) could be observed on increasing the SDS concentration

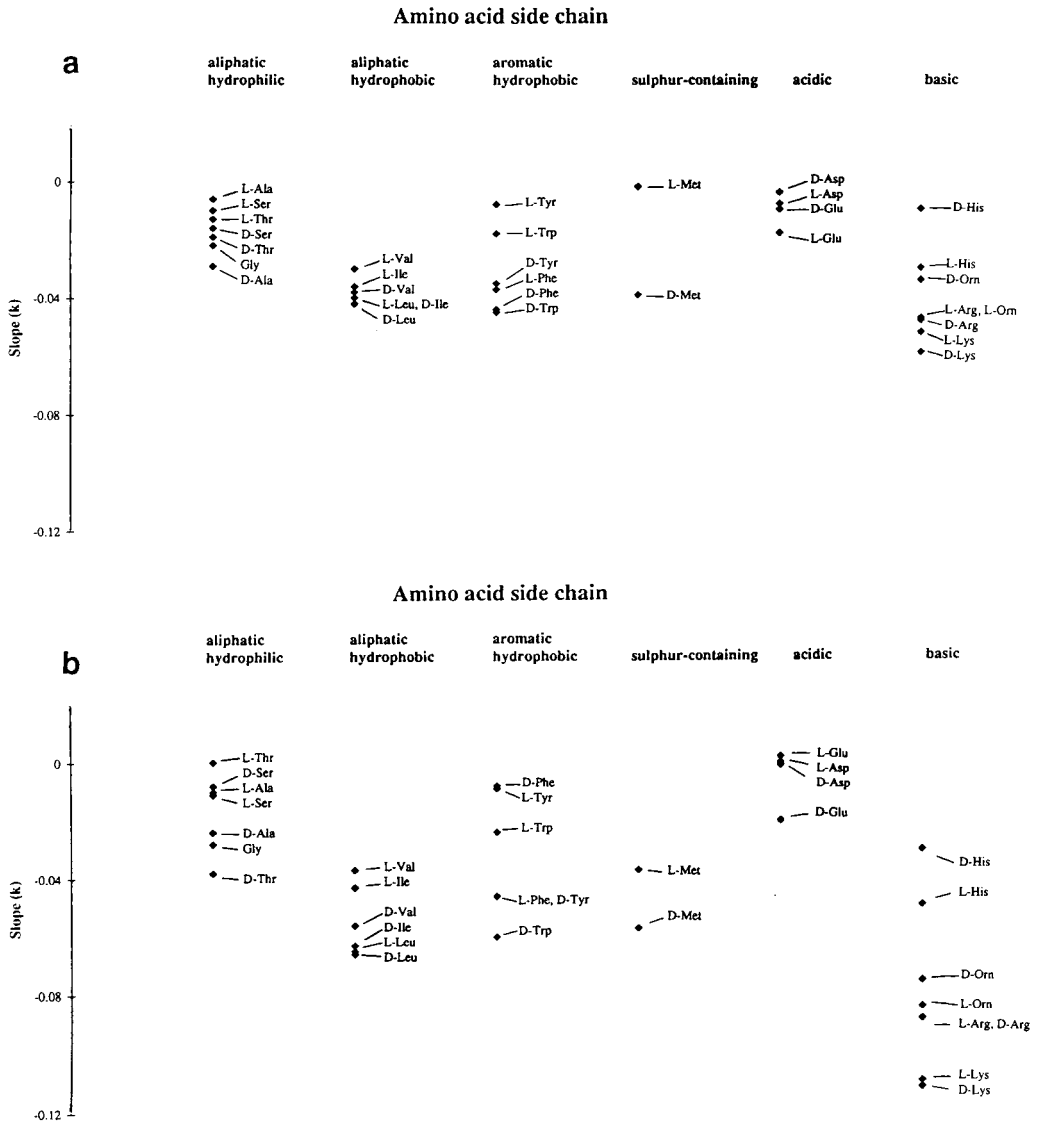

Fig. 5. Effect of organic modifier on OPA/TATG–amino acid derivative MEKC retention and selectivity. Plot of the slope k from linear regression of log k' vs. modifier concentration for data in Figs. 3 and 4. The derivatives are grouped based on the characteristics of their respective amino acid side chain. Data for (a) methanol and (b) acetonitrile.

from 45 to 55 mM. In fact, this change will only prolong the analysis time. Experimental data on the effective retention factor, k', selectivity factor, α, and resolution, R_s, for 14 OPA/TATG–D- and L-amino acid derivatives from an MEKC separation with 40 mM borate buffer (pH 9.5) containing 45 mM SDS and 4% acetonitrile are given in Table 1. The resolution of the derivatives of the D- and L-forms of a specific amino acid was generally very high (mean $R_s = 14.3$). This is predominantly a result of the high separation efficiency, mean plate number = 130 000, which corresponds to 680 000 plates/m. Notably, the value of the selectivity factor, α, was con-

Table 1
Experimental data on effective retention factor, selectivity and resolution for fourteen OPA/TATG–DL-amino acid derivatives as after MEKC separation

Amino acid	k'(L)	k'(D)	α	R_s
Ser	0.86	0.98	1.5	3.9
Thr	0.92	1.7	1.8	15
His	0.85	1.1	1.3	8.3
Trp	1.7	3.6	2.2	20
Tyr	0.92	1.7	1.9	18
Ala	0.98	1.7	1.7	12
Val	1.7	3.4	2.0	18
Ile	2.8	6.0	2.2	23
Phe	2.3	5.8	2.5	28
Leu	4.3	8.3	1.9	18
Met	1.9	3.4	1.8	17
Arg	14	37	2.6	12
Lys	47	410	8.6	6.8
Orn	82	98	1.2	0.79

Effective retention factor calculated from Eq. 2, selectivity factor $\alpha = k'_2/k'_1$ and resolution $R_s = 2(t_{R_2} - t_{R_1})/(w_{b_1} + w_{b_2})$. Conditions: Buffer, sodium borate buffer (pH 9.55, $I = 0.04$ M) containing 0.045 M SDS and 4% acetonitrile; untreated fused-silica capillary, 27 cm (19 cm to detector) $\times$ 50 μm I.D.; field strength, 405 V/cm (ca. 52 μA).

sistently slightly higher than that previously obtained in reversed-phase LC for the same derivatives and organic modifiers [20]. In addition, the same elution order between the amino acid L- and D-forms was obtained in the MEKC system as previously in HPLC, i.e., the L-amino acid derivative elutes before the D-amino acid derivative.

3.4. Time optimization

Several aspects must be considered in the course of time optimization in MEKC in order to arrive finally at a good compromise between overall resolution and analysis time. In addition to what has been discussed in previous sections, the length of the separation capillary is also an important parameter. As in conventional column chromatographic techniques, in MEKC the retention time for a solute, and consequently the analysis time, is a strong function of the capillary length ($t_R \propto L$), whereas resolution is a weak function ($R_s \propto \sqrt{N}$). The latter statement assumes that peak broadening is independent of capillary length and net velocity, which is not valid in general but, for the sake of giving guidelines in MEKC time optimization, can be used as an approximation. The influence of capillary length on both resolution and time optimization has hardly been discussed in the literature [40,41]. A practical limitation regarding capillary length is that most commercially available CE instruments only permit capillaries with a total length down to 25–30 cm. Another restriction may emanate from the detector electronics and timed control of hydrodynamic injection, which must be optimized for fast separations and the use of short separation capillaries. Moreover, the separation speed can be increased by the use of high voltages, but this will be limited by reaching too high a current, which causes problems with Joule heating deteriorating the performance. With the automated CE system used in this study, a 27-cm capillary could be mounted in the capillary cassette holder. The voltage was increased to give a field strength of 405 V/cm (ca. 52 μA), which is equal to a power per unit length of 2.1 W/m. This is close to the upper limit in terms of the heating effect reported by Sepaniak and Cole [42] for MEKC separations. An MEKC separation in less than 5 min of 34 D- and L-amino acids labelled with OPA/TATG is demonstrated in Fig. 6. Regarding the overall resolution of the amino acid derivatives, it is interesting to compare our results with the theoretical equations derived for MEKC optimization by Foley [41]. If no change in plate number and selectivity is assumed while optimizing the resolution at varying k', optimum resolution is obtained at

$$k'_{opt} = (t_{MC}/t_0)^{0.5} \quad (7)$$

Eq. 7 was derived for neutral solutes [41]. Although the retention factor of an acidic solute is the weighted average of the retention factor of its undissociated and dissociated forms, a separation buffer pH of 9.55 is well above the pK_a for the acidic derivatives. Hence, only minor effects of pH on retention for the majority of the derivatives are expected at this pH. This is also consistent with our findings, as discussed above. Therefore, Eq. 7 can be used to calculate an

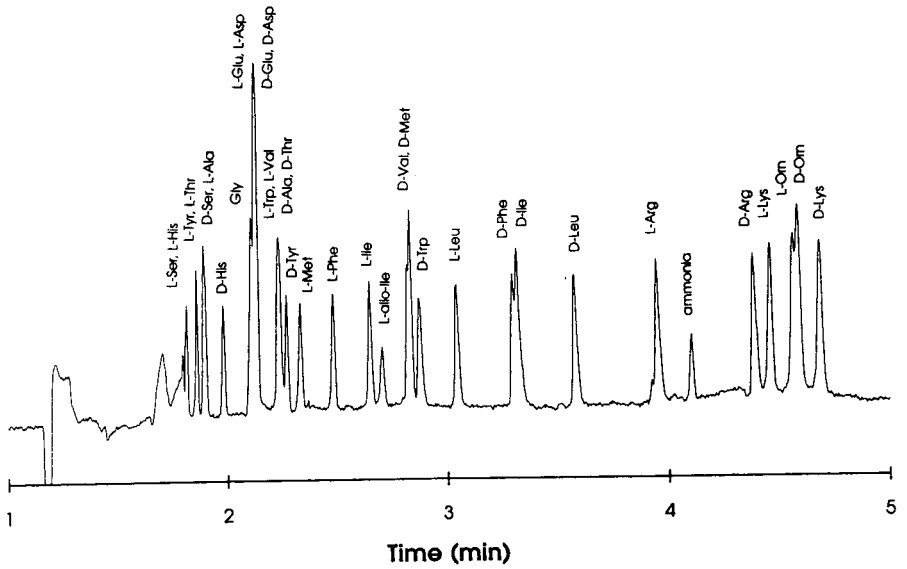

Fig. 6. MEKC separation of OPA/TATG–D,L-amino acid derivatives. Conditions: buffer, sodium borate buffer (pH 9.55, $I = 0.04$ M) containing 0.045 M SDS and 4% (v/v) acetonitrile; untreated fused-silica capillary, 27 cm (19 cm to detector) × 50 μm I.D.; field strength, 405 V/cm (ca. 52 μA); hydrodynamic injection (2 s at 0.5 p.s.i.); UV detection at 340 nm.

approximate theoretical value of the optimum retention factor for comparison with our experimental data. Calculating k'_{opt} for the separation in Fig. 6 gives a value of 1.99 for the retention factor where optimum resolution is obtained. In spite of the fact that the OPA/TATG–amino acid derivatives cover a wide k' range in that separation (0.85–410, see Table 1), it is interesting that the MEKC retention window is centred so that the derivative eluting in the middle has a k' between 3 and 5. Recalling that the k' scale is logarithmic if aligned with the t_R scale, our result for the experimental MEKC optimization of the retention of OPA/TATG–amino acid derivatives is in the vicinity of the theoretically predictable optimum.

3.5. Microchemical analysis

Although an in-depth evaluation of the utility of the present MEKC method for microchemical analysis is beyond the scope of this study, some results of interest for that purpose are given here. When using the automated CE system and UV detection, the mass limit of detection (MLOD) for the OPA/TATG–amino acid derivatives was similar for detection at 254 nm with detection at 340 nm. Injection of a 3.6-nl samples (257 fmol) of L-leucie, labelled with OPA/TATG, was detected after MEKC separation with a signal-to-noise ratio (S/N) of 23 and 20, respectively (noise measured peak-to-peak). Extrapolating to $S/N = 3$ gives MLODs of 33 and 38 fmol, respectively. This is equal to a concentration limit of detection (CLOD) of ca. 10 μM. When performing UV detection at the lower wavelength both the derivatives and also the excess of reagent, i.e., OPA, are detected. Fortunately, most of the peaks emanating from the reagent elute in front of the derivatives; however, some co-elution occurs between the reagent and the first-eluting derivatives, which is why detection at 340 nm should be used in quantitative and qualitative analytical applications. The MLOD when using the laboratory-built CE instrument with the modified HPLC fluoroscence detector was 64 fmol ($S/N = 3$), which is just above that obtained for UV detection with the automated CE system. Although the optical configuration of the HPLC fluorescence detector is not entirely perfect for on-capillary detection, fluorescence is more selective

than UV absorption for the detection of the OPA/TATG-labelled amino acids.

In addition, the method detection limit may be significantly improved if laser-induced fluorescence detection is utilized with excitation with either a helium–cadmium laser (325 nm) [20] or an argon ion laser (351–364 nm) [21]. In order to take full advantage of the present method for the rapid separation of labelled D- and L-amino acids, methods for rapid sample pretreatment should be available. For example, in studies of amino acid racemization in peptides and proteins, a rapid hydrolysis procedure is desirable. Regarding the chiral labelling of the amino acid enantiomers, the derivatization time needed should be minimized and, moreover, for the analysis of nanolitre sample volumes the derivatization reaction should preferably be carried out on-column in the separation capillary to avoid any sample dilution. Such studies are in progress [43].

4. Conclusions

Through optimization of one MEKC separation parameter a time we have obtained a method which permits the rapid screening of OPA/TATG-labelled D- and L-protein amino acids for use in microchemical analytical work. The method is versatile since the diastereomers formed can be detected by both UV and fluorescence detection, and laser-induced fluorescence detection may be employed if ultra-high sensitivity is required. An advantage with this chiral labelling is the very high resolution of the derivatives of the D- and L-form of each amino acid achieved. This high resolution is obtained simultaneously in a single run for all amino acids. This should be compared with the use of achiral labelling in combination with chiral additives in the separation buffer, e.g., cyclodextrins, which commonly gives good resolution only for a partial group of a large set of amino acids in a single MEKC run. It may be argued that a more dedicated method for MEKC optimization might have given the same result but saving experimental effort. Unfortunately, there is still a lack of a comprehensive theory of MEKC resolution quantitatively relating simultaneously efficiency, selectivity, capacity factor, retention window and analysis time and, moreover, which is applicable to both ionic and non-ionic solutes and can also take into account changes in analyte–micellar interactions when using organic modifiers. Dedicated strategies presented for MEKC separations [31,32,36,44,45] are commonly based on a global approach for optimization of resolution and the retention window, since several experimental parameters are interactive and cannot be optimized in isolation from each other. So far, however, such studies have usually only involved the simultaneous optimization of a limited number of the many experimental parameters of interest in MEKC: separation buffer pH, ionic strength, surfactant concentration, type of buffer, type of surfactant, surfactant counter ion, type and concentration of organic modifiers, voltage, temperature, capillary length, etc. Besides, before a global optimization can be successful, a number of initial experiments must be carried out to arrive at a preliminary system in order to permit proper judgements regarding the experimental design. However, optimization in the traditional way as carried out here is justified from the need to characterize the detailed behaviour of separation buffer modifiers on analyte retention and selectivity. This is essential to permit fine tuning of the separation conditions and is of particular importance when resolving complex mixtures such as large sets of amino acids. To the best of our knowledge, a separation of 34 D,L-amino acids in less than 5 min, with only a few peaks co-eluting, has not previously been demonstrated. For the purpose of gaining further insight into the MEKC separation selectivity, a multivariate analysis of the presented retention data, using various solute structural descriptors, will be the subject of a subsequent report.

Acknowledgements

This work was supported by the Swedish Natural Science Research Council, the Helge Ax:son Johnson Foundation, the Adlerbert Foundation, the Paul och Marie Berghaus

Foundation and the Elisabeth and K.G. Lennander Foundation. We acknowledge the California Separation Science Society for a student travel grant to Anna Tivesten which made possible the presentation of part of this work at the Sixth International Symposium on High Performance Capillary Electrophoresis (HPCE '94), San Diego, USA. Heléne Holgersson and Anna-Maija Alatalo are greatly thanked for help with the experimental work. We thank Jan Bergmark of Beckman Instruments (Sweden) for the loan of the P/ACE system and Liz Turner for linguistic help.

References

[1] M. Tanaka, S. Asano, M. Yoshinago, Y. Kawaguchi, T. Tetsumi and T. Shono, Fresenius' J. Anal. Chem., 339 (1991) 63–64.
[2] T. Ueda, R. Mitchell, F. Kitamura, T. Metcalf, T. Kuwana and A. Nakamoto, J. Chromatogr., 593 (1992) 265–274.
[3] S. Terabe, Y. Miyashita, Y. Ishihama and O. Shibata, J. Chromatogr., 636 (1993) 47–55.
[4] R. Kuhn, F. Stoecklin and F. Erni, Chromatographia, 33 (1992) 32–36.
[5] P. Gozel, E. Gassmann, H. Michelsen and R.N. Zare, Anal. Chem., 59 (1987) 44–49.
[6] K. Otsuka and S. Terabe, J. Chromatogr., 515 (1990) 221–226.
[7] A. Dobashi, T. Ono, S. Hara and J. Yamaguchi, J. Chromatogr., 480 (1989) 413–420.
[8] K. Otsuka and S. Terabe, Electrophoresis, 11 (1990) 982–984.
[9] K. Otsuka, J. Kawahara, K. Tatekawa and S. Terabe, J. Chromatogr., 559 (1991) 209–214.
[10] Y. Ishihami and S. Terabe, J. Liq. Chromatogr., 16 (1993) 933–944.
[11] S. Terabe, M. Shibata and Y. Miyashita, J. Chromatogr., 480 (1989) 403–411.
[12] S. Mayer and V. Shurig, J. High Resolut. Chromatogr., 15 (1992) 129–131.
[13] D.W. Armstrong, Y. Tang, T. Ward and M. Nichols, Anal. Chem., 65 (1993) 1114–1117.
[14] S. Terabe, K. Otsuka and H. Nishi, J. Chromatogr. A, 666 (1994) 295–319.
[15] K. Blau and J. Halket, Handbook of Derivatives for Chromatography, Wiley, Chichester, 2nd ed., 1993.
[16] A.D. Tran, T. Blanc and E.J. Leopold, J. Chromatogr., 516 (1990) 241–249.
[17] H. Nishi, T. Fukuyama and M. Matsuo, J. Microcol. Sep., 2 (1990) 234–240.
[18] L. Kang and R.H. Buck, Amino Acids, 2 (1992) 103–109.
[19] R.J.H. Houben, H. Gielen and Sj. van der Wal, J. Chromatogr., 634 (1993) 317–322.
[20] S. Einarsson, S. Folestad and B. Josefsson, J. Liq. Chromatogr., 10 (1987) 1589–1601.
[21] A. Tivesten, M.-L. Johanson and S. Folestad, in preparation.
[22] R.G. Bates and V.E. Bower, Anal. Chem., 28 (1956) 1322–1324.
[23] A.S. Cohen, D.R. Najarian and B.L. Karger, J. Chromatogr., 516 (1990) 49–60.
[24] D.Y. Chen, H.P. Swedlow, H.R. Harke, J.Z. Zhang and N.J. Dovichi, J. Chromatogr., 559 (1991) 237–246.
[25] H.-F. Yin, J.A. Lux and G. Shomburg, J. High Resolut. Chromatogr., 13 (1990) 624–627.
[26] S. Terabe, K. Otsuka, K. Ichikawa, A. Tsuichiya and T. Ando, Anal. Chem., 56 (1984) 111–113.
[27] S. Terabe, K. Otsuka and T. Ando, Anal. Chem., 57 (1985) 834–841.
[28] J.H. Knox, J. Chromatogr. A., 680 (1994) 3–13.
[29] H.T. Rasmussen and H.M. McNair, J. Chromatogr., 516 (1990) 223–231.
[30] J.C. Giddings, Anal. Chem., 39 (1967) 1027–1028.
[31] E. Skocir, J. Vindevogel and P. Sandra, Chromatographia, 39 (1994) 7–10.
[32] M.G. Khaledi, S.C. Smith and J.K. Strasters, Anal. Chem., 63 (1991) 1820–1830.
[33] G.L. McIntiere, CRC Crit. Rev. Anal. Chem., 21 (1990) 257–278.
[34] L.J. Cline Love, J.G. Habarta and J.G. Dorsey, Anal. Chem., 56 (1984) 1132A–1148A.
[35] B. Lindman and H. Wennerström, Top. Curr. Chem., 87 (1980) 24–26 and 57–58.
[36] J. Vindevogel and P. Sandra, Anal. Chem., 63 (1991) 1530–1536.
[37] J. Gorse, A.T. Balchunas, D.F. Swaile and M.J. Sepaniak, J. High Resolut. Chromatogr. 11 (1988) 554–559.
[38] D.R. Lide (Editor), CRC Hanbook of Chemistry and Physics, CRC Press, Boca Raton, FL, 1991, p. 7-1.
[39] W.L. Hinze and D.W. Armstrong, Ordered Media in Chemical Separations (ACS Symposoum Series, No. 342), American Chemical Society, Washington, DC, 1987, pp. 15–17.
[40] H.T. Rasmussen, L.K. Goebel and H.M. McNair, J. High Resolut. Chromatogr., 14 (1991) 25–28.
[41] J.P. Foley, Anal. Chem., 62 (1990) 1302–1308.
[42] M.J. Sepaniak and R.O. Cole, Anal. Chem., 59 (1987) 472–476.
[43] A. Tivesten, E. Örnskov and S. Folestad, in preparation.
[44] Y.F. Yik and S.F.Y. Li, Chromatgraphia, 35 (1993) 560–566.
[45] M. Castagnola, D.V. Rossetti, L. Cassiano, R. Rabino, G. Nocca and G. Giardina, J. Chromatogr., 638 (1993) 327–334.

ELSEVIER

Journal of Chromatography A, 708 (1995) 339–350

JOURNAL OF CHROMATOGRAPHY A

Capillary zone electrophoretic determination of C_2–C_{18} linear saturated free fatty acids with indirect absorbance detection

R. Roldan-Assad[a], P. Gareil[b,*]

[a] *Laboratoire de Chimie Analytique (URA CNRS 437), Ecole Supérieure de Physique et Chimie Industrielles de La Ville de Paris, 10 Rue Vauquelin, 75231 Paris cedex 05, France*

[b] *Laboratoire d'Electrochimie et de Chimie Analytique (URA CNRS 216), Ecole Nationale Supérieure de Chimie de Paris, 11 Rue Pierre et Marie Curie, 75231 Paris cedex 05, France*

First received 18 January 1995; revised manuscript received 15 March 1995; accepted 27 March 1995

Abstract

The potential of capillary zone electrophoresis for the separation of linear saturated fatty acids in their free form was evaluated. With increasing chain length, difficulties arise from decreasing analyte solubility in aqueous media, increasing occurrence of analyte aggregation and decreasing separation selectivity between successive homologues. A solution was to use electrolytes containing cyclodextrins (CDs) and methanol. The separation of C_2–C_{14} fatty acid homologues differing in only one carbon atom was achieved in less than 10 min using a purely aqueous electrolyte with trimethyl-β-CD as an additive. The separation of C_7–C_{18} homologues was completed in under 20 min with electrolytes containing up to 60% methanol, in addition to the aforementioned CD. In the presence of the CD, analyte solubility is enhanced through the inclusion of the alkyl chain of the acid in the CD cavity, while separation selectivity is improved because the stability constants of the inclusion complexes increase with increasing chain length of the acid. The lack of a suitable chromophore moiety was circumvented through the optimization of indirect absorbance detection conditions. *p*-Anisate was selected as the chromogenic species. The minimum detectable concentrations are of the order of $(1–2)\cdot 10^{-6}$ mol l^{-1} (0.2–0.5 ppm) and detection linearity was established over at least three orders of magnitude of concentration. The quantitative analysis of a coco oil extract sample is presented, showing results almost identical with those obtained by gas chromatography. Owing to the close values for response factors resulting from the indirect detection principles, a rapid percentage composition can be obtained by corrected peak area normalization.

1. Introduction

During the last decade, the development of capillary electrophoresis (CE) and related electrokinetic techniques has led to interest in widely varying fields of applications involving separations of ionic and non-ionic, polar or apolar, small or large (macro-) molecules. Especially the potential of these techniques for the analysis of ionic surfactant mixtures has recently been addressed and very promising results have emerged for linear alkylsulphonates [1] and alkylsulphates [2], linear and branched alkylbenzenesulphonates [3], and alkyl- and alkylbenzyl quaternary ammonium compounds [4].

Free fatty acids (FFA) constitute an important class of naturally occurring compounds of wide origin which are met as complex mixtures in

* Corresponding author.

0021-9673/95/$09.50
SSDI 0021-9673(95)00390-8

animals, plants and even fossil fuels. They differ by their chain length and branching, degree of unsaturation and position and configuration of their double bonds. Some of these natural sources are used as raw materials for the industrial synthesis of various surfactants. There is therefore a stringent demand for their determination in various matrices. However, the separation methods employed often involve a preliminary derivatization step. In the most popular method, gas chromatography (GC) with flame ionization detection, methyl or silyl esters are formed to enhance the analyte volatility prior to introduction on to capillary columns [5–9]. More recently, liquid chromatographic (LC) methods in reversed-phase [5,10–18] or ion-pair modes [19] have also appeared, but the lack of a strongly absorbing chromophore generally precludes the direct use of spectrophotometric detection. Many precolumn derivatization reagents have therefore been proposed to induce sensitivities of more practical interest for absorbance [11,13,15] or fluorescence detection [5,12,14–17]. The determination of amide FFA derivatives by liquid chromatography–mass spectrometry has also been reported [20].

However, a much smaller number of methods that permit the direct determination of FFA in their original form entails the use of specifically designed stationary phases in GC [21,22], nonpolar packed [23,24] or open-tubular capillary columns [25] in supercritical fluid chromatography (SFC) and of refractive index [18], conductivity [19] or low-wavelength UV detection [10] in LC. In addition to the form in which FFA are actually separated, these methods provide slightly different selectivities, viz., for unsaturated species, as a result of their different retention mechanisms. Nevertheless, for compounds having surfactant properties, any technique involving the use of a solid stationary phase is likely to induce undesirable adsorption phenomena. This is why CE techniques performed in free solutions should also be of interest. The first attempts were achieved in capillary isotachophoresis (CITP) and successfully applied to the determination of short-chain ($<C_8$) FFA in formation waters [26] and of C_1–C_{18} linear FFA in hydrocarbonaceous matrices [27]. Additional benefits lie in the fact that no sample pretreatment is generally required and that conductivity is a fairly sensitive mode of detection in CITP owing to the absence of any background electrolyte in the analyte zone. More attractive approaches are those of capillary zone electrophoresis (CZE) or micellar electrokinetic chromatography (MEKC) which bring about more operational flexibility in addition to their high resolving power. So far, CZE and MEKC separations of FFA have only been reported for chain lengths of $<C_7$ [1,28–31]. The methods described differ in the speed and direction of the electroosmotic flow carrying the analytes simultaneously to electromigration, the use of ionic micelles [31] and in the detection modes, conductivity [28,29] or indirect absorbance [1,30,31].

The purpose of this work was to investigate the separability of long-chain linear saturated FFA by CZE and to assess their detection sensitivity by indirect absorbance. As the chain length of FFA increases, several analytical difficulties arise with such separations owing to the lower and lower analyte solubilities, micelle formation in the separation electrolyte and decreasing separation selectivity between the consecutive homologues. These problems were solved for chain lengths up to C_{18} by optimizing the composition of electrolytes containing methanol and a derivatized cyclodextrin (CD). The conditions for indirect absorbance detection were also studied with regard to linearity and limit of detection. The quantitative aspects are illustrated with the determination of FFA in a coco oil extract sample.

2. Experimental

Experiments were performed with a Perkin-Elmer/Applied Biosystems (ABI, Foster City, CA, USA) Model 270A capillary electrophoresis instrument, equipped with a variable-wavelength absorbance detector. Fused-silica capillaries of 50 μm I.D. from ABI were used in all experiments. The detection window was located 22 cm from the capillary outlet. Samples were intro-

duced in the hydrostatic injection mode using the vacuum depression line of 16.9 kPa on the outlet side of the capillary provided with the instrument. Detector signals were recorded and processed with a Thermo Separation Products/Spectra-Physics Model 4400 integrator (Spectra-Physics, San Jose, CA, USA). The choice of capillary length and the settings for temperature, injection time, separation voltage and detection wavelength are specified according to the sample in the course of the discussion and in the figure captions.

Most of the chemicals used for the electrolytes and the standard samples were of analytical-reagent grade from Aldrich (Milwaukee, WI, USA) or Sigma (St. Louis, MO, USA). Tris–anisate electrolytes were prepared by partially neutralizing Tris base with *p*-anisic acid (both from Aldrich) to the desired pH. The cyclodextrins were gifts from Wacker Chemie (Munich, Germany), except trimethyl-β-CD, which was purchased from Sigma. The sample of coco oil extract was of commercial origin. Water used throughout was of Milli-Q quality (Millipore, Milford, MA, USA).

New capillaries were conditioned by flushing successively with 1 mol l^{-1} sodium hydroxide for 10 min, water for 5 min, 0.5 mol l^{-1} sodium chloride, 6 mmol l^{-1} sodium hydroxide solution for 10 min, water for 5 min and finally with the operating electrolyte for 10 min. With the ABI instrument used, three capillary volumes are displaced in 5 min. Between runs, the capillaries were rinsed with the operating electrolyte for 5 min.

3. Results and discussion

3.1. Overall separation strategy

The first papers dealing with the CZE separation of carboxylic acid homologues suggested conditions that were simply adapted from those derived for UV-transparent small inorganic or organic anions. These conditions generally involved the use of a cationic surfactant to reverse the electroosmotic flow and hence shorten the analysis time [1,28,29], but this configuration was detrimental to resolution for anionic species. In fact, reversal of the natural cathodic electroosmotic flow is mainly suitable for analytes having their effective mobility in excess, or of the order of the electroosmotic mobility, which is not the case for long-chain FFA. Cathodic electroosmotic flow has already been used by Ackermans et al. [30] for C_1–C_7 FFA and by Nielen [2] for C_2–C_{12} alkylsulphates. Under such conditions, FFA are detected in order of decreasing chain length, i.e., in the reversed order of GC and LC methods, which could be of practical relevance. MEKC was also assessed for the separation of C_4–C_7 FFA using mixed dodecylsulphate–dodecylbenzenesulphonate micelles for indirect absorbance detection [31]. Although a correct resolution was achieved, this approach did not provide satisfactory signal stability and sensitivity. This investigation was therefore concentrated on counter-electroosmotic flow CZE.

As far as detection is concerned, promising results were reported by Huang and co-workers [28,29] with on-column conductivity measurement, but so far this mode has not been easily accessible using commercial instrumentation. In this work, the capability of low-wavelength UV detection was first tested for C_7, C_8 and C_9 FFA with bicine (pH 8.3) and glycine (pH 8.8) buffers at 210 and 200 nm, respectively. However, negative peaks were obtained, indicating that the buffer species absorbed more than the analytes. With a still more transparent buffer such as phosphate–borate (pH 8.9), positive peaks were observed at 200 nm but the sensitivity was poor. Indirect absorbance detection, as already implemented for C_1–C_7 FFA using a chromogenic species (benzoate) in the electrolyte [1,30], was selected for further optimization.

Another relevant parameter is pH. As linear FFA homologues have almost identical acid–base pK values [32], their separation cannot be based on differences in effective charges. Full ionization of the analytes should rather be sought for separation according to absolute mobilities. A pH range of 8–11 was therefore selected, which also increases the cathodic electroosmotic flow and the solubility of long-chain

FFA. Nevertheless, beyond a certain chain length that needed to be determined, the achievement of a sufficient analyte solubility and the suppression of analyte aggregation require the use of an organic solvent or a specific additive in the electrolyte. Tetrahydrofuran (THF), acetonitrile and methanol were chosen for evaluation. Preliminary solubilization assays in water were also conducted for octadecanoic acid with additives such as sodium dodecyl sulphate, urea, sodium deoxycholate and dimethyl-β-CD. None of these additives succeeded in solubilizing octadecanoic acid at a $2 \cdot 10^{-4}$ mol l^{-1} concentration, even in basic medium, except the cyclodextrin (CD). This last behaviour suggested the inclusion of the long chain of the acid in the CD cavity. Further assays were subsequently undertaken with other CDs to optimize this effect.

The last aspect to consider is that homologues become increasingly difficult to separate as their chain length increases. As will be shown below, the formation of an inclusion complex between fatty acids and CDs turned out to play a key role in the separation of long-chain FFA, as it allows a selective adjustment of their effective mobility.

3.2. Indirect absorbance detection conditions

For optimized indirect absorbance detection of FFA, the chromophore should preferably bear a negative charge and have a high molar absorptivity for high sensitivity, and its effective mobility must be close to that of the analytes to reduce electromigration dispersion. The separation electrolyte should not contain any other negatively charged species than the chromophore and its total absorbance should not exceed the upper limit of linear range of Beer's law, for a linear detector response. These conditions also dictate the choice of a cationic buffer pH. The chromogenic species tested are given in Table 1 with the resulting conclusions. Of all the species, *p*-anisate gave the most satisfactory baseline stability, peak symmetry and sensitivity and was therefore selected for further investigation. The choice of *p*-anisate concentration and detection wavelength were made with regard to electrolyte absorbance and conductivity. Fig. 1 shows a Beer's law plot obtained by filling the whole capillary with electrolytes of various *p*-anisate concentrations and measuring the resulting absorbance using the ABI detector. Absorbance appears to be linearly related to *p*-anisate concentration within the range 0–0.11 absorbance, which is in agreement with results previously reported for similar detector and cell geometries [34]. In addition, the spectrum of *p*-anisate in a basic methanol–water (50:50, v/v) medium presents a maximum for a wavelength of ca. 245 nm. At this wavelength, the maximum *p*-anisate concentration permitted for an electrolyte absorbance of 0.11 is only 3 mmol l^{-1}, which was too low to ensure adequate sample capacity and conductivity. The *p*-anisate concentration and the wavelength were then fixed at 10 mmol l^{-1}

Table 1
List of chromophores studied for indirect absorbance detection

Chromophore	Concentration (mmol l^{-1})	Absolute mobility at 25°C [33] (10^{-5} cm^2 V^{-1} s^{-1})	Detection wavelength (nm)	Remarks
Naphthoate	10		254	Insufficient purity, baseline instability
2-Naphthalenesulfonate	10	31.3	254	Low water solubility
2,3-Dihydroxybenzoate	10	33.0	254	Baseline instability
Picrate	10	31.5	300	Baseline instability
Benzoate	40	33.6	254	Low sensitivity
Chromate	5	81.1	254	Fronting peaks
p-Anisate	10	30.0	270	Adequate baseline stability and sensitivity

Tris electrolyte (pH 8.2) in THF–water (30:70, v/v). Test mixture: linear C_7–C_9 FFA.

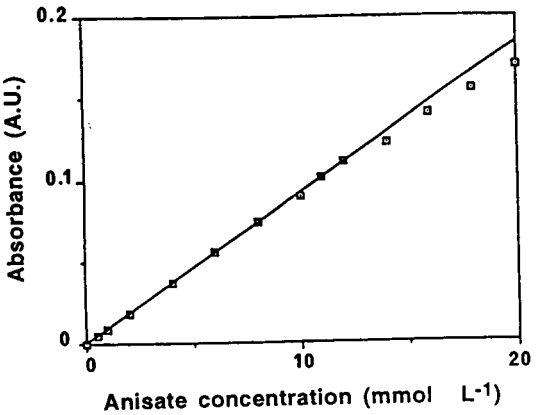

Fig. 1. Plot of absorbance versus *p*-anisate concentration. Optical cell, 50 μm I.D.; 320 μm O.D. fused-silica capillary. Tris–*p*-anisate buffer (pH 8.1) in methanol–water (50:50, v/v). Wavelength, 270 nm.

and 270 nm, respectively. It was also ascertained that, even if the electrolyte absorbance is kept near to the upper limit of the Beer's law linear range, doubling the *p*-anisate concentration to 20 mmol l^{-1} while shifting the wavelength to 275 nm resulted, as expected, in a decrease in sensitivity. No other anionic species should be introduced in the electrolyte other than the *p*-anisate chromophore. Hence setting the *p*-anisate concentration also sets the electrolyte ionic strength. Several cationic buffering species were successively tried in the pH range 8–11 in methanol–water (50:50, v/v): Tris (pH 8.1), Ammediol (pH 8.8), ethanolamine (pH 9.5) and cyclohexylamine (pH 10.8). Of these, Tris was selected for further optimization, as it produced the highest baseline stability. The separation of a C_2–C_{14} linear FFA standard mixture obtained with a purely aqueous electrolyte is shown in Fig. 2a. The electropherogram illustrates the progressive loss of resolution for homologues differing by only one carbon atom as the chain length increases, especially in the range of the C_{10}–C_{14} FFA. A marked decrease in peak height also occurs for C_{13} and C_{14} acids, indicating either incomplete solubilization or aggregate formation.

3.3. Sample solubility and selectivity

The achievement of adequate solubility, aggregate breaking and selectivity of long-chain FFA required the use of some organic solvents and/or specific additives. However, the organic solvent content in the electrolyte should be kept low, as an increase in solvent content results in a decrease in electroosmotic mobility, which in turn drastically affects the migration times of anions. Among the solvents tested, THF produced the

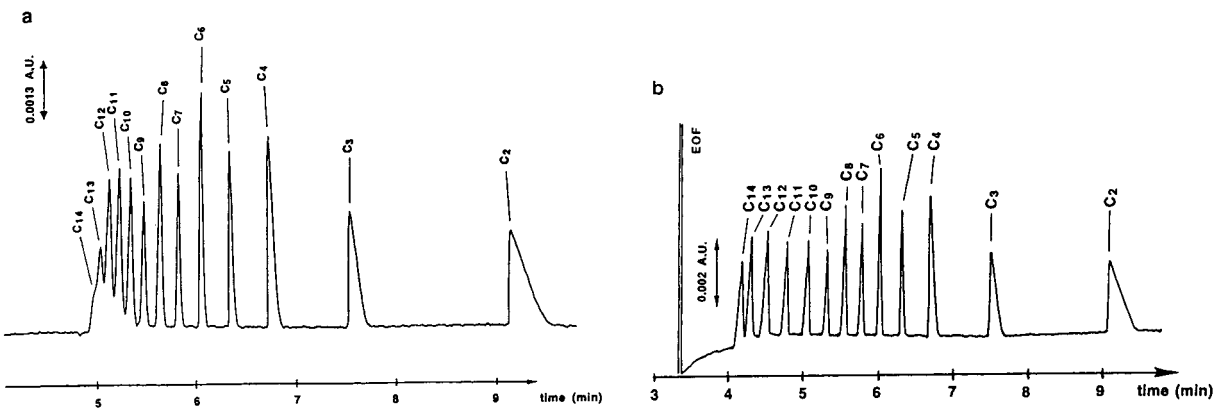

Fig. 2. Effect of addition of a β-CD derivative on the separation of C_2–C_{14} linear FFA standard mixture (0.5 mmol l^{-1} each in methanol) in a purely aqueous electrolyte. Fused-silica capillary, 50 μm I.D. × 72 cm (50 cm to detector). Electrotyte, 20 mmol l^{-1} Tris–10 mmol l^{-1} *p*-anisate (pH 8.2): (a) without any additive; (b) with 0.75 mmol l^{-1} trimethyl-β-CD added. Applied voltage, 30 kV ($I = 3$ μA). Temperature, 30°C. Indirect absorbance detection at 270 nm. Hydrodynamic injection for 1 s. EOF = electroosmotic flow.

highest solubilizing power, but a very noisy baseline in the region of anions, even if an unstabilized quality of THF (i.e. free from di-*tert.*-butyl-*p*-cresol) was employed. Acetonitrile was the least detrimental to electroosmotic flow, but solubility was impaired with respect to THF. Finally, methanol led to the best compromise for the most critical FFA in the study, i.e. the C_{14}–C_{18} FFA. Resolution between homologues increased with increasing methanol percentage at the expense of the total analysis time, which became prohibitively long beyond a content of ca. 60%.

In order to minimize the proportion of methanol, the positive effect of CDs was next investigated more deeply. A series of 20 mmol l^{-1} Tris–10 mmol l^{-1} *p*-anisate buffers (pH 8.2) in methanol–water (50:50, v/v) containing 1 mmol l^{-1} of various CDs were examined for solubility and resolution of the C_{16}–C_{18} FFA pair. The CDs tested were the natural α-, β- and γ-CD and the following derivatized CDs: dimethyl-β-CD (degree of substitution, *DS*, 1.8), trimethyl-β-CD (*DS* 3.0), hydroxyethyl-β-CD (*DS* 1.0), hydroxypropyl-β-CD (*DS* 0.9), hydroxypropyl-α-CD (*DS* 0.6) and hydroxypropyl-γ-CD (*DS* 0.6). The best results were obtained with dimethyl- and especially with trimethyl-β-CD. On increasing the CD concentration, the peak shapes improved continuously, whereas the resolution passed through a maximum for a concentration of the order of 1 mmol l^{-1}. Fig. 2b highlights the improvement in resolution of linear C_{10}–C_{14} FFA achieved when the aqueous electrolyte was supplemented with 0.75 mmol l^{-1} trimethyl-β-CD [35]. It must be emphasized that up to that chain length no organic solvent at all was needed and the electroosmotic mobility is about $60 \cdot 10^{-5}$ cm^2 V^{-1} s^{-1}. The formation of an inclusion complex between FFA and CD causes the effective mobility of the analyte to decrease with increase in CD concentration, as shown in Fig. 3, and this phenomenon becomes more pronounced as the complex stability increases. In fact, using a method described previously [36], the stability constants can easily be derived from the determination of the inflection point on the curves represented in Fig. 3. Table 2 shows that, as expected, the stability of the inclusion complexes increases with increasing hydrophobicity of the guest compounds, i.e., with increasing chain length of the FFA. In the case of partial complex formation, the differences in stability constants between neighbouring homologues result in an increase in the difference between the effective mobilities of these homologues. How-

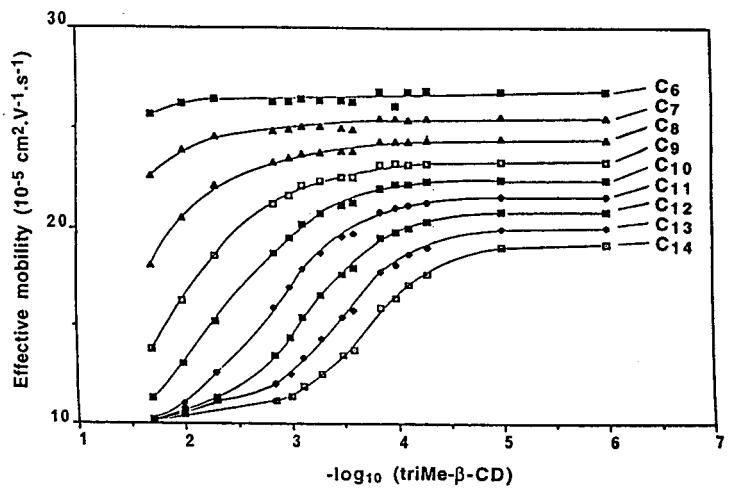

Fig. 3. Variation of the effective mobilities (absolute values) of C_6–C_{14} FFA on addition of trimethyl-β-CD at various concentrations. Operating conditions as in Fig. 2, except for the concentration of the CD. Effective mobilities are calculated as the difference between apparent mobility and electroosmotic mobility.

Table 2
Stability constants, K_f, for inclusion complex formation between linear FFA and trimethyl-β-CD (*DS* 3.0), determined by CZE

Linear FFA	Log K_f
C_{14}	3.77 ± 0.05
C_{13}	3.58 ± 0.05
C_{12}	3.13 ± 0.05
C_{11}	2.6 ± 0.1
C_{10}	2.2 ± 0.2
C_9	1.9 ± 0.3

Electrolyte, aqueous 20 mmol l^{-1} Tris–10 mmol l^{-1} *p*-anisate buffer (pH 8.2); temperature, 30°C.

ever, if the CD concentration is increased up to the point where complex formation becomes complete, the effective mobilities of FFA homologues become almost identical owing to the high molecular mass of the CD, and resolution is lost. This phenomenon is reminiscent of what was observed and described for the CZE separation of enantiomers using CDs as chiral additives [37].

Fig. 4 shows the separation of a standard mixture of linear C_7–C_{18} FFA using methanol–water (50:50,v/v) containing 1 mmol l^{-1} trimethyl-β-CD. In this special case, the resolution can be considered as too large. The proper methanol concentration can be adjusted according to the qualitative and quantitative compositions of each real sample.

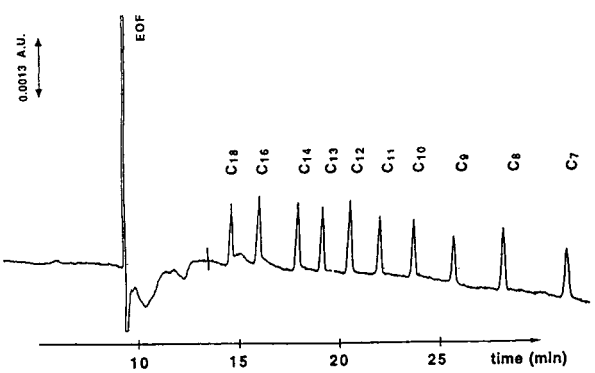

Fig. 4. Separation of a C_7–C_{18} linear FFA standard mixture (0.5 mmol l^{-1} each in methanol). Fused-silica capillary, 50 μm I.D. × 72 cm (50 cm to detector). Electrotyte, 20 mmol l^{-1} Tris–10 mmol l^{-1} *p*-anisate (pH 8.2) containing 1 mmol, l^{-1} trimethyl-β-CD in methanol–water (50:50, v/v). Applied voltage, 30 kV ($I = 3$ μA). Temperature, 30°C. Indirect absorbance detection at 270 nm. Hydrodynamic injection for 1 s.

3.4. Total analysis time

The main factors contributing to the total analysis time were electrolyte methanol content, temperature, separation voltage and capillary length. The analysis time is closely related to the amount of methanol needed to produce suitable sample solubility and resolution of the longest FFA. It was also seen that increasing temperature shortened the analysis time significantly, but this caused the resolution to decrease slightly. The temperature of the capillary compartment was set to 30°C. The low ionic strength and conductivity of the electrolyte allowed the separation voltage to be set at 30 kV; the resulting current for a 72 cm × 50 μm I.D. capillary was 3 μA. Fig. 5 shows the impact of simultaneously

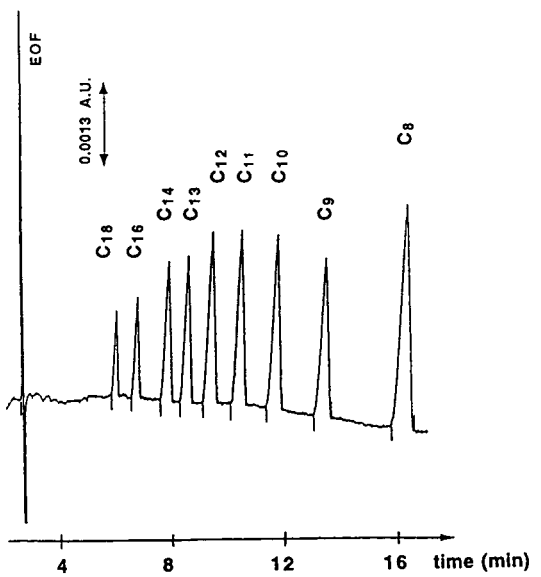

Fig. 5. Separation of a C_8–C_{18} linear FFA reference mixture using optimized capillary length and methanol content. Operating conditions as for Fig. 4, except capillary length, 40 cm (22 cm to detector); electrolyte solvent composition, methanol–water (60:40, v/v) ($I = 4$ μA). The quantitative composition of the reference mixture is given in Table 3, second column.

reducing the total length of the capillary from 72 cm (effective length to the detector cell 50 cm) to 40 cm (effective length 22 cm) and raising the methanol content from 50 to 60%. In spite of the increased methanol content, which brought about more flexibility with respect to the longest FFA, the total analysis time up to the detection of octanoic acid was markedly shortened.

3.5. Quantitative aspects

Special attention was next devoted to the aspects related to method validation, such as detection linearity, precision and detection limits.

A series of samples of a C_8–C_{18} standard mixture of known concentration were first analysed at different dilution factors under the conditions given in Fig. 5, each sample being injected twice. Five successive dilutions differing from one another by a factor of two were performed, so that the range of concentrations covered extended over a factor of 32. The sampling time was kept constant at 1 s, which corresponded to a volume of about 6.4 nl. The plots of migration time-corrected peak areas versus analyte concentration exhibited good linearity over this whole range, as testified by the regression data given in Table 3. No attempt was made to determine the upper concentration limit for signal linearity. Except for octanoic acid, the values determined for the slopes, which correspond to the sensitivity of the method, increased with increasing alkyl chain length of the FFA, i.e., when the analyte absolute mobility decreased, in agreement with indirect absorbance detection theory [2,30].

A series of five consecutive injections of the C_8–C_{18} standard mixture at a concentration corresponding to the median of the concentration range studied before ($C_0/4$) was next performed for the determination of precision. The results given in Table 4 show that the precisions on migration times were ca. $\leq 1\%$, while those on time-corrected peak areas were within the

Table 4
Precision expressed as relative standard deviation (R.S.D.) for migration times (t_M) and time-corrected peak areas (A/t_M) of linear FFA

FFA	R.S.D. ($n = 5$) (%)	
	t_M	A/t_M
C_{18}	0.7	6.2
C_{16}	0.8	5.2
C_{14}	0.9	9.1
C_{13}	1.0	6.8
C_{12}	1.0	4.0
C_{11}	1.0	4.0
C_{10}	1.0	2.8
C_9	1.1	6.1
C_8	1.1	7.3

Operating conditions as for Fig. 6, except concentration of the standard mixture used = $C_0/4$.

Table 3
Linear regression data of migration time-corrected peak areas vs. injected concentration of FFA homologue

FFA	C_0 (mmol l^{-1})	Slope (10^5 μV l mol^{-1})	Intercept (μV)	Regression coefficient (R^2)
C_{18}	0.38	1.46	0.25	0.991
C_{16}	0.47	1.21	0.17	0.991
C_{14}	0.80	1.22	0.13	0.996
C_{13}	0.82	1.17	−0.16	0.997
C_{12}	1.18	1.14	0.61	0.997
C_{11}	1.06	1.10	0.67	0.996
C_{10}	1.06	1.03	0.61	0.996
C_9	1.00	0.87	0.33	0.995
C_8	1.00	1.33	0.39	0.999

For each analyte, the range of concentration studied extended from the analyte concentration in the initial standard mixture, C_0, to $C_0/32$. 1 μV corresponds to 1 absorbance unit. Operating conditions as for Fig. 6.

range 3–7%. It can be noted that peak integration was not performed with highly efficient software but simply using a basic integrator.

The minimum detectable concentrations (MDC) were evaluated after a brief determination of the maximum sampling time consistent with still limited extra-column band broadening. The sampling time was raised to 6 s, which corresponded to a volume of 38 nl. A new series of five samples of the C_8–C_{18} standard mixture differing in their dilution factors was injected. The concentrations ranged this time from $C_0/512$ to $C_0/32$, C_0 being the initial concentration of the standard mixture given in Table 3. Linear plots were still obtained in this range for the corrected peak areas versus analyte concentration (so called calibration graphs) with regression coefficients R^2 varying between 0.970 (C_{16}) and 0.998 (C_8). The MDCs were calculated either using peak heights as the analyte concentration producing a signal-to-noise ratio of three, or using corrected peak areas as the concentration producing a signal equal to the intercept of the calibration graph plus three times its standard deviation. The results obtained can be compared in Table 5. The MDCs derived from peak areas were slightly higher than those derived from the peak heights, but no further tendency was observed.

3.6. Qualitative and quantitative analysis of FFA in a coco oil extract

The methods were applied to the determination of FFA in a coco oil extract sample of commercial origin. Using first the purely aqueous electrolyte, peaks corresponding to the even-carbon-number C_6–C_{14} FFA were recognized (Fig. 6), but the presence of heavier FFA could not be established. The same sample was next analysed with the methanol-rich electrolyte. FFA having even-carbon-number chain lengths up to C_{18} were clearly identified, with dodecanoic acid being apparently the major component (Fig. 7). Moreover, no peak other than those of linear C_8–C_{18} FFA was detected, which agrees well with the fact that coco oils are known to mainly contain linear saturated fatty acids.

These last conditions were used to determine the quantitative composition of the coco oil extract. The reference mixture was the standard mixture of C_8–C_{18} FFA diluted twice (concentration $C_0/2$, see Table 3), the concentrations of which were of the same order of magnitude as those in the extract. Undecanoic acid was chosen as the internal standard and was introduced in the sample of coco oil extract at exactly the same concentration as it was in the reference standard mixture. Three methods were implemented to derive the quantitative composition: direct use of the calibration graph (time-corrected peak areas versus analyte concentration, see Table 3) (method A); use of the peak areas obtained with the reference mixture as a single-point calibration and of the ratio of internal standard peak areas for correction of injection conditions (method B); and use of the peak areas obtained with the reference mixture in keeping with the slopes of the calibration graphs and of the ratio of internal standard peak areas (method C). The

Table 5
Minimum detectable concentrations (MDC) of linear FFA determined from peak heights and peak areas

MDC	Units	FFA								
		C_{18}	C_{16}	C_{14}	C_{13}	C_{12}	C_{11}	C_{10}	C_9	C_8
From peak heights	μmol l^{-1}	0.7	0.6	1.1	2.2	1.4	1.3	1.7	2.4	2.5
	ppm	0.2	0.1	0.2	0.5	0.3	0.2	0.3	0.4	0.4
From peak areas	μmol l^{-1}	2.0	3.6	2.9	2.3	2.2	3.4	2.0	2.4	1.3
	ppm	0.6	0.9	0.7	0.5	0.4	0.6	0.3	0.4	0.2

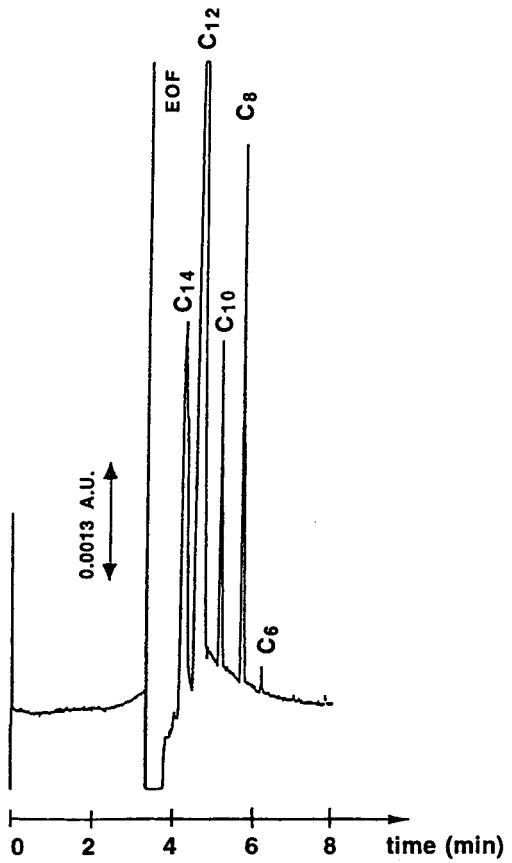

Fig. 6. Electropherogram of the coco oil extract sample dissolved in methanol (260 mg per 100 ml) showing C_6–C_{14} FFA. Operating conditions as for Fig. 2b.

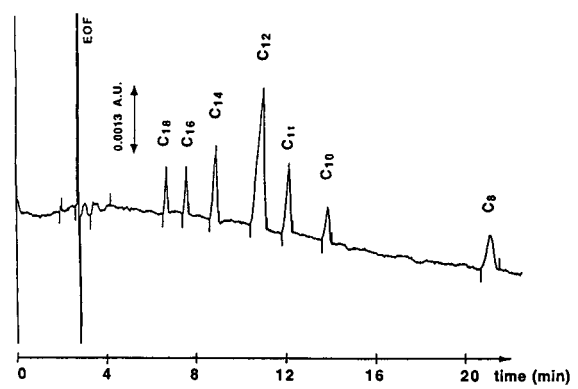

Fig. 7. Electropherogram of the coco oil extract sample dissolved in methanol (65 mg per 100 ml) spiked with undecanoic acid as an internal standard, showing C_8–C_{18} FFA. Operating conditions as for Fig. 5.

Table 6
Molar composition (in mmol l^{-1}) of a commercial coco oil extract, dissolved in methanol (65 mg per 100 ml)

FFA	Method		
	A	B	C
C_{18}	0.180	0.282	0.263
C_{16}	0.223	0.342	0.324
C_{14}	0.468	0.674	0.678
C_{12}	1.333	1.937	1.931
C_{10}	0.169	0.253	0.253
C_8	0.150	0.220	0.230

Method A: direct use of the calibration graphs (see Table 3). Method B: use of the peak areas obtained with the reference mixture as a single-point calibration and of the ratio of internal standard peak areas. Method C: use of the peak areas obtained with the reference mixture in keeping with the slopes of the calibration graphs and of the ratio of internal standard peak areas. Operating conditions as in Fig. 6.

last method allowed us to take advantage of a better estimate of the response factors. Table 6 shows that very close results were obtained by methods B and C, whereas method A leads to markedly lower values, probably because the viscosity of the coco oil extract was higher than that of the standard mixture. This shows that the injection conditions can be an important source of error. Finally, Table 7 gives the composition of the coco oil extract sample in mass percent calculated from the results given in Table 6,

Table 7
Percentage mass composition of the coco oil extract sample calculated from results given in Table 6, method C, and corresponding R.S.D. ($n = 5$), together with the composition of this sample calculated directly from corrected areas (A/t_M) and the average composition of similar samples determined by GC, from supplier's source

FFA	A/t_M (%)	Mass-%	R.S.D. (%)	Mass-% (average, GC)
C_{18}	8.7	10.0	4.3	11[a]
C_{16}	9.0	10.7	2.3	9
C_{14}	18.9	19.8	2.0	18
C_{12}	50.4	49.6	1.3	49
C_{10}	5.9	5.6	4.9	6
C_8	3.1	4.2	3.3	7

[a] Total for $C_{18:0}$, $C_{18:1}$ and $C_{18:2}$ FFA.

method C, with their corresponding relative standard deviations. This composition is not very different from that directly calculated from area normalization, ignoring the response factors. This is a known advantage of indirect absorbance detection [2]. The average composition, determined by GC from the supplier's source, of similar coco oil extracts is also included in Table 7, for the sake of comparison. It should be noted that the present CZE method was not capable of discriminating between the saturated and the mono- and di-unsaturated octadecanoic acids. Apart from this discrepancy and taking into account local and climatic composition variations, it can be considered that a very close agreement was found between the CZE and GC techniques.

4. Conclusion

CZE with indirect absorbance detection has turned out to be a valuable approach for the direct determination of free fatty acids with chain lengths up to C_{18}. Purely aqueous electrolytes can be employed to separate C_2–C_{14} FFA using a CD derivative, while electrolytes containing both 50–60% methanol and the CD are needed to resolve C_8–C_{18} FFA mixtures adequately. CZE appears to be complementary to existing chromatographic methods. While the total analysis times (15–25 min) are similar for the electrophoretic and chromatographic techniques, CZE does not need gradient conditions. The detection order of FFA in CZE is the reverse of that commonly obtained by chromatographic techniques. In the absence of a sample enrichment procedure and with conventional capillaries, the minimum detectable concentrations are at the very low micromolar level (ca. 0.2–0.5 ppm). The linear response range extends over at least three orders of magnitude, from ca. 10^{-6} to 10^{-3} mol l^{-1}, and a rapid mass composition can be obtained from direct corrected area normalization. Sample preparation prior to injection is also less stringent in CZE than in chromatography.

The capability of CZE to resolve long-chain FFA with chain lengths up to C_{18} extends the field of applications of the technique. From the experience gained through this investigation, it seems doubtful that FFA of longer chains can be separated using this approach, since their solubility will require still higher methanol contents, which will be detrimental to inclusion in the CDs, the selectivity and the analysis time. Work is in progress to assess the separability of unsaturated fatty acids.

Acknowledgements

Financial support by Rhône-Poulenc-Chimie (RPC, Courbevoie, France) is gratefully acknowledged. The authors also thank Dr. F. Marcenac (RPC, Centre de Recherches de Saint-Fons, France) and Dr. J.L. Schuppiser (RPC, Courbevoie, France) for their special interest and stimulating discussions.

References

[1] J. Romano, P. Jandik, W.R. Jones and P.E. Jackson, J. Chromatogr., 546 (1991) 411–421.
[2] M.W.F. Nielen, J. Chromatogr., 588 (1991), 321–326.
[3] P.L. Desbène, C. Rosny, B. Desmazières and J.C. Jaquier, J. Chromatogr., 608 (1992) 375–383.
[4] C.S. Weiss, J.S. Hazlett, I.H. Datta and M.H. Danzer, J. Chromatogr., 608 (1992) 325–332.
[5] J.D. Baty, R.G. Willis and R. Tavendale, J. Chromatogr., 353 (1986) 319–328.
[6] W.W. Christie, Gas Chromatography and Lipids, Oily Press, Ayr, 1989.
[7] N.C. Shantha and G.E. Napolitano, J. Chromatogr., 624 (1992) 37–51.
[8] K. Eder, A.M. Reichlmayr-Lais and M. Kirchgessner, J. Chromatogr., 598 (1992) 33–42.
[9] E. Ballesteros, S. Cardenas, M. Gallego and M. Valcarcel, Anal. Chem., 66 (1994) 628–634.
[10] A.K. Batta, V. Dayal, R.W. Colman, A.K. Sinha, S. Sheffer and G. Salen, J. Chromatogr., 284 (1984) 257–260.
[11] H. Miwa, C. Hiyama and M. Yamamoto, J. Chromatogr., 321 (1985) 165–174.
[12] W.W. Christie, HPLC and Lipids, Pergamon Press, Oxford, 1987.
[13] J.F. Lawrence and C.F. Charbonneau, J. Chromatogr., 445 (1988) 189–197.

[14] G. Kargas, T. Rudy, T. Spennetta, K. Takayama, N. Querishi and E. Shrago, J. Chromatogr., 526 (1990) 331–340.
[15] Y. Yasaka, M. Tanaka, T. Shono, T. Tetsumi and J. Katakawa, J. Chromatogr., 508 (1990) 133–140.
[16] J.S. Yoo and V.L. McGuffin, J. Chromatogr., 627 (1992) 87–96.
[17] F. Zonta, B. Stanger, P. Bognoni and P. Masotti, J. Chromatogr., 594 (1992) 137–144.
[18] C.B. Ching, K. Hidajat and M.S. Rao, J. Liq. Chromatogr., 16 (1993) 527–540.
[19] Y. Tsuyama, T. Uchida and T. Goto, J. Chromatogr., 596 (1992) 181–184.
[20] T. Kusaka and M. Ikeda, J. Chromatogr., 639 (1993) 165–173.
[21] K.I. Sakodynsky, G.A. Smolyaninov, V.Y. Zelvensky and N.A. Glotova, J. Chromatogr., 172 (1979), 93–105.
[22] C. de Jong and H.T. Badings, J. High Resolut. Chromatogr., 13 (1990) 94–98.
[23] A. Nomura, J. Yamada, K. Tsunoda, K. Sakaki and T. Yokochi, Anal. Chem., 61 (1989) 2076–2078.
[24] Y. Liu, F. Yang and C.J. Pohl, J. Microcol. Sep., 2 (1990) 245–254.
[25] J.W. King, J. Chromatogr., 28 (1990) 9–14.
[26] T. Barth, Anal. Chem., 59 (1987) 2232–2237.
[27] M. Koval, D. Kaniansky, M. Hutta and R. Lacko, J. Chromatogr., 325 (1985) 151–160.
[28] X. Huang, J.A. Luckey, M.J. Gordon and R.N. Zare, Anal. Chem., 61 (1989) 766–770.
[29] X. Huang, M.J. Gordon and R.N. Zare, J. Chromatogr., 480 (1989) 285–288.
[30] M.T. Ackermans, F.M. Everaerts and J.L. Beckers, J. Chromatrogr., 549 (1991) 345–355.
[31] R. Szücs, J. Vindevogel and P. Sandra, J. High Resolut. Chromatogr., 14 (1991) 692–693.
[32] G. Kortum, W., Vogel and K. Andrussow, Dissociation Constants of Organic Acids in Aqueous Solution, Butterworths, London, 1961.
[33] T. Hirokawa, M. Nishino, N. Aoki, Y. Kiso, Y. Sawamoto, T. Yagi and J.-I. Akiyama, J. Chromatogr., 271 (1983) D1–D106.
[34] F. Foret, S. Fanali, L. Ossicini and P. Bocek, J. Chromatogr., 470 (1989) 299–308.
[35] P. Gareil, R. Roldan-Assad and F. Lelièvre, Analusis, 21 (1993) M35–M38.
[36] P. Gareil, D. Pernin, J.-P. Gramond and F. Guyon, J. High Resolut. Chromatogr., 16 (1993) 195–197.
[37] S.A. Wren and R.C. Rowe, J. Chromatogr., 603 (1992) 235–241.

ELSEVIER

Journal of Chromatography A, 708 (1995) 351–355

JOURNAL OF CHROMATOGRAPHY A

Short communication

Detection of olive oil adulteration by measuring its authenticity factor using reversed-phase high-performance liquid chromatography

Ali H. El-Hamdy*, Naima K. El-Fizga

Department of Food Science, Faculty of Agriculture, University of Al-Fateh, P.O. Box 91752, Tripoli, Libya

First received 12 December 1994; revised manuscript received 31 March 1995; accepted 31 March 1995

Abstract

Addition of as little as 1% of linoleic-rich vegetable oils to olive oil can be detected easily and quantitatively by reversed-phase high-performance liquid chromatography on an octyl-bonded silica stationary phase (Supelcosil-LC 8). The mobile phase was acetone–acetonitrile (70:30, v/v), used isocratically. The chromatogram of pure olive oil was compared with those of mixtures of soybean, sunflower and corn oils with olive oil. The results indicate the possibility of the detection of adulteration by less than 1% of linoleic-rich vegetable oils in olive oil qualitatively and quantitatively in less than 15 min. An olive oil authenticity factor was established as a rapid indicator of adulteration and a simple equation for determining the extent of adulteration was derived.

1. Introduction

In Libya, olive oil is the main oil used in food preparation, cooking and frying and large volumes are imported every year. However, recently other oils such as corn, sunflower and soybean oils have also been imported. The Libyan Secretariat of Agriculture buys local olive oil at a higher price than imported olive oil, to encourage farmers not to neglect olive trees. However, frequent adulteration of both imported and local olive oil with the cheaper oils high in linoleic acid required a rapid method for the detection of adulteration to protect the economy and the consumer. Fatty acids have been used as indicators of adulteration [1–6], but their wide range in the adulterant and adulterated oils make them unsuitable for this purpose. Unsaponifiables have also been used as adulteration indicators [3–8], but extraction and processing operations make them unreliable. As fatty acids are distributed on glycerol molecules according to certain position-specific patterns, triacylglycerols are considered as fingerprints of natural oils. A combination of chemical, physical and/or chromatographic methods [9–17] has been used to determine the triacylglycerol composition of oils as a means of detecting possible adulteration. Peak ratios of triacylglycerols separated by HPLC have been used as a measure of olive oil adulteration [16].

This work was undertaken to develop a simple, rapid method for the detection of oils high in linoleic acid in olive oil by reversed-phase

* Corresponding author.

0021-9673/95/$09.50
SSDI 0021-9673(95)00415-7

high-performance liquid chromatography (RP-HPLC) and a simple authenticity factor and a derived equation to determine the extent of adulteration with a one short chromatographic step, completed in less than 15 min.

2. Experimental

Commercial vegetable oils (soybean, sunflower and corn oils) high in linoleic acid were used as adulterants and mixed with a virgin olive oil sample.

2.1. RP-HPLC

The HPLC system consisted of a Model 2249 gradient pump (LKB, Bromma, Sweden) connected to two 150 × 4.5 mm I.D. stainless-steel columns packed with an octyl-bonded silica stationary phase (Supelcosil-LC 8) (Supelco, Bellefonte, PA, USA). Samples were injected through a Rheodyne (Cotati, CA, USA) Model 7125 injector equipped with a 20-ml sample loop and an LKB differential refractometric detector connected to an LKB Model 2221 integrator recorder. The isocratic mobile phase was acetone–acetonitrile (70:30, v/v). Samples were dissolved in the mobile phase and injected without any prior treatment.

3. Results and discussion

Fig. 1 shows typical chromatograms of olive, corn, soybean and sunflower oil triacylglycerols separated according to their equivalent carbon number (*ECN*). Soybean oil contains 1.2% of triacylglycerols with *ECN* 38 and 7.0% of *ECN* 40 triacylglycerols. The *ECN* 42 triacylglycerol contents in corn, sunflower and soybean are 24.2 ± 0.04, 22.4 ± 0.10 and 24.9 ± 0.11%, respectively (Table 1), while that in olive oil is 1.0 ± 0.02%. The *ECN* 42 triaclyglycerol group was used as an indicator of adulteration because it shows the greatest difference in triacylglycerol content between olive oil and the high linoleic acid oils.

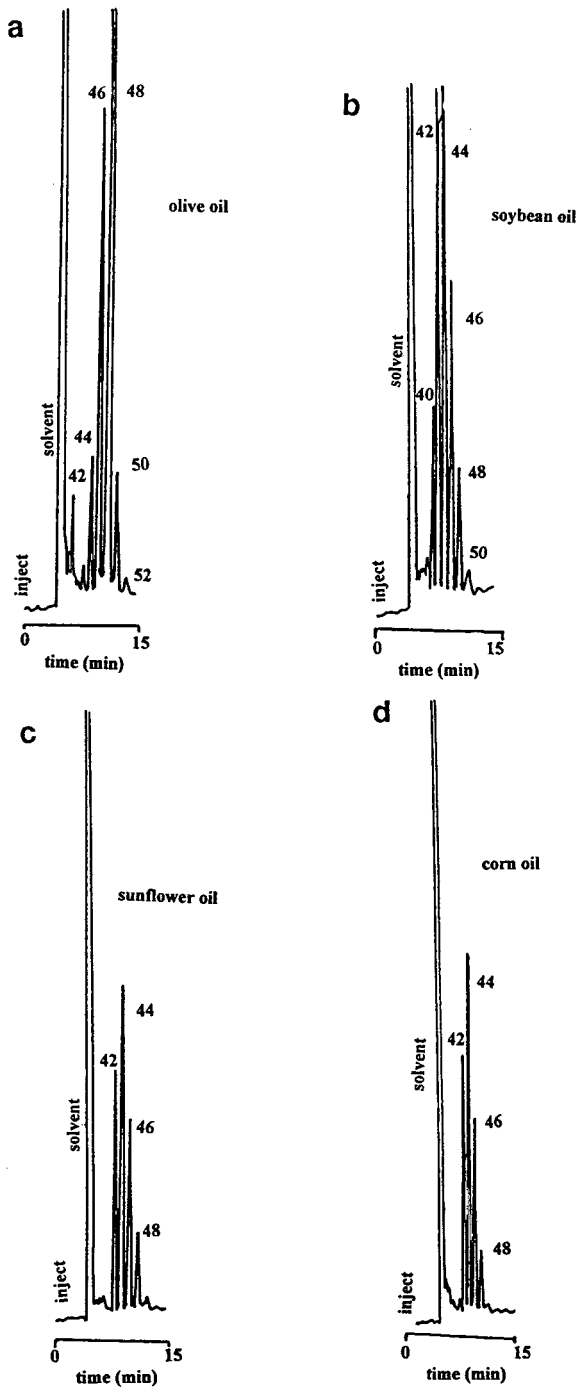

Fig. 1. Separation of triacylglycerols on Supelcosil-LC 8 with acetone–acetonitrile (70:30, v/v) as the mobile phase and refractive index detection. Flow-rate, 1.0 ml/min. (a) Olive oil; (b) soybean oil; (c) sunflower oil; (d) corn oil.

Table 1
Triacylglycerol composition (%) (± S.D., $n = 9$) and authenticity factors (Au) of olive, corn, soybean and sunflower oils separated by RP-HPLC

Triacylglycerol *ECN*	Oil			
	Corn	Sunflower	Soybean	Olive
38	nd[a]	nd	1.2 ± 0.04	nd
40	nd	nd	7.0 ± 0.02	nd
42	24.2 ± 0.04	22.4 ± 0.10	24.9 ± 0.11	1.0 ± 0.02
44	38.2 ± 0.40	35.2 ± 0.16	30.8 ± 0.32	5.7 ± 0.51
46	23.6 ± 0.21	25.0 ± 0.16	21.6 ± 0.54	23.2 ± 0.37
48	9.2 ± 0.04	12.7 ± 0.03	10.5 ± 0.13	60.1 ± 1.25
50	1.4 ± 0.01	1.1 ± 0.09	2.7 ± 0.22	6.8 ± 0.19
52	1.5 ± 0.10	2.2 ± 0.11	0.9 ± 0.12	0.9 ± 0.13
Au	3.2 ± 0.05	3.5 ± 0.03	3.1 ± 0.03	100.0 ± 2.73

[a] Not detected.

The presence of vegetable oils of high linoleic acid content in olive oil can be detected by measuring its authenticity factor (Au) as follows

$$Au = \frac{100 - ECN\,42(\%)}{ECN\,42(\%)} \quad (1)$$

Virgin olive oil separated by RP-HPLC has $Au = 98.2 \pm 3.86$. The authenticity factors of corn, sunflower and soybean oils are 3.2 ± 0.02, 3.5 ± 0.06 and 3.2 ± 0.19, respectively. Fig. 2 shows that addition of as little as 1% of corn, sunflower and soybean oils decreased the olive oil Au to 81.6 ± 2.5, 80.3 ± 4.05 and 79.0 ± 3.54, respectively, and additions of 5% of these oils decreased Au to 46.2 ± 1.38, 48.3 ± 1.26 and 46.4 ± 1.70, respectively.

Table 2
Change in authenticity factor (Au) and *ECN* 42 triacylglycerol content due to change in added high linoleic acid oils

Oil (%)[a]	*ECN* 42 ± S.D.[b] (%)	*Au* ± S.D.[b]
0.0	1.0 ± 0.02	95.2 ± 3.86
1.0	1.3 ± 0.04	78.4 ± 2.56
2.0	1.5 ± 0.04	66.5 ± 1.94
3.0	1.7 ± 0.05	57.8 ± 1.62
4.0	1.9 ± 0.05	51.0 ± 1.43
5.0	2.1 ± 0.06	45.6 ± 1.31
6.0	2.4 ± 0.07	41.3 ± 1.23
7.0	2.6 ± 0.08	37.7 ± 1.16
8.0	2.8 ± 0.09	34.6 ± 1.10
9.0	3.0 ± 0.10	32.0 ± 1.05
10.0	3.2 ± 0.11	39.8 ± 1.00
100.0	23.1 ± 1.08	3.3 ± 0.20

[a] Percentage of oils high in linoleic acid in olive oil.
[b] $n = 27$.

Plotting the percentage of added high linoleic acid oil versus the percentage of *ECN* 42 triacylglycerol group (Fig. 3) showed the possibility of measuring the extent of olive oil adulteration by the simple equation

$$\text{added oil}(\%) = \frac{ECN\,42(\%) - b}{a} \quad (2)$$

where a and b are constants. The constants a and b differ slightly according to the oil added. Thus, corn, sunflower and soybean oils added to olive oil can be calculated using the following equations:

$$\text{corn oil}(\%) = \frac{ECN\,42(\%) - 0.9820}{0.2326} \quad (3)$$

$$\text{sunflower oil}(\%) = \frac{ECN\,42(\%) - 0.9954}{0.2142} \quad (4)$$

$$\text{soybean oil}(\%) = \frac{ECN\,42(\%) - 0.9801}{0.2388} \quad (5)$$

The overall equation for oils added to olive oil is

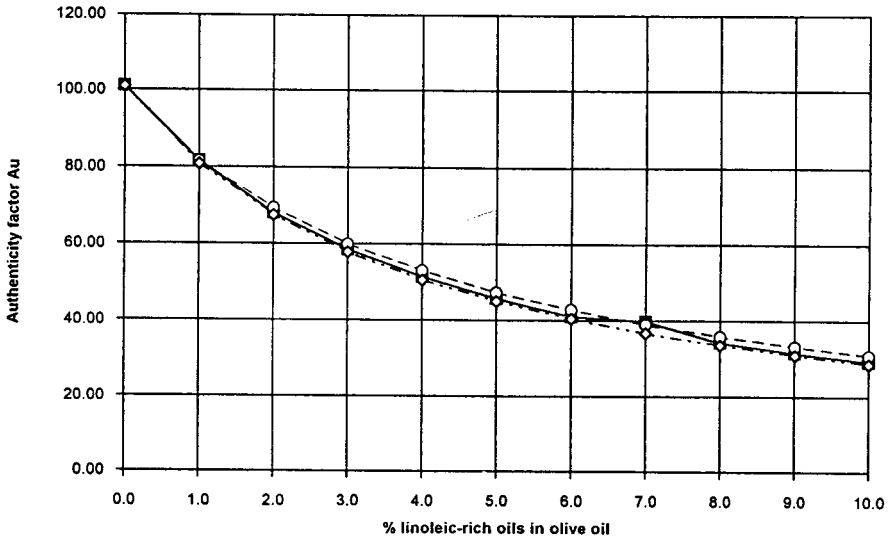

Fig. 2. Change of authenticity factors (*Au*) of olive oil as a result of addition of vegetable oils of high linoleic acid content. ■ = Corn oil; ○ = sunflower oil; ◇ = soybean oil.

$$\text{added oil}(\%) = \frac{ECN\,42(\%) - 0.9850}{0.2285} \qquad (6)$$

This study indicates the possibility of detecting and determining as little as 1% of oils high in linoleic acid in olive oil, and suggests the use of an authenticity factor as a simple and rapid indicator of adulteration. The whole analysis requires less than 15 min. However, oleic acid rich oils such as residue or re-esterified olive oils require emphasis on triacylglycerol groups other than *ECN* 42. A similar detection method for

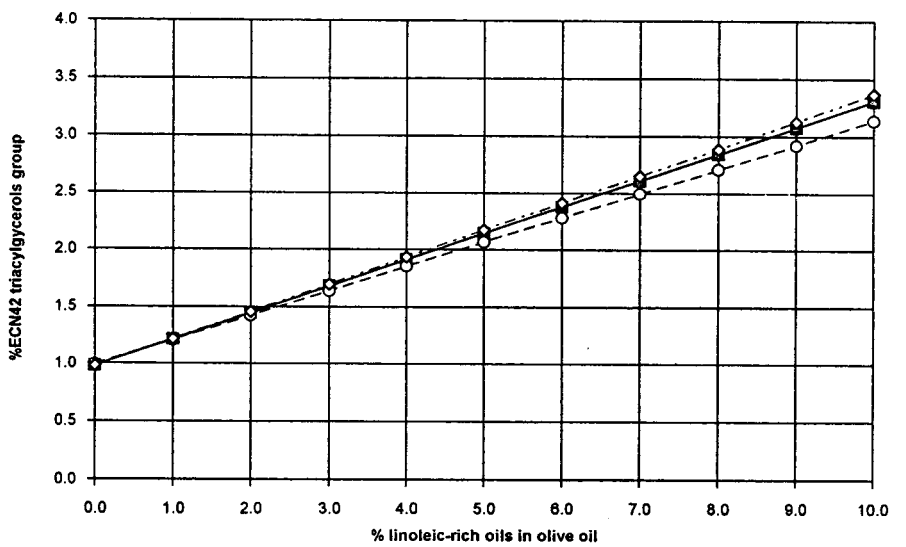

Fig. 3. Change of *ECN* 42 triacylglycerol content in olive oil due to change of added high linoleic acid vegetable oils. ■ = Corn oil; ○ = sunflower oil; ◇ = soybean oil.

such oils is under development using an octadecyl-bonded phase.

References

[1] G.F. Spencer, S.F. Herb and P.J. Gormisky, J. Am. Oil Chem. Soc., 53 (1976) 94.
[2] R.S. Farag, S.H. Abu-Raya, F.A. Ahmed, F.M. Hewedi and K.H. Khalifa, J. Am. Oil Chem. Soc., 60 (1983) 1669.
[3] J.B. Rossell, B. King and M.J. Downes, J. Am. Oil Chem. Soc., 60 (1983) 333.
[4] A.M. Abu-Hadeed and A.R. Kotb, J. Am. Oil Chem. Soc., 65 (1988) 1922.
[5] D. Firestone and J.L. Summers, J. Am. Oil Chem. Soc., 62 (1985) 1558.
[6] D. Firestone, Karen L. Carson and R.J. Reina, J. Am. Oil Chem. Soc., 65 (1988) 788.
[7] R.S. Farag, F.A. Ahmed, A.A. Shehata, S.H. Abu-Raya and A.F. Abdalla, J. Am. Oil Chem. Soc., 59 (1982) 557.
[8] M.H. Gordon and R.E. Griffith, Food Chem. 43 (1992) 71.
[9] V.M. Kapoulas and S. Passaloglon-Emmanouiliolou, J. Am. Oil Chem. Soc., 58 (1981) 694.
[10] D.S. Galanos, V.M. Kapoulas and E.C. Vondouris, J. Am. Oil Chem. Soc., 45 (1968) 825.
[11] D.S. Galanos and V.M. Kapoulas, J. Am. Oil Chem. Soc., 42 (1965) 815.
[12] D. Gegiou and K. Staphylakis, J. Am. Oil Chem. Soc., 62 (1985) 1047.
[13] C. Merritt, Jr., M.J. Vajdi, S.C. Kayser, J.W. Halliday and M.C. Bazinet, J. Am. Oil Chem. Soc., 59 (1982) 422.
[14] S. Synouri-Vrettaken, M.E. Komaitis and E.C. Vondouris, J. Am. Oil Chem. Soc., 61 (1984) 1051.
[15] R.V. Flor, J. Am. Oil Chem. Soc., 66 (1989) 431.
[16] V.M. Kapoulas and N.M. Andrikopoulos, J. Chromatogr., 366 (1986) 311.
[17] M. Proto, Ind. Aliment., 31 (1992) 36.

ELSEVIER

Journal of Chromatography A, 708 (1995) 356–361

JOURNAL OF CHROMATOGRAPHY A

Short communication

Performance of a physically adsorbed high-molecular-mass polyethyleneimine layer as coating for the separation of basic proteins and peptides by capillary electrophoresis

F. Bedia Erim[1], Alejandro Cifuentes, Hans Poppe, Johan C. Kraak*

Laboratory for Analytical Chemistry, University of Amsterdam, Nieuwe Achtergracht 166, 1018 WV Amsterdam, Netherlands

First received 17 November 1994; revised manuscript received 27 March 1995; accepted 27 March 1995

Abstract

A simple method for the preparation of a polyethyleneimine (PEI) coating on the inner surface of fused-silica capillaries for capillary electrophoresis (CE) is reported. The PEI layer can be coated on the silica surface by just flushing the capillary with a solution containing high-molecular-mass PEI. The physically adsorbed layer appears to be very stable and can be used in a pH range of 3–11. In comparison to described methods to fabricate an immobilized PEI layer, the proposed method does not require an immobilization step, is simple and the preparation time of the coating is less than two hours. Good reproducibilities of migration times of basic proteins and peptides were obtained on the same PEI-coated capillary as well as on different PEI-coated capillaries. For basic proteins efficiencies ranging from 300 000–500 000 plates per meter were normally found.

1. Introduction

In CE analysis of proteins, interaction of the biopolymers with the capillary wall seems to be the main reason for the loss in efficiency compared to that predicted by theory. Furthermore, protein adsorption on the internal surface of the capillary can cause poor reproducibility of migration time and low protein recovery. The adsorption is believed to be due to the electrostatic interactions between positively charged residues of the protein and the negatively charged silanol groups which are intrinsic to the fused-silica surface.

Different methods have been developed in CE to diminish interaction between proteins and the silica surface (see Refs. [1–4] for exhaustive and up-to-date reviews). The most successful methods are the ones whereby the silanol groups are shielded by a polymer layer [5–14]. The use of such polymeric coatings has led to high efficiencies and reproducible protein separations.

The PEI coating as developed by Towns and Regnier [8], and adapted by others [10,12,15], seems to be a very interesting solution to this problem. This coating is different from most polymer layers because the surface bears a positive charge. The PEI coating is particularly suited for the separation of basic proteins since at acidic pH the surface and proteins have the same positive charge. Under these conditions the proteins are repelled from the surface in analogy

* Corresponding author.

[1] Present address: Department of Chemistry, Technical University of Istanbul, Maslak 80626, Istanbul, Turkey.

0021-9673/95/$09.50
SSDI 0021-9673(95)00394-0

to what has been described by Lauer and McManigill [16]. The PEI coating has the additional advantage that the separation of basic compounds is fast, because the basic analytes move to the anode, i.e. in the same direction as the electroosmotic flow.

When testing a high-molecular-mass PEI (M_r $6 \cdot 10^5$–$1 \cdot 10^6$) as additive to the buffer in another CE study, we discovered that PEI sticks irreversibly on the silica surface, even under harsh conditions such as flushing the capillary with strong basic and acidic solutions. It is well known that polymers strongly adsorb onto silica surfaces and their adsorption has been applied to mask the silanol groups on the surface of fused-silica capillaries [11,17]. Since the preparation of an immobilized bonded PEI coating is rather laborious and time-consuming (as for most polymer coatings), we found it worthwhile to investigate whether a physically adhered PEI layer can be used as coating as well. The study was focused on the reproducibility, the efficiency and the long-term stability of the coating, using some basic proteins and peptides as test compounds.

2. Materials and methods

2.1. Instrumentation

Separations were carried out using a Prince (Lauer-Labs, Emmen, Netherlands) injection system with temperature controller, connected to a Linear M-200 variable-wavelength UV–Vis detector (Linear Ins. Corp., Reno, NV, USA) operated at 214 nm. Fused-silica capillaries (Polymicro Technologies Inc., Phoenix, AZ, USA) with 75 μm I.D. and 360 μm O.D. were used; the total and effective (from the injection point to the detector) lengths of the capillaries are indicated in the figures. The injection was carried out at the cathodic side using controlled pressure for a fixed time.

2.2. Samples and chemicals

Lysozyme (chicken egg white), cytochrome c (horse heart), ribonuclease A (bovine pancreas), trypsinogen and α-chymotrypsinogen (bovine pancreas) were purchased from Sigma Chemical Co. (St. Louis, MO, USA) and used as received. All the short peptides were from Nutritional Biochemicals Corporation (Cleveland, OH, USA) and the long ones from Bachem Feinchemikalien AG (Bubendorf, Switzerland). Proteins and peptides were dissolved at the concentrations indicated (ranging from 0.2 to 2 mg/ml) in water, previously purified by passage through a PSC filter assembly (Barnstead, Boston, MA, USA). The samples were stored at −20°C and warmed to room temperature before use. Polyethyleneimine (PEI, molecular mass range $6 \cdot 10^5$–$1 \cdot 10^6$) was from Fluka (Fluka AG, Buchs, Switzerland). Acetic acid and formic acid (E. Merck, Darmstadt, Germany), succinic acid (BDH Laboratory Chemicals Division, Poole, UK), chloro-acetic acid, malonic acid, Tricine (N-tris[hydroxymethyl]methyl-glycine), CAPS (3-cyclohexylamino-1-propanesulfonic acid) and MES (all from Aldrich, Axel, Netherlands) were used in the various running buffers. These buffers were used in a 50 mM concentration and at pH values of 3 (chloro-acetic), 5.5 (acetic, MES, succinic, malonic), 7 and 7.5 (MES), 8 and 8.5 (Tricine), 9–11 (CAPS). The buffers were stored at 4°C and warmed to room temperature before use.

2.3. Coating procedure

Before coating the capillary with PEI the external polyimide coating was burned-off over a length of 5 mm in order to make the detection window. The fused-silica capillary was first etched by flushing the capillary with a solution of 1 M sodium hydroxide for 30 min at 1 bar and with water for 15 min at the same pressure. Then the capillary was flushed with a solution of PEI in water at 1.5 bar for 10 min and the PEI solution left in the capillary for one hour. Next the polymer solution was pressed out of the capillary with air at 1.5 bar. Finally the capillary was rinsed with water for 15 min and with running buffer for 15 min. A washing step of 1 min with buffer was used between injections. This procedure can be carried out by using the

Prince instrument in automatic mode, which allows to coat each capillary unattendedly overnight.

3. Results and discussion

The PEI molecule has many positive charges and interacts strongly with negatively charged silanol groups on the surface of the fused-silica capillary [8]. This irreversible adsorption creates a PEI layer on the capillary wall and thus masks the underlying silanol groups from unwanted interactions with biopolymers. Moreover, the adsorbed PEI layer has a positive charge over a wide pH range, which results in an electroosmotic flow towards the anode. This anodic electrophoretic flow favours the separation speed of substances with a positive charge such as basic proteins and peptides.

3.1. Effect of the PEI concentration in the coating solution

In order to determine whether the PEI concentration in the coating solution has an effect on the nature of the dynamically generated PEI layer, the electroosmotic flow was measured as function of the pH on capillaries coated with 0.1–10% (w/v) solutions of PEI. Different buffers were used to cover the pH range of 3–10.4. Fig. 1 shows the effect of the pH on the electroosmotic flow. As can be seen the electroosmotic flow is always towards the anode over the investigated pH range. This behaviour indicates that the basic PEI molecules are strongly adsorbed on the silica surface and that the residual amine groups of the PEI create a positively charged surface. The electroosmotic flow is relatively constant over the pH range 3–6 and then gradually decreases at higher pH. This latter effect can be attributed to deprotonation of the amine groups and the higher ionization of silanol groups on the capillary wall [8].

From Fig. 1 it can be seen that capillaries coated with 1, 5 and 10% of PEI exhibit similar behaviour. However, in the capillary coated with 0.1% PEI a significantly larger electroosmotic

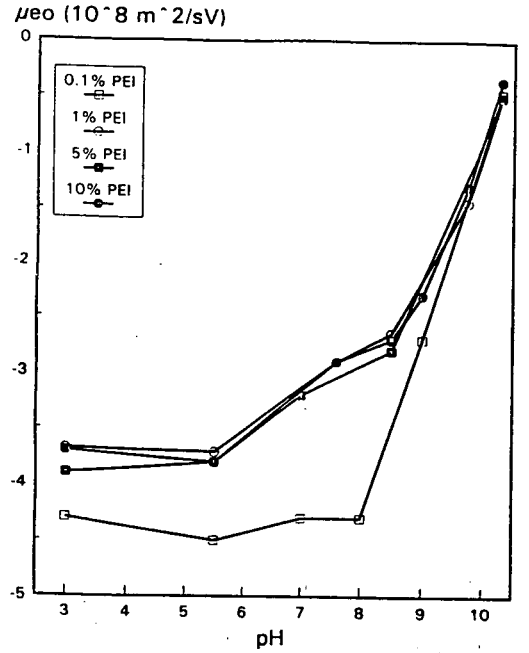

Fig. 1. Plots of electroosmotic flow versus pH on capillaries coated with 0.1, 1, 5 and 10% (w/v) PEI solutions in water. Acetone was employed as neutral marker.

flow (EOF) was found. A similar behaviour has been observed by other authors [8].

In order to ascertain that the effects described above were indeed due to changes in the pH and degree of coating, all the experiments described above were repeated using the same buffers but adding different quantities of NaCl in order to keep the current the same (ionic strength is then also approximately constant). Some EOF values changed slightly; however, the same trend as shown in Fig. 1 was observed.

3.2. Effect of type of buffer and pH

The effect of the type of buffer on the electroosmotic flow was investigated on a 10% PEI capillary using acetone as neutral marker. Four different buffers at pH 5.5, i.e. malonic acid, succinic acid, MES and acetic acid, at the same concentration (50 m*M*) were employed. It appeared that the electroosmotic flow was strongly dependent on the type of anion. The electro-

osmotic mobilities with malonic acid, succinic acid, MES and acetic acid were found to be $-18 \cdot 10^{-9}$, $-18 \cdot 10^{-9}$, $-50 \cdot 10^{-9}$ and $-45 \cdot 10^{-9}$ $m^2 s^{-1} V^{-1}$, respectively. As can be seen, the divalent acids, i.e. malonic and succinic acid, have the same electroosmotic flow, but the value is much smaller than those found with the monovalent acids, i.e. acetic acid and MES. A similar behaviour was observed when NaCl was added to the buffers in order to get similar ionic strength, as done above. A strong electrostatic interaction between the divalent anions and the amine groups of PEI, which decreases the charge on the coating and thus the zeta potential, seems to take place, which may explain this effect.

3.3. Efficiency of the PEI coating for biological compounds

The performance of the PEI-coated capillaries was investigated with proteins and peptides. Fig. 2 shows a typical electrophoretogram of a mixture of basic proteins on a 10% PEI-coated capillary at pH 5.5. The PEI coating appears to be very efficient for basic proteins, and plate numbers ranging from 300 000–500 000 plates/m were normally found. Similar efficiencies were found with the 0.1, 1 and 5% PEI coating solutions. Unfortunately acidic proteins interact strongly with the coating and the performance is very poor.

The PEI coating appears to be also suitable for the separation of other types of samples. As an illustration, Figs. 3A and 3B show a separation of a mixture of di- and tripeptides at pH 8.2 and a separation of longer peptides at pH 9.75, respectively. As can be seen, very efficient and fast separations can be realized.

3.4. Reproducibility and long-term stability of the PEI coating

The reproducibility and the long-term stability of the PEI coating was investigated by measuring the plate numbers and retention times of some basic proteins on three 10% PEI coated capillaries. The run-to-run reproducibilities of the migration times of the proteins on the three

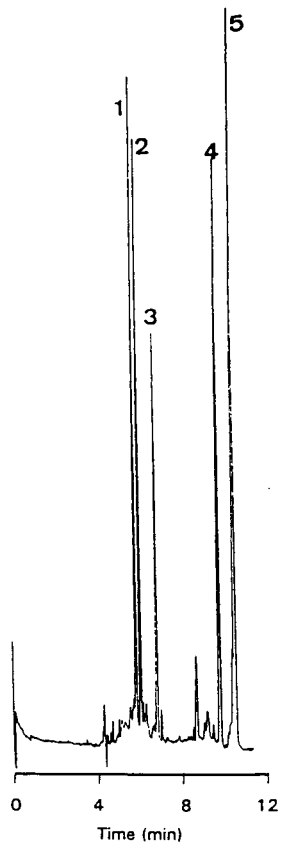

Fig. 2. Separation of five basic proteins. 10% PEI-coated capillary, total length 63.5 cm, effective length 46.5 cm, I.D. 75 μm. Buffer: 50 m*M* acetate, pH 5.5. Run voltage −28.8 kV. Injection 10 mbar for 6 s. Sample: (1) trypsinogen 0.32 mg/ml, (2) α-chymotrypsinogen 0.32 mg/ml, (3) ribonuclease A 0.72 mg/ml, (4) cytochrome C 0.32 mg/ml and (5) lysozyme 0.32 mg/ml. UV detection at 214 nm.

capillaries were excellent and the relative standard deviations (%R.S.D.) in migration times ranged from 0.5 to 1.5% ($n = 6$). The R.S.D. values for column-to-column reproducibilities of the migration times ranged from 1.9 to 2.8% ($n = 18$) and the R.S.D. in the plate numbers ranged from 10 to 15%.

The long-time reproducibility of the migration times of proteins was followed on one capillary for one month. During this period 70 injections of the test proteins were performed. The migration times changed about 5% and no noticeable loss in efficiency was observed.

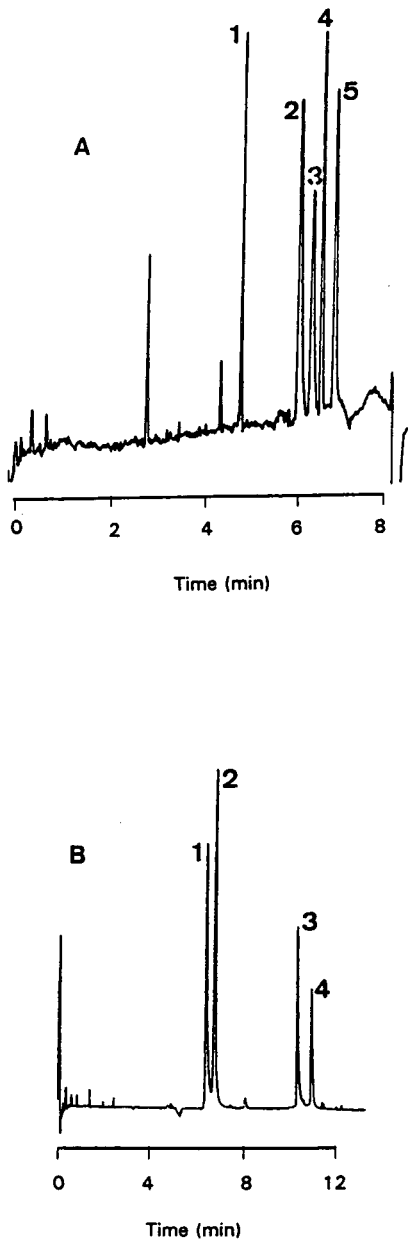

Fig. 3. Separation of short peptides (A) and long peptides (B) on a 5% PEI-coated capillary. Total length 85 cm, effective length 50 cm, I.D. 75 μm. Run voltage −24 kV. Injection 10 mbar for 6 s. Sample concentration ranging from 0.2 to 0.6 mg/ml. UV detection at 214 nm. (A) Buffer: 50 m*M* Tricine, pH 8.2; peptides: (1) GE, (2) GGG, (3) LGF, (4) AA, (5) SGG. (B) Buffer: 50 m*M* CAPS, pH 9.75; peptides (1) WAGGDASGE, (2) ELAGAPPEPA, (3) SYSMEHPRWG, (4) LQAAPALDKL.

In order to test the stability of the coating at very basic pHs we left a 50 m*M* CAPS buffer at pH 11 in a 5% PEI-coated capillary for 60 h. Analysis times were measured before and after this experiment using the five basic proteins as analytes at pH 5.5. After 60 h the migration times of all proteins were slightly increased, i.e. about 3%, while the efficiency was not altered. This result indicates that the dynamically generated PEI layer is more or less irreversibly attached to the silica surface.

4. Conclusions

A stable high-molecular-mass PEI layer can be dynamically generated on the inside surface of fused-silica capillaries by just filling the capillary with a solution of a high-molecular-mass PEI (M_r $6 \cdot 10^5$–$1 \cdot 10^6$) and flushing the capillary after a certain time. The preparation of the coating is very simple, reproducible and takes less than two hours. The coating is very stable in the pH range 3–11. For basic proteins efficiencies of 300 000–500 000 plates/m were obtained. The coating appears to be suitable for the separation of biological compounds such as basic proteins and peptides but cannot be recommended for acidic proteins.

Acknowledgements

A.C. would like to acknowledge the financial support of the European Communities (Human Capital and Mobility Programme, bursary #ERB4001GT920989).

References

[1] W.G. Kuhr, Anal. Chem., 62 (1990) 403R.
[2] W.G. Kuhr and C.A. Monning, Anal. Chem., 64 (1992) 389R.
[3] C.A. Monning and R.T. Kennedy, Anal. Chem., 66 (1994) 280R.
[4] S.F. Yi, Capillary Electrophoresis: Principles, Practice and Applications, Elsevier, Amsterdam, 1992.
[5] S. Hjertén, J. Chromatogr., 347 (1985) 191.

[6] R.M. Mc Cormick, Anal. Chem., 60 (1988) 2322.
[7] G.J.M. Bruin, J.P. Chang, R.H. Kulman, K. Zegers, J.C. Kraak and H. Poppe, J. Chromatogr., 471 (1989) 429.
[8] J.K. Towns and F.E. Regnier, J. Chromatogr., 516 (1990) 69.
[9] A. Cifuentes, J.M. Santos, M. de Frutos and J.C. Diez-Masa, J. Chromatogr. A, 652 (1993) 161.
[10] J.T. Smith and Z. El Rassi, Electrophoresis, 14 (1993) 396.
[11] M. Gilges, M.H. Kleemiss and G. Schomburg, Anal. Chem., 66 (1994) 2038.
[12] M. Huang, W.P. Vorkink and M.L. Lee, J. Microcol. Sep., 4 (1992) 233.
[13] W. Nasabeh and Z. El Rassi, J. Chromatogr., 559 (1991) 367.
[14] Y.F. Maa, K.J. Hyver and S.A. Swedberg, J. High Resolut. Chromatogr. Chromatogr. Commun., 14 (1991) 65.
[15] T. Wang and R.A. Hartwick, J. Chromatogr., 594 (1992) 325.
[16] H.H. Lauer and D. McManigill, Anal. Chem., 58 (1986) 166.

ELSEVIER

Journal of Chromatography A, 708 (1995) 363

JOURNAL OF CHROMATOGRAPHY A

Erratum

Erratum to "Determination of phylloquinone in intravenous fat emulsions and soybean oil by high-performance liquid chromatography" [J. Chromatogr. A, 664 (1994) 189]☆

Fathi Moussa

Faculté de Pharmacie de Tours, Service de Chimie Analytique, 2 Bis Boulevard Tonnellé, 37042 Tours Cedex, France

In the paragraph "Preparation of calibration graph" a sentence was omitted. Before "Pipette into each tube. . . ." (p. 191, left column, line 4) the following sentence has to be inserted: "Redissolve the residues in 50 μl of absolute ethanol".

☆ SSDI of original article: 0021-9673(93)E0046-W.

0021-9673/95/$09.50
SSDI 0021-9673(95)00392-4

ELSEVIER

Journal of Chromatography A, 708 (1995) 364

JOURNAL OF CHROMATOGRAPHY A

Erratum

Erratum to "Study of the enantioselective binding between BOF-4272 and serum albumins by means of high-performance frontal analysis" [J. Chromatogr. A, 694 (1995) 81]☆

Akimasa Shibukawa[a,*], Miki Kadohara[a], Jing-yi He[a], Masuhiro Nishimura[b], Shinsaku Naito[b], Terumichi Nakagawa[a]

[a]*Faculty of Pharmaceutical Sciences, Kyoto University, Sakyo-ku, Kyoto 606, Japan*

[b]*Laboratory of Drug Metabolism Research, Naruto Research Institute, Otsuka Pharmaceutical Factory, Inc., Naruto-shi, Tokushima 772, Japan*

In Table 2 on page 86 the number of determinations has been incorrectly cited. All samples were analyzed five times except for the 400 μM BOF-4272/550 μM albumin solution which was analyzed in duplicate.

The first entry in this table should read BOF-4272 instead of BOV-4272.

☆ SSDI of original article: 0021-9673(94)000653-9.

0021-9673/95/$09.50
SSDI 0021-9673(95)00543-9

Author Index Vol. 708

Adachi, S., Mizuno, T. and Matsuno, R.
Concentration dependence of the distribution coefficient of maltooligosaccharides on a cation-exchange resin 708(1995)177
Aflalaye, A., Sternberg, R., Raulin, F. and Vidal-Madjar, C.
Gas chromatography of Titan's atmosphere. VI. Analysis of low-molecular-mass hydrocarbons and nitriles with BPX5 capillary columns 708(1995)283
Andersson, B., see Kussak, A. 708(1995)55
Andersson, K., see Kussak, A. 708(1995)55
Arnold, F.H., see Plunkett, S.D. 708(1995)19
Bedia Erim, F., Cifuentes, A., Poppe, H. and Kraak, J.C.
Performance of a physically adsorbed high-molecular-mass polyethyleneimine layer as coating for the separation of basic proteins and peptides by capillary electrophoresis 708(1995)356
Bellomonte, G., see Carratù, B. 708(1995)203
Boniglia, C., see Carratù, B. 708(1995)203
Brønnum-Hansen, K., see Ekelund, J. 708(1995)253
Bruno, T.J., Wertz, K.H. and Caciari, M.
Retention of halocarbons on a hexafluoropropylene epoxide-modified graphitized carbon black. IV. Propane-based compounds 708(1995)293
Caciari, M., see Bruno, T.J. 708(1995)293
Cao, X., see Hunt, A.J. 708(1995)61
Carratù, B., Boniglia, C. and Bellomonte, G.
Optimization of the determination of amino acids in parenteral solutions by high-performance liquid chromatography with precolumn derivatization using 9-fluorenylmethyl chloroformate 708(1995)203
Carta, G., see Gervais, D.P. 708(1995)41
Casal, V., see Herraiz, T. 708(1995)209
Cavallaro, A., see Longo, M. 708(1995)303
Cifuentes, A., see Bedia Erim, F. 708(1995)356
Cont, M., see Larsen, B. 708(1995)115
Dash, A.K. and Harrison, J.S.
Ion-pair chromatographic method for the analysis of mafenide acetate 708(1995)83
Diamandis, E.P., see Goldberg, D.M. 708(1995)89
Dimond, P., see Hunt, A.J. 708(1995)61
Doi, T., see Furuta, R. 708(1995)245
Ehwald, R., see Woehlecke, H. 708(1995)263
Ekelund, J., Van Arkens, A., Brønnum-Hansen, K., Fich, K., Olsen, L. and Petersen, P.V.
Chiral separations of β-blocking drug substances using chiral stationary phases 708(1995)253
El-Fizga, N.K., see El-Hamdy, A.H. 708(1995)351
El-Hamdy, A.H. and El-Fizga, N.K.
Detection of olive oil adulteration by measuring its authenticity factor using reversed-phase high-performance liquid chromatography 708(1995)351
Fich, K., see Ekelund, J. 708(1995)253
Folestad, S., see Tivesten, A. 708(1995)323
Freimanis, J., see Loža, E. 708(1995)231
Furuta, R. and Doi, T.
Enantiomeric separation of a thiazole derivative by high-performance liquid chromatography and micellar electrokinetic chromatography 708(1995)245
Gareil, P., see Roldan-Assad, R. 708(1995)339
Gervais, D.P., Laughinghouse, W.S. and Carta, G.
Study of radial compression high-performance liquid chromatographic columns for preparative chromatography 708(1995)41
Goldberg, D.M., Ng, E., Karumanchiri, A., Yan, J., Diamandis, E.P. and Soleas, G.J.
Assay of resveratrol glucosides and isomers in wine by direct-injection high-performance liquid chromatography 708(1995)89
Gordon, N.F., see Hunt, A.J. 708(1995)61
Guiochon, G., see Lin, B. 708(1995)1
Haginaka, J., Miyano, Y., Saizen, Y., Seyama, C. and Murashima, T.
Separation of enantiomers on a pepsin-bonded column 708(1995)161
Hamilton, R.A., see Hunt, A.J. 708(1995)61
Harrison, J.S., see Dash, A.K. 708(1995)83
Hayakawa, K., see Nishimura, M. 708(1995)195
Hayashi, M., see Nishimura, M. 708(1995)195
He, J.-y., see Shibukawa, A. 708(1995)364
Herod, A.A. and Kandiyoti, R.
Fractionation by planar chromatography of a coal tar pitch for characterisation by size-exclusion chromatography, UV fluorescence and direct-probe mass spectrometry 708(1995)143
Herraiz, T. and Casal, V.
Evaluation of solid-phase extraction procedures in peptide analysis 708(1995)209
Hoque, E.
High-performance size-exclusion chromatographic characterization of water-soluble polymeric substances produced by *Phanerochaete chrysosporium* from free and wheat cell wall bound 3,4-dichloroaniline 708(1995)273
Horikawa, T., see Nishimura, M. 708(1995)195
Hunt, A.J., Lynch, P.D., Londo, T., Dimond, P., Gordon, N.F., McCormack, T., Schutz, A., Percoskie, M., Cao, X., McGrath, J.P., Putney, S. and Hamilton, R.A.
Development and monitoring of purification process for nerve growth factor fusion antibody 708(1995)61
Jarrett, H.W.
Preparation of cDNA–silica using reverse transcriptase and its DNA sequence determination 708(1995)13
Kadohara, M., see Shibukawa, A. 708(1995)364
Kandiyoti, R., see Herod, A.A. 708(1995)143
Karpe, P., Kirchner, S. and Rouxel, P.
Thermal desorption–gas chromatography–mass spectrometry–flame ionization detection–sniffer multi-coupling: A device for the determination of odorous volatile organic compounds in air 708(1995)105

Karumanchiri, A., see Goldberg, D.M. 708(1995)89
Kelly, M.T., see Walshe, M. 708(1995)31
Kemme, A., see Loža, E. 708(1995)231
Kim, J.-H., see Oh, C.-H. 708(1995)131
Kim, K.-R., see Oh, C.-H. 708(1995)131
Kirchner, S., see Karpe, P. 708(1995)105
Kraak, J.C., see Bedia Erim, F. 708(1995)356
Kussak, A., Andersson, B. and Andersson, K.
Determination of aflatoxins in airborne dust from feed factories by automated immunoaffinity column clean-up and liquid chromatography 708(1995)55
Larsen, B., Cont, M., Montanarella, L. and Platzner, N.
Enhanced selectivity in the analysis of chlorobiphenyls on a carborane phenylmethylsiloxane copolymer gas chromatography phase (HT-8) 708(1995)115
Laughinghouse, W.S., see Gervais, D.P. 708(1995)41
Léonil, J., see Mollé, D. 708(1995)223
Lin, B., Yun, T., Zhong, G. and Guiochon, G.
Shock layer analysis for a single-component in preparative elution chromatography 708(1995)1
Lionetti, C., see Longo, M. 708(1995)303
Loļa, D., see Loža, E. 708(1995)231
Londo, T., see Hunt, A.J. 708(1995)61
Longo, M., Lionetti, C. and Cavallaro, A.
Determination of N-nitrosodimethylamine in beer by gas chromatography–stable isotope dilution chemical ionization mass spectrometry 708(1995)303
Loža, E., Loļa, D., Kemme, A. and Freimanis, J.
Enantiomeric enrichment of partially resolved 4-hydroxy-2-carboxymethylcyclopentanone derivatives by achiral phase chromatography 708(1995)231
Lynch, P.D., see Hunt, A.J. 708(1995)61
Mabry, T.J., see Oh, C.-H. 708(1995)131
Mank, A.J.G. and Yeung, E.S.
Diode laser-induced fluorescence detection in capillary electrophoresis after pre-column derivatization of amino acids and small peptides 708(1995)309
Matsuno, R., see Adachi, S. 708(1995)177
McCalley, D.V.
Influence of organic solvent modifier and solvent strength on peak shape of some basic compounds in high-performance liquid chromatography using a reversed-phase column 708(1995)185
McCormack, T., see Hunt, A.J. 708(1995)61
McGrath, J.P., see Hunt, A.J. 708(1995)61
Miyano, Y., see Haginaka, J. 708(1995)161
Miyazaki, M., see Nishimura, M. 708(1995)195
Mizuno, T., see Adachi, S. 708(1995)177
Mollé, D. and Léonil, J.
Heterogeneity of the bovine κ-casein caseinomacropeptide, resolved by liquid chromatography on-line with electrospray ionization mass spectrometry 708(1995)223
Montanarella, L., see Larsen, B. 708(1995)115
Mou, S., see Sun, Q. 708(1995)99
Moussa, F.
Erratum to "Determination of phylloquinone in intravenous fat emulsions and soybean oil by high-performance liquid chromatography" [J. Chromatogr. A, 664 (1994) 189] 708(1995)363
Murashima, T., see Haginaka, J. 708(1995)161
Naito, S., see Shibukawa, A. 708(1995)364
Nakagawa, T., see Shibukawa, A. 708(1995)364
Ng, E., see Goldberg, D.M. 708(1995)89
Nishimura, M., see Shibukawa, A. 708(1995)364
Nishimura, M., Hayashi, M., Yamamoto, A., Horikawa, T., Hayakawa, K. and Miyazaki, M.
Study on how mobile phase buffer composition effects the retention behavior of the system peak in non-suppressed ion chromatography 708(1995)195
Nott, R., see Sundaram, K.M.S. 708(1995)71
Oh, C.-H., Kim, J.-H., Kim, K.-R. and Mabry, T.J.
Rapid gas chromatographic screening of edible seeds, nuts and beans for non-protein and protein amino acids 708(1995)131
Olsen, L., see Ekelund, J. 708(1995)253
Percoskie, M., see Hunt, A.J. 708(1995)61
Petersen, P.V., see Ekelund, J. 708(1995)253
Platzner, N., see Larsen, B. 708(1995)115
Plunkett, S.D. and Arnold, F.H.
Molecularly imprinted polymers on silica: selective supports for high-performance ligand-exchange chromatography 708(1995)19
Poppe, H., see Bedia Erim, F. 708(1995)356
Putney, S., see Hunt, A.J. 708(1995)61
Raulin, F., see Aflalaye, A. 708(1995)283
Ritchie, H., see Walshe, M. 708(1995)31
Robertson, J., see Trenerry, V.C. 708(1995)169
Roldan-Assad, R. and Gareil, P.
Capillary zone electrophoretic determination of C_2–C_{18} linear saturated free fatty acids with indirect absorbance detection 708(1995)339
Rouxel, P., see Karpe, P. 708(1995)105
Saizen, Y., see Haginaka, J. 708(1995)161
Schutz, A., see Hunt, A.J. 708(1995)61
Seyama, C., see Haginaka, J. 708(1995)161
Shibukawa, A., Kadohara, M., He, J.-y., Nishimura, M., Naito, S. and Nakagawa, T.
Erratum to "Study of the enantioselective binding between BOF-4272 and serum albumins by means of high-performance frontal analysis" [J. Chromatogr. A, 694 (1995) 81] 708(1995)364
Smyth, M.R., see Walshe, M. 708(1995)31
Soleas, G.J., see Goldberg, D.M. 708(1995)89
Sternberg, R., see Aflalaye, A. 708(1995)283
Sun, Q., Wang, H. and Mou, S.
Rapid determination of germanium and tin by ion chromatography 708(1995)99
Sundaram, K.M.S. and Nott, R.
Simultaneous determination of tebufenozide and five of its intact metabolites from forestry matrices by high-performance liquid chromatography 708(1995)71
Tivesten, A. and Folestad, S.
Separation of precolumn-labelled D- and L-amino acids by micellar electrokinetic chromatography with UV and fluorescence detection 708(1995)323
Trenerry, V.C., Robertson, J. and Wells, R.J.
Analysis of illicit amphetamine seizures by capillary electrophoresis 708(1995)169
Van Arkens, A., see Ekelund, J. 708(1995)253

Vidal-Madjar, C., see Aflalaye, A. 708(1995)283
Walshe, M., Kelly, M.T., Smyth, M.R. and Ritchie, H. Retention studies on mixed-mode columns in high-performance liquid chromatography 708(1995)31
Wang, H., see Sun, Q. 708(1995)99
Wells, R.J., see Trenerry, V.C. 708(1995)169
Wertz, K.H., see Bruno, T.J. 708(1995)293
Woehlecke, H. and Ehwald, R. Characterization of size-permeation limits of cell walls and porous separation materials by high-performance size-exclusion chromatography 708(1995)263
Yamamoto, A., see Nishimura, M. 708(1995)195
Yan, J., see Goldberg, D.M. 708(1995)89
Yeung, E.S., see Mank, A.J.G. 708(1995)309
Yun, T., see Lin, B. 708(1995)1
Zhong, G., see Lin, B. 708(1995)1

AVAILABLE AT YOUR FINGERTIPS: **NOW AVAILABLE:**

ELSEVIER SCIENCE COMPLETE CATALOGUE

THE 1995 ON

These catalogues feature all journals, books and major reference works from Elsevier Science. Furthermore they allow you to access information about the electronic and CD-ROM products now published by Elsevier Science. Demonstration examples of some of these products are included.

Features include:

ELSEVIER SCIENCE

Cj

Catalogue on **INTERNET**

- All the journals, with complete information about journal editors and editorial boards
- Listings of special issues and volumes
- Listings of recently published papers for many journals
- Complete descriptions and contents lists of book titles
- Clippings of independent reviews of published books
- Book series, dictionaries, reference works
- Electronic and CD-ROM products
- Demonstration versions of electronic products
- Free text search facilities
- Ordering facilities
- Print options
- Hypertext features

ELSEVIER SCIENCE

Ccd

Catalogue on **CD-ROM**

Extra features with the Catalogue on Internet

- Alerting facility for new & forthcoming publications
- Updated monthly

ELSEVIER SCIENCE COMPLETE CATALOGUE INTERNET: TRY IT TODAY!

gopher to: gopher.elsevier.nl
WWW: http://www.elsevier.nl/

CD-ROM (published yearly, free of charge)

Please contact:

Customer Service Department
Tel.: +31 (20) 485 3757
Fax: +31 (20) 485 3432
e-mail: nlinfo-f@elsevier.nl

ELSEVIER | PERGAMON | NORTH HOLLAND | EXCERPTA MEDICA

Flow–Through (Bio)Chemical Sensors

By **M. Valcárcel** and **M.D. Luque de Castro**

Techniques and Instrumentation in Analytical Chemistry Volume 16

Flow-through sensors are more suitable than classical probe-type sensors for addressing real (non-academic) problems. The external shape and operation of flow-through (bio)chemical sensors are of great practical significance as they facilitate sample transport and conditioning, as well as calibration and sensor preparation, maintenance and regeneration, all of which result in enhanced analytical features and a wider scope of application. This is a systematic presentation of flow-through chemical and biochemical sensors based on the permanent or transient immobilization of any of the ingredients of a (bio)chemical reaction (i.e. the analyte, reagent, catalyst or product) where detection is integrated with the analytical reaction, a separation process (dialysis, gas diffusion, sorption, etc.) or both.

The book deals critically with most types of flow-through sensors, discussing their possibilities and shortcomings to provide a realistic view of the state-of-the-art in the field. The large numbers of figures, the wealth of literature references and the extensive subject index complement the text.

Contents: 1. Sensors in Analytical Chemistry. Analytical chemistry at the turn of the XXI century. Analytical information. What is a sensor? Sensors and the analytical process. Types of sensors. General features of (bio)chemical sensors. (Bio)chemical sensors and analytical properties. Commercial availability. Trends in sensor development. **2. Fundamentals of Continuous-Flow (Bio)Chemical Sensors.** Definition. Classification. The active microzone. Flow-through cells. Continuous configurations. Regeneration modes. Transient signals. Measurement modes. The role of kinetics. Requirements for proper sensor performance. **3. Flow-Through Sensors Based on Integrated Reaction and Detection.** Introduction. Flow-through sensors based on an immobilized catalyst. Flow-through immunosensors. Flow-through sensors based on an immobilized reagent. Flow-through sensors based on an *in situ* produced reagent. **4. Flow-Through Sensors Based on Integrated Separation and Detection.** Introduction. Integrated gas diffusion and detection. Integrated liquid-liquid separation and detection. Integrated retention and detection. Flow-through sensors for multideterminations based on integrated retention and detection. Ion-selective electrodes (ISEs) and ion-sensitive field-effect transistors (ISFETs). **5. Flow-Through Sensors Based on Integrated Reaction, Separation and Detection.** Introduction. Integration of gas-diffusion, reaction and detection. Integration of dialysis, reaction and detection. Integration of sorption, reaction and detection. **Index.**

©1994 332 pages Hardbound
Price: Dfl. 355.00 (US$ 208.75)
ISBN 0-444-89866-2

ELSEVIER
An imprint of Elsevier Science

ORDER INFORMATION

ELSEVIER SCIENCE
Customer Service Department
P.O. Box 211
1000 AE Amsterdam
The Netherlands
Fax: +31 (20) 485 3432

For USA and Canada:
ELSEVIER SCIENCE
Customer Service Department
P.O. Box 945, New York
NY 10159-0945
Fax: +1 (212) 633 3764

US$ prices are valid only for the USA & Canada and are subject to exchange rate fluctuations; in all other countries the Dutch guilder price (Dfl.) is definitive. Customers in the European Union should add the appropriate VAT rate applicable in their country to the price(s). Books are sent postfree if prepaid.

PUBLICATION SCHEDULE FOR THE 1995 SUBSCRIPTION

Journal of Chromatography A and *Journal of Chromatography B: Biomedical Applications*

MONTH	1994	Jan–June	J	A	S	
Journal of Chromatography A	Vols. 683–688	Vols. 689–705	706/1 + 2 707/1 707/2 708/1	708/2 709/1 709/2 710/1	710/2 711/1 711/2 712/1	The publication schedule for further issues will be published later.
Bibliography Section		713			714/1	
Journal of Chromatography B: Biomedical Applications		663–668	669/1 669/2	670/1 670/2	671/1 + 2	

INFORMATION FOR AUTHORS

(Detailed *Instructions to Authors* were published in *J. Chromatogr. A*, Vol. 657, pp. 463–469. A free reprint can be obtained by application to the publisher, Elsevier Science B.V., P.O. Box 330, 1000 AH Amsterdam, Netherlands.)

Types of Contributions. The following types of papers are published: Regular research papers (full-length papers), Review articles, Short Communications and Discussions. Short Communications are usually descriptions of short investigations, or they can report minor technical improvements of previously published procedures; they reflect the same quality of research as full-length papers, but should preferably not exceed five printed pages. Discussions (one or two pages) should explain, amplify, correct or otherwise comment substantively upon an article recently published in the journal. For Review articles, see inside front cover under Submission of Papers.

Submission. Every paper must be accompanied by a letter from the senior author, stating that he/she is submitting the paper for publication in the *Journal of Chromatography A* or *B*.

Manuscripts. Manuscripts should be typed in **double spacing** on consecutively numbered pages of uniform size. The manuscript should be preceded by a sheet of manuscript paper carrying the title of the paper and the name and full postal address of the person to whom the proofs are to be sent. As a rule, papers should be divided into sections, headed by a caption (*e.g.*, Abstract, Introduction, Experimental, Results, Discussion, etc.). All illustrations, photographs, tables, etc., should be on separate sheets.

Abstract. All articles should have an abstract of 50–100 words which clearly and briefly indicates what is new, different and significant. No references should be given.

Introduction. Every paper must have a concise introduction mentioning what has been done before on the topic described, and stating clearly what is new in the paper now submitted.

Experimental conditions should preferably be given on a *separate* sheet, headed "Conditions". These conditions will, if appropriate, be printed in a block, directly following the heading "Experimental".

Illustrations. The figures should be submitted in a form suitable for reproduction, drawn in Indian ink on drawing or tracing paper. Each illustration should have a caption, all the *captions* being typed (with double spacing) together on a *separate sheet*. If structures are given in the text, the original drawings should be provided. Coloured illustrations are reproduced at the author's expense, the cost being determined by the number of pages and by the number of colours needed. The written permission of the author and publisher must be obtained for the use of any figure already published. Its source must be indicated in the legend.

References. References should be numbered in the order in which they are cited in the text, and listed in numerical sequence on a separate sheet at the end of the article. Please check a recent issue for the layout of the reference list. Abbreviations for the titles of journals should follow the system used by *Chemical Abstracts*. Articles not yet published should be given as "in press" (journal should be specified), "submitted for publication" (journal should be specified), "in preparation" or "personal communication".

Vols. 1–651 of the *Journal of Chromatography*; *Journal of Chromatography, Biomedical Applications* and *Journal of Chromatography, Symposium Volumes* should be cited as *J. Chromatogr.* From Vol. 652 on, *Journal of Chromatography A* (incl. Symposium Volumes) should be cited as *J. Chromatogr. A* and *Journal of Chromatography B: Biomedical Applications* as *J. Chromatogr. B.*

Dispatch. Before sending the manuscript to the Editor please check that the envelope contains four copies of the paper complete with references, captions and figures. One of the sets of figures must be the originals suitable for direct reproduction. Please also ensure that permission to publish has been obtained from your institute.

Proofs. One set of proofs will be sent to the author to be carefully checked for printer's errors. Corrections must be restricted to instances in which the proof is at variance with the manuscript.

Reprints. Fifty reprints will be supplied free of charge. Additional reprints can be ordered by the authors. An order form containing price quotations will be sent to the authors together with the proofs of their article.

Quality Assurance for Environmental Analysis

Method Evaluation within the Measurements and Testing Programme (BCR)

Edited by **Ph. Quevauviller**, **E.A. Maier** and **B. Griepink**

Techniques and Instrumentation in Analytical Chemistry, Volume 17

Quality assurance (QA) for environmental analysis is a growing feature of the nineties as is illustrated by the number of QA guidelines and systems which are being implemented nowadays. This book focuses on the technical aspects of quality assurance. The techniques used in different analytical fields are critically reviewed and existing tools for evaluating their performance are described. Particular reference is made to the activities of the Measurements and Testing Programme (BCR) of the European Commission towards the improvement of quality control of environmental analysis.

Contents: 1. Quality assurance for environmental analysis (Ph. Quevauviller *et al.*). 2. Development of ICPMS and ID-ICPMS with the determination of Pb and Hg in environmental matrices as an example (M. Campbell). 3. Detection of sources of error in the determination of Cr in environmental matrices by FAAS and ETAAS (G. Rauret *et al.*). 4. Analysis of environmental and biological samples by atomic spectroscopic methods (M. Hoenig, M.F. Gunn). 5. Validation of neutron activation analysis techniques (K. Heydorn). 6. Flow-through (bio)chemical sensors in environmental analysis (M.D. Luque de Castro, M. Válcarcel). 7. Fiber optical sensors applied to field measurements (C. Cámara *et al.*). 8. Chromium speciation in environmental and biological samples (K. Vercoutere, R. Cornelis). 9. Determination of aluminium species in natural waters (B. Fairman, A. Sanz-Medel). 10. Selenium speciation analyses in water and sediment matrices (C. Cámara *et al.*). 11. Antimony speciation in water (M.B. de la Calle- Guntiñas *et al.*). 12. Arsenic speciation in environmental matrices (A. Amran *et al.*). 13. Mercury speciation in biological matrices (I. Drabæk, Å Iverfeldt). 14. Speciation analysis of organolead compounds. Status and future prospects (R. Lobinski *et al.*). 15. Speciation analysis of organotin by GC-AAS and GC-AES after extraction and derivatization (W.M.R. Dirkx *et al.*). 16. High performance liquid chromatography - isotope dilution - inductively coupled plasma - mass spectrometry for lead and tin speciation in environmental samples (S.J. Hill *et al.*). 17. Speciation of organotin compounds in environmental samples by GC-MS (R. Morabito *et al.*). 18. Development of supercritical fluid extraction procedures for the determination of organotin compounds in sediment (J.M. Bayona). 19. Hydride generation for speciation analyses using GC/AAS (R. Ritsema *et al.*). 20. Single and sequential extraction schemes for trace metal speciation in soil and sediment (A.M. Ure *et al.*). 21. Methods for the determination of chlorinated biphenyls in air (M. Morosini, K. Balschmitter). 22. Sample handling and determination of carbamate pesticides and their transformation products in various matrices (M. Honing *et al.*). 23. Method development for the determination of polycyclic aromatic hydrocarbons (PAHs) in environmental matrices (J. Jacob). 24. Method validation for the determination of dioxins (T. Rymen). Subject index.

©1995 670 pages Hardbound
Price: Dfl. 475.00 (US$279.50)
ISBN 0-444-89955-3

ELSEVIER
An imprint of Elsevier Science

ORDER INFORMATION

ELSEVIER SCIENCE
Customer Service Department
P.O. Box 211
1000 AE Amsterdam
The Netherlands
Fax: +31 (20) 485 3432

For USA and Canada:
ELSEVIER SCIENCE
Customer Service Department
P.O. Box 945, New York
NY 10159-0945
Fax: +1 (212) 633 3764

US$ prices are valid only for the USA & Canada and are subject to exchange rate fluctuations; in all other countries the Dutch guilder price (Dfl.) is definitive. Customers in the European Union should add the appropriate VAT rate applicable in their country to the price(s). Books are sent postfree if prepaid.